TRANSCRANIAL MAGNETIC STIMULATION PROMOTES MOTOR REHABILITATION THROUGH NEURAL PLASTICITY

EDITED BY: Dongsheng Xu, Oscar Arias-Carrion and Ti-Fei Yuan

PUBLISHED IN: Frontiers in Neural Circuits and Frontiers in Human Neuroscience

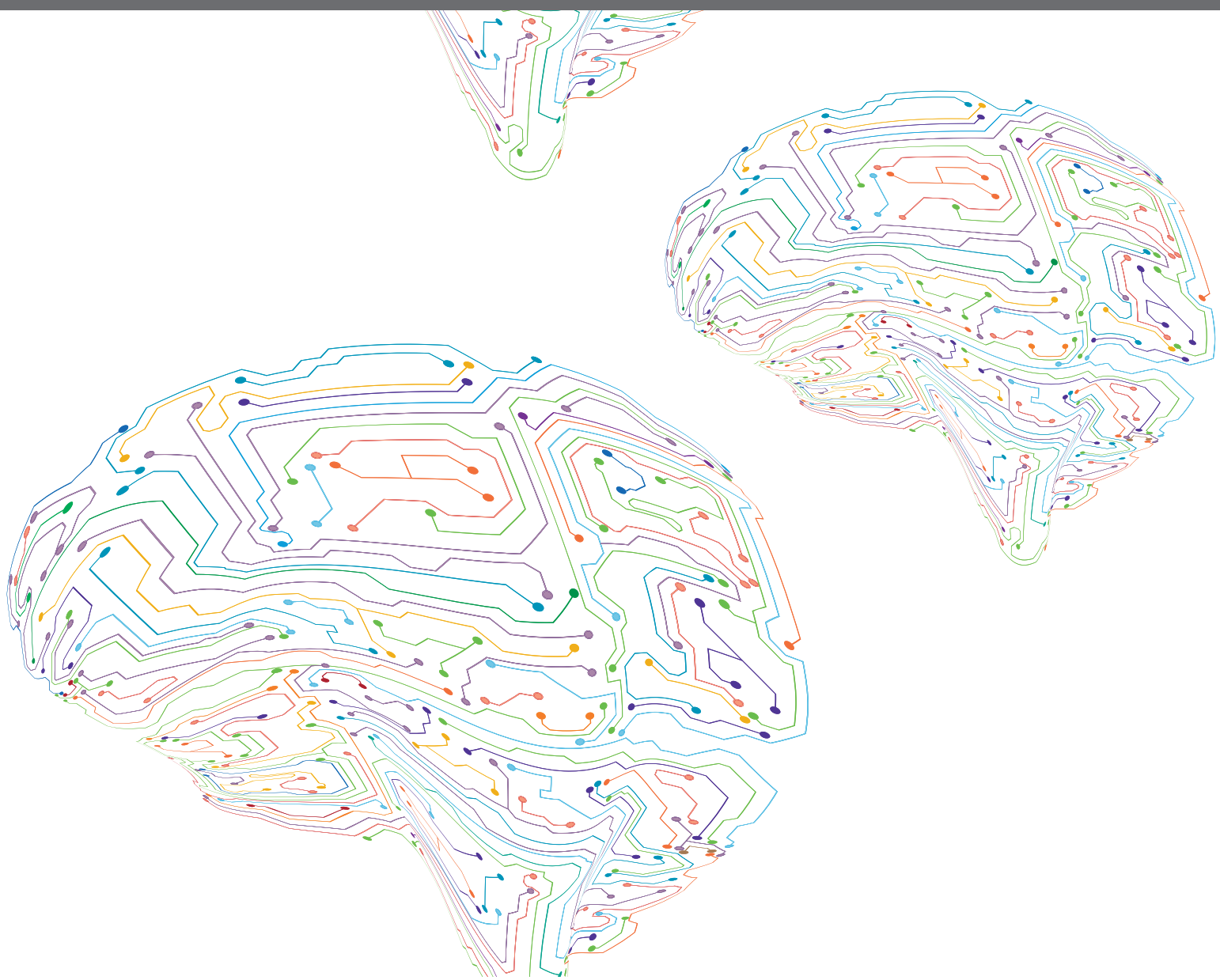

frontiers Research Topics

frontiers

Frontiers eBook Copyright Statement

The copyright in the text of individual articles in this eBook is the property of their respective authors or their respective institutions or funders. The copyright in graphics and images within each article may be subject to copyright of other parties. In both cases this is subject to a license granted to Frontiers.

The compilation of articles constituting this eBook is the property of Frontiers.

Each article within this eBook, and the eBook itself, are published under the most recent version of the Creative Commons CC-BY licence. The version current at the date of publication of this eBook is CC-BY 4.0. If the CC-BY licence is updated, the licence granted by Frontiers is automatically updated to the new version.

When exercising any right under the CC-BY licence, Frontiers must be attributed as the original publisher of the article or eBook, as applicable.

Authors have the responsibility of ensuring that any graphics or other materials which are the property of others may be included in the CC-BY licence, but this should be checked before relying on the CC-BY licence to reproduce those materials. Any copyright notices relating to those materials must be complied with.

Copyright and source acknowledgement notices may not be removed and must be displayed in any copy, derivative work or partial copy which includes the elements in question.

All copyright, and all rights therein, are protected by national and international copyright laws. The above represents a summary only. For further information please read Frontiers' Conditions for Website Use and Copyright Statement, and the applicable CC-BY licence.

ISSN 1664-8714
ISBN 978-2-88974-353-7
DOI 10.3389/978-2-88974-353-7

About Frontiers

Frontiers is more than just an open-access publisher of scholarly articles: it is a pioneering approach to the world of academia, radically improving the way scholarly research is managed. The grand vision of Frontiers is a world where all people have an equal opportunity to seek, share and generate knowledge. Frontiers provides immediate and permanent online open access to all its publications, but this alone is not enough to realize our grand goals.

Frontiers Journal Series

The Frontiers Journal Series is a multi-tier and interdisciplinary set of open-access, online journals, promising a paradigm shift from the current review, selection and dissemination processes in academic publishing. All Frontiers journals are driven by researchers for researchers; therefore, they constitute a service to the scholarly community. At the same time, the Frontiers Journal Series operates on a revolutionary invention, the tiered publishing system, initially addressing specific communities of scholars, and gradually climbing up to broader public understanding, thus serving the interests of the lay society, too.

Dedication to Quality

Each Frontiers article is a landmark of the highest quality, thanks to genuinely collaborative interactions between authors and review editors, who include some of the world's best academicians. Research must be certified by peers before entering a stream of knowledge that may eventually reach the public - and shape society; therefore, Frontiers only applies the most rigorous and unbiased reviews.
Frontiers revolutionizes research publishing by freely delivering the most outstanding research, evaluated with no bias from both the academic and social point of view. By applying the most advanced information technologies, Frontiers is catapulting scholarly publishing into a new generation.

What are Frontiers Research Topics?

Frontiers Research Topics are very popular trademarks of the Frontiers Journals Series: they are collections of at least ten articles, all centered on a particular subject. With their unique mix of varied contributions from Original Research to Review Articles, Frontiers Research Topics unify the most influential researchers, the latest key findings and historical advances in a hot research area! Find out more on how to host your own Frontiers Research Topic or contribute to one as an author by contacting the Frontiers Editorial Office: frontiersin.org/about/contact

TRANSCRANIAL MAGNETIC STIMULATION PROMOTES MOTOR REHABILITATION THROUGH NEURAL PLASTICITY

Topic Editors:
Dongsheng Xu, Tongji University, China
Oscar Arias-Carrion, Hospital General Dr. Manuel Gea Gonzalez, Mexico
Ti-Fei Yuan, Shanghai Jiao Tong University, China

Citation: Xu, D., Arias-Carrion, O., Yuan, T.-F., eds. (2022). Transcranial Magnetic Stimulation Promotes Motor Rehabilitation Through Neural Plasticity. Lausanne: Frontiers Media SA. doi: 10.3389/978-2-88974-353-7

Table of Contents

frontiers in Human Neuroscience

ORIGINAL RESEARCH
published: 21 May 2020
doi: 10.3389/fnhum.2020.00190

Corticomotor Excitability Changes Associated With Freezing of Gait in People With Parkinson Disease

Ya-Yun Lee[1], Min-Hao Li[1,2], Chun-Hwei Tai[3]† and Jer-Junn Luh[1,4]*†*

[1] School and Graduate Institute of Physical Therapy, College of Medicine, National Taiwan University, Taipei, Taiwan, [2] Department of Physical Medicine and Rehabilitation, National Taiwan University Hospital, Taipei, Taiwan, [3] Department of Neurology, National Taiwan University Hospital, Taipei, Taiwan, [4] College of Education, Fu-Jen Catholic University, Taipei, Taiwan

OPEN ACCESS

Edited by:
Oscar Arias-Carrión,
Hospital General Dr. Manuel Gea Gonzalez, Mexico

Reviewed by:
Silmar Teixeira,
Federal University of Piauí, Brazil
Benito de Celis Alonso,
Meritorious Autonomous University of Puebla, Mexico

***Correspondence:**
Chun-Hwei Tai
chtai1502@ntu.edu.tw;
chtai66@gmail.com
Jer-Junn Luh
jerjunnluh@gmail.com

†These authors have contributed equally to this work

Specialty section:
This article was submitted to Brain Imaging and Stimulation, a section of the journal Frontiers in Human Neuroscience

Received: 06 March 2020
Accepted: 28 April 2020
Published: 21 May 2020

Citation:
Lee Y-Y, Li M-H, Tai C-H and Luh J-J (2020) Corticomotor Excitability Changes Associated With Freezing of Gait in People With Parkinson Disease. Front. Hum. Neurosci. 14:190. doi: 10.3389/fnhum.2020.00190

Background and Purpose: Freezing of gait (FOG) is a debilitating gait disorder in people with Parkinson's disease (PD). While various neuroimaging techniques have been used to investigate the pathophysiology of FOG, changes in corticomotor excitability associated with FOG have yet to be determined. Research to date has not concluded if changes in corticomotor excitability are associated with gait disturbances in this patient population. This study aimed to use transcranial magnetic stimulation (TMS) to investigate corticomotor excitability changes associated with FOG. Furthermore, the relationship between corticomotor excitability and gait performances would be determined.

Methods: Eighteen participants with PD and FOG (PD + FOG), 15 without FOG (PD − FOG), and 15 non-disabled adults (Control) were recruited for this study. Single and paired-pulse TMS paradigms were used to assess corticospinal and intracortical excitability, respectively. Gait performance was measured by the 10-Meter-Walk test. Correlation analysis was performed to evaluate relationships between TMS outcomes and gait parameters.

Results: Compared with the Control group, the PD + FOG group showed a significantly lower resting motor threshold and reduced short intracortical inhibition (SICI). Correlation analysis revealed a relationship between resting motor evoked potential and step length, and between SICI and walking velocity in the Control group. While the silent period correlated with step length in the PD − FOG group, no significant relationship was observed in the PD + FOG group.

Discussion and Conclusion: Compared to the Control group, the PD + FOG group exhibited reduced corticomotor inhibition. Distinct correlations observed among the three groups suggest that the function of the corticomotor system plays an important role in mediating walking ability in non-disabled adults and people with PD − FOG, while people with PD + FOG may rely on neural networks other than the corticomotor system to control gait.

Keywords: Parkinson's disease, freezing of gait, transcranial magnetic stimulation, corticomotor excitability, gait

INTRODUCTION

Freezing of gait (FOG) is a debilitating phenomenon of Parkinson disease (PD) characterized by transient incapability or difficulty to move the feet forward despite an intention to do so (Nutt et al., 2011). It has been reported that ∼54.8% of people with PD experienced freezing episodes that increased in prevalence as disease progressed (Amboni et al., 2015). Even with "ON" medication status, 38.2% of individuals with PD experienced FOG (Perez-Lloret et al., 2014). Although freezing episodes may last only a few seconds, they significantly increase the risk of falls, affect daily activities, and reduce quality of life. A comprehensive understanding of the neurophysiological changes associated with FOG may facilitate the development of more effective treatment approaches (Nutt et al., 2011).

Functional magnetic resonance imaging (fMRI) and functional near infrared spectroscopy (fNIRS) have been used to provide insights into brain activation changes associated with FOG (Vercruysse et al., 2014). It was observed that people with FOG demonstrated a decreased activation of the motor, basal ganglia and ventral attention networks when performing freezing-provoking tasks in virtual reality (Shine et al., 2013). A study using fNIRS, that more directly evaluated the changes in oxygenated hemoglobin (HbO_2) during walking, found that HbO_2 of the prefrontal areas increased before and during freezing episodes (Maidan et al., 2015). These studies provided valuable information regarding changes in FOG associated cortical activations; it remains unclear whether increased (or decreased) activations of brain regions represents enhanced (or reduced) neural excitability. Increased brain activation may suggest an increased inhibitory process within that region (Sack and Linden, 2003). Hence, transcranial magnetic stimulation (TMS) becomes an invaluable tool for researchers to understand the changes in corticomotor excitability associated with certain disorders or disease phenotype.

Various TMS paradigms, such as single-pulse and paired-pulse paradigms, are available to evaluate the excitability of the corticospinal tract and intracortical neuronal network within the primary motor cortex (M1) (Vucic and Kiernan, 2017). Changes in corticomotor excitability of the upper-extremity muscles have been widely studied with TMS in people with PD. The studies found that PD during "ON" medication status displayed increased excitability of the corticospinal pathway and decreased intracortical inhibition compared with non-disabled adults (Cantello et al., 1991; Valls-Sole et al., 1994; Ni and Chen, 2015). Very few studies have determined the corticomotor excitability changes of lower-extremity muscles in people with PD. Since upper-extremity and lower-extremity muscles have different descending projections and functional requirement (Tremblay and Tremblay, 2002), understanding the neurophysiological changes of lower-extremity muscles is important. Enhanced corticospinal excitability in the quadriceps muscle has been reported in persons with PD (Tremblay and Tremblay, 2002). When targeting the tibialis anterior (TA) muscle, excitability of the corticospinal tract for individuals with PD did not differ from control subjects. The only observed difference was that persons with PD had significantly lower intracortical facilitation during "OFF" medication (Vacherot et al., 2010a,b). Additionally, after pooling the data from PD ("ON" and "OFF" medication) and control subjects, it was found that changes in intracortical facilitation correlated significantly with gait velocity and stride length (Vacherot et al., 2010b). These studies provided preliminary evidence of the corticomotor abnormality in the lower-extremity muscles of PD.

Since people with FOG have greater gait disturbances than those without FOG, the corticomotor excitability may change along with the symptoms. To date, no studies have evaluated differences in corticomotor excitability of lower extremity muscles between freezers and non-freezers using TMS. Understanding the potential direction of changes in corticomotor excitability may facilitate the development of appropriate interventions. This study also aimed to investigate whether changes in corticomotor excitability would correlate with walking ability in people with FOG, since gait disturbances are one of the major causes of poor quality of life for these individuals.

MATERIALS AND METHODS

Participants

Forty-eight subjects, including 18 participants with PD and FOG (PD + FOG), 15 individuals without FOG (PD − FOG), and 15 age-matched non-disabled control subjects (Control) participated in this study. The baseline characteristics of the participants are presented in **Table 1**. Before joining, the participants signed an informed consent form approved by the Institutional Review Board of National Taiwan University Hospital and completed a TMS safety questionnaire. The study procedure conformed to the World Medical Association Declaration of Helsinki. The participants were excluded if they had any contraindications or concerns for receiving TMS. The participants with PD were classified as freezers and non-freezers based on the New Freezing of Gait Questionnaire (NFOG-Q) (Nieuwboer et al., 2009). A medical history chart review verified the classification of the participants with PD.

TMS Assessments

All TMS assessments were performed with a double-cone coil (110 mm) connected to a paired-pulse magnetic stimulator (The Magstim® BiStim^2; The Magstim Company Ltd., Whitland,

TABLE 1 | Clinical characteristics of the participants.

	PD + FOG	PD − FOG	Control	*p*
Age (years)	68.2 ± 1.8	65.1 ± 1.4	68.0 ± 1.4	0.295
Gender (male/female)	10/8	8/7	6/9	0.641
Disease duration (years)	8.2 ± 1.4	3.9 ± 0.7	–	0.009*
UPDRS-III (scores)	21.1 ± 1.7	15.1 ± 1.8	–	0.022*
Levodopa equivalent dosage (mg/day)	822.3 ± 119.4	489.7 ± 76.4	–	0.032*

*Values are presented as mean ± standard error for continuous variables and frequency for categorical variables. UPDRS-III: part-III of Unified Parkinson's Disease Rating Scale. *p < 0.05.*

United Kingdom). The target muscle was the TA of the more affected side for participants with PD and the non-dominant side for the Control participants. After skin preparation, surface electromyographic (EMG) electrodes were placed over the TA muscle belly, and a ground electrode was placed over the lateral epicondyle of the femur. EMG signal sampling rate was 4000 Hz with 0–1000 Hz band-pass filter. TMS pulses were applied over the cortical representation area (i.e., hotspot) of the TA on the M1 to activate the corticospinal tract and generate motor evoked potentials (MEPs) (Ni and Chen, 2015). Consistent with the international guidelines (Rossini et al., 1994), the hotspot of the TA and resting motor threshold (RMT) were first determined. With single-pulse TMS, 10–15 trials of MEPs were elicited using an intensity at 130% of RMT under resting and active conditions. In the resting condition, participants were instructed to sit and relax their TA muscles with ankle dorsiflexion at 90°; under the active condition, participants were asked to conduct a low-level isometric ankle dorsiflexion contraction to touch a lever bar placed above the first metatarsal shaft. The height of the bar was adjusted to 30° of dorsiflexion for each participant (Fisher et al., 2016). Peak-to-peak MEP amplitude of each trial was recorded, and mean MEP amplitude was calculated for each condition. Cortical silent period (CSP), a period when EMG activity is suppressed for a few hundred milliseconds after MEP, was also recorded during the active muscle contraction condition (Kobayashi and Pascual-Leone, 2003).

Using the paired-pulse stimulation paradigm, short intracortical inhibition (SICI) and intracortical facilitation (ICF) were obtained. Two stimuli, the conditioning stimulus and the testing stimulus, were applied to the TA hotspot. The conditioning stimulus was set at 80% of RMT, while the testing stimulus was set at 130% of RMT (Vacherot et al., 2010b). The SICI can be obtained when the inter-stimuli intervals are tuned at 2–5 ms, while ICF is measured when the inter-stimuli intervals are set between 7 and 15 ms (Vucic and Kiernan, 2017). In this study, stimuli were applied when inter-stimulus intervals were set at 2 and 3 ms for SICI ($SICI_{2ms}$, $SICI_{3ms}$, respectively), and 12 and 15 ms for ICF (ICF_{12ms}, ICF_{15ms}, respectively). The stimulation order was randomly assigned to each subject. Peak-to-peak MEP values obtained from the paired-pulse paradigm were normalized to the single-pulse resting MEP value to determine the inhibition or facilitation of the intracortical neurons.

Gait Performances

The 10-Meter Walk Test (10MWT) was used to evaluate walking ability. Participants were instructed to walk at a comfortable walking speed along a 10-m walkway three times. The investigator recorded the time and the number of steps that the participants took during the 10-m walk, and further calculated mean walking velocity, stride length, and cadence. Good to excellent test-retest reliability for these gait parameters have been established for individuals with PD (Lang et al., 2016).

Statistical Analysis

Baseline characteristics of the three groups (PD + FOG, PD − FOG, and Control) were analyzed with a chi-square test and one-way analysis of variance (ANOVA) for dichotomous and continuous variables, respectively. The dataset distribution was checked before analyzing the data. Since most of the outcome measures were not normally distributed, the Kruskal-Wallis test was used to determine group differences. Dunn's *post-hoc* tests with Bonferroni corrections were performed when a significant main effect was found. In addition to *p*-values, the effect sizes (η^2) were calculated to determine the amount of group differences (Tomczak and Tomczak, 2014). Spearman's rho test was used to determine the relationship between TMS outcomes and gait performance. During the correlation analysis, TMS data of $SICI_{2ms}$ and $SICI_{3ms}$ were pooled to represent an averaged intracortical inhibition, and ICF_{12ms} and ICF_{15ms} were averaged to represent intracortical facilitation. Only gait velocity and step length were chosen for the correlation analysis because these gait parameters were mostly affected in people with FOG. All data acquired were analyzed with IBM SPSS 22.0 software (IBM Corporation, Armonk, NY, United States) using $\alpha = 0.05$ for significance.

RESULTS

Analysis of the clinical characteristics of the participants revealed no significant differences in age and gender among the groups. The PD + FOG group had significantly longer disease duration, greater disease severity, and higher levodopa medication usage than the PD − FOG group (**Table 1**).

TMS Outcomes

The TMS outcomes are presented in **Table 2**. Statistical analysis revealed a significant difference in RMT among the three groups [$\chi^2(2) = 6.977$, $p = 0.031$, $\eta^2 = 0.111$]. Dunn's *post-hoc* with Bonferroni corrections revealed that the PD + FOG group had lower RMT than the control group ($p = 0.025$), while there were no differences between the PD + FOG and PD − FOG groups ($p = 0.854$) or the PD − FOG and control groups ($p = 0.400$). The three groups did not differ in resting MEP [$\chi^2(2) = 0.019$, $p = 0.991$, $\eta^2 = 0.044$], active MEP [$\chi^2(2) = 0.862$, $p = 0.650$, $\eta^2 = 0.026$], and CSP [$\chi^2(2) = 0.701$, $p = 0.701$, $\eta^2 = 0.029$].

The results of the paired-pulse paradigm are shown in **Figure 1**. Significant group difference was found in $SICI_{2ms}$ [$\chi^2(2) = 8.993$, $p = 0.011$, $\eta^2 = 0.155$], but not in $SICI_{3ms}$ [$\chi^2(2) = 2.197$, $p = 0.333$, $\eta^2 = 0.004$], ICF_{12ms} [$\chi^2(2) = 1.830$, $p = 0.400$, $\eta^2 = 0.004$], or ICF_{15ms} [$\chi^2(2) = 1.869$, $p = 0.393$, $\eta^2 = 0.003$]. *Post-hoc* analysis of $SICI_{2ms}$ showed that the PD + FOG group had larger normalized MEPs than the Control group ($p = 0.008$), but no significance was found between the PD + FOG and PD − FOG groups ($p = 0.749$) nor the PD − FOG and Control groups ($p = 0.235$). This suggests that the participants with PD + FOG had less intra-cortical inhibition at $SICI_{2ms}$ than the Control participants.

Since baseline demographic comparison revealed that the participants with FOG group had greater disease severity with longer disease duration and higher levodopa usage than those without FOG, it was unclear whether the TMS results might be affected by these factors. To scrutinize the findings of

TABLE 2 | Corticomotor excitability and gait performances of the three groups.

	PD + FOG	PD − FOG	Control	*p*	η^2
Single-pulse TMS					
RMT (%MSO)	41.9 ± 2.4*	45.3 ± 2.4	53.4 ± 3.4	0.031	0.111
Resting MEP (μV)	1013.5 ± 206.8	1074.9 ± 245.4	1000.7 ± 177.8	0.991	0.044
Active MEP (μV)	2271.2 ± 269.0	2502.6 ± 298.3	2777.4 ± 356.5	0.566	0.026
CSP (s)	0.150 ± 0.008	0.141 ± 0.104	0.153 ± 0.014	0.701	0.029
Paired-pulse TMS					
$SICI_{2ms}$ (%)	45.6 ± 6.7*	41.1 ± 9.5	19.3 ± 3.7	0.011	0.155
$SICI_{3ms}$ (%)	47.5 ± 9.6	44.0 ± 9.5	27.9 ± 5.8	0.333	0.004
ICF_{12ms} (%)	91.4 ± 18.0	69.0 ± 13.7	109.3 ± 21.5	0.274	0.004
ICF_{15ms} (%)	94.7 ± 24.1	71.2 ± 17.2	109.1 ± 29.3	0.433	0.003
Gait performances					
Walking velocity (m/s)	0.91 ± 0.06*	1.09 ± 0.05	1.22 ± 0.04	0.003	0.214
Step length (m)	0.48 ± 0.03*†	0.60 ± 0.03	0.66 ± 0.02	<0.001	0.307
Cadence (step/s)	1.88 ± 0.04	1.81 ± 0.03	1.87 ± 0.06	0.175	0.033

*Values are presented as mean ± standard error. RMT, resting motor threshold; MSO, maximal stimulator output; MEP, motor evoked potentials; CSP, cortical silent period; SICI, short-interval intracortical inhibition; ICF, intracortical facilitation. *Significant difference between PD + FOG group and Control group ($p < 0.05$). †Significant difference between PD + FOG group and PD − FOG group ($p < 0.05$).*

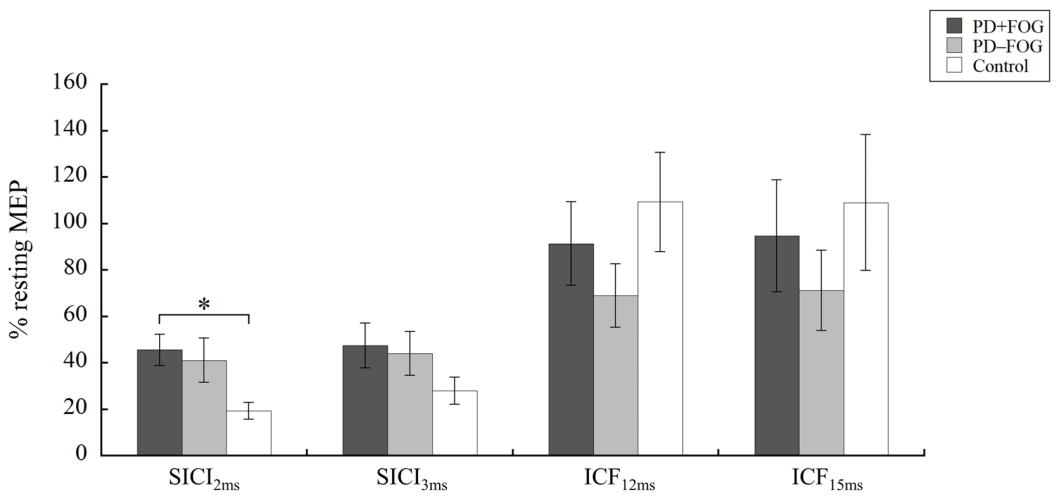

FIGURE 1 | Paired-pulse TMS. Means and standard errors of the means of the PD + FOG (dark gray), PD − FOG (light gray), and Control (white) group. MEP, motor evoked potential; SICI, short intracortical inhibition; ICF, intracortical facilitation. *$P < 0.05$.

the TMS outcomes, we re-analyzed the data by removing the individuals who had disease duration longer than 10 years and/or UPDRS III score greater than 25, leaving 13 participants in the PD − FOG group and 10 in the PD + FOG group. After removing these cases, there were no significant differences between the PD − FOG and PD + FOG groups in disease duration ($p = 0.283$), severity ($p = 0.066$), and medication usage ($p = 0.434$). When re-analyzing the TMS data of the remaining subjects, the results still showed significant group differences in RMT [$\chi^2(2) = 8.602$, $p = 0.014$] and $SICI_{2ms}$ [$\chi^2(2) = 7.739$, $p = 0.021$], suggesting that the observed changes in corticomotor excitability were associated with FOG but not due to other factors.

Gait Performances

Significant group differences were found for walking velocity [$\chi^2(2) = 11.613$, $p = 0.003$, $\eta^2 = 0.214$]. *Post-hoc* analysis showed that participants with PD + FOG had slower walking velocity than Control subjects ($p = 0.002$), but no differences were found between the PD + FOG and PD − FOG groups ($p = 0.215$) or between the PD − FOG and Control groups ($p = 0.381$). While no group difference was found in cadence [$\chi^2(2) = 3.489$, $p = 0.175$, $\eta^2 = 0.033$], a significant group difference was observed in step length [$\chi^2(2) = 15.807$, $p < 0.001$, $\eta^2 = 0.307$]. *Post-hoc* analysis of step length revealed that the PD + FOG group had significantly smaller step length than the Control ($p < 0.001$) and the PD − FOG ($p = 0.036$) groups. However, the PD − FOG and Control groups did not differ significantly in step length ($p = 0.562$).

To justify the above findings, gait parameters were re-analyzed by removing the subjects who had longer disease duration, greater disease severity and higher levodopa usage as described in the previous section. Secondary analysis still revealed a significant

group difference in walking velocity [$\chi^2(2) = 11.959$, $p = 0.003$] and step length [$\chi^2(2) = 11.960$, $p = 0.003$], supporting our original findings.

Correlation Analysis

Spearman's rho tests were performed separately for all groups (**Table 3**). In the Control group, significant correlation was found between walking velocity and SICI [$\rho_{(13)} = 0.556$, $p = 0.031$], while no other TMS parameters correlated with walking velocity. Step length negatively correlated with resting MEP [$\rho_{(13)} = -0.585$, $p = 0.022$]. No other correlations were observed between gait outcomes and TMS measures.

For the PD − FOG group, a positive correlation was observed between step length and CSP [$\rho_{(13)} = 0.559$, $p = 0.030$], while a borderline correlation was found between gait velocity and SICI [$\rho_{(13)} = 0.504$, $p = 0.055$]. No other correlations were observed between the gait parameters and TMS outcomes in this group. Different from the other two groups, there was no relationship found between the gait parameters and any of the TMS outcomes in the PD + FOG group. Since some relationships were found between SICI and velocity in the Control and PD − FOG groups but not in the PD + FOG group, **Figure 2** is drawn to illustrate the different correlation patterns among the three groups.

DISCUSSION

This study aimed to determine the changes in corticomotor excitability in participants with PD + FOG compared to those without FOG and control subjects. Additionally, we wanted to understand whether corticomotor excitability correlates with gait performance. The results showed that, during "ON" medication, participants with PD + FOG had significantly lower RMT and reduced $SICI_{2ms}$ than the Control subjects. Relationships was found between SICI and walking velocity, and between resting MEP and step length in the Control group. Only the CSP correlated with step length in the PD − FOG group, while no correlation was found between gait parameters and TMS outcomes in the PD + FOG group.

TABLE 3 | Correlation results between gait performances and TMS outcomes.

Correlation (ρ)	RMT	Rest MEP	Active MEP	CSP	SICI	ICF
Control						
Velocity	0.240	−0.043	−0.211	0.318	0.556*	0.300
Step length	0.250	−0.585*	−0.185	−0.318	0.404	0.465
PD − FOG						
Velocity	0.011	−0.036	−0.061	0.399	0.504	0.013
Step length	0.126	−0.116	−0.133	0.559*	0.418	0.115
PD + FOG						
Velocity	−0.109	0.156	0.044	−0.133	−0.260	−0.020
Step length	−0.200	0.213	0.017	−0.126	−0.342	−0.055

*Values are presented as Spearman's rho. RMT, resting motor threshold; MEP, motor evoked potentials; CSP, cortical silent period; SICI, short-interval intracortical inhibition; ICF, intracortical facilitation. *p < 0.05.*

Resting motor threshold is an important single-pulse TMS parameter reflecting how easily the corticomotoneurons in the M1 are excited when the target muscle is at rest, and thus can represent the neuronal membrane excitability of the corticospinal tract (Vucic and Kiernan, 2017). Earlier studies conducted on upper-extremity muscles showed that RMT was similar in persons with PD and non-disabled adults, regardless of medication status (Leon-Sarmiento et al., 2013; Ni and Chen, 2015). While Vacherot et al. (2010b) did not find significant differences in RMT of the TA between the PD and Control groups (Vacherot et al., 2010b), Tremblay and Tremblay (2002) showed that individuals with PD had a significantly lower RMT of the quadriceps muscle (Tremblay and Tremblay, 2002). The inconsistent findings in RMT among the studies may be hampered by the lack of patient classification or consideration of their principal features (Cantello et al., 2002). Cantello et al. (1991) recruited participants with PD who had asymmetric body rigidity and found that RMT was lower on the rigid side than the contralateral side or than on healthy adults (Cantello et al., 1991). It was suggested that the motoneurons from the corticospinal system of the rigid side were hyperexcited, and the subliminal excitation of the alpha-motoneurons led to a lower RMT (Cantello et al., 1991, 2002). Our study provided additional evidence showing that participants with PD + FOG had significantly lower RMT than control subjects, also suggesting enhanced excitability of the corticomotor system. We could not exclude the possibility that the reduction of RMT was due to greater rigidity in people with PD + FOG even though no obvious background EMG activities were observed in these participants throughout the study. Nevertheless, appropriate patient classification may be an important factor to consider in future studies to unravel neurophysiological changes in patient populations.

Paired-pulse paradigm may be one of the most sensitive tools to highlight corticomotor abnormalities in PD (Vacherot et al., 2010a). The current study found that the PD + FOG group had significantly larger normalized MEP at $SICI_{2ms}$ in comparison to the Control group, suggesting a decreased intracortical inhibition in people with FOG. However, no significant differences were observed between PD − FOG and Control groups. Our results partly support Vacherot et al.'s (2010b) finding of no significant differences in $SICI_{2ms}$ of the TA muscle between people with PD and control participants regardless of medication status (Vacherot et al., 2010b). Targeting the first dorsal interosseous muscle, a significantly reduced $SICI_{2ms}$ was found during "OFF" medication, but the reduction in intracortical inhibition was restored during the "ON" state (Ridding et al., 1995). Our study is the first to show that individuals with FOG have a reduced $SICI_{2ms}$ of the TA muscle even during the "ON" medication status, suggesting that the intracortical inhibition is impaired in persons with PD + FOG, and dopaminergic medication could not fully restore the intracortical inhibitory control of these individuals. This reduced intracortical inhibition corresponds to the finding of decreased RMT, suggesting a compensatory hyperexcitation of the corticomotor system in people with PD + FOG. Using fMRI combined with a motor imagery of walking task, Snijders et al. (2011) found that patients with

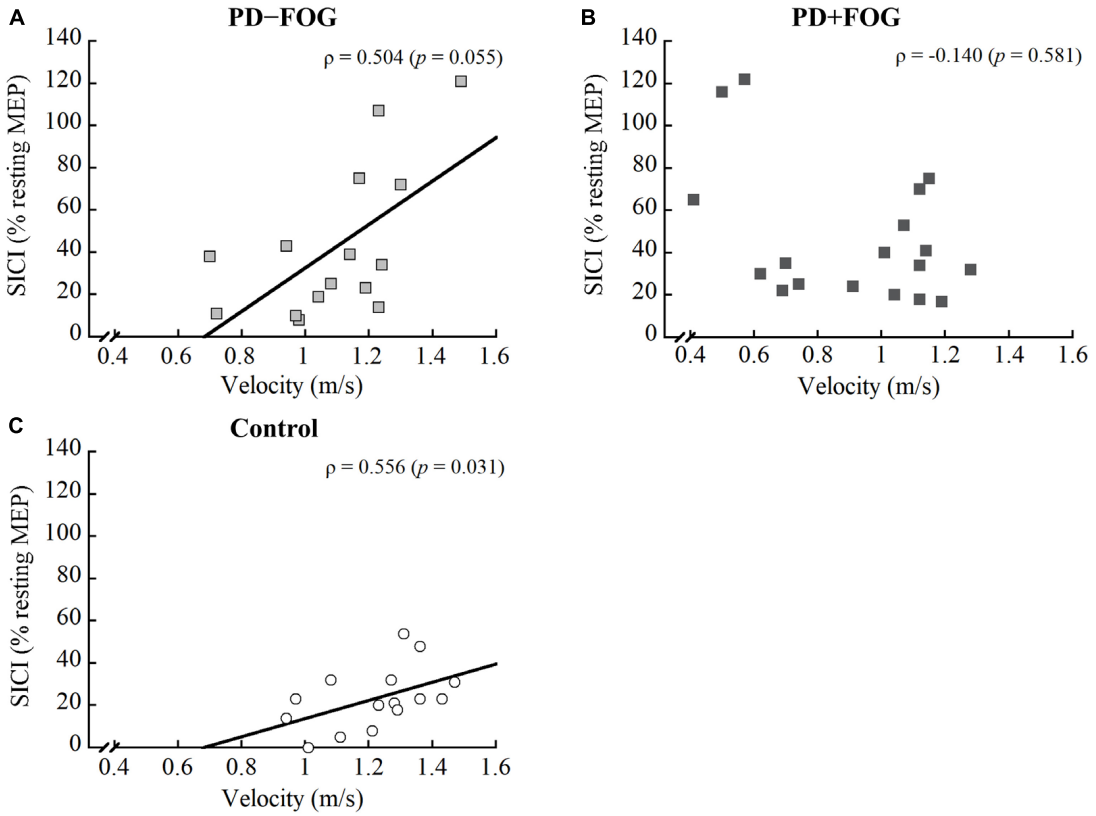

FIGURE 2 | Correlation between SICI and gait velocity of the **(A)** PD − FOG, **(B)** PD + FOG, and **(C)** Control groups. SICI, short intracortical inhibition.

FOG, compared to those without FOG, showed a compensatory increased activation of the mesencephalic locomotor network in order to maintain motor imagery of gait (Snijders et al., 2011). Our TMS findings further supported the idea that the corticomotor system of people with FOG may be hyperexcited in order to compensate for the impaired basal ganglia.

Beyond the findings of RMT and $SICI_{2ms}$, no statistically significant group differences were observed in other TMS variables. This is consistent with the results reported by Vacherot et al. (2010a), who also did not find any statistically significant differences in resting MEP, active MEP, CSP, and $SICI_{3ms}$ between people with PD, regardless of "ON" or "OFF" medication, and control subjects. However, the study found impaired intracortical facilitation in the PD group during "OFF" medication, but the group difference was not evident during "ON" state. Thus, the authors suggested that dopamine substitution therapy could partially restore the function of the intracortical facilitation (Vacherot et al., 2010a,b). Since the subjects in our study were tested during "ON" medication state; it is not known whether any of the TMS variables may become impaired during the "OFF" status.

There is still a lack of comprehensive knowledge regarding how corticomotor excitability correlates with gait performance, particularly in people with PD + FOG (Swanson and Fling, 2018). Hence, the relationships between TMS outcome measures and gait variables were determined in this study. Distinct correlation patterns were observed within the three groups. For the Control group, a negative correlation was found between step length and resting MEP, while gait velocity positively correlated with the combined SICI score. As for the PD − FOG, a positive correlation was observed between step length and CSP, and a borderline correlation between walking velocity and SICI (ρ = 0.504, p = 0.055). The results from the PD − FOG group support those observed in the Control group. Since smaller resting MEP indicated less excited corticospinal tract and longer CSP represented greater inhibitory control of the corticospinal tract (Vucic and Kiernan, 2017), the results suggest that the modulation of appropriate step length in non-disabled adults and non-freezers relies on the inhibitory control of the corticospinal pathway. On the other hand, gait velocity correlated with SICI, indicating that walking velocity may be modulated by the intracortical inhibitory control. Individuals who had less intracortical inhibition also walked faster.

Contrary to the findings from the Control and PD − FOG groups, no significant relationships existed in the PD + FOG group. Although a good explanation for these distinct correlation patterns is lacking, we speculate that it could be related to the function or integrity of the motor circuit, connections between the sensorimotor cortex and the basal ganglia. The motor circuit plays an important role in modifying and executing motor plans during locomotion (Kesar et al., 2018). The motor circuit is presumably intact in non-disabled adults, while it is mildly to

moderately affected in persons with PD − FOG. Thus, greater integrity of the motor circuit should be associated with better walking ability. However, the motor circuit is severely disrupted in people with FOG, and those individuals would rely more on the cognitive process (i.e., the frontostriatal circuit) when they intend to walk (Redgrave et al., 2010). Moreover, people with PD + FOG may use all available neural resources when executing movements. Thus, no correlation was observed in this patient population.

One limitation of this study is that participants were tested only during "ON" medication. The reason for testing the participants during the "ON" state was that persons with PD should take medication regularly. However, even with the usage of medication, many individuals, especially those with FOG, have discernable gait disturbances. Therefore, we wanted to understand whether there were any abnormalities in corticomotor excitability in persons with PD + FOG during the "ON" state. Since several earlier studies found greater changes in corticomotor excitability during "OFF" state, future studies should test the participants during "OFF" medication to understand the neurophysiological changes associated with FOG. Another limitation of the study is that the participants in the PD + FOG and PD − FOG groups were not matched in disease duration and severity. The participants were recruited using convenient sampling; thus, baseline demographic data were not fully controlled. As presented in the results, we reanalyzed the data by removing participants who had longer disease duration and greater disease severity to further scrutinize our findings. Secondary analysis still revealed significant group differences for the RMT and $SICI_{2ms}$, supporting our initial findings. Future studies should consider disease duration- and severity-matched individuals when recruiting participants with FOG. The third limitation of the study was the potential insufficient sample size of the participants. This study recruited 33 participants with PD (18 with FOG and 15 without) according to the sample sizes being used in previous studies (Cantello et al., 2002; Tremblay and Tremblay, 2002; Vacherot et al., 2010b). A *post-hoc* power analysis revealed that the power of the study was 0.73 using $SICI_{2ms}$ or 0.89 using velocity as the primary outcome. Nevertheless, more sample size in the future studies will facilitate the generalization of this study. Lastly, we did not pool the data of all participants with PD when performing the correlation analysis because we were more interested in understanding the association of corticomotor excitability and gait performance in each subgroup population. Investigating the relationships within each subgroup may provide additional insights regarding how the central nervous system modulates walking ability in healthy and pathological brains.

CONCLUSION

Using TMS to explore the changes in corticomotor excitability associated with FOG in people with PD, it was found that freezers had a lower RMT and a reduced $SICI_{2ms}$ when compared with non-disabled adults. Additionally, gait performances appeared to correlate with some TMS outcomes in non-disabled adults and people with PD − FOG, but not in people with PD + FOG. These findings may add a piece of information for unraveling the pathophysiology of FOG.

DATA AVAILABILITY STATEMENT

The datasets generated for this study are available on request to the corresponding author.

ETHICS STATEMENT

The studies involving human participants were reviewed and approved by National Taiwan University Hospital Research Ethics Committee. The patients/participants provided their written informed consent to participate in this study.

AUTHOR CONTRIBUTIONS

Y-YL conceived and designed the study, performed the experiment, conducted the statistical analysis, and drafted the manuscript. M-HL conducted the statistical analysis and helped to draft the manuscript. C-HT helped coordinate the study and reviewed the manuscript. J-JL helped conceive the study and reviewed the manuscript.

FUNDING

This study was funded by the Ministry of Science and Technology of Taiwan (MOST 105-2314-B-002-202 and 106-2314-B-002-044-MY3).

REFERENCES

Amboni, M., Stocchi, F., Abbruzzese, G., Morgante, L., Onofrj, M., Ruggieri, S., et al. (2015). Prevalence and associated features of self-reported freezing of gait in Parkinson disease: the DEEP FOG study. *Parkinsonism Relat. Disord.* 21, 644–649. doi: 10.1016/j.parkreldis.2015.03.028

Cantello, R., Gianelli, M., Bettucci, D., Civardi, C., De Angelis, M. S., and Mutani, R. (1991). Parkinson's disease rigidity: magnetic motor evoked potentials in a small hand muscle. *Neurology* 41, 1449–1456.

Cantello, R., Tarletti, R., and Civardi, C. (2002). Transcranial magnetic stimulation and Parkinson's disease. *Brain Res. Brain Res. Rev.* 38, 309–327.

Fisher, B. E., Piraino, A., Lee, Y. Y., Smith, J. A., Johnson, S., Davenport, T. E., et al. (2016). The effect of velocity of joint mobilization on corticospinal excitability in individuals with a history of ankle sprain. *J. Orthop. Sports Phys. Ther.* 46, 562–570. doi: 10.2519/jospt.2016.6602

Kesar, T. M., Stinear, J. W., and Wolf, S. L. (2018). The use of transcranial magnetic stimulation to evaluate cortical excitability of lower limb musculature: challenges and opportunities. *Restor. Neurol. Neurosci.* 36, 333–348. doi: 10.3233/rnn-170801

Kobayashi, M., and Pascual-Leone, A. (2003). Transcranial magnetic stimulation in neurology. *Lancet Neurol.* 2, 145–156.

Lang, J. T., Kassan, T. O., Devaney, L. L., Colon-Semenza, C., and Joseph, M. F. (2016). Test-retest reliability and minimal detectable change for the 10-meter

walk test in older adults with Parkinson's disease. *J. Geriatr. Phys. Ther.* 39, 165–170. doi: 10.1519/jpt.0000000000000068

Leon-Sarmiento, F. E., Rizzo-Sierra, C. V., Bayona, E. A., Bayona-Prieto, J., Doty, R. L., and Bara-Jimenez, W. (2013). Novel mechanisms underlying inhibitory and facilitatory transcranial magnetic stimulation abnormalities in Parkinson's disease. *Arch. Med. Res.* 44, 221–228. doi: 10.1016/j.arcmed.2013.03.003

Maidan, I., Bernad-Elazari, H., Gazit, E., Giladi, N., Hausdorff, J. M., and Mirelman, A. (2015). Changes in oxygenated hemoglobin link freezing of gait to frontal activation in patients with Parkinson disease: an fNIRS study of transient motor-cognitive failures. *J. Neurol.* 262, 899–908. doi: 10.1007/s00415-015-7650-6

Ni, Z., and Chen, R. (2015). Transcranial magnetic stimulation to understand pathophysiology and as potential treatment for neurodegenerative diseases. *Transl. Neurodegener.* 4:22.

Nieuwboer, A., Rochester, L., Herman, T., Vandenberghe, W., Emil, G. E., Thomaes, T., et al. (2009). Reliability of the new freezing of gait questionnaire: agreement between patients with Parkinson's disease and their carers. *Gait Posture* 30, 459–463. doi: 10.1016/j.gaitpost.2009.07.108

Nutt, J. G., Bloem, B. R., Giladi, N., Hallett, M., Horak, F. B., and Nieuwboer, A. (2011). Freezing of gait: moving forward on a mysterious clinical phenomenon. *Lancet Neurol.* 10, 734–744. doi: 10.1016/s1474-4422(11)70143-0

Perez-Lloret, S., Negre-Pages, L., Damier, P., Delval, A., Derkinderen, P., Destee, A., et al. (2014). Prevalence, determinants, and effect on quality of life of freezing of gait in Parkinson disease. *JAMA Neurol.* 71, 884–890.

Redgrave, P., Rodriguez, M., Smith, Y., Rodriguez-Oroz, M. C., Lehericy, S., Bergman, H., et al. (2010). Goal-directed and habitual control in the basal ganglia: implications for Parkinson's disease. *Nat. Rev. Neurosci.* 11, 760–772. doi: 10.1038/nrn2915

Ridding, M. C., Inzelberg, R., and Rothwell, J. C. (1995). Changes in excitability of motor cortical circuitry in patients with Parkinson's disease. *Ann. Neurol.* 37, 181–188. doi: 10.1002/ana.410370208

Rossini, P. M., Barker, A. T., Berardelli, A., Caramia, M. D., Caruso, G., Cracco, R. Q., et al. (1994). Non-invasive electrical and magnetic stimulation of the brain, spinal cord and roots: basic principles and procedures for routine clinical application. Report of an IFCN committee. *Electroencephalogr. Clin. Neurophysiol.* 91, 79–92. doi: 10.1016/0013-4694(94)90029-9

Sack, A. T., and Linden, D. E. (2003). Combining transcranial magnetic stimulation and functional imaging in cognitive brain research: possibilities and limitations. *Brain Res. Brain Res. Rev.* 43, 41–56. doi: 10.1016/s0165-0173(03)00191-7

Shine, J. M., Matar, E., Ward, P. B., Frank, M. J., Moustafa, A. A., Pearson, M., et al. (2013). Freezing of gait in Parkinson's disease is associated with functional decoupling between the cognitive control network and the basal ganglia. *Brain* 136(Pt 12), 3671–3681. doi: 10.1093/brain/awt272

Snijders, A. H., Leunissen, I., Bakker, M., Overeem, S., Helmich, R. C., Bloem, B. R., et al. (2011). Gait-related cerebral alterations in patients with Parkinson's disease with freezing of gait. *Brain* 134(Pt 1), 59–72. doi: 10.1093/brain/awq324

Swanson, C. W., and Fling, B. W. (2018). Associations between gait coordination, variability and motor cortex inhibition in young and older adults. *Exp. Gerontol.* 113, 163–172. doi: 10.1016/j.exger.2018.10.002

Tomczak, M., and Tomczak, E. (2014). The need to report effect size estimates revisited. An overview of some recommended measures of effect size. *Trends Sport Sci.* 1, 19–25.

Tremblay, F., and Tremblay, L. E. (2002). Cortico-motor excitability of the lower limb motor representation: a comparative study in Parkinson's disease and healthy controls. *Clin. Neurophysiol.* 113, 2006–2012. doi: 10.1016/s1388-2457(02)00301-2

Vacherot, F., Attarian, S., Eusebio, A., and Azulay, J. P. (2010a). Excitability of the lower-limb area of the motor cortex in Parkinson's disease. *Neurophysiol. Clin.* 40, 201–208. doi: 10.1016/j.neucli.2010.04.002

Vacherot, F., Attarian, S., Vaugoyeau, M., and Azulay, J. P. (2010b). A motor cortex excitability and gait analysis on Parkinsonian patients. *Mov. Disord.* 25, 2747–2755. doi: 10.1002/mds.23378

Valls-Sole, J., Pascual-Leone, A., Brasil-Neto, J. P., Cammarota, A., McShane, L., and Hallett, M. (1994). Abnormal facilitation of the response to transcranial magnetic stimulation in patients with Parkinson's disease. *Neurology* 44, 735–741.

Vercruysse, S., Gilat, M., Shine, J. M., Heremans, E., Lewis, S., and Nieuwboer, A. (2014). Freezing beyond gait in Parkinson's disease: a review of current neurobehavioral evidence. *Neurosci. Biobehav. Rev.* 43, 213–227. doi: 10.1016/j.neubiorev.2014.04.010

Vucic, S., and Kiernan, M. C. (2017). Transcranial magnetic stimulation for the assessment of neurodegenerative disease. *Neurotherapeutics* 14, 91–106. doi: 10.1007/s13311-016-0487-6

Conflict of Interest: The authors declare that the research was conducted in the absence of any commercial or financial relationships that could be construed as a potential conflict of interest.

Copyright © 2020 Lee, Li, Tai and Luh. This is an open-access article distributed under the terms of the Creative Commons Attribution License (CC BY). The use, distribution or reproduction in other forums is permitted, provided the original author(s) and the copyright owner(s) are credited and that the original publication in this journal is cited, in accordance with accepted academic practice. No use, distribution or reproduction is permitted which does not comply with these terms.

frontiers in Neural Circuits

ORIGINAL RESEARCH
published: 17 June 2020
doi: 10.3389/fncir.2020.00035

Electroacupuncture-Related Metabolic Brain Connectivity in Neuropathic Pain due to Brachial Plexus Avulsion Injury in Rats

*Ao-Lin Hou[1†], Mou-Xiong Zheng[2†], Xu-Yun Hua[2†], Bei-Bei Huo[3], Jun Shen[3,4] and Jian-Guang Xu[3]**

[1]Shanghai Eighth People Hospital, Shanghai, China, [2]Department of Traumatology and Orthopedics, Yueyang Hospital, Shanghai University of Traditional Chinese Medicine, Shanghai, China, [3]School of Rehabilitation Science, Shanghai University of Traditional Chinese Medicine, Shanghai, China, [4]Department of Orthopedics, Guanghua Hospital of Integrative Chinese and Western Medicine, Shanghai, China

Objective: The present study aimed to investigate the analgesic effect of electroacupuncture (EA) in neuropathic pain due to brachial plexus avulsion injury (BPAI) and related changes in the metabolic brain connectivity.

Methods: Neuropathic pain model due to BPAI was established in adult female Sprague–Dawley rats. EA stimulations (2/15 Hz, 30 min/day, 5-day intervention followed by 2-day rest in each session) were applied to the fifth–seventh cervical "Jiaji" acupoints on the noninjured side from 1st to 12th weeks following BPAI (EA group, $n = 8$). Three control groups included sham EA (nonelectrical acupuncture applied to 3 mm lateral to the real "Jiaji" acupoints), BPAI-only, and normal rats (no particular intervention; eight rats in each group). Thermal withdrawal latency (TWL) of the noninjured forepaw was regularly tested to evaluate the threshold of thermalgesia. Small animal [fluorine-18]-fluoro-2-deoxy-$_D$-glucose (^{18}F-FDG) PET/CT scans of brain were conducted at the end of 4th, 12th, and 16th weeks to explore metabolic alterations of brain.

Results: In the EA group, the TWL of the noninjured forepaw significantly decreased following BPAI and then increased following EA stimulation, compared with sham EA ($P < 0.001$). The metabolic brain connectivity among somatosensory cortex (SC), motor cortex (MC), caudate putamen (Cpu), and dorsolateral thalamus (DLT) in bilateral hemispheres decreased throughout the 16 weeks' observation in the BPAI-only group, compared with the normal rats ($P < 0.05$). In the EA group, the strength of connectivity among the above regions were found to be increased at the end of 4th week following BPAI modeling, decreased at 12th week, and then increased again at 16th week ($P < 0.05$). The changes in metabolic connectivity were uncharacteristic and dispersed in the sham EA group.

Conclusion: The study revealed long-term and extensive changes of metabolic brain connectivity in EA-treated BPAI-induced neuropathic pain rats. Bilateral sensorimotor

OPEN ACCESS

Edited by:
Ti-Fei Yuan,
Shanghai Jiao Tong University, China

Reviewed by:
Sangma Xie,
Hangzhou Dianzi University, China
Lijuan Ao,
Kunming Medical University, China

****Correspondence:***
Jian-Guang Xu
xjg@shutcm.edu.cn

†These authors have contributed equally to this work

Received: *19 March 2020*
Accepted: *12 May 2020*
Published: *17 June 2020*

Citation:
Hou A-L, Zheng M-X, Hua X-Y, Huo B-B, Shen J and Xu J-G (2020) Electroacupuncture-Related Metabolic Brain Connectivity in Neuropathic Pain due to Brachial Plexus Avulsion Injury in Rats. Front. Neural Circuits 14:35. doi: 10.3389/fncir.2020.00035

and pain-related brain regions were mainly involved in this process. It indicated that modulation of brain metabolic connectivity might be an important mechanism of analgesic effect in EA stimulation for the treatment of neuropathic pain.

Keywords: neuropathic pain, brachial plexus avulsion injury, electroacupuncture, thermal withdrawal latency, metabolic connectivity

INTRODUCTION

Brachial plexus avulsion injury (BPAI), which is often caused by motorcycle accident, is one of the most devastating peripheral nerve injuries. Partial or global BPAI would lead to sensory and motor dysfunction. Neuropathic pain is another intractable problem caused by BPAI. It is reported that 70–90% BPAI patients suffer from persistent neuropathic pain (Teixeira et al., 2015). This kind of pain is usually described as hot-burning, tingling, pricking, pins-and-needles, sharp, shooting, squeezing, cold, electric, or shock-like quality of pain (Widerström-Noga, 2017). Functional and structural changes in the nervous system involve the peripheral nerve fibers, spine, brain, and several pain pathways (Teixeira et al., 2015). These factors would contribute to both development and maintenance of neuropathic pain (Gierthmühlen and Baron, 2016; Zilliox, 2017). Neuropathic pain following BPAI was reported to be largely refractory to the conventional treatment, and evidenced-based treatments for it are scarce (Parry, 1980; Teixeira et al., 2015). Investigation on the mechanisms underlying neuropathic pain due to BPAI would be necessary for seeking the solve for neuropathic pain.

Several other guidelines have focused on the clinical practice of pharmacological medicine (Attal et al., 2010). Nonpharmacological therapy, such as direct current stimulation with (or without) visual illusion, transcutaneous electrical stimulation, dorsal root entry zone lesioning, and acupuncture are recommended for neuropathic pain after spinal cord injury (Davis and Lentini, 1975; Spaić et al., 2002; Soler et al., 2010; Cohen and Mao, 2014; Ngernyam et al., 2015). However, chronic neuropathic pain is still a challenging problem (Zilliox, 2017). Acupuncture is a popular practice of traditional Chinese medicine. It modulates the flow of Qi and blood through the meridians of the body and restores the balance among five main organs (heart, liver, spleen, kidney, and lung) to maintain homeostasis (Rong et al., 2011). Acupuncture or electroacupuncture (EA) has been used as alternative therapy in the treatment of several diseases (Li et al., 2014; Lu et al., 2014). Chronic pain is one of its major indications, including inflammatory pain, cancer-related pain, visceral pain, and neuropathic pain (Ju et al., 2017; Zhang et al., 2014). However, the underlying mechanism is largely unknown.

As the development of neuroimaging technology, [fluorine-18]-fluoro-2-deoxy-$_D$-glucose (^{18}F-FDG) PET has been used as a method for measuring the cerebral metabolic rate of glucose from 1980 (Phelps et al., 1980). It directly measures the glucose metabolism as a marker of neural activity and reflects the whole brain activity, which is in the steady state. Compared with blood-oxygen-level-dependent imaging (BOLD) functional magnetic resonance imaging (fMRI), ^{18}F-FDG-PET is less dependent on neurovascular coupling (Yakushev et al., 2017). Metabolic connectivity reflects metabolism relationships between different brain regions, which could provide a novel insight of brain connectivity (Yakushev et al., 2017). It has been used in many diseases such as Alzheimer's disease (AD; Morbelli et al., 2012; Herholz et al., 2018), dementia (Caminiti et al., 2016), and amyotrophic lateral sclerosis (Pagani et al., 2016).

In the present study, the BPAI-induced neuropathic pain was established in rats. Sham EA, BPAI-only (model), and normal groups were set up for control. The changes in thermalgesia threshold were evaluated. Meanwhile, ^{18}F-FDG traced positron emission tomography/computed tomography (PET/CT) was acquired to assess the change in brain metabolism. Metabolic connectivity was further calculated to explore the underlying mechanisms of neural activity in BPAI rats.

MATERIALS AND METHODS

Animals

A total of 32 female Sprague–Dawley rats weighing 180–200 g were included. All the rats were provided by Shanghai Slack Laboratory Animal Limited Liability Company (Shanghai, China). They were raised under the conditions with 12-h light/dark cycle and unrestricted food or water supply. The rats were kept in cages for at least 7 days before any further intervention or assessment started. The rats were randomly assigned to four groups: the normal, model, sham EA, and EA groups (eight rats in each group).

All procedures were in agreement with the Guide for the Care and Use of Laboratory Animals described by the US National Institutes of Health and were approved by the Animal Ethical Committee of Shanghai University of Traditional Chinese Medicine. The flow diagram is shown in **Figure 1**.

Surgical Procedure

The global BPAI (C5-T1 cervical nerve roots) procedure was performed on the right side in the rats of model, sham EA, and EA groups according to the method described in our previous study (Shen et al., 2019a). During the procedure, the rat was anesthetized *via* intraperitoneal injection with sodium pentobarbital (40 mg/kg) and then placed in a prone position on a clean operation table. An incision of 4 cm was made through the dorsal midline from the occiput to the scapular angulus superior. Under an operation microscope (magnification, 10×), longissimus capitis muscle, semispinal muscle of the neck, biventer cervicis, and complex muscle were divided. The muscles on vertebral plate and

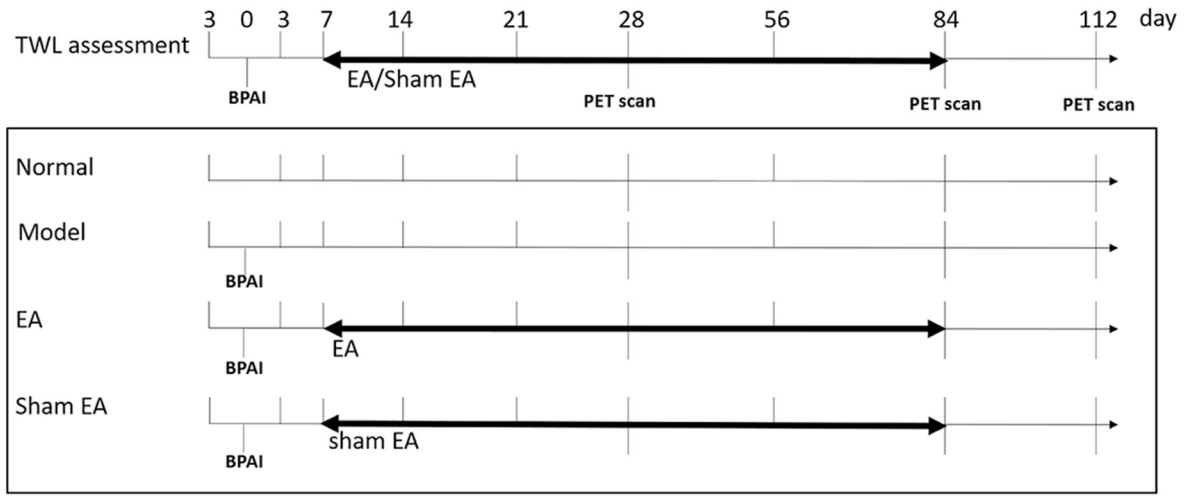

FIGURE 1 | Flow chart of whole experiment. Right side brachial plexus avulsion injury (BPAI) was made on day 0. TWL assessment was conducted on 3rd day before BPAI and 3th, 7th, 14th, 21th, 28th, 56th, 84th, and 112th day following BPAI, respectively. (^{18}F-FDG) PET/CT scan was performed on 28th, 84th, and 112th day following BPAI, respectively. EA/sham EA intervention was performed from 7th to 84th day, which lasted for 11 weeks. BPAI, brachial plexus avulsion; TWL, thermal withdrawal latency; EA, electroacupuncture.

the spinous process were removed, and hemilaminectomies from C4 to T1 were performed to expose the nerve roots on the right side. The roots of C5, C6, C7, C8, and T1 nerves were identified under direct vision. Both dorsal and ventral rootlets were grasped with forceps and completely extracted from the spinal cord by traction. The rootlets and dorsal ganglions were visually confirmed to ensure a preganglionic injury. Glutin sponge was applied for hemostasis, and the incision was covered with penicillin powder to prevent infection.

EA/Sham EA Interventions

The EA and sham EA interventions were conducted at the same time of the day since first week following BPAI. The rats were placed in a self-made immobilization apparatus, with the right hindlimb and low back exposed and the rest of the body fixed. Room temperature was controlled to 25.0 ± 1.0°C, with noise and light controlled. The rats acclimated for at least 3 days before the interventions started.

In the EA stimulation, three disposable sterile stainless-steel needles (0.3 mm in diameter and 13 mm in length; Huatuo, Suzhou Medical Appliance Factory, Suzhou, China) were inserted into the left C5–C7 "Jiaji" acupoints (EX-B2, 5 mm lateral to the left C5–C7 spinous, 3–5 mm in depth). Then, the needles' tails were connected to the output terminal of an electrical stimulator (Huatuo SDZ-II nerve and muscle stimulator, Suzhou Medical Appliance Factory, Suzhou, China). The frequency of disperse-dense wave of EA was 2/15 Hz, and the intensity was modulated to induce slight contraction of target muscles. The intervention was performed for 30 min per day, five times per week for 11 weeks.

In the sham EA group, three needles were inserted into sham acupoints (8 mm lateral to the left C5–C7 spinous, 3–5 mm in depth) without electrical output.

Behavioral Assessments

Thermal withdrawal latency (TWL) of the noninjured (left) forepaw was tested 3 days pre-BPAI, 3rd day, and at the end of the 1st, 2nd, 3rd, 4th, 8th, 12th, and 16th weeks after BPAI (Rodrigues-Filho et al., 2003; Challa, 2015). Before the first evaluation, the rats were trained 5 days per week for 2 weeks.

The TWL tests were performed with the Plantar Test Apparatus (Hargreaves Method) for Mice and Rats (IITC Life Science Inc., Woodland Hills, CA, United States). The rats were placed on a glass platform for 15 min before the test to ensure acclimation. Then, a high-intensity moveable radiant heat source was placed underneath. The lateral palmar surface of the noninjured (left) forepaw was exposed to the radiant heat source. The time when the rat withdraws or moves the forepaw after placement of the heat source was recorded, with shorter latencies indicating lower thermalgesia thresholds. The heat source automatically cut off at 20 s to avoid tissue damage. Five consecutive tests were conducted in each rat, with intervals of 5 min in between. The average value was recorded as the final result.

^{18}F-FDG PET/CT Scanning

^{18}F-FDG PET scanning were acquired at the end of the 4th, 12th, and 16th weeks following BPAI, respectively. Images were acquired from a small animal PET/CT scanner (Concorde Microsystems, Knoxville, TN, USA).

Before PET/CT scanning, the rats stayed with water supply only for 12 h to enhance ^{18}F-FDG uptake. ^{18}F-FDG (0.5 m Ci) was injected through the tail vein, and then, the rat stayed in a quiet room for 30 min to ensure adequate take-up of tracer. Rats were induced with 5% halothane and maintained with 1.5%. The scan processes were conducted as previous study described (Shen et al., 2019a). During scanning, the rat was placed in prone position on the bed of PET/CT, which consisted of a 15-cm-diameter ring of 96-position sensitive ray scintillation detectors and provided a 10.8-cm transaxial and a 7.8-cm axial field of view (FOV) with an intrinsic resolution of 1.8 mm. The timing resolution was <1.5 ns. The CT images were obtained for coregistration and attenuation correction. The collected images were recombined in the OSEM3D mode with a 128 × 128 matrix. Parameters of CT image acquisition were set as follows: spherical tube voltage = 80 kV, current = 500 μA, and acquisition time = 492 s.

Image Preprocessing

Data preprocessing was conducted using the Statistical Parametric Mapping 8 toolbox (SPM 8)[1] based on Matlab 2014a (Mathworks, Inc., Natick, MA, USA). The raw PET images in DICOM format were converted into NIFTI format using ImageJ software (Image Processing and Analysis in Java, National Institutes of Health, Bethesda, MD, USA). The skull-stripped brain PET images of each rat were extracted by using a hand drawing mask. All the three directions (i.e., *x*, *y*, and *z*) of the voxels were upscaled by 10 to fit the algorithm implemented in SPM8. Based on a standard rat brain template (Schwarz et al., 2006), the orientation of individual PET images was adjusted by modifying pitch/roll/yaw parameters, and the origin was reset. As only one brain volume of standard uptake value (SUV) was obtained during one image acquisition period, the realignment procedure for correction of head motion among different volumes was inapplicable, thus not conducted. All individual brain PET images were then spatially normalized to the template and resampled to 2 × 2 × 2 mm^3 resolution. The images were smoothed with a Gaussian kernel of a full-width at half-maximum (FWHM) twice of the voxel size (i.e., FWHM = 4 mm), to enhance the signal/noise ratio. The FDG uptake value of each voxel was normalized by the global mean uptake value to correct for variability across subjects.

Metabolic Connectivity Construction

In the current study, a matrix of intersubject metabolic brain connectivity was constructed for each group of rats. The process is shown in **Figure 2**. In the matrix, a set of nodes represented selected brain regions, while their edges denoted functional relationship between nodes. Our previous report has revealed significantly altered glucose metabolism in bilateral motor cortex (MC), sensory cortex (SC), caudate putamen (Cpu), and dorsolateral thalamus (DLT) following BPAI (Shen et al., 2019a,b). Therefore, these above eight brain regions were defined as nodes, and they were drawn out by registering the stereotaxic rat brain atlas (Schwarz et al., 2006) with the normalized brain PET images of each rat. The mean SUV of each selected brain region from each rat was extracted and compiled into separate vectors. The cross-subject Pearson's correlation coefficients between paired brain regions were calculated. Then, an adjacency 8 × 8 correlation matrix for each group was constructed with brain regions labeled on the *x*- and *y*-axes and *P*-values of correlation coefficients as the elements in rows and columns.

Statistical Analysis

The SPSS 22.0 statistical software (SPSS Inc., New York, NY, USA) was used to analyze the behavioral data. The data were shown as mean ± standard deviation. Least significance difference (LSD) test was used to analyze the differences among the four groups at each time point. $P < 0.05$ were considered statistically significant.

After metabolic connectivity construction, a two-sample *t*-test was performed in the intragroup comparison of metabolic brain images (i.e., EA vs. sham EA, model vs. normal, sham EA vs. model, EA vs. model) with a significance level of $P = 0.05$ [false discovery rate (FDR) correction]. The analysis was performed using the Statistical Parametric Mapping 8 toolbox (SPM 8)[1] based on Matlab 2014a (Mathworks, Inc., Natick, MA, USA).

RESULTS

Animals

All rats were in good condition and active after BPAI modeling. They showed slight weakness within the first three postinjury days and then largely recovered to baseline level. No obviously abnormal foraging activity or instability was observed, and no infection was noted. Most rats in model, sham EA, and EA groups showed autotomy in the right (injured) forepaws, such as biting off the nails and digits. Horner's sign (i.e., ptosis, concave eyeballs, and constriction of pupils) was presented on the right (injured) side in all rats.

Behavioral Assessment

Before BPAI, there was no significant difference in TWL assessments of the noninjured (left) forepaw among the four groups ($P > 0.05$). On the third day, and first and second weeks after BPAI, TWL of the model, sham EA, and EA groups significantly decreased compared with the normal group ($P < 0.05$). However, there was no significant difference between the sham EA and EA groups ($P > 0.05$). Since the third week after BPAI, the average TWL of the model group was still lower than that in the normal group ($P < 0.001$), and the TWL in the EA group started to be significantly higher than that in the sham EA group ($P < 0.001$). The changing curve is shown in **Figure 3**.

Metabolic Brain Connectivity

On the fourth week following BPAI (i.e., 3 weeks of EA/sham EA intervention), significantly decreased metabolic connectivity

[1]http://www.fil.ion.ucl.ac.uk/spm/

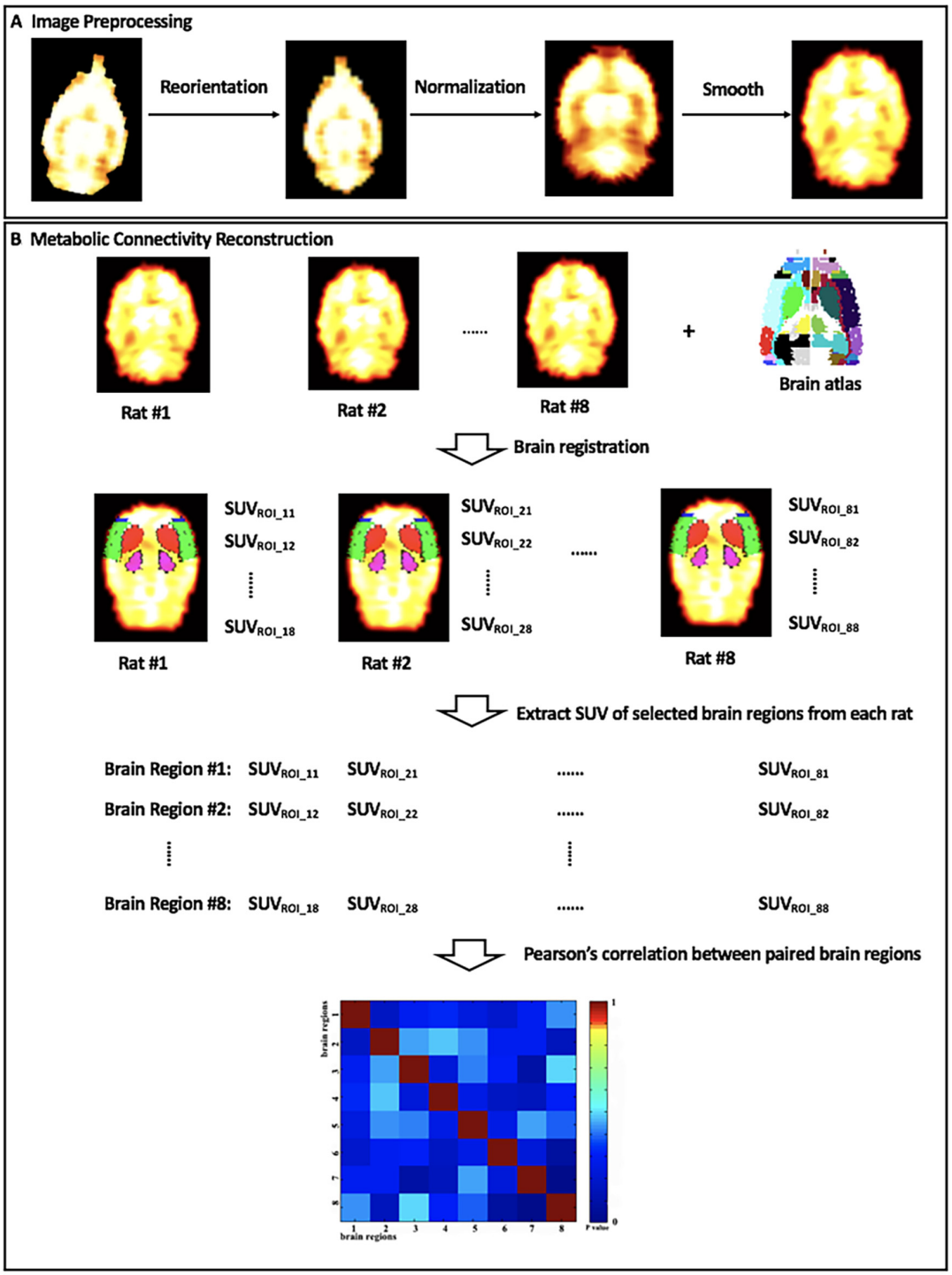

FIGURE 2 | The diagram of **(A)** image preprocessing and **(B)** metabolic connectivity construction. $SUV_{ROI_{ij}}$, the standard uptake value (SUV) of brain region #*j* in rat #*i*.

was observed in bilateral motor, sensory, and pain-related brain regions (**Figures 4D,H**). Increased metabolic connectivity between regions related to motor and sensory regions in the right hemisphere, as well as decreased metabolic connectivity in the left hemisphere were observed in the sham EA group, compared with the model group (**Figures 4C,G**). However, significantly increased metabolic connectivity in bilateral hemispheres was observed in the EA group

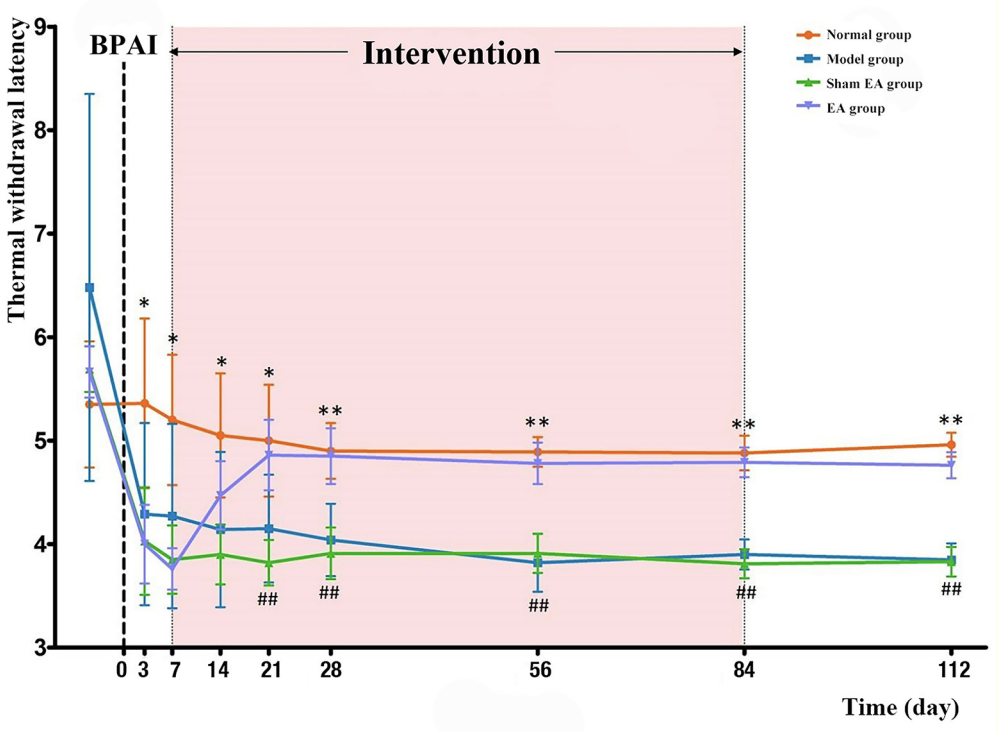

FIGURE 3 | Comparison of TWL of the rats' left (noninjured) forepaw in the normal, model, sham EA, and EA groups. BPAI was made on day 0. * and ** Indicate significant differences between the model and normal groups at the same timepoint (model–normal; $^{*}P < 0.05$; $^{**}P < 0.001$). $^{\#\#}$Indicates significant differences between the EA and sham EA groups at the same timepoint (EA–sham EA; $P < 0.001$). BPAI, brachial plexus avulsion injury; EA, electroacupuncture.

compared with the sham EA (**Figures 4A,E**) and model group (**Figures 4B,F**).

At the end of the 12th week after BPAI (i.e., 11 weeks of EA/sham EA intervention), metabolic connectivity in bilateral hemispheres still decreased in the model group (**Figures 5D,H**). However, metabolic connectivity increased in the left hemisphere (contralateral to the injured limb) in the sham EA group (**Figures 5C,G**). Decreased metabolic connectivity in bilateral hemispheres was observed in the EA group compared with the sham EA group (**Figures 5A,E**) or with the model group (**Figures 5B,F**).

At the end of the 16th week after BPAI (i.e., 4 weeks after EA/sham EA intervention), increased metabolic connectivity was observed in bilateral hemispheres in the EA group compared with the sham EA group (**Figures 6A,E**) or the model group (**Figures 6B,F**). In the model (**Figures 6D,H**) and sham EA groups (**Figures 6C,G**), the changes were similar with those of previous timepoints (12 weeks).

DISCUSSION

Neuropathic pain is a persistent chronic pain that is associated with abnormal functioning caused by a lesion or disease affecting the somatosensory system (Treede et al., 2008). Many diseases could cause persistent chronic pain, such as diabetic peripheral neuropathy, nondiabetic neuropathy, postherpetic neuralgia, trigeminal neuralgia, and spinal cord injury (Bril et al., 2011; Finnerup et al., 2014; Mulla et al., 2015). BPAI is a specific type of brachial plexus injury that causes preganglionic disruption of nerve roots from the spinal cord (Murphey et al., 1947). High prevalence of neuropathic pain is also acknowledged in BPAI (Santana et al., 2016).

Although accumulating studies have focused on neuropathic pain (Zilliox, 2017), the treatment of neuropathic pain induced by BPAI is still challenging. For example, the American Academy of Neurology (ANN) has published practice guidelines including pharmacological and nonpharmacological treatment of painful diabetic neuropathy, postherpetic neuralgia, and trigeminal neuralgia (Gronseth et al., 2008; Bril et al., 2011). However, for neuropathic pain due to BPAI, reported guideline is still limited. Paszcuk et al. (2011) reported potential effect of cannabinoid and cannabinoid agonists in treating neuropathic pain following BPAI in mice (Paszcuk et al., 2011). However, the adverse effects associated with the use of "medical cannabis" and the safety of inhaling pyrolysis products in cannabis smoking process still need further investigation and improvement (Donvito et al., 2018). Previous study also demonstrated that motor cortex stimulation and deep brain stimulation may be effective for treating neuropathic pain following peripheral nerve injury (Levy et al., 2010). However, complications

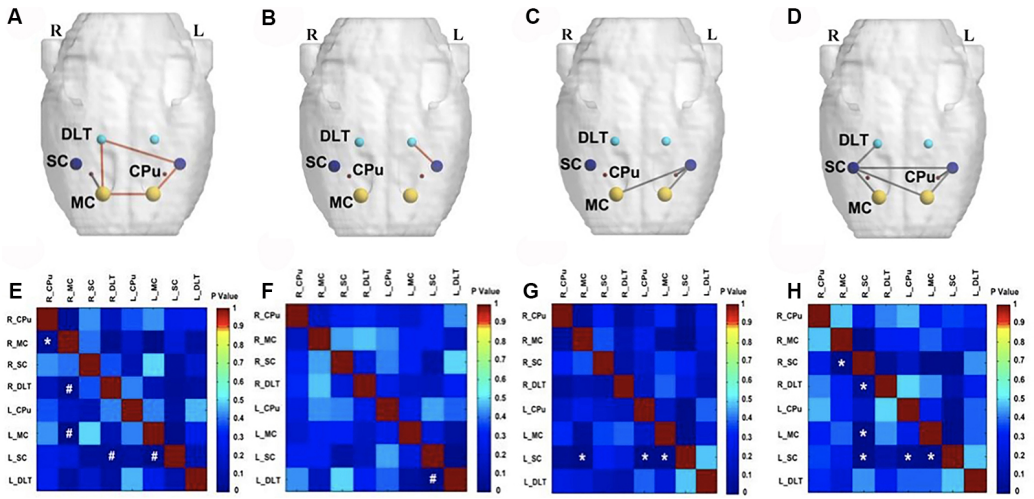

FIGURE 4 | Comparison of metabolic connectivity among four groups at fourth week (i.e., 3 weeks of EA/sham EA intervention) after BPAI. **(A,E)** Significantly increased metabolic connectivity was observed among the right DLT, right motor cortex, left motor cortex, and left somatosensory cortex in the EA group, compared with the sham EA group. **(B,F)** Significantly increased metabolic connectivity was observed among the dorsolateral thalamus and left somatosensory cortex in the EA group, compared with the model. **(C,G)** Significantly increased metabolic connectivity among the left caudate putamen and left somatosensory cortex, as well as decreased metabolic connectivity between the right motor cortex and left somatosensory cortex, left motor cortex, and left somatosensory cortex was observed in the sham EA group, compared with the model group. **(D,H)** Changes in metabolic connectivity in the whole brain after BPAI (*$P < 0.05$; $^{\#}P < 0.001$). Red line, increased metabolic connectivity; gray line, decreased metabolic connectivity. BPAI, brachial plexus avulsion injury; EA, electroacupuncture; SC, somatosensory cortex; DLT, dorsolateral thalamus; MC, motor cortex; CPu, caudate putamen.

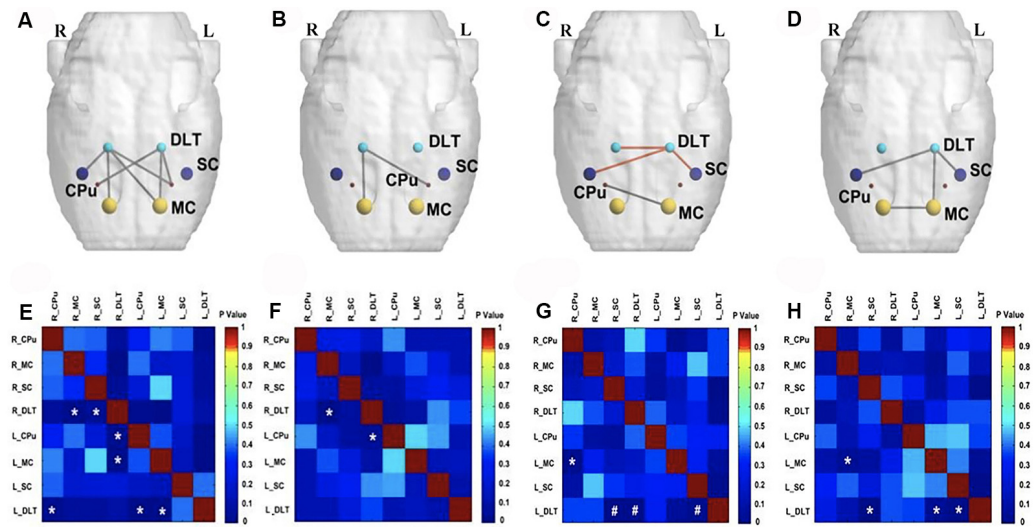

FIGURE 5 | Comparison of metabolic connectivity among four groups at 12th week (i.e., 11 weeks of EA/sham EA intervention) after BPAI. **(A,E)** Significantly increased metabolic connectivity was observed among the bilateral DLT, bilateral motor cortex, bilateral caudate putamen, and right somatosensory cortices in the EA group compared with the sham EA group. **(B,F)** Significantly decreased metabolic connectivity was observed among the right DLT, right motor cortex, and left caudate putamen in the EA group compared with the model group. **(C,G)** Significantly increased metabolic connectivity between the left DLT and bilateral somatosensory cortices, as well as decreased metabolic connectivity between left motor cortex and right somatosensory cortex were observed in the sham EA group compared with the model group. **(D,H)** Changes of metabolic connectivity in the whole brain after BPAI (*$P < 0.05$; $^{\#}P < 0.001$). Red line, increased metabolic connectivity; gray line, decreased metabolic connectivity. BPAI, brachial plexus avulsion injury; EA, electroacupuncture; SC. somatosensory cortex; DLT, dorsolateral thalamus; MC, motor cortex; CPu, caudate putamen.

of the surgery, such as intracranial bleeding, infection, and permanent neurological deficits, need to be considered (Nguyen et al., 1999).

EA, originated from traditional acupuncture, is combined use of needles and electrical stimulation (Ju et al., 2017). Cope (2016) reported that repeated EA contributes to significant

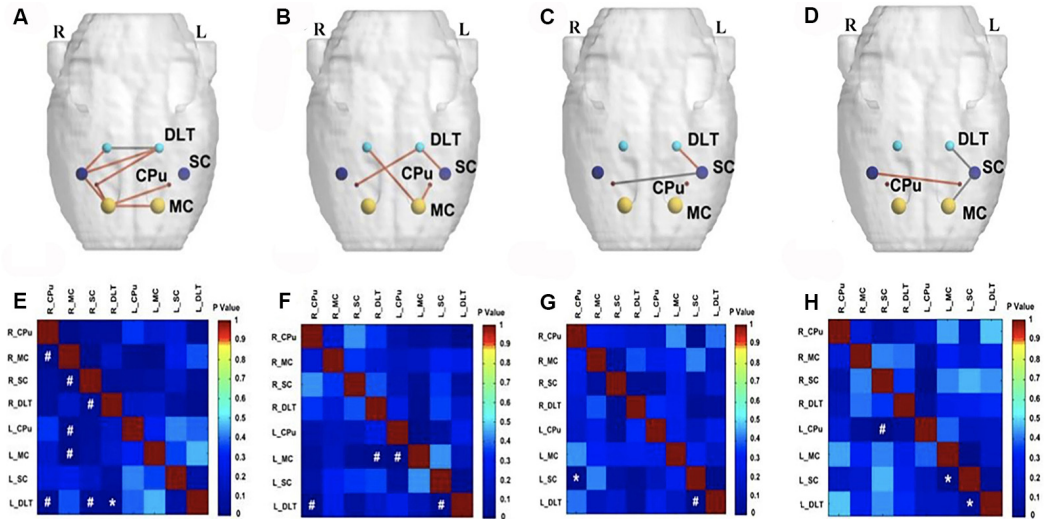

FIGURE 6 | Comparison of metabolic connectivity among four groups at 16th week (i.e., 4 weeks after EA/sham EA intervention) after BPAI. **(A,E)** Significantly increased metabolic connectivity among the bilateral motor cortex, bilateral caudate putamen, bilateral DLT, and right somatosensory cortex, as well as significantly decreased metabolic connectivity between bilateral DLT were observed in the EA group compared with the sham EA group. **(B,F)** Significantly increased metabolic connectivity was observed among the bilateral DLT, left motor cortex, left somatosensory cortex, and right caudate putamen in the EA group compared with the model. **(C,G)** Significantly increased metabolic connectivity between the left DLT and left somatosensory cortex, as well as decreased metabolic connectivity between left somatosensory cortex and right caudate putamen were observed in the sham EA group compared with the model group. **(D,H)** Changes of metabolic connectivity in the whole brain after BPAI ($^{*}P < 0.05$; $^{\#}P < 0.001$). Red line, increased metabolic connectivity; gray line, decreased metabolic connectivity. BPAI, brachial plexus avulsion injury; EA, electroacupuncture; SC, somatosensory cortex; DLT, dorsolateral thalamus; MC, motor cortex; CPu, caudate putamen.

analgesic effects in treating brachial plexus neuralgia induced by administration of cobra venom (Cope, 2016). Zhang et al. (2014) reported that EA intervention can relieve neuropathic pain in BPAI patients.

Therefore, we established the neuropathic pain model by BPAI. Thermalgesia threshold of the noninjured forepaw was significantly decreased after BAPI, which is consistent with our previous studies. We found that thermalgesia threshold of the noninjured forepaw was elevated after application of 2/15 Hz EA stimulation in the "Jiaji" acupoints (EX-C5–C7). These demonstrated that EA could potentially release neuropathic pain following BPAI, and the treatment may persist after the cease of intervention.

The mechanism of neuropathic pain in BPAI is complicated. In BPAI, both peripheral nerve fibers and spinal cord were injured (Teixeira et al., 2015). Thus, several neural pathways are involved in the occurrence and development of neuropathic pain following BPAI. Peripheral nerve injury leads to sensitization of primary afferents inputs *via* the changes in the expression of neurotransmitters, neuromodulators, growth factors, and neuroactive molecules located in the dorsal root ganglion (Jaggi and Singh, 2011). Aside from that, BPAI also leads to hyperactivity of neuron in the posterior horn of the spinal cord (Denny-Brown et al., 1973; Powers et al., 1984), resulting in sensitization in the spinal cord (Jaggi and Singh, 2011). With the development of brain imaging and electrophysiological technology, a number of studies have reported that the brain has a network of cortical and subcortical areas that constitutes the "pain matrix" (Moisset and Bouhassira, 2007; Iannetti and Mouraux, 2010) that are associated with the sensory-discriminative (Hsieh et al., 1996; Apkariana et al., 2005; Moisset and Bouhassira, 2007), affective-emotional (Hsieh et al., 1996; Moisset and Bouhassira, 2007), and cognitive aspects (Apkariana et al., 2005; Moisset and Bouhassira, 2007) of pain. The "pain matrix" may provide insight of cerebral mechanism of neuropathic pain following BPAI.

There also have been some researches in the mechanism of acupuncture/EA in treating neuropathic pain. Li et al. (2019) found that 6 weeks of EA intervention could activate μ-opioid receptors, inhibit spinal dorsal horn neuron, and thus release pain. Low frequency of EA inhibits neuropathic pain more effectively than high frequency. It is reported that 2 Hz of EA induced a robust and longer-lasting decreased mechanical allodynia threshold than 100 Hz in caudal trunk nerve injury-induced neuropathic pain (Kim et al., 2004). In an L5/L6 nerve ligation-induced neuropathic pain model, 2 Hz also decreased mechanical and thermal hypersensitivity more powerfully than 100 Hz (Sun et al., 2002). Aside from that, spinal serotonin and norepinephrine participate in EA inhibition of neuropathic pain. EA can activate 5-HT1ARs to inhibit *N*-methyl-D-aspartate receptor (NMDAR) activities (Zhang et al., 2014). Park et al. (2010) also found that EA could reduce the release of excitatory amino acids and promote the release of inhibitory amino acid neurotransmitters in spinal cord (Park et al., 2010). Jiang et al. (2016) found that EA could inhibit secretion of prostaglandin E2 in the spinal cord and reduce pain by

inserting bilateral L5 "Jiaji" (EX-B2), "Dachangshu" (BL25), "Weizhong" (BL40), and "Kunlun" (BL60) acupoints in rats. Other mechanisms include inhibiting of glial cells and inducing of numerous bioactive chemicals in the spinal cord (Zhang et al., 2014). Zhang et al. reported that EA stimulation could attenuate neuropathic pain after brachial plexus injury through upregulating β-endorphin expression (Zhang et al., 2014). Our previous studies revealed that application of EA induced activation and subsequent deactivation of somatosensory area and pain-related regulating cortical areas, including insula, thalamus, and cingulate cortex in a sciatic nerve transection model (Wu et al., 2018b). We also found that EA could induce both regional and extensive neuroplasticity in bilateral hemispheres (Wu et al., 2018a).

^{18}FDG-PET has been widely used to evaluate regional brain glucose metabolic connectivity in many diseases to provide further understanding of neural functional connectivity (Morbelli et al., 2012; Caminiti et al., 2016; Pagani et al., 2016; Herholz et al., 2018). Horwitz et al. (1987) suggested that metabolic connectivity was the across-subject correlations of glucose metabolism between different brain regions (Horwitz et al., 1987). The altered metabolic connectivity revealed the changes in brain functional network, which was associated with pathophysiology of disorders. Our previous study also showed that neuropathic pain following BPAI induced metabolic connectivity changes significantly among sensorimotor-related areas and pain-related area in bilateral hemispheres (Huo et al., 2020). The specific neuroplasticity pattern might provide further insights to the mechanism of neuropathic pain following BPAI.

In the present research, we used ^{18}FDG-PET to assess the changes of metabolic connectivity in neuropathic pain following BPAI. We found that decreased metabolic connectivity between bilateral sensorimotor cortices from 4th to 14th weeks. The decreased activation of sensorimotor cortex (SMC) could be attributable to the lack of neural input signals from periphery (Yoshikawa et al., 2012). We noted increased metabolic connectivity between SMC and pain-related areas in bilateral hemispheres at 4th week and decreased metabolic connectivity at 12th week following EA intervention. However, at 16th week, increased metabolic connectivity was found between SMC and pain-related areas in bilateral hemisphere. The specific activation pattern may be associated with the central mechanism of EA intervention in treating neuropathic pain after BPAI.

Caudate and putamen, which constitute the dorsal striatum, are the gateway to the basal ganglia (Kreitzer and Malenka, 2008). The Cpu receives inputs from all cortical areas and projects to frontal lobe areas (prefrontal, premotor, and supplementary motor areas) throughout the thalamus, which are concerned with motor planning (Herrero et al., 2002). Lanz et al. (2011) reported that increased activity of Cpu was associated with sensation of thermal pain. In the present experiment, the decreased metabolic connectivity between SC and Cpu in the left hemisphere (contralateral to the injured forelimb) may be the part explanation of the neuroplasticity evoked by chronic neuropathic pain and the dysfunction of motor and sensory function.

The thalamus is a key relay station for the transmission of nociceptive information to the cerebral cortex. It receives somatosensory inputs from the skin, deep structures, and visceral organs and then projects to the cortex. The dorsal thalamus contains the principal somatosensory thalamic nuclei (Yen and Lu, 2013). Previous studies have revealed the importance of thalamus in neuromodulation of chronic pain. Iadarola et al. (1995) reported reduced regional blood flow in the thalamus contralateral to the injured limb in patients with spontaneous pain. Application of deep brain stimulation in thalamus was demonstrated to be efficient for release of chronic neuropathic pain after traumatic amputation and BPAI (Pereira et al., 2013). In our study, decreased metabolic connectivity between ipsilateral DLT and SC was related with BPAI-induced neuropathic pain.

However, the present study still has some limitations. The natural difference between human and rodents should not be neglected. The acupoints are empirical proof in human that need further evidence. Further researches in human and brain microstructures are still needed before full confirmation is made.

DATA AVAILABILITY STATEMENT

The raw data supporting the conclusions of this article will be made available by the authors, without undue reservation.

ETHICS STATEMENT

All procedures were in agreement with the Guide for the Care and Use of Laboratory Animals described by the US National Institutes of Health and were reviewed and approved by the Animal Ethical Committee of Shanghai University of Traditional Chinese Medicine.

AUTHOR CONTRIBUTIONS

A-LH and B-BH designed the study and monitored the progress, data collection, and analysis. M-XZ and X-YH analyzed and interpreted the data and made critical revision of the article. JS and X-YH designed the study and collected the data. J-GX supervised the progress of the study.

FUNDING

This work was supported by Shanghai Rising-Star Program (grant number 19QA1409000), Shanghai Municipal Commission of Health and Family Planning (grant number 2018YQ02), Shanghai "Rising Stars of Medical Talent" Youth Development Program (grant number RY411.19.01.10) and the National Key R&D Program of China (grant number: 2018YFC2001600).

SUPPLEMENTARY MATERIAL

The Supplementary Material for this article can be found online at: https://www.frontiersin.org/articles/10.3389/fncir.2020.00035/full#supplementary-material.

REFERENCES

Apkariana, A. V., Bushnell, M. C., Treede, R. D., and Zubieta, J. K. (2005). Human brain mechanisms of pain perception and regulation in health and disease. *Eur. J. Pain* 9, 463–484. doi: 10.1016/j.ejpain.2004.11.001

Attal, N., Cruccu, G., Baron, R., Haanpää, M., Hansson, P., Jensen, T. S., et al. (2010). EFNS guidelines on the pharmacological treatment of neuropathic pain: 2010 revision. *Eur. J. Neurol.* 17, e1113–e1188. doi: 10.1111/j.1468-1331.2010.02999.x

Bril, V., England, J., Franklin, G. M., Backonja, M., Cohen, J., Toro, D. D., et al. (2011). Evidence-based guideline: treatment of painful diabetic neuropathy: report of the american academy of neurology, the american association of neuromuscular and electrodiagnostic medicine and the american academy of physical medicine and rehabilitation. *Muscle Nerve* 3, 345–352. doi: 10.1002/mus.22092

Caminiti, S. P., Tettamanti, M., Sala, A., Presotto, L., and Perani, D. (2016). Metabolic connectomics targeting brain pathology in dementia with Lewy bodies. *J. Cereb. Blood Flow Metab.* 37, 1311–1325. doi: 10.1177/0271678X16654497

Challa, S. R. (2015). Surgical animal models of neuropathic pain: pros and Cons. *Int. J. Neurosci.* 125, 170–174. doi: 10.3109/00207454.2014.922559

Cohen, S. P., and Mao, J. (2014). Neuropathic pain: mechanisms and their clinical implications. *BMJ* 348:f7656. doi: 10.1136/bmj.f7656

Cope, D. K. (2016). Analgesic effects and neuropathology changes of electroacupuncture on curing a rat model of brachial plexus neuralgia induced by cobra venom. *Pain Physician* 19:E435.

Davis, R., and Lentini, R. (1975). Transcutaneous nerve stimulation for treatment of pain in patients with spinal cord injury. *Surg. Neurol.* 4, 100–101.

Denny-Brown, D., Kirk, E. J., and Yanagisawa, N. (1973). The tract of Lissauer in relation to sensory transmission in the dorsal horn of spinal cord in the macaque monkey. *J. Comp. Neurol.* 151, 175–200. doi: 10.1002/cne.901510206

Donvito, G., Nass, S. R., Wilkerson, J. L., Curry, Z. A., Schurman, L. D., Kinsey, S. G., et al. (2018). The endogenous cannabinoid system: a budding source of targets for treating inflammatory and neuropathic pain. *Neuropsychopharmacology* 43, 52–79. doi: 10.1038/npp.2017.204

Finnerup, N. B., Norrbrink, C., Trok, K., Piehl, F., Johannesen, I. L., Sørensen, J. C., et al. (2014). Phenotypes and predictors of pain following traumatic spinal cord injury: a prospective study. *J. Pain* 15, 40–48. doi: 10.1016/j.jpain.2013.09.008

Gierthmühlen, J., and Baron, R. (2016). Neuropathic pain. *Semin. Neurol.* 36, 462–468. doi: 10.1055/s-0036-1584950

Gronseth, G., Cruccu, G., Alksne, J., Argoff, C., Brainin, M., Burchiel, K., et al. (2008). Practice parameter: the diagnostic evaluation and treatment of trigeminal neuralgia (an evidence-based review): report of the Quality Standards Subcommittee of the American Academy of Neurology and the European Federation of Neurological Societies. *Neurology* 71, 1183–1190. doi: 10.1212/01.wnl.0000326598.83183.04

Herholz, K., Haense, C., Gerhard, A., Jones, M., Anton-Rodriguez, J., Segobin, S., et al. (2018). Metabolic regional and network changes in Alzheimer's disease subtypes. *J. Cereb. Blood Flow Metab.* 38, 1796–1806. doi: 10.1177/0271678X17718436

Herrero, M. T., Barcia, C., and Navarro, J. (2002). Functional anatomy of thalamus and basal ganglia. *Childs Nerv. Syst.* 18, 386–404. doi: 10.1007/s00381-002-0604-1

Horwitz, B., Grady, C. L., Schlageter, N. L., Duara, R., and Rapoport, S. I. (1987). Intercorrelations of regional glucose metabolic rates in Alzheimer's disease. *Brain Res.* 407, 294–306. doi: 10.1016/0006-8993(87)91107-3

Hsieh, J. C., Ståhle-Bäckdahl, M., Hägermark, O., Stone-Elander, S., Rosenquist, G., and Ingvar, M. (1996). Traumatic nociceptive pain activates the hypothalamus and the periaqueductal gray: a positron emission tomography study. *Pain* 64, 303–314. doi: 10.1016/0304-3959(95)00129-8

Huo, B. B., Shen, J., Hua, X. Y., Zheng, M. X., Lu, Y. C., Wu, J. J., et al. (2020). Alteration of metabolic connectivity in a rat model of deafferentation pain: a 18F-FDG PET/CT study. *J. Neurosurg.* 132, 1295–1303. doi: 10.3171/2018.11.JNS181815

Iadarola, M. J., Max, M. B., Berman, K. F., Byas-Smith, M. G., Coghill, R. C., Gracely, R. H., et al. (1995). Unilateral decrease in thalamic activity observed with positron emission tomography in patients with chronic neuropathic pain. *Pain* 63, 55–64. doi: 10.1016/0304-3959(95)00015-k

Iannetti, G. D., and Mouraux, A. (2010). From the neuromatrix to the pain matrix (and back). *Exp. Brain Res.* 205, 1–12. doi: 10.1007/s00221-010-2340-1

Jaggi, A. S., and Singh, N. (2011). Role of different brain areas in peripheral nerve injury-induced neuropathic pain. *Brain Res.* 1381, 187–201. doi: 10.1016/j.brainres.2011.01.002

Jiang, H., Yu, X., Ren, X., and Tu, Y. (2016). Electroacupuncture alters pain-related behaviors and expression of spinal prostaglandin E2 in a rat model of neuropathic pain. *J. Tradit. Chin. Med.* 36, 85–91. doi: 10.1016/s0254-6272(16)30013-9

Ju, Z. Y., Wang, K., Cui, H. S., Yao, Y., Liu, S. M., Zhou, J., et al. (2017). Acupuncture for neuropathic pain in adults. *Cochrane Database Syst. Rev.* 12:CD012057. doi: 10.1002/14651858.CD012057.pub2

Kim, J. H., Min, B. H., Na, H. S., and Park, D. S. (2004). Relieving effects of electroacupuncture on mechanical allodynia in neuropathic pain model of inferior caudal trunk injury in rat: mediation by spinal opioid receptors. *Brain Res.* 998, 230–236. doi: 10.1016/j.brainres.2003.11.045

Kreitzer, A. C., and Malenka, R. C. (2008). Striatal plasticity and basal ganglia circuit function. *Neuron* 60, 543–554. doi: 10.1016/j.neuron.2008.11.005

Lanz, S., Seifert, F., and Maihöfner, C. (2011). Brain activity associated with pain, hyperalgesia and allodynia: an ALE meta-analysis. *J. Neural Transm.* 118, 1139–1154. doi: 10.1007/s00702-011-0606-9

Levy, R., Deer, T. R., and Henderson, J. (2010). Intracranial neurostimulation for pain control: a review. *Pain Phys.* 13, 157–165.

Li, H., Liu, H., Liu, C., Shi, G., Zhou, W., Zhao, C., et al. (2014). Effect of "Deqi" during the study of needling "Wang's Jiaji" acupoints treating spasticity after stroke. *Evid. Based Complement. Alternat. Med.* 2014:715351. doi: 10.1155/2014/715351

Li, H. P., Su, W., Shu, Y., Yuan, X. C., Lin, L. X., Hou, T. F., et al. (2019). Electroacupuncture decreases Netrin-1-induced myelinated afferent fiber sprouting and neuropathic pain through mu-opioid receptors. *J. Pain Res.* 12, 1259–1268. doi: 10.2147/jpr.s191900

Lu, Y., Yong, H., Tang, C., Shan, B., Cui, S., Yang, J., et al. (2014). Brain areas involved in the acupuncture treatment of AD model rats: a PET study. *BMC Complement. Altern. Med.* 14:178. doi: 10.1186/1472-6882-14-178

Moisset, X., and Bouhassira, D. (2007). Brain imaging of neuropathic pain. *NeuroImage* 37, S80–S88. doi: 10.1016/j.neuroimage.2007.03.054

Morbelli, S., Drzezga, A., Perneczky, R., Frisoni, G. B., Caroli, A., van Berckel, B. N., et al. (2012). Resting metabolic connectivity in prodromal Alzheimer's disease. A European Alzheimer Disease Consortium (EADC) project. *Neurobiol. Aging* 33, 2533–2550. doi: 10.1016/j.neurobiolaging.2012.01.005

Mulla, S. M., Wang, L., Khokhar, R., Izhar, I., Agarwal, A., Couban, R., et al. (2015). Management of central poststroke pain: systematic review of randomized controlled trials. *Stroke* 46, 2853–2860. doi: 10.1161/STROKEAHA.115.010259

Murphey, F., Hartung, W., and Kirklin, J. W. (1947). Myelographic demonstration of avulsing injury of the brachial plexus. *Am. J. Roentgenol. Radium Ther.* 58:102.

Ngernyam, N., Jensen, M. P., Arayawichanon, P., Auvichayapat, N., Tiamkao, S., Janjarasjitt, S., et al. (2015). The effects of transcranial direct current stimulation in patients with neuropathic pain from spinal cord injury. *Clin. Neurophysiol.* 126, 382–390. doi: 10.1016/j.clinph.2014.05.034

Nguyen, J. P., Lefaucheur, J. P., Decq, P., Uchiyama, T., Carpentier, A., Fontaine, D., et al. (1999). Chronic motor cortex stimulation in the treatment of central and neuropathic pain. Correlations between clinical, electrophysiological and anatomical data. *Pain* 82, 245–251. doi: 10.1016/s0304-3959(99)00062-7

Pagani, M., Öberg, J., De Carli, F., Calvo, A., Moglia, C., Canosa, A., et al. (2016). Metabolic spatial connectivity in amyotrophic lateral sclerosis as revealed by independent component analysis. *Hum. Brain Mapp.* 37, 942–953. doi: 10.1002/hbm.23078

Park, J. H., Han, J. B., Kim, S. K., Park, J. H., and Go, D. H. (2010). Spinal GABA receptors mediate the suppressive effect of electroacupuncture on

cold allodynia in rats. *Brain Res.* 1322, 24–29. doi: 10.1016/j.brainres.2010.02.001

Parry, C. B. (1980). Pain in avulsion lesions of the brachial plexus. *Pain* 9, 41–53. doi: 10.1016/0304-3959(80)90027-5

Paszcuk, A. F., Dutra, R. C., da Silva, K. A., Quintao, N. L., Campos, M. M., and Calixto, J. B. (2011). Cannabinoid agonists inhibit neuropathic pain induced by brachial plexus avulsion in mice by affecting glial cells and MAP kinases. *PLoS One* 6:e24034. doi: 10.1371/journal.pone.0024034

Pereira, E. A., Boccard, S. G., Linhares, P., Chamadoira, C., Rosas, M. J., Abreu, P., et al. (2013). Thalamic deep brain stimulation for neuropathic pain after amputation or brachial plexus avulsion. *Neurosurg. Focus* 35:E7. doi: 10.3171/2013.7.focus1346

Phelps, M. E., Huang, S. C., Hoffman, E. J., Selin, C., Sokoloff, L., and Kuhl, D. E. (1980). Tomographic measurement of local cerebral glucose metabolic rate in humans with (F-18)2-fluoro-2-deoxy-D-glucose: validation of method. *Ann. Neurol.* 6, 371–388. doi: 10.1002/ana.410060502

Powers, S. K., Adams, J. E., Edwards, M. S., Boggan, J. E., and Hosobuchi, Y. (1984). Pain relief from dorsal root entry zone lesions made with argon and carbon dioxide microsurgical lasers. *J. Neurosurg.* 61, 841–847. doi: 10.3171/jns.1984.61.5.0841

Rodrigues-Filho, R., Santos, A. R. S., Bertelli, J. A., and Calixto, J. B. (2003). Avulsion injury of the rat brachial plexus triggers hyperalgesia and allodynia in the hindpaws: a new model for the study of neuropathic pain. *Brain Res.* 982, 186–194. doi: 10.1016/s0006-8993(03)03007-5

Rong, P., Zhu, B., Li, Y., Gao, X., Hui, B., Li, Y., et al. (2011). Mechanism of acupuncture regulating visceral sensation and mobility. *Front. Med.* 5, 151–156. doi: 10.1007/s11684-011-0129-7

Santana, M. V. B., Bina, M. T., Paz, M. G., Santos, S. N., Teixeira, M. J., Raicher, I., et al. (2016). High prevalence of neuropathic pain in the hand of patients with traumatic brachial plexus injury: a cross-sectional study. *Arq. Neuropsiquiatr.* 74, 895–901. doi: 10.1590/0004-282x20160149

Schwarz, A. J., Danckaert, A., Reese, T., Gozzi, A., Paxinos, G., Watson, C., et al. (2006). A stereotaxic MRI template set for the rat brain with tissue class distribution maps and co-registered anatomical atlas: application to pharmacological MRI. *NeuroImage* 32, 538–550. doi: 10.1016/j.neuroimage.2006.04.214

Shen, J., Huo, B. B., Hua, X. Y., Zheng, M. X., and Xu, J. G. (2019a). Cerebral^{18} F-FDG metabolism alteration in a neuropathic pain model following brachial plexus avulsion: a PET/CT study in rats. *Brain Res.* 1712, 132–138. doi: 10.1016/j.brainres.2019.02.005

Shen, J., Huo, B. B., Zheng, M. X., Hua, X. Y., Shen, H., Lu, Y. C., et al. (2019b). Evaluation of neuropathic pain in a rat model of total brachial plexus avulsion from behavior to brain metabolism. *Pain Physician* 22, E215–E224.

Soler, M. D., Kumru, H., Pelayo, R., Vidal, J., Tormos, J. M., Fregni, F., et al. (2010). Effectiveness of transcranial direct current stimulation and visual illusion on neuropathic pain in spinal cord injury. *Brain* 133, 2565–2577. doi: 10.1093/brain/awq184

Spaić, M., Marković, N., and Tadić, R. (2002). Microsurgical DREZotomy for pain of spinal cord and cauda equina injury origin: clinical characteristics of pain and implications for surgery in a series of 26 patients. *Acta Neurochir.* 144, 453–462. doi: 10.1007/s007010200066

Sun, R. Q., Wang, H. C., and Yun, W. (2002). Effect of electroacupuncture with different frequencies on neuropathic pain in a rat model. *Chinese J. Appl. Physiol.* 18, 128–131. doi: 10.3969/j.issn.1000-6834.2002.02.007

Teixeira, M. J., da Paz, M. G. S., Bina, M. T., Santos, S. N., Raicher, I., Galhardoni, R., et al. (2015). Neuropathic pain after brachial plexus avulsion—central and peripheral mechanisms. *BMC Neurol.* 15:73. doi: 10.1186/s12883-015-0329-x

Treede, R. D., Jensen, T. S., Campbell, J. N., Cruccu, G., Dostrovsky, J. O., Griffin, J. W., et al. (2008). Neuropathic pain: redefinition and a grading system for clinical and research purposes. *Neurology* 70, 1630–1635. doi: 10.1212/01.wnl.0000282763.29778.59

Widerström-Noga, E. (2017). Neuropathic pain and spinal cord injury: phenotypes and pharmacological management. *Drugs* 77, 967–984. doi: 10.1007/s40265-017-0747-8

Wu, J.-J., Lu, Y.-C., Hua, X.-Y., Ma, S.-J., Shan, C.-L., and Xu, J.-G. (2018a). Cortical remodeling after Electroacupuncture Therapy in peripheral nerve repairing model. *Brain Res.* 1690, 61–73. doi: 10.1016/j.brainres.2018.04.009

Wu, J.-J., Lu, Y.-C., Hua, X.-Y., Ma, S.-J., and Xu, J.-G. (2018b). A longitudinal mapping study on cortical plasticity of peripheral nerve injury treated by direct anastomosis electroacupuncture in rats. *World Neurosurg.* 114, e267–e282. doi: 10.1016/j.wneu.2018.02.173

Yakushev, I., Drzezga, A., and Habeck, C. (2017). Metabolic connectivity: methods and applications. *Curr. Opin. Neurol.* 30, 677–685. doi: 10.1097/wco.0000000000000494

Yen, C. T., and Lu, P. L. (2013). Thalamus and pain. *Acta Anaesthesiol. Taiwan.* 51, 73–80. doi: 10.1016/j.aat.2013.06.011

Yoshikawa, T., Hayashi, N., Tajiri, Y., Satake, Y., and Ohtomo, K. (2012). Brain reorganization in patients with brachial plexus injury: a longitudinal functional MRI study. *ScientificWorldJournal* 2012:501751. doi: 10.1100/2012/501751

Zhang, R., Lao, L., Ren, K., and Berman, B. M. (2014). Mechanisms of acupuncture-electroacupuncture on persistent pain. *Anesthesiology* 120, 482–503. doi: 10.1097/aln.0000000000000101

Zhang, S., Tang, H., Zhou, J., and Gu, Y. (2014). Electroacupuncture attenuates neuropathic pain after brachial plexus injury. *Neural Regen. Res.* 9, 1365–1370. doi: 10.4103/1673-5374.137589

Zilliox, L. A. (2017). Neuropathic pain. *Continuum* 23, 512–532. doi: 10.1212/CON.0000000000000462

Conflict of Interest: The authors declare that the research was conducted in the absence of any commercial or financial relationships that could be construed as a potential conflict of interest.

Copyright © 2020 Hou, Zheng, Hua, Huo, Shen and Xu. This is an open-access article distributed under the terms of the Creative Commons Attribution License (CC BY). The use, distribution or reproduction in other forums is permitted, provided the original author(s) and the copyright owner(s) are credited and that the original publication in this journal is cited, in accordance with accepted academic practice. No use, distribution or reproduction is permitted which does not comply with these terms.

frontiers in Human Neuroscience

ORIGINAL RESEARCH
published: 17 September 2020
doi: 10.3389/fnhum.2020.551470

Abnormal Spatial Patterns of Intrinsic Brain Activity in Osteonecrosis of the Femoral Head: A Resting-State Functional Magnetic Resonance Imaging Study

Shengyi Feng[1†], Bo Li[1†], Gang Li[2], Xuyun Hua[1], Bo Zhu[1], Xuejia Li[2], Wenting Lu[3] and Jianguang Xu[4*]*

[1]Center of Traumatology and Orthopedics, Yueyang Hospital of Integrated Traditional Chinese and Western Medicine, Shanghai University of Traditional Chinese Medicine, Shanghai, China, [2]Department of Orthopedics, Affiliated Hospital of Shandong University of Traditional Chinese Medicine, Shanghai, China, [3]Quyang Community Health Service Center of Hongkou District, Shanghai, China, [4]School of Rehabilitation Science, Shanghai University of Traditional Chinese Medicine, Shanghai, China

OPEN ACCESS

Edited by:
Dongsheng Xu,
Tongji University, China

Reviewed by:
Jiu Chen,
Nanjing Medical University, China
Sangma Xie,
Hangzhou Dianzi University, China
Yutong Liu,
University of Nebraska Medical Center, United States

***Correspondence:**
Bo Li
libo@shyueyanghospital.com
Jianguang Xu
jianguangxu@fudan.edu.cn

[†]These authors have contributed equally to this work

Specialty section:
This article was submitted to Brain Imaging and Stimulation, a section of the journal Frontiers in Human Neuroscience

Received: 13 April 2020
Accepted: 27 August 2020
Published: 17 September 2020

Citation:
Feng S, Li B, Li G, Hua X, Zhu B, Li X, Lu W and Xu J (2020) Abnormal Spatial Patterns of Intrinsic Brain Activity in Osteonecrosis of the Femoral Head: A Resting-State Functional Magnetic Resonance Imaging Study. Front. Hum. Neurosci. 14:551470. doi: 10.3389/fnhum.2020.551470

Objective: Osteonecrosis of the femoral head (ONFH) is a common condition that is encountered in clinical practice, and yet, little is known about its characteristics and manifestations in the brain. Therefore, in this study, we aimed to use resting-state functional magnetic resonance imaging (rs-fMRI) to investigate the spatial patterns of spontaneous brain activity in the brain of ONFH patients.

Methods: The study included ONFH patients and healthy controls. The pattern of intrinsic brain activity was measured by examining the amplitude of low-frequency fluctuations (ALFF) of blood oxygen level-dependent signals using rs-fMRI. Meanwhile, we also used Harris hip scores to evaluate the functional performance of ONFH patients and healthy controls.

Result: Ten ONFH patients and 10 health controls were investigated. We found global ALFF differences between the two groups throughout the occipital, parietal, frontal, prefrontal, and temporal cortices. In the ONFH patients, altered brain activity was found in the brain regions in the sensorimotor network, pain-related network, and emotion and cognition network. The results of the correlation investigations also demonstrated that the regions with ALFF changes had significant correlations with the functional performance of the patients evaluated by Harris hip scores.

Abbreviations: ONFH, Osteonecrosis of the femoral head; rs-fMRI, Resting-state functional magnetic resonance imaging; fALFF, fractional amplitude of low-frequency fluctuation; MMSE, Mini-Mental State Examination; DPARSF, Data Processing Assistant for rsfMRI; MOG, middle occipital gyrus; PHG, parahippocampal gyrus; PreCG, precentral gyrus; IFGtri, right triangular part of the inferior frontal gyrus; PoCG, postcentral gyrus.

Conclusions: Our study has revealed the abnormal pattern of brain activity in ONFH patients, and our findings could be used to aid in understanding the mechanisms behind the gait abnormality and intractable pain associated with ONFH at the central level.

Keywords: osteonecrosis of the femoral head, magnetic resonance imaging, spatial patterns, spontaneous brain activity, amplitude of low-frequency fluctuations, Harris hip scores, sensorimotor network, osteonecrosis

INTRODUCTION

Osteonecrosis of the femoral head (ONFH) is caused by impaired or interrupted vascular supply, and it may occur in individuals of all ages (Sultan et al., 2019). Subsequently, it may lead to the necrotization of the osteocytes. ONFH may originate from both traumatic and non-traumatic aetiologies. As the area of necrosis increases, the manifestations of ONFH progress to structural modifications and the collapse of the femoral head. As a consequence, ONFH may be accompanied by varying levels of pain and the functional disability of the hip joint. Among all of its symptoms, pain is usually the most significant and sustained, especially in advanced-stage ONFH [Association Research Circulation Osseous (ARCO) III° and IV°; Pyda et al., 2015; Kuroda et al., 2016].

Nowadays, owing to the advances in brain imaging techniques, a larger number of researchers are focusing on the central mechanism of arthritic disorders. The pathophysiologies of several motor system diseases have been investigated using functional magnetic resonance imaging (fMRI) techniques. In patients with osteoarthritis, Chen et al. (2015) reported that acupuncture might relieve knee osteoarthritis-related pain by modulating the functional connectivity between the right frontoparietal network, executive control network, and descending pain modulatory pathway. Within the networks, the rostral anterior cingulate cortex and medial prefrontal cortex were found to exhibit enhanced functional connectivity (Chen et al., 2015). A study based on the moxibustion treatment of knee osteoarthritis demonstrated increased fractional amplitude of low-frequency fluctuation (fALFF) values in the bilateral cerebrum, extra-nucleus, left cerebellum, and white matter. Simultaneously, the fALFF values of the precentral gyrus (PreCG), frontal lobe, and occipital lobe were found to be decreased (Xie et al., 2013). In rheumatoid arthritis patients, Flodin et al. (2016) reported that the supplementary motor areas, midcingulate cortex, and primary sensorimotor cortex exhibited enhanced functional connectivity. A recent multi-modal MRI study revealed that positive connections between the inferior parietal lobule, medial prefrontal cortex, and multiple brain networks, as well as reductions in inferior parietal lobule Gray Matter (GM), could be monitored to predict the development of fatigue, pain, and cognitive dysfunction in rheumatoid arthritis patients (Schrepf et al., 2018). Further, a neuroimaging study has reported that patients with chronic osteoarthritis pain exhibit significantly higher levels of anticorrelation between the right anterior insula and default mode network regions, thereby suggesting an altered brain state at rest characterised by the increased inhibitory effect of the salience network on the default mode network (Ryan et al., 2018).

Most studies focus on the pain-related symptoms following the onset of osteoarthritis and rheumatoid arthritis. However, in patients suffering from ONFH, gait abnormality is also an important symptom that may cause a dramatic reorganization in the motor-related brain networks. Thus, it is assumed that multiple brain networks may be involved in the adaptive plasticity following the development of ONFH and that resting-state fMRI (rs-fMRI) could be an effective modality for investigating the corresponding changes in the whole brain. Despite this, little is known about the characteristics and manifestations of ONFH in the brain.

Therefore, in the present study, we aimed to investigate the changes in intrinsic or spontaneous brain activity in ONFH patients *via* the use of rs-fMRI to examine the regional amplitude of low-frequency fluctuations (ALFF) across the bilateral hemispheres.

MATERIALS AND METHODS

Subjects

This study was approved by the Medical Research Ethics Committee of the authors' affiliated institutions and was registered in the national clinical trial registry. Twenty right-handed subjects (10 ONFH patients and 10 healthy controls) participated in this study after providing written informed consent. The participants with ONFH were recruited from among patients who had consulted orthopedic clinics at the authors' affiliated institutions for hip pain. The healthy controls were recruited from the local community by advertisements.

The inclusion criteria for ONFH patients were as follows: (1) had been diagnosed as ONFH following the 2015 Guideline for Diagnostic and Treatment of ONFH (Li, 2015); (2) were the first time to suffer from ONFH; (3) had no previous treatment of medication; and (4) underwent a complete physical and radiological examination, standard laboratory tests, and an extensive number of neuropsychological assessments.

The criteria for the selection of the healthy controls were as follows: (1) no neurological or psychiatric disorders, such as stroke, depression, or epilepsy; (2) no neurological deficiencies, such as visual or hearing loss; (3) no abnormal findings, such as infarction or focal lesion in conventional brain MRI; (4) no cognitive complaints; and (5) Mini-Mental State Examination (MMSE) scores of 28 or higher.

The exclusion criteria for the patients with ONFH were as follows: (1) presence of neurological or psychiatric disorders, such as stroke, depression, or epilepsy; (2) presence of neurological deficiencies, such as visual or hearing loss; (3) presence of abnormal findings, such as infarction or focal lesion, in conventional brain MRI; (4) cognitive complaints;

TABLE 1 | Demographic data and clinical characteristics of the ONFH patients and healthy controls.

Characteristic	ONFH	Controls	*P*-value
Number (*n*)	10	10	/
Male/female (*n*)	6/4	4/6	0.371[#]
Age (mean ± SD, years)	54.30 ± 19.00	55.7 ± 10.72	0.842[##]
MMSE scores	28.90 ± 2.85	29.60 ± 0.84	0.465[##]
Harris scores	73.10 ± 5.19	97.40 ± 3.53	<0.001[##]

ONFH, Osteonecrosis of the femoral head; MMSE, Mini-Mental State Examination; SD, standard deviation; [#]indicates that P-values for sex distribution between the groups were obtained by a chi-square test; [##]indicates that P-values were obtained by a two-tailed t-test.

(5) MMSE scores of less than 28; and (6) the inability to tolerate fMRI scans.

The clinical and demographic data of the 20 participants are presented in **Table 1**. There were no significant differences between the two groups in terms of sex, age, MMSE scores, and Harris hip scores.

Data Acquisition

The MRI data were acquired by scans performed with a Siemens Verio 3 Tesla scanner (Siemens, Erlangen, Germany). Head-huggers and earplugs were used to limit head motion and reduce the volume of noise produced by the MRI scanner. The subjects were instructed to relax, hold still, keep their eyes closed, keep awake, and not think about anything in particular. Functional images were captured axially using an echo-planar imaging (EPI) sequence with the following settings: a repetition time of 3,000 ms, echo time of 30 ms, a flip angle of 90°, a field of view of 24 cm, a resolution of 64 × 64 matrices, 43 slices with a thickness of 3 mm, a voxel size of 3.75 × 3.75 × 3 mm^3, and bandwidth of 2,232 Hz/pixel. The scan lasted for 600 s. All the subjects had not fallen asleep based on the responses in a simple questionnaire filled after the scan. Three-dimensional T1-weighted magnetization-prepared rapid gradient echo (MPRAGE) sagittal images were captured using the following parameters: a repetition time of 1,900 ms, echo time of 2.93 ms, an inversion time of 900 ms, a flip angle of 9°, a resolution of a 256 × 256 matrix, 160 slices with a thickness of 1.0 mm, and a voxel size of 1 × 1 × 1 mm^3.

Data Preprocessing

In this study, fMRI image data processing was carried out using the Data Processing Assistant for rsfMRI (DPARSF; Yan et al., 2016); this toolbox is based on Statistical Parametric Mapping 8 (SPM8[1]) and is run in MATLAB R2014a (MathWorks Inc., Natick, MA, USA). The preprocessing steps were based on a recent mainstream protocol (Wang et al., 2011): the first 10 volumes of images were discarded owing to signal equilibrium and to allow the participants to adapt to the noise produced by the MRI scanner. All the slices of the remaining 190 volumes were corrected for different signal acquisition times by shifting the signal measured in each slice relative to the acquisition time of the slice acquired in the middle of each repetition time. Subsequently, to minimize the confounding of head motion, we utilized the Friston 24-parameter model to regress out head motion effects (Friston et al., 1996). The Friston 24-parameter model (i.e., six head motion parameters, six head motion parameters one time-point before, and the 12 corresponding squared items) was chosen based on prior work that higher-order models remove head motion effects better (Satterthwaite et al., 2013; Mistry et al., 2016). The motion-corrected functional volumes were spatially normalized to the EPI template space and resampled to 3 mm isotropic voxels using the normalization parameters estimated and recorded during unified segmentation. Following this, the functional images were spatially smoothed with a 6-mm full width at half maximum Gaussian kernel. Finally, using DPRSF, linear trend subtraction and temporal filtering (0.01–0.10 Hz) were performed on the time series of each voxel in order to reduce the effect of low-frequency drifts and high-frequency noise. As a quality check of fMRI date, large head motion in any direction corresponding to >3 mm or any rotation >3° would be excluded in our study.

[1]http://www.fil.ion.ucl.ac.uk/spm

Harris Hip Scoring System

The Harris Hip Scale, a widely adopted approach for assessing hip function, has been demonstrated to be effective for evaluating changes in hip function, and it has been shown to have high validity, reliability, and responsiveness (Mistry et al., 2016). Consequently, we used this approach to evaluate the pain, hip function, deformity level, and motion range of ONFH patients.

ALFF Analyses

We used the DPARSF to calculate the ALFF value, as described in previous studies (Yu et al., 2014; Golestani et al., 2017; Zhou et al., 2017). The preprocessed data were subjected to detrend and bandpass filtering (0.01–0.1 Hz). The time courses were first converted to the frequency domain *via* the fast Fourier transform algorithm. The square root of the power spectrum was computed and then averaged across 0.01–0.10 Hz at each voxel. This averaged square root was recorded as the ALFF. To reduce the global effects of variability across the participants, the ALFF of each voxel was divided by the global mean ALFF value of each subject, resulting in a relative ALFF. The global mean ALFF value was calculated for each participant within a group GM mask obtained by selecting a threshold of 0.2 on the mean GM map of all the 20 subjects. The relative ALFF value in a given voxel reflects the degree of its raw ALFF value relative to the average ALFF value of the whole brain.

Statistical Analyses

Intergroup ALFF Analysis

To determine the ALFF differences between the two groups, a two-sample *t*-test was performed at each voxel (within the AAL mask and GM mask). The statistical threshold was set at $|T| > 1.73$ ($P < 0.05$) and the cluster size at >10 voxels (=270 mm^3), which corresponded to a corrected *P*-value of <0.05, and the corrections were conducted using Gaussian random field (GRF).

Correlation Analysis of ALFF and Harris Hip Scores

To investigate the relationship between the ALFF and functional performance in all the subjects, we computed the Pearson's correlation coefficients between the ALFF and Harris hip scores in both the ONFH and healthy control groups combined in a voxel-wise way. The statistical threshold was set at $|T| > 1.73$ ($P < 0.05$) and the cluster size at > 50 voxels (=1,350 mm^3), which corresponded to a corrected P of <0.05 (Wang et al., 2011).

RESULTS

Demographic Characteristics and Hip Function Test

Eventually, after excluding subjects with excessive head movements, 10 ONFH subjects and 10 HC subjects entered the statistical analysis stage. The demographic characteristics, neuropsychological scores, and hip function scores are presented in **Table 1**. There were no significant differences between the two groupsin terms of sex, age, and MMSE scores; however, the Harris hip scores were significantly different between the two groups ($P < 0.001$). **Figure 1** demonstrates that the correlation between age and Harris scores was significant. The differences among the affected sides were significant ($P < 0.001$) since there was a larger proportion of patients with ONFH affecting the left side in the experimental group. The distribution of sides affected with ONFH is presented in **Figure 2**.

ALFF Differences Between ONFH Patients and Healthy Controls

Figure 3 presents the ALFF differences between ONFH patients and healthy controls. The most significant ALFF increases in the ONFH patients were found in the right middle occipital gyrus (MOG), right inferior parietal lobule, left angular gyri, right insula, right superior temporal gyrus, right lingual gyrus, and left median cingulate and paracingulate gyri, left precuneus, left cuneus, and right parahippocampal gyrus (PHG) while increases were also observed in the right middle temporal gyrus, the left calcarine fissure and surrounding cortex, both-sides of the PreCG, the right inferior frontal gyrus, the right triangular part of the inferior frontal gyrus (IFGtri), the right middle frontal gyrus, both-sides of the postcentral gyrus (PoCG), the right anterior cingulate, and the paracingulate gyri. Significant ALFF decreases associated with ONFH were not observed.

Figure 4A shows the individual MOG ALFF in ONFH patients and healthy controls. The group means were different between the two groups and exhibited a trend of $ALFF_{HC} < ALFF_{ONFH,}$ where HC represents healthy control. There were significant differences between ONFH patients and healthy controls ($t = 3.387$, $P = 0.0033$).

Correlations Between the ALFF and Harris Hip Scores

Figure 4B depicts the correlation maps between the ALFF and Harris hip scores in the ONFH and HC groups combined. Per the results of linear regression analysis, there were significant negative correlations ($r^2 = 0.3195$, $P = 0.0094$) in the MOG ALFF.

DISCUSSION

ONFH may lead to intractable pain and the functional disability of the hip joint. Chronic pain and gait abnormality could influence the spatial patterns of intrinsic brain activity (Xie et al., 2013; Chen et al., 2015; Flodin et al., 2016; Ryan et al., 2018; Schrepf et al., 2018). Our study investigated the ONFH-related changes in the intrinsic or spontaneous brain activity by measuring the ALFF values of resting-state fMRI signals. Based on the current literature, this is the first time that a study has investigated the brain plasticity in ONFH patients. We found that there were global differences in ALFF values when comparing them between the ONFH patients and healthy controls, including in the right MOG, right inferior parietal lobule, left angular gyri, right insula, right superior temporal gyrus, right lingual gyrus, left median cingulate and paracingulate gyri, left precuneus, left cuneus, and right PHG while differences

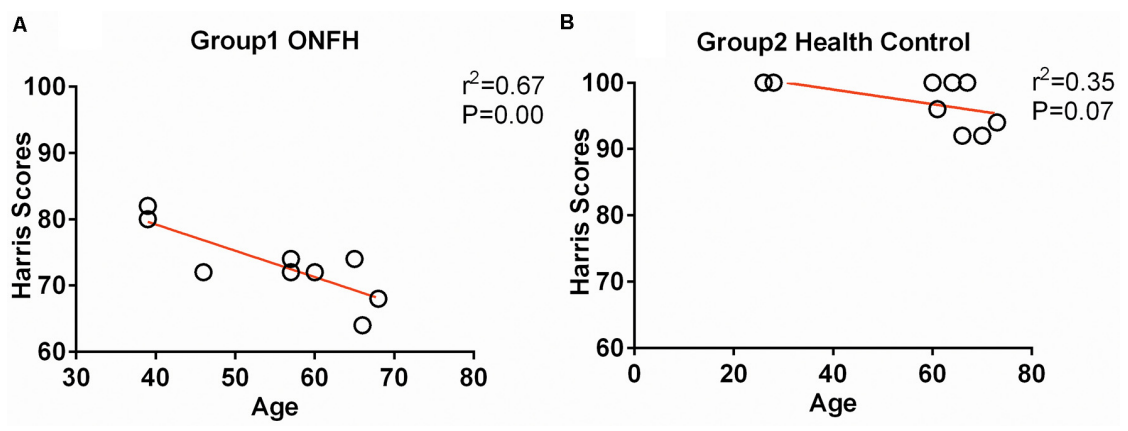

FIGURE 1 | Correlation between age and Harris hip score. **(A)** The scatter plots between the Harris scores and age of the osteonecrosis of the femoral head (ONFH) participants. **(B)** The scatter plots between the Harris scores and age of healthy control participants.

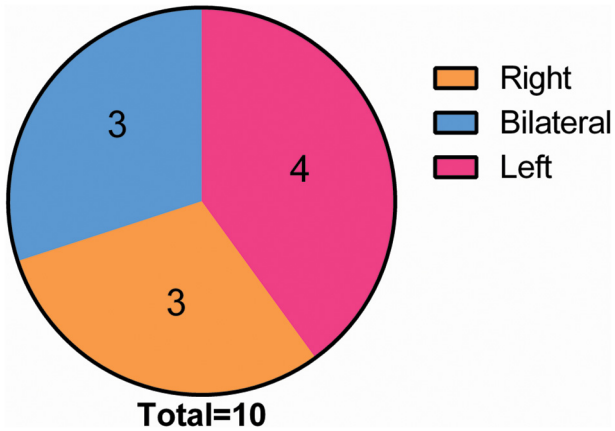

FIGURE 2 | Distribution of the incidence location in the ONFH Group. Among all of the 10 ONFH patients, the condition was present in the right hip in three patients and in the left hip in four patients, and it was bilateral in three patients. Abbreviations: ONFH, osteonecrosis of the femoral head.

were also observed in the right middle temporal gyrus, the left calcarine fissure and surrounding cortex, both sides of the PreCG, the bilateral PoCG, the right IFGtri, the right middle frontal gyrus, and the right paracingulate gyri. Our results imply that measuring the ALFF value of intrinsic or spontaneous brain activity could be useful in characterizing the pathophysiology of ONFH.

Sensorimotor Dysfunction

Dysfunction, including chronic pain and movement disorder of the hip joint, has long plagued ONFH patients and may lead to functional and structural plasticity in the sensorimotor system. The primary motor cortex is predominantly located in the PreCG while the primary somatosensory cortex is located in the PoCG. Previous studies have revealed that PreCG is the primary region of the motor network that is involved in planning and executing movements (Stinear et al., 2009). In clinical practice, despite the pain they experience, the major complaint of arthritis patients is regarding the impairment of motor function, and typically, the sensorimotor cortex is the main area that is analyzed (Canavero and Bonicalzi, 2013). Interestingly, in the present study, we found the enhanced activation of the bilateral PreCG and PoCG in the ONFH patients compared to in the healthy controls. It is known that patients with ONFH may continue to use the affected hip joint with an abnormal gait. The brain tries to compensate for the unusual walking posture and enhances its motor control *via* adaptive plasticity. The occipital lobe contains most of the anatomical region of the visual cortex and contributes to visual information processing and communication with the cerebral cortex (Tu et al., 2013), the increasing of ALFF in MOG also could be evidence of *via* enhancing visual-spatial abilities to assist motor control.

Pain

Most of the previous studies have focused on the influences between fair of pain and pain perception, and the results have revealed that several brain regions, including the insular, prefrontal cortex, and anterior cingulate cortex may be involved in the development of fair of pain (Lumley et al., 2011; Lyby et al., 2011). ONFH patients had verified degrees of pain, resulting in increased ALFF values in the insula, paracingulate gyri, and IFGtri. The IFGtri is a part of the frontal gyrus of the frontal lobe. It is known that the anterior cingulate cortex is a critical hub for pain-induced mood disorders (Barthas et al., 2015). The insular cortex is critical for the perception, modulation, and chronification of pain (Lu et al., 2016). The prefrontal cortex is related to negative emotions and the descending pain inhibitory system (Maeoka et al., 2012). Based on our results, the contralateral (right-side) insula, paracingulate gyri, and IFGtri exhibited significant changes in the ALFF value. It may be inferred that ONFH-induced chronic pain could result in the functional remodeling of the brain. The pain matrix may be activated, and the pain-loop at the central level could be another adaptive plasticity response in ONFH patients, which could be an effective factor for poor clinical outcomes.

Emotion and Cognition

Previous studies have demonstrated that chronic pain may lead to various emotional and cognitive disorders (Lyby et al., 2011). The limbic system contributes to information processing related to motivation, emotion, learning, cognition, and memory. Our results revealed increased ALFF values in the right PHG. The PHG surrounds the hippocampus and is an important part of the limbic system. The PHG plays an important role in emotion processing, center-periphery organization, high spatial frequencies, expertise, and cognition (Levy et al., 2001; Van den Stock et al., 2014). The PHG transfers major polysensory input to the hippocampus and is the recipient of different combinations of sensory information (Burwell, 2000). The enhanced ALFF value in the PHG may indicate information recoding and an integration disorder in ONFH patients (Ranganath and Ritchey, 2012). Meanwhile, the hippocampus has been considered as the brain region that contributes to processing negative emotions, such as fear and anxiety (Kajimura et al., 2015). In the present study, the obvious increase in the ALFF value of the PHG could be evidence of a compensatory reaction for abnormal emotions in ONFH patients. Some studies also elucidated the obvious abnormal resting-state activity and increase in functional connectivity of the MOG in major depressive disorder (Teng et al., 2018), it also could be evidence of a compensatory reaction for abnormal emotions in ONFH patients. Further research should be performed to investigate the psychosocial alterations associated with ONFH since a proportion of ONFH patients suffer from anxiety, depression, and other mental illnesses.

Moreover, significant ALFF decreases associated with ONFH were not observed in the present study. In all the ONFH patients, the control of the healthy side may be enhanced to adapt to the chronic pain and functional disability. Further, this may enhance the activation of extensive brain regions.

In conclusion, we have presented the changes in the ALFF value in ONFH patients using rs-fMRI. We found that

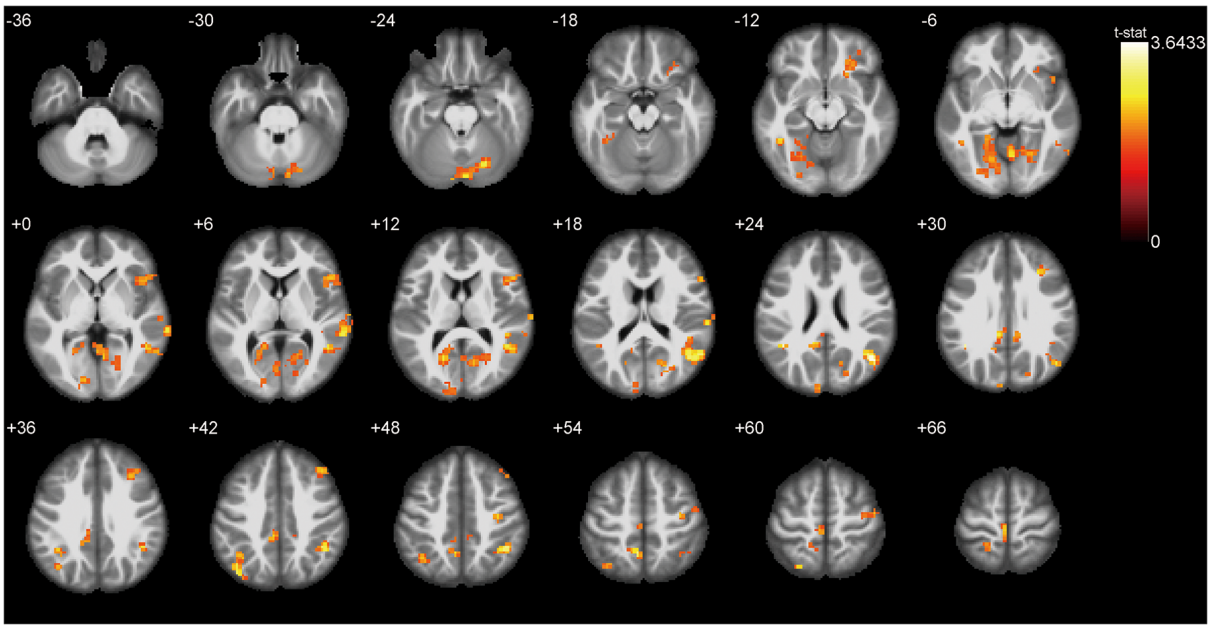

FIGURE 3 | *T*-test statistical difference maps between the ONFH patients and healthy controls. There were significant ALFF differences between the two groups in the right middle occipital gyrus (MOG), right inferior parietal lobule, left angular gyri, right insula, right superior temporal gyrus, right lingual gyrus, left median cingulate and paracingulate gyri, left precuneus, left cuneus, and right parahippocampal gyrus (PHG) while differences were also observed in the right middle temporal gyrus, the left calcarine fissure, both sides of the precentral gyrus (PreCG), the bilateral postcentral gyrus (PoCG), the right triangular part of the inferior frontal gyrus (IFGtri), the right middle frontal gyrus, and the right paracingulate gyri. For the details of the regions, see **Table 2**. Abbreviations: ONFH, osteonecrosis of the femoral head; ALFF, amplitude of low-frequency fluctuations.

TABLE 2 | Regions exhibiting ALFF differences between the ONFH patients and healthy controls (with GRF correction).

Region	Side	MNI coordinates			*t*-value	Cluster size (*k*)
		x	*y*	*z*		
Middle occipital gyrus	R	48	−66	24	3.64	238
Inferior parietal	R	42	−48	45	3.45	85
Angular gyri	L	−42	−51	24	3.41	150
Insula	R	30	12	−18	3.38	29
Superior temporal gyrus	R	69	−33	3	3.25	110
Lingual gyrus	R	6	−63	−3	3.22	786
Median cingulate and paracingulate gyri	L	−9	−39	33	3.21	786
Precuneus	L	−6	−54	54	3.17	72
Cuneus	L	−6	−96	27	3.15	786
Parahippocampal gyrus	R	18	−6	−21	3.08	41
Middle temporal gyrus	R	48	−54	3	2.83	238
Calcarine fissure and surrounding cortex	L	−18	−63	12	2.74	786
Precentral gyrus	R	36	−15	51	2.71	52
Inferior frontal gyrus, triangular part	R	48	21	9	2.61	122
Middle frontal gyrus	R	30	27	30	2.60	85
Inferior temporal gyrus	L	−45	−48	−12	2.59	786
Paracentral lobule	R	0	−27	69	2.58	52
Superior parietal gyrus	L	−24	−69	60	2.56	150
Superior occipital gyrus	R	21	−78	21	2.42	786
Anterior cingulate and paracingulate gyri	R	6	51	9	2.37	14
Postcentral gyrus	L	−24	−45	69	2.41	72
Lingual gyrus	L	−21	−48	−6	2.25	786
Precentral gyrus	L	−27	−21	57	2.22	11
Fusiform	R	24	−72	−6	2.05	786

This table shows all the local maxima separated by more than 20 mm. Regions were automatically labeled using the automated anatomical labeling (AAL) 2 atlas. x, y, and z = Montreal Neurological Institute (MNI) coordinate in the left-right, anterior-posterior, and inferior-superior dimensions, respectively. The statistical threshold was set at $P < 0.05$ and the cluster volume at 10 voxels between the ONFH patients and healthy controls corrected by a GRF correction. ONFH, Osteonecrosis of the femoral head; GRF, Gaussian random field; ALFF, amplitude of low-frequency fluctuations.

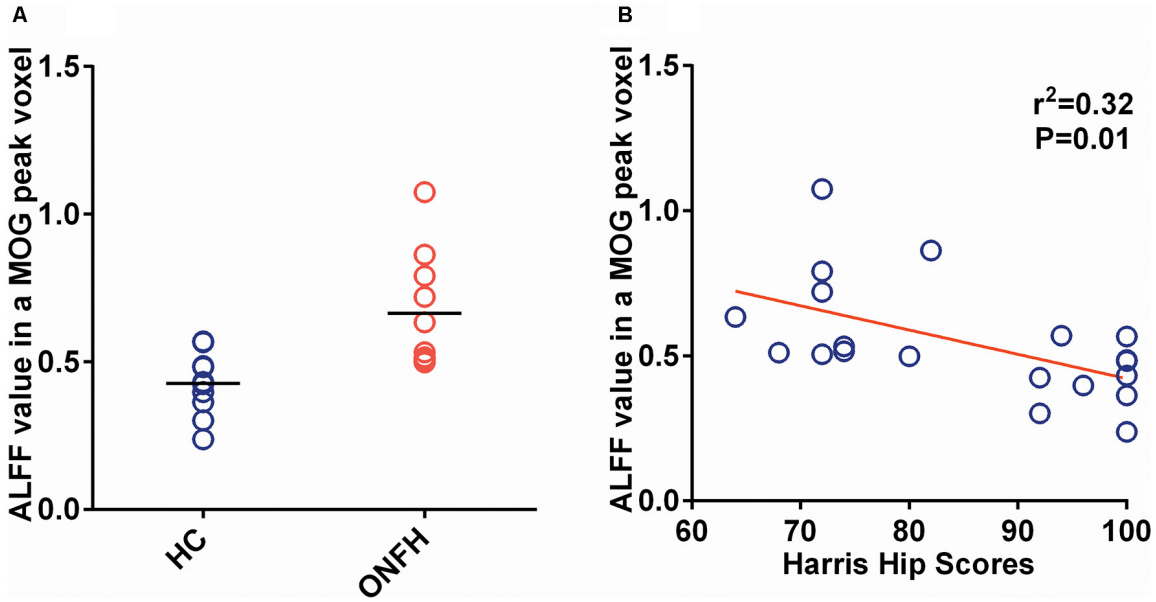

FIGURE 4 | The ALFF of the MOG and Correlation of the ALFF and Harris Hip Score. **(A)** A scatter plot representing the individual MOG ALFF values in the ONFH patients and healthy controls. The group means were different between the two groups and exhibited the following trend: $ALFF_{ONFH} < ALFF_{HC}$, where HC represents healthy control. There were significant differences between ONFH patients and healthy controls ($t = 3.387$, $P = 0.0033$). **(B)** The scatter plot between MOG ALFF and Harris hip scores, which has a linear regression as a significant negative correlation ($r^2 = 0.3195$, $P = 0.0094$). Abbreviations: ALFF, amplitude of low-frequency fluctuations; MOG, middle occipital gyrus; ONFH, osteonecrosis of the femoral head.

the MOG exhibits the most significant group difference in terms of the ALFF. Our results have demonstrated that the abnormal spontaneous intrinsic activity of several brain regions could be the underlying pathophysiology and brain region interconnecting relation in ONFH. Furthermore, the abnormal spontaneous activity of the MOG and frontal lobe leads to several problems that should be considered. In further studies, the following steps should be taken. First, a larger sample size should be used, and sex- and age-related changes should be investigated in different sexes and ages. Second, longitudinal studies on the changes in the intrinsic or spontaneous brain should be conducted in patients with ONFH. Third, patient groups with different stages of ONFH should be enrolled for group investigations.

DATA AVAILABILITY STATEMENT

The raw data supporting the conclusions of this article will be made available by the authors, without undue reservation.

ETHICS STATEMENT

The studies involving human participants were reviewed and approved by Medical Research Ethics Committee of Yueyang Hospital of Integrated Traditional Chinese and Western Medicine, Shanghai University of Traditional Chinese Medicine (2018-041-01). The patients/participants provided their written informed consent to participate in this study.

AUTHOR CONTRIBUTIONS

SF and XH performed statistical analysis and wrote the manuscript. XL, BZ, GL, and WL were involved in the fMRI scanning and data collection. BL and JX were responsible for the study design and research funding. All authors contributed to the article and approved the submitted version.

FUNDING

This work was supported by the Project of Improving TCM Characteristic Diagnosis and Treatment Technology, Shanghai Municipal Commission of Health and Family Planning (Grant No. Zyjx-2017006), Budget Item of Shanghai University of Traditional Chinese Medicine (Grant No. 18TS091), Preventive Health Program, Shanghai Municipal Health Committee [Grant No. ZY (2018–2020)-ZWB-1001-CPJS49)], and the National Key R&D Program of China (Grant No. 2018YFC2001600). The funding agencies had no role in the study design, data collection, data analysis, article writing, or decision in submitting the work for publication.

ACKNOWLEDGMENTS

We would like to thank the Department of Medical Imaging, Yueyang Hospital of Integrated Traditional Chinese and Western Medicine, Shanghai University of Traditional Chinese Medicine, Shanghai, China for the support in fMRI scanning.

REFERENCES

Barthas, F., Sellmeijer, J., Hugel, S., Waltisperger, E., Barrot, M., and Yalcin, I. (2015). The anterior cingulate cortex is a critical hub for pain-induced depression. *Biol. Psychiatry* 77, 236–245. doi: 10.1016/j.biopsych.2014.08.004

Burwell, R. D. (2000). The parahippocampal region: corticocortical connectivity. *Ann. N Y Acad. Sci.* 911, 25–42. doi: 10.1111/j.1749-6632.2000.tb06717.x

Canavero, S., and Bonicalzi, V. (2013). Role of primary somatosensory cortex in the coding of pain. *Pain* 154, 1156–1158. doi: 10.1016/j.pain.2013.02.032

Chen, X., Spaeth, R. B., Freeman, S. G., Scarborough, D. M., Hashmi, J. A., Wey, H. Y., et al. (2015). The modulation effect of longitudinal acupuncture on resting state functional connectivity in knee osteoarthritis patients. *Mol. Pain* 11:67. doi: 10.1186/s12990-015-0071-9

Flodin, P., Martinsen, S., Altawil, R., Waldheim, E., Lampa, J., Kosek, E., et al. (2016). Intrinsic brain connectivity in chronic pain: a resting-State fMRI study in patients with rheumatoid arthritis. *Front. Hum. Neurosci.* 10:107. doi: 10.3389/fnhum.2016.00107

Friston, K. J., Williams, S., Howard, R., Frackowiak, R. S., and Turner, R. (1996). Movement-related effects in fMRI time-series. *Magn. Reson. Med.* 35, 346–355. doi: 10.1002/mrm.1910350312

Golestani, A. M., Kwinta, J. B., Khatamian, Y. B., and Chen, J. J. (2017). The effect of low-frequency physiological correction on the reproducibility and specificity of resting-state fMRI metrics: functional connectivity, ALFF, and ReHo. *Front. Neurosci.* 11:546. doi: 10.3389/fnins.2017.00546

Kajimura, S., Kochiyama, T., Nakai, R., Abe, N., and Nomura, M. (2015). Fear of negative evaluation is associated with altered brain function in nonclinical subjects. *Psychiatry Res.* 234, 362–368. doi: 10.1016/j.pscychresns.2015.10.001

Kuroda, Y., Matsuda, S., and Akiyama, H. (2016). Joint-preserving regenerative therapy for patients with early-stage osteonecrosis of the femoral head. *Inflamm. Regen.* 36:4. doi: 10.1186/s41232-016-0002-9

Levy, I., Hasson, U., Avidan, G., Hendler, T., and Malach, R. (2001). Center-periphery organization of human object areas. *Nat. Neurosci.* 4, 533–539. doi: 10.1038/87490

Li, Z. R. (2015). Guideline for diagnostic and treatment of osteonecrosis of the femoral head. *Orthop. Surg.* 7, 200–207. doi: 10.1111/os.12193

Lu, C., Tao, Y., Zhao, H., Ming, Z., Meng, F., Hao, F., et al. (2016). Insular cortex is critical for the perception, modulation, and chronification of pain. *Neurosci. Bull.* 32, 191–201. doi: 10.1007/s12264-016-0016-y

Lumley, M. A., Cohen, J. L., Borszcz, G. S., Cano, A., Radcliffe, A. M., Porter, L. S., et al. (2011). Pain and emotion: a biopsychosocial review of recent research. *J. Clin. Psychol.* 67, 942–968. doi: 10.1002/jclp.20816

Lyby, P. S., Aslaksen, P. M., and Flaten, M. A. (2011). Variability in placebo analgesia and the role of fear of pain—an ERP study. *Pain* 152, 2405–2412. doi: 10.1016/j.pain.2011.07.010

Maeoka, H., Matsuo, A., Hiyamizu, M., Morioka, S., and Ando, H. (2012). Influence of transcranial direct current stimulation of the dorsolateral prefrontal cortex on pain related emotions: a study using electroencephalographic power spectrum analysis. *Neurosci. Lett.* 512, 12–16. doi: 10.1016/j.neulet.2012.01.037

Mistry, J. B., Jauregui, J. J., Lerner, A. L., Chughtai, M., Elmallah, R. K., and Mont, M. A. (2016). An assessment of the comprehensiveness of various hip outcome scores. *Surg. Technol. Int.* 28, 267–274.

Pyda, M., Koczy, B., Widuchowski, W., Widuchowska, M., Stoltny, T., Mielnik, M., et al. (2015). Hip resurfacing arthroplasty in treatment of avascular necrosis of the femoral head. *Med. Sci. Monit.* 21, 304–309. doi: 10.12659/msm.891031

Ranganath, C., and Ritchey, M. (2012). Two cortical systems for memory-guided behaviour. *Nat. Rev. Neurosci.* 13, 713–726. doi: 10.1038/nrn3338

Ryan, K., Goncalves, S., Bartha, R., and Duggal, N. (2018). Motor network recovery in patients with chronic spinal cord compression: a longitudinal study following decompression surgery. *J. Neurosurg. Spine* 28, 379–388. doi: 10.3171/2017.7.spine1768

Satterthwaite, T. D., Elliott, M. A., Gerraty, R. T., Ruparel, K., Loughead, J., Calkins, M. E., et al. (2013). An improved framework for confound regression and filtering for control of motion artifact in the preprocessing of resting-state functional connectivity data. *NeuroImage* 64, 240–256. doi: 10.1016/j.neuroimage.2012.08.052

Schrepf, A., Kaplan, C. M., Ichesco, E., Larkin, T., Harte, S. E., Harris, R. E., et al. (2018). A multi-modal MRI study of the central response to inflammation in rheumatoid arthritis. *Nat. Commun.* 9:2243. doi: 10.1038/s41467-018-04648-0

Stinear, C. M., Coxon, J. P., and Byblow, W. D. (2009). Primary motor cortex and movement prevention: where Stop meets Go. *Neurosci. Biobehav. Rev.* 33, 662–673. doi: 10.1016/j.neubiorev.2008.08.013

Sultan, A. A., Mohamed, N., Samuel, L. T., Chughtai, M., Sodhi, N., Krebs, V. E., et al. (2019). Classification systems of hip osteonecrosis: an updated review. *Int. Orthop.* 43, 1089–1095. doi: 10.1007/s00264-018-4018-4

Teng, C., Zhou, J., Ma, H., Tan, Y., Wu, X., Guan, C., et al. (2018). Abnormal resting state activity of left middle occipital gyrus and its functional connectivity in female patients with major depressive disorder. *BMC Psychiatry* 18:370. doi: 10.1186/s12888-018-1955-9

Tu, S., Qiu, J., Martens, U., and Zhang, Q. (2013). Category-selective attention modulates unconscious processes in the middle occipital gyrus. *Conscious. Cogn.* 22, 479–485. doi: 10.1016/j.concog.2013.02.007

Van den Stock, J., Vandenbulcke, M., Sinke, C. B., and de Gelder, B. (2014). Affective scenes influence fear perception of individual body expressions. *Hum. Brain Mapp.* 35, 492–502. doi: 10.1002/hbm.22195

Wang, Z., Yan, C., Zhao, C., Qi, Z., Zhou, W., Lu, J., et al. (2011). Spatial patterns of intrinsic brain activity in mild cognitive impairment and Alzheimer's disease: a resting-state functional MRI study. *Hum. Brain Mapp.* 32, 1720–1740. doi: 10.1002/hbm.21140

Xie, H., Xu, F., Chen, R., Luo, T., Chen, M., Fang, W., et al. (2013). Image formation of brain function in patients suffering from knee osteoarthritis treated with moxibustion. *J. Tradit. Chin. Med.* 33, 181–186. doi: 10.1016/s0254-6272(13)60122-3

Yan, C. G., Wang, X. D., Zuo, X. N., and Zang, Y. F. (2016). DPABI: data processing and analysis for (resting-state) brain imaging. *Neuroinformatics* 14, 339–351. doi: 10.1007/s12021-016-9299-4

Yu, R., Chien, Y. L., Wang, H. L., Liu, C. M., Liu, C. C., Hwang, T. J., et al. (2014). Frequency-specific alternations in the amplitude of low-frequency fluctuations in schizophrenia. *Hum. Brain Mapp.* 35, 627–637. doi: 10.1002/hbm.22203

Zhou, F., Huang, S., Zhuang, Y., Gao, L., and Gong, H. (2017). Frequency-dependent changes in local intrinsic oscillations in chronic primary insomnia: a study of the amplitude of low-frequency fluctuations in the resting state. *Neuroimage Clin.* 15, 458–465. doi: 10.1016/j.nicl.2016.05.011

Conflict of Interest: The authors declare that the research was conducted in the absence of any commercial or financial relationships that could be construed as a potential conflict of interest.

Copyright © 2020 Feng, Li, Li, Hua, Zhu, Li, Lu and Xu. This is an open-access article distributed under the terms of the Creative Commons Attribution License (CC BY). The use, distribution or reproduction in other forums is permitted, provided the original author(s) and the copyright owner(s) are credited and that the original publication in this journal is cited, in accordance with accepted academic practice. No use, distribution or reproduction is permitted which does not comply with these terms.

frontiers in Neural Circuits

ORIGINAL RESEARCH
published: 30 September 2020
doi: 10.3389/fncir.2020.563777

Effects of rTMS Treatment on Cognitive Impairment and Resting-State Brain Activity in Stroke Patients: A Randomized Clinical Trial

Mingyu Yin[1†], Yuanwen Liu[1†], Liying Zhang[1], Haiqing Zheng[1], Lingrong Peng[2], Yinan Ai[1], Jing Luo[1] and Xiquan Hu[1*]*

[1] Department of Rehabilitation Medicine, The Third Affiliated Hospital, Sun Yat-sen University, Guangzhou, China,
[2] Department of Radiology, The Third Affiliated Hospital, Sun Yat-sen University, Guangzhou, China

Background: Repetitive transcranial magnetic stimulation (rTMS) has been employed for motor function rehabilitation for stroke patients, but its effects on post-stroke cognitive impairment (PSCI) remains controversial.

Objective: To identify the effects of rTMS intervention on PSCI patients and its potential neural correlates to behavioral improvements.

Methods: We recruited 34 PSCI patients for 20 sessions of 10 Hz rTMS or no-stim control treatments over the left dorsal lateral prefrontal cortex (DLPFC). Cognitive function was evaluated with the Montreal Cognitive Assessment Scale, Victoria Stroop Test, Rivermead Behavior Memory Test, and Activities of Daily Living (ADL) assessed with the Modified Barthel Index. 14 patients received functional MRI scan, a useful non-invasive technique of determining how structurally segregated and functionally specialized brain areas were interconnected, which was reflected by blood oxygenation level–dependent signals. The amplitude of low-frequency fluctuation (ALFF) and functional connectivity (FC) were applied as the analytical approaches, which were used to measure the resting-state brain activity and functional connection.

Results: rTMS improved cognitive functions and ADLs for PSCI patients relative to patients who received no-stim control treatment. The cognitive improvements correlated to increased ALFF of the left medial prefrontal cortex, and increased FC of right medial prefrontal cortex and right ventral anterior cingulate cortex.

Conclusion: 10 Hz rTMS at DLPFC could improve cognitive function and quality of life for PSCI patients, which is associated with an altered frontal cortical activity.

Clinical Registration: Chinese Clinical Trial Registry, ChiCTR-IPR-17011908, http://www.chictr.org.cn/index.aspx.

Keywords: stroke, cognitive impairment, transcranial magnetic stimulation, amplitude of low frequency fluctuation, functional connectivity

OPEN ACCESS

Edited by:
Dongsheng Xu,
Tongji University, China

Reviewed by:
Simon Arthur Sharples,
University of St Andrews, United Kingdom
Anna Poggesi,
University of Florence, Italy

***Correspondence:**
Jing Luo
jill_272@foxmail.com
Xiquan Hu
xiquhu@hotmail.com

† These authors have contributed equally to this work

Received: *19 May 2020*
Accepted: *07 September 2020*
Published: *30 September 2020*

Citation:
Yin M, Liu Y, Zhang L, Zheng H, Peng L, Ai Y, Luo J and Hu X (2020) Effects of rTMS Treatment on Cognitive Impairment and Resting-State Brain Activity in Stroke Patients: A Randomized Clinical Trial. Front. Neural Circuits 14:563777. doi: 10.3389/fncir.2020.563777

INTRODUCTION

Post-stroke cognitive impairment (PSCI) impairs quality of life in stroke patients. One-third of all stroke patients have varying levels of cognitive impairment and 7% post-stroke patients develop dementia within 1 year (Leys et al., 2005; Sachdev et al., 2006). The core domains for PSCI include executive function, memory, attention, language, and visuospatial function while executive dysfunction and memory disorder are the most common clinical manifestation (Iadecola et al., 2019). With the development of the study of the brain network, cognitive impairments cannot be completely explained by the location after stroke but can be attributed to impairment of brain regions remote to the lesions. For these remote effects, it can be explained that the disruption of neuronal input is vital to the function of that remote brain region or of a certain network (Tuladhar et al., 2013). It has been widely accepted that stroke-induced damage to part of a brain network could have harmful effects on its entire function (Dijkhuizen et al., 2014). Functional MRI (fMRI) is a common imaging technique that has been used to investigate the functional change in the brains of patients with several psychiatric and neurological disorders (Sun et al., 2011). Among them, resting-state fMRI (rs-fMRI) measures spontaneous fluctuations in neural signaling, detected as low-frequency blood oxygenation level–dependent oscillations, which are synchronized among functionally connected brain regions (Dijkhuizen et al., 2014). Previous studies have applied the rs-fMRI technique, which suggested that the patients with PSCI have less functional connectivity within the brain networks (Ding et al., 2014; Dacosta-Aguayo et al., 2015).

The interventions of PSCI included controlling vascular risk factors, pharmacological treatments such as cholinesterase inhibitors (galantamine, donepezil, rivastigmine), the *N*-methyl D-aspartate antagonist memantine, and various Chinese medicines, cognitive training, and non-invasive stimulation (Beristain and Golombievski, 2015; Iadecola et al., 2019). Recently, repetitive transcranial magnetic stimulation (rTMS) is a non-invasive and relatively safe electrophysiological technique, based on the principle of electromagnetic induction of an electric field in the brain, that has been widely used in the field of rehabilitation of post-stroke dysfunctions such as motor disorder, neglect, and swallowing impairment (Winstein et al., 2016; Dionisio et al., 2018; Lefaucheur et al., 2020). Nevertheless, there are few studies about the treatment of PSCI by rTMS, and its therapeutic effects remain unclear. Rektorova et al. (2005) observed that high-frequency rTMS applied over the left DLPFC may induce positive effects on executive functioning in patients with cerebrovascular disease. However, the sample size was only seven and further studies involving larger sample sizes needed to be performed. Although some studies have not detected significant effects, others have found that the effects of rTMS treatment are not as significant as that of cognitive training, which may be related to factors such as choice of scale, rTMS parameters, and insufficient sample size (Kim et al., 2010; Park and Yoon, 2015). Therefore, the therapeutic effects of rTMS for PSCI patients remain controversial and further research is required.

In the present study, we examined the effects of rTMS on cognitive functions by expanding the sample size, modifying the rTMS parameters, and evaluating the overall cognitive function, especially the executive and memory function, and activities of daily living (ADL) that is closely related to cognition recovery. We measured two markers for resting-state fMRI including the amplitude of low-frequency fluctuations (ALFF) (0.01–0.08 Hz) of the blood oxygenation level–dependent signal used to reflect spontaneous neural activity and functional connectivity (FC) used to investigate the functional relationship between different regions at a network level (Liu et al., 2014; Lei et al., 2017; Pan et al., 2017). We expect to identify potential neural correlates to behavioral improvements following rTMS intervention on these PSCI patients.

MATERIALS AND METHODS

Participants

A total of 34 PSCI patients were recruited for the present study between August 2017 and August 2019, which were subdivided for rTMS (n = 16) and no-stim control (n = 18) treatment groups using a computer-generated list of random numbers. MRI scanning was completed in seven patients in each group (**Figure 1**). Demographics and clinical characteristics are presented in **Tables 1**, **2**. There was no difference between the two groups in terms of demographic and clinical characteristics.

Written informed consent was obtained from all patients before the treatments and the study was approved by the Institutional Ethics Committee of The Third Affiliated Hospital of Sun Yat-sen University and registered at Chictr.org (Chinese Clinical Trial Registry Unique Identifier: ChiCTR-IPR-17011908, date of registration: July 8, 2017).

The inclusion criteria were as follows: (1) stroke patients in accordance with the diagnostic criteria established by the fourth National Cerebrovascular Disease Academic Conference in 1995 confirmed by a brain CT or MRI; (2) first-ever stroke, course of stroke between 1 and 6 months; (3) right-handed; (4) aged 30–75 years; (5) the presence of cognitive impairments (Montreal Cognitive Assessment, MoCA $<$ 26); (6) no severe aphasia and able of accomplishing cognitive tests; (7) stable vital signs, no progression of neurological symptoms; (8) normal cognitive functions before stroke; (9) capable of tolerating MRI scan; (10) voluntary participation and signed the informed consent.

The exclusion criteria were as follows: (1) non-first stroke; (2) complete left prefrontal cortex injury confirmed by CT/MRI; (3) transcranial surgery or skull defect; (4) metal or cardiac pacemaker implants; (5) history of brain tumor, brain trauma, seizures, and risks of seizures; (6) cognitive function recession before stroke; (7) any neuropsychiatric comorbidity and affective disorder that could influence the test outcomes; (8) any other factors that could affect cognitive assessments and treatments.

Outcome Measurements

The primary outcome measure, Montreal Cognitive Assessment (MoCA), was used for evaluating the general cognitive function. The secondary outcome measures were Victoria Stroop Test

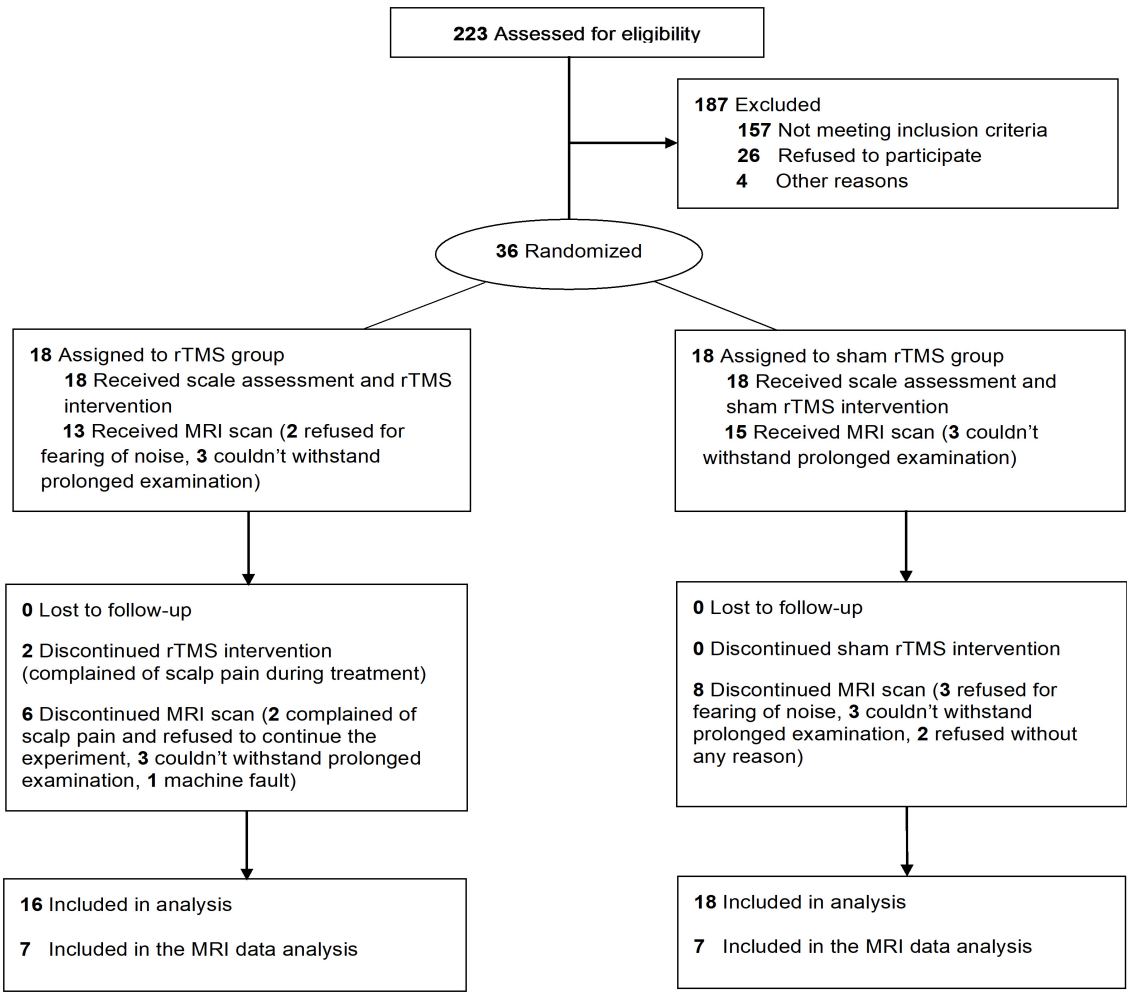

FIGURE 1 | Trial flowchart.

(VST), Rivermead Behavior Memory Test (RBMT), and Modified Barthel Index (MBI), which were used for evaluating executive function, memory, and activities of daily living (ADL). All the assessments were conducted before treatments, after 2-week treatments, and after 4-week treatments (the day after the final treatments) by an independent occupational therapist.

MoCA is widely used for evaluating cognitive functions containing seven cognitive subtests: visual-executive, naming, attention, language, abstraction, delayed recall, and orientation. One point is added for patients with or less than 12 years of schooling (Nasreddine et al., 2005).

VST, a brief version of Stroop test, is more suitable for patients with brain injury, which consists of three test cards: a colored dots trail (A), a neutral words trail (B), and an incongruent-colored words trail (C). Each card contains 24 dots/words and the outcome measures are the time consumed and the number of making errors when reading (Bayard et al., 2011; Tremblay et al., 2016).

RBMT is designed to evaluate daily memory ability, which is made up of 11 subtests: remembering names, remembering hidden belongings, remembering an appointment, picture recognition, prose recall, recalling a short route, remembering an errand, orientation, and date and face recognition (Lu et al., 2015).

MBI is used to assess the ADL including 10 subtests: personal hygiene, bathing, feeding, toileting, stair climbing, dressing, bowel control, bladder control, ambulation, or wheelchair and chair–bed transfer (Leung et al., 2007).

rTMS Procedure

rTMS treatment was conducted with a MagPro X100 magnetic stimulators (The MagVenture Company, Denmark) and a standard figure-of-eight air-cooled coil (MCF-B65). To detect motor evoked potentials, we used the disposable ECG electrode from Xi'an fude (SEAg-J-22 × 32). Acquisition software was MAGPRO G3. Amplifier type was differential digital amplifier named Magpro MEP Monitor. Filter was high pass 20 Hz–low pass 10 kHz. The sampling rate was 100 kHz. Magnification factor was common mode rejection ratio, > 55 dB. Before stimulating, a recording electrode was attached to the contralesional first dorsal

TABLE 1 | Baseline characteristics of all the patients with PSCI enrolled.

Variables	rTMS (*N* = 16)	No-stim control (*N* = 18)	*P*	χ^2/ *t*/*z* value	*df*
Sex (male/female)	14/2	16/2	0.90	0.02	1
Age, mean (SD), years	56.69 (12.92)	58.17 (11.27)	0.72	−0.36	32
Type of stroke (hemorrhagic/ischemic)	5/11	6/12	0.90	0.02	1
Side of stroke (left/right/bilateral)	4/6/6	6/7/5	0.91	0.51	2
Education, mean (SD), years	10.03 (4.15)	9.33 (3.87)	0.62	0.51	32
Disease duration, median (IQR), days	52 (38.25–98.75)	55 (39.75–94.75)	0.88	−0.16	
MoCA score, mean (SD)	13.06 (6.90)	14.72 (5.76)	0.45	−0.76	32
VST-A: time, median (IQR), s	42 (35.50–63)	42.50 (33.50–51.25)	0.80	−0.26	
VST-B: time, median (IQR), s	67.50 (48.50–92.50)	48.50 (37.75–120)	0.57	−0.57	
VST-C: time, mean (SD), s	100.13 (41.38)	107.72 (61.35)	0.68	−0.42	32
VST-A: error words, median (IQR)	0.50 (0–1)	1.50 (0–2)	0.12	−1.56	
VST-B: error words, median (IQR)	1.50 (0–4)	2.50 (0–6)	0.46	-0.74	
VST-C: error words, mean (SD)	4.94 (2.67)	5.72 (3.89)	0.50	-0.68	32
RBMT score, mean (SD)	7.75 (4.36)	9.33 (5.76)	0.38	-0.90	32
MBI score, mean (SD)	48.06 (19.52)	50.33 (24.03)	0.77	-0.30	32

PSCI, post-stroke cognitive impairment; rTMS, repetitive transcranial magnetic stimulation; MoCA, Montreal Cognitive Assessment Scale; VST, Victoria Stroop Test; RBMT, Rivermead Behavior Memory Test; MBI, Modified Barthel Index. Data presented as mean (SD) or median (interquartile range, IQR).

TABLE 2 | Baseline characteristics of PSCI patients with fMRI scan.

Variables	rTMS (*N* = 7)	No-stim control (*N* = 7)	*P*	χ^2/ *t*/*z* value	*df*
Sex (male/female)	6/1	5/2	0.52	0.42	1
Age, median (IQR), years	58 (41–65)	62 (40–63)	1	0.00	
Type of stroke (hemorrhagic/ischemic)	3/4	3/4	1	0.00	1
Side of stroke (left/right/bilateral)	3/3/1	3/3/1	1	0.00	2
Education, median (IQR), years	12 (12–16)	11 (3–12)	0.21	−1.32	
Disease duration, mean (SD), days	84.86 (50.43)	76.14 (48.79)	0.75	0.33	12
MoCA score, mean (SD)	13.29 (7.65)	11.29 (6.50)	0.61	0.53	12
VST-A: time, mean (SD), s	42.14 (17.31)	56 (33.90)	0.35	−0.96	12
VST-B: time, median (IQR), s	61 (50–70)	38 (33–123)	0.95	−0.06	
VST-C: time, mean (SD), s	88.71 (24.62)	108.71 (61.02)	0.44	−0.80	12
VST-A: error words, median (IQR)	0 (0–1)	2 (0–4)	0.24	−1.17	
VST-B: error words, median (IQR)	0 (0–3)	4 (0–7)	0.42	-0.80	
VST-C: error words, mean (SD)	4.14 (3.13)	5.86 (3.53)	0.36	-0.96	
RBMT score, mean (SD)	7.86 (6.26)	7.71 (5.35)	0.96	0.05	
MBI score, median (IQR)	27 (26–70)	45 (37–65)	0.48	-0.70	

PSCI, post-stroke cognitive impairment; fMRI, functional MRI; rTMS, repetitive transcranial magnetic stimulation; MoCA, Montreal Cognitive Assessment Scale; VST, Victoria Stroop Test; RBMT, Rivermead Behavior Memory Test; MBI, Modified Barthel Index. Data presented as mean (SD) or median (interquartile range, IQR).

interosseous (FDI) muscle of the patients as the target muscle and the minimal stimulus intensity required to produce motor evoked potential $> 50\ \mu V$ in more than 5 out of 10 trials was defined as resting motor threshold (MT) (Rossi et al., 2009).

Then, 10-Hz rTMS was applied at 80% RMT, with trains of 5-s duration (50 pulses per train), 25-s inter-train interval, and a of total 40 trains (2000 pulses) costing 20 min on the left side of the DLPFC each day. We determined the optimum position for activation of the right FDI muscle by moving the coil in 0.5-cm steps around the presumed hand area of the left M1. The site at which stimuli of slightly suprathreshold intensity consistently produced the largest MEPs in the target muscle was marked as the "FDI hot spot." For L-DLFPC stimulation, the rTMS coil was positioned 5 cm anterior to the left "FDI hot spot" (Rektorova et al., 2005). For rTMS group, the stimulating coil was placed tangentially to the surface of the skull, whereas for the no-stim control group, the coil was placed perpendicularly to the surface of the skull inducing no magnetic field. All patients received treatments once a day, 5 days per week for 4 weeks.

After rTMS treatments, patients received a 30-min computer-assisted cognitive rehabilitation referring to attention, executive function, memory, calculation, language and visuospatial skills, etc. Therapists were blinded to assignments. Besides, during hospitalization, patients received conventional drug treatments recommended by the 2016 American Heart Association/American Stroke Association recommendation (Winstein et al., 2016).

MRI Image Acquisition and Data Pre-processing

Images were obtained before treatments and after the last rTMS treatments using a 3.0-T Discovery MR 750 Scanner (General Electric Company, United States) with an eight-channel phased array head coil. Patients were required to remain awake with their eyes closed without thinking anything. High-resolution T1-weighted structural MRI was acquired with a 3D T1-BRAVO echo sequence with parameters as follows: repetition time/echo time = 7.8 ms/3.0 ms, flip angle = 13°, field of view = 256 × 256 mm, matrix = 256 × 256, slice thickness = 1.0 mm, voxel size = 1 mm × 1 mm × 1 mm, and 176 slices. Resting fMRI was acquired using an echo-planar-imaging sequence: repetition time/echo time = 2000/30 ms, flip angle = 90°, field of view = 230 × 230 mm, matrix = 64 × 64, slices = 33, slice thickness = 3.6 mm, gap = 0.6 mm, voxel size = 3.6 mm × 3.6 mm × 3.6 mm, and total volumes = 240.

Functional images were preprocessed with the Data Processing Assistant for Resting-State fMRI software (DPARSF[1]) (Chao-Gan and Yu-Feng, 2010), which is based on Statistical Parametric Mapping 8. For each subject, the first 10 volumes were discarded to allow the mean magnetization to reach a steady state and the participants to get familiar to the MR scan environment. The remaining data were then corrected for the acquisition time difference between the 2D image slices and were realigned to the first volume to correct head motions. The maximum translational motion of all subjects was less than 3 mm and the maximum rotation was less than 3°. Images were registered with the 3D T1-weighted structural MRI and subsequently registered into the MNI standard space using the transform defined based on the registration process of the T1-weighted MRI (to the MNI space). They were then smoothed with an isotropic 3D Gaussian kernel with a full width at half maximum of 6 mm^3. Finally, band-pass filtering ($0.01 < f < 0.08$ Hz) was performed and a linear trend was removed.

ALFF and FC Analysis

ALFF analysis was performed using the Resting-State fMRI Data Analysis Toolkit (REST V1.8[2]) (Chao-Gan and Yu-Feng, 2010). In summary, for a given voxel, a fast Fourier transformation was used to convert the time course to the frequency domain. The mean square root, being computed and averaged throughout 0.01–0.08 Hz at each voxel, was regarded as the ALFF. Also, individual ALFF map was divided by the global mean ALFF within the mask for standardization purposes. Finally, all ALFF maps were spatially smoothed with a 6-mm full-width at half-maximum Gaussian kernel.

Regions showing significant ALFF differences after rTMS treatments were finally defined as regions of interest (ROIs), which were chosen as the seeds for FC analysis. Then, correlation analysis was performed between the seed and the whole brain in a voxel-wise manner. Finally, an entire brain *z*-value map was created after normalizing these FC values calculated from the correlation analysis by Fisher r-to-z transformation.

Statistical Analysis

Statistical analyses were performed with SPSS V.22.0 software (IBM, Armonk, NY, United States). Shapiro–Wilk tests were used to examine the normal distribution. Two-way repeated-measures ANOVA with Bonferroni correction for *post hoc* comparisons was conducted to assess the dynamic differences within and between groups over time for clinical assessments including MoCA, VST, RBMT, and MBI scales (a log or square-root transformation was applied to achieve a normal distribution when the data were non-normally distributed). Two-sample *t*-test and non-parametric Mann–Whitney tests were used to compare two groups in terms of continuous variables, and the χ^2 test was used for categorical variables. Pearson correlations were used to measure the association between primary outcome and secondary outcomes. Normally distributed data were expressed as mean (SD) whereas non-normally distributed data were expressed as the median (interquartile range). The significance threshold was set to $P < 0.05$. Paired *t*-test and one-sample *t*-test were performed on the maps of ALFF and FC to obtain functional differences (cluster-wise false discovery rate (FDR) corrected, voxel-level $P < 0.005$). Regions showing significant ALFF and FC differences after rTMS treatments were defined as regions of interest (ROIs). ALFF and FC values were subsequently extracted from the seed regions within each subject. Pearson correlations were calculated to measure the association between the change of neuropsychological test and the change of ALFF and FC values.

RESULTS

Primary Outcome Changes

For the primary outcome, two-way repeated measures ANOVA of MoCA test revealed a significant interaction effect between group and time ($F = 17.5$, $df = 1.5$, $P < 0.001$). Pairwise comparisons showed that the MoCA score in both groups increased significantly after 2 and 4 weeks ($P < 0.05$) and the score for rTMS group was significantly higher than that in the no-stim control group after 4-week treatments ($P = 0.03$) (**Figure 2A**).

Secondary Outcome Changes

Referring to memory ability, two-way repeated measures ANOVA of RBMT revealed a significant interaction effect between group and time ($F = 5.2$, $df = 2$, $P = 0.008$). Pairwise comparisons showed that RBMT score increased significantly for rTMS group after 2- and 4-week treatments ($P < 0.001$), and for no-stim control group after 4-week treatment ($P = 0.003$) (**Figure 2B**).

[1]http://www.rfmri.org/DPARSF

[2]http://restfmri.net/forum/REST

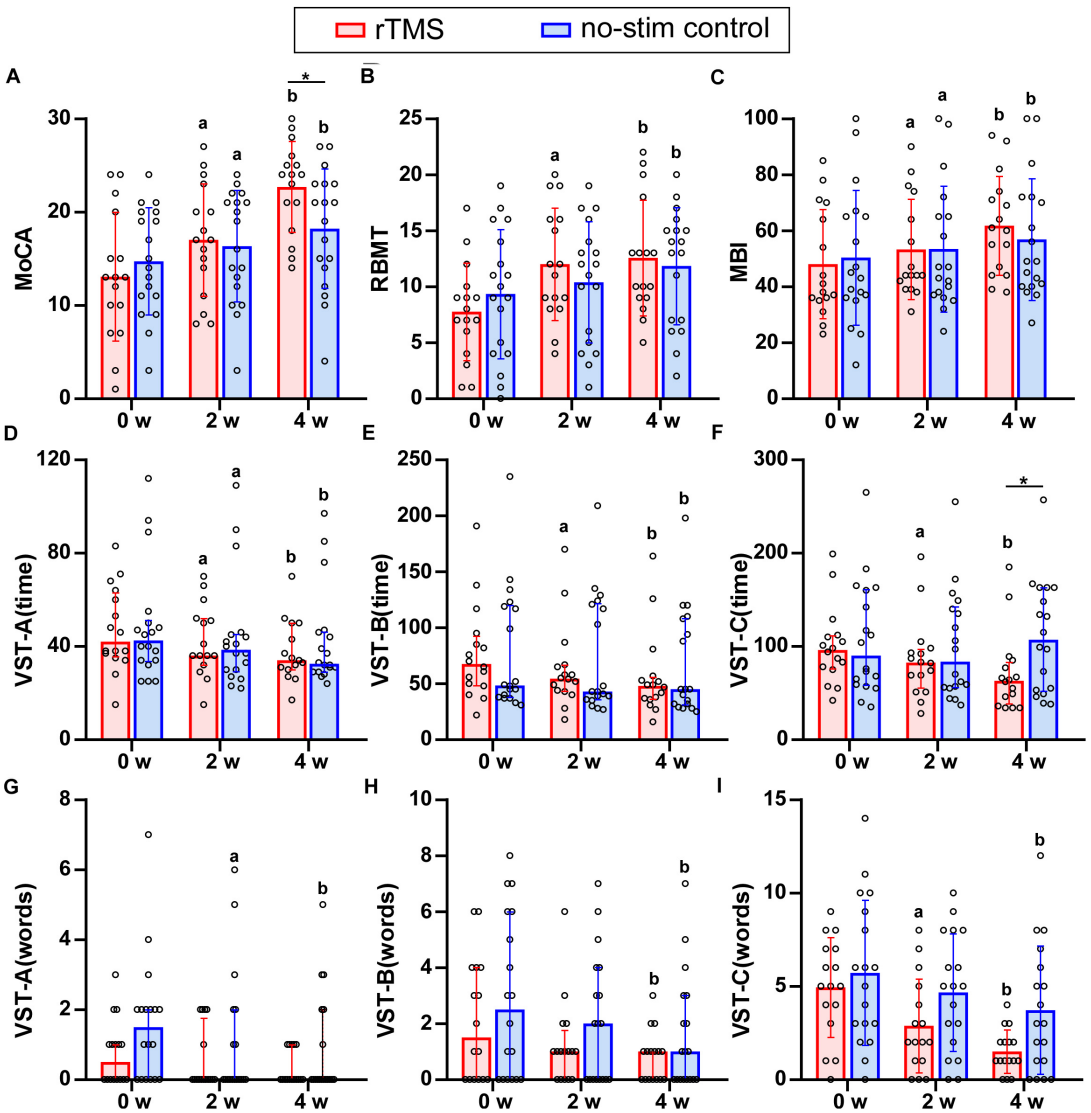

FIGURE 2 | Results of neuropsychological test for rTMS group or no-stim control group. **(A)** Differences in MoCA score. **(B)** Differences in RBMT score. **(C)** Differences in MBI score. **(D–I)** Differences in the time consumed and number of making error words of VST scale. Data are analyzed by two-way repeated measures ANOVA. **(A,B,C,I)** Tops of column indicate mean and vertical lines demote SD. **(D–H)** Tops of column indicate median and vertical lines denote 25th and 75th percentiles. rTMS group is colored in red and no-stim control group is colored in blue. $^{a}P < 0.05$: intra-group comparison (0w vs. 2w). $^{b}P < 0.05$: intra-group comparison (0w vs. 4w). $^{*}P < 0.05$: inter-group comparison.

Regarding the ADL, two-way repeated measures ANOVA of MBI test showed a significant interaction effect between group and time ($F = 5.74$, $df = 1.25$, $P = 0.02$). Pairwise comparisons showed that MBI scores increased significantly after 2 and 4 weeks of treatments for both groups ($P < 0.05$) (**Figure 2C**).

There was no significant difference in the group-by-time interaction for the two-way repeated measures ANOVA of VST-A (time) ($F = 1.07$, $df = 1.39$, $P = 0.33$), VST-A (error words) ($F = 0.70$, $df = 2$, $P = 0.50$), VST-B (error words) ($F = 0.58$, $df = 2$, $P = 0.94$), and VST-C (error words) ($F = 2.91$, $df = 2$, $P = 0.06$), whereas a significant interaction between group and time was found in VST-B (time) ($F = 4.81$, $df = 1.29$, $P = 0.03$) and VST-C (time) ($F = 10.11$, $df = 1.21$, $P = 0.002$). Pairwise comparisons revealed that the time consumed of VST-C in rTMS group was significantly lower than that in the no-stim control group after 4 weeks of treatments ($P = 0.03$) (**Figures 2D–I**).

Comparison of the Improvement of Neuropsychological Test Between rTMS Group and No-Stim Control Group

Two-sample *t*-tests were used for the analysis of VST-A (time), VST-C (error words) (4w), and RBMT (4w) and non-parametric Mann–Whitney *U* tests were used for the analysis of MoCA, RBMT (2w), and the other parts of VST test. The improvement of the MoCA score for rTMS group was significantly higher than

that in the no-stim control group after 2 weeks ($Z = -3.25$, $P = 0.001$) and 4 weeks of treatments ($Z = -4$, $P < 0.001$) (**Figure 3A**). The improvement of the RBMT score for rTMS group was significantly higher than that in the no-stim control group after 2 weeks ($Z = -2.46$, $P = 0.01$) and 4 weeks of treatments ($F = 1.15$, $t = 2.29$, df = 32, $P = 0.03$) (**Figure 3B**). Moreover, the improvement of the MBI score for rTMS group was significantly higher than that in the no-stim control group after 4 weeks of treatments ($Z = -3.08$, $P = 0.002$) (**Figure 3C**). There was no difference between the two groups in the reduction of time consumed of VST-A (**Figure 3D**). The reduction of time consumed of VST-B was significantly higher than that in the no-stim control group after 2 weeks (Z = −2.56, $P = 0.01$) and 4 weeks of treatments ($Z = -2.13$, $P = 0.03$) (**Figure 3E**), and similar results were found in VST-C (2 weeks, $Z = -2.17$, $P = 0.03$; 4 weeks, Z = −3.18, $P = 0.001$) (**Figure 3F**). There was no difference between the two groups in the reduction of number of making error words of VST-A and VST-B (**Figure 3G–H**). The reduction of the number of making error words of VST-C for rTMS group was significantly higher than that in the no-stim control group after 4 weeks of treatments ($F = 1.29$, $t = 2.16$, df = 32, $P = 0.04$) (**Figure 3I**). The number of making error words of VST-C for rTMS group was also significantly higher than that in the no-stim control group after 4 weeks of treatments ($F = 1.29$, $t = 2.16$, df = 32, $P = 0.04$) (**Figure 3I**).

Changes of MoCA Test for Sub-Items

By using two-way repeated measures ANOVA for analyzing the seven sub-items of the MoCA test, significant interaction effects between group and time were found in the cognitive domain of visuospatial and executive functioning ($F = 20.27$, $df = 1.49$, $P = 0.001$), attention ($F = 4.42$, $df = 1.66$, $P = 0.02$), and delayed

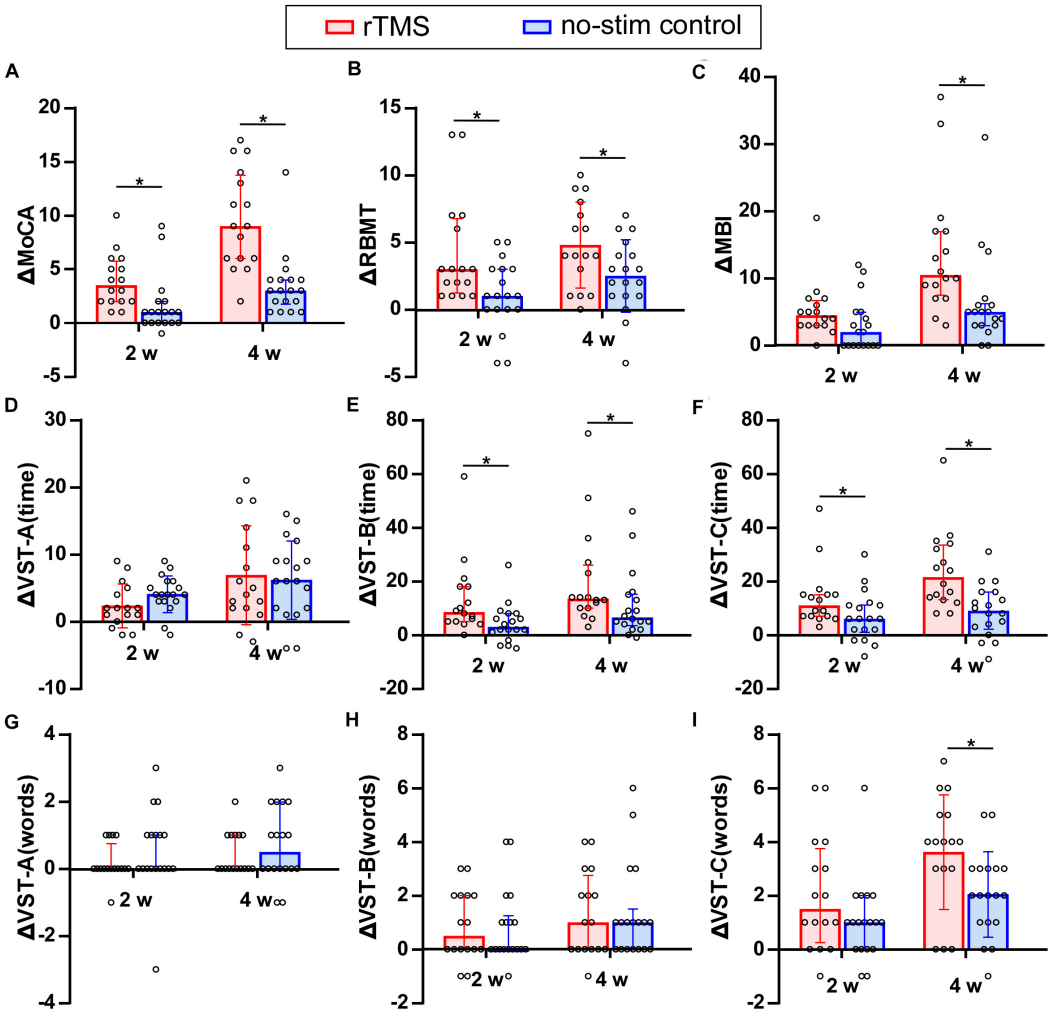

FIGURE 3 | Comparison of the improvement of neuropsychological test between rTMS group and no-stim control group. **(A)** Differences in MoCA score. **(B)** Differences in RBMT score. **(C)** Differences in MBI score. **(D–I)** Differences in the time consumed and number of making error words of VST scale. The panels **(A,B-2w,C,E–H,I-2w)** are non-normally distributed data and analyzed by non-parametric Mann–Whitney *U* test. Tops of column indicate median and vertical lines demote 25th and 75th percentiles. The panels **(B-4w,D,I-4w)** are normally distributed data and analyzed by two-sample *t*-test. Tops of column indicate mean and vertical lines denote SD. rTMS group is colored in red and no-stim control group is colored in blue. *$P < 0.05$: inter-group comparison.

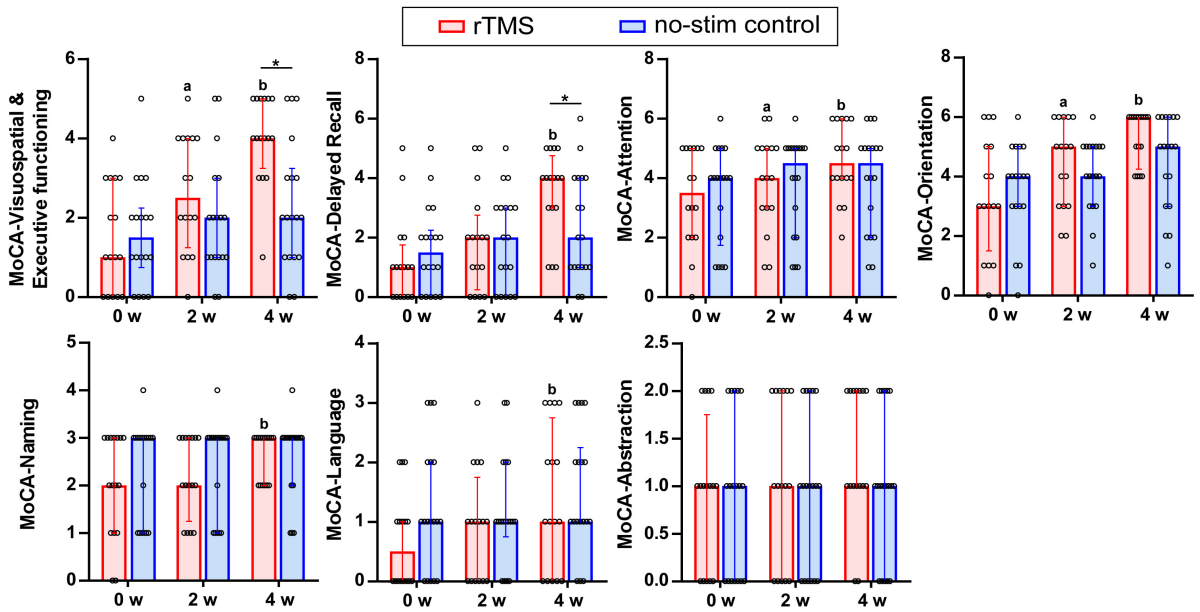

FIGURE 4 | Sub-items of the MOCA test in detail. Data are analyzed by two-way repeated measures ANOVA. Tops of column indicate median and vertical lines demote 25th and 75th percentiles. rTMS group is colored in red and no-stim control group is colored in blue. $^{a}P < 0.05$: intra-group comparison (0w vs. 2w). $^{b}P < 0.05$: intra-group comparison (0w vs. 4w). $^{*}P < 0.05$: inter-group comparison.

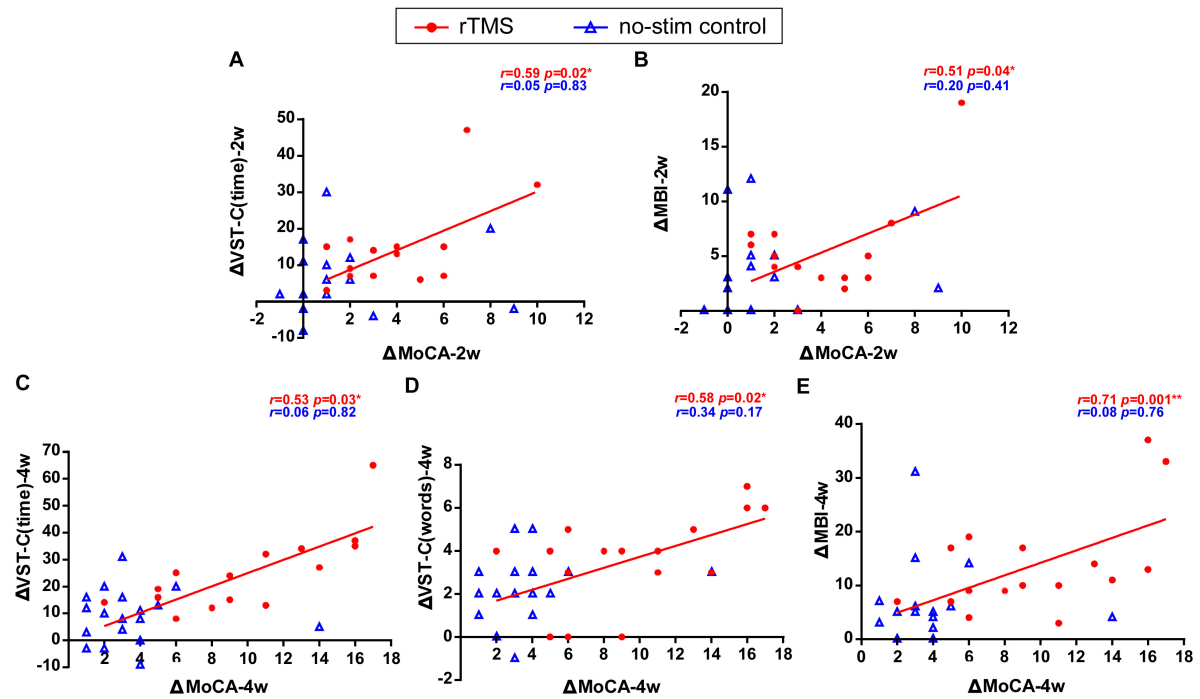

FIGURE 5 | Correlation of changes for the primary outcome and the secondary outcomes. Data are analyzed by Pearson correlations. **(A)** The improvement of the score of MoCA test positively correlated with the reduction of the time consumed of VST-C after 2 weeks of rTMS treatments. **(B)** The improvement of the score of MoCA test positively correlated with the improvement of the score of MBI test after 2 weeks of rTMS treatments. **(C)** The improvement of the score of MoCA test positively correlated with the reduction of the time consumed of VST-C after 4 weeks of rTMS treatments. **(D)** The improvement of the score of MoCA test positively correlated with the reduction of the number of making error words of VST-C after 4 weeks of rTMS treatments. **(E)** The improvement of the score of MoCA test positively correlated with the improvement of the score of MBI test after 4 weeks of rTMS treatments.

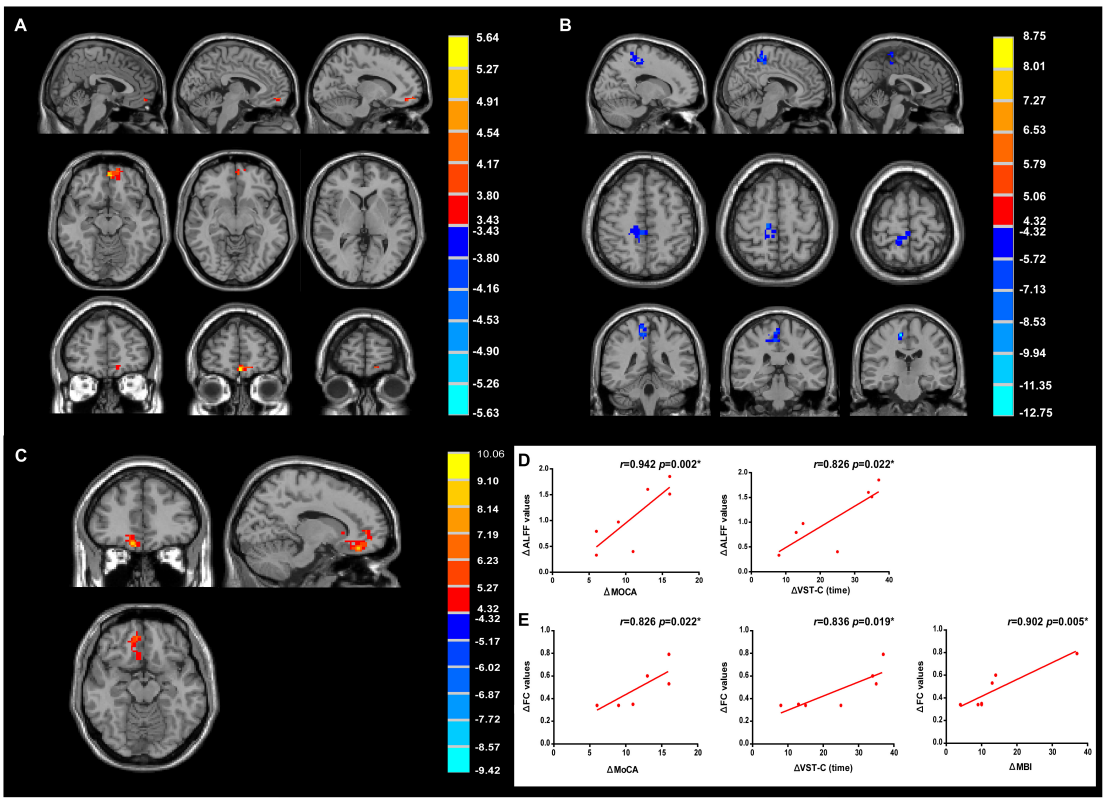

FIGURE 6 | Modulation of amplitude of low-frequency fluctuation (ALFF) and functional connectivity (FC) after treatments. **(A)** Change of ALFF in rTMS group. **(B)** Change of ALFF in no-stim control group. **(C)** Increased FC in rTMS group. Significance level was defined at $P < 0.005$, cluster size > 51 voxels. FDR corrected. The left side of the image corresponds to the right side of the brain. **(D)** The improvement of MoCA and VST-C test positively correlated with the change of ALFF values. **(E)** The improvement of MoCA, VST-C, and MBI test positively correlated with the change of FC values.

recall ($F = 6.90$, $df = 2$, $P = 0.002$). Pairwise comparisons showed that rTMS group differed significantly from no-stim control group in executive functioning ($P = 0.003$) as well as delayed recall ($P = 0.04$) (**Figure 4**).

Correlation of Changes for the Primary Outcome and the Secondary Outcomes

The correlation results showed that the change of the scores of MoCA test after 2 weeks of rTMS treatments positively correlated with the reduction of time consumed of VST-C test ($r = 0.59$, $P = 0.02$) (**Figure 5A**) and the improvement of the scores of MBI test ($r = 0.51$, $P = 0.04$) (**Figure 5B**). Besides, after 4 weeks of rTMS treatments, the change of scores of MoCA test positively correlated with the reduction of time consumed of VST-C test ($r = 0.53$, $P = 0.03$) (**Figure 5C**), the reduction of numbers of making error words of VST-C test ($r = 0.58$, $P = 0.02$) (**Figure 5D**), and the improvement of the scores of MBI test ($r = 0.71$, $P = 0.001$) (**Figure 5E**).

Effects of rTMS Treatment on Neural Activity and Connectivity

With 10 Hz left DLPFC rTMS treatments, ALFF in the left medial prefrontal cortex (peak MNI coordinates: $x = -5$, $y = 57$, $z = -15$, $P < 0.005$, $t = 5.64$, voxels = 53, corrected by FDR) (**Figure 6A** and **Table 3**) was significantly increased, whereas for no-stim control treated group, significantly decreased ALFF was found in the right posterior parietal cortex (peak MNI coordinates: $x = 12$, $y = -24$, $z = 57$, $P < 0.005$, $t = -12.75$, voxels = 135, corrected by FDR) (**Figure 6B** and **Table 3**).

Further FC analysis was based on the ROIs (the regions showing significant ALFF differences after rTMS treatments), and the results showed that FC increased significantly in the right medial prefrontal cortex (peak MNI coordinates: $x = 9$, $y = 45$, $z = -18$, $P < 0.005$, $t = 7.19$, voxels = 69, corrected by FDR) and the right ventral anterior cingulate cortex (vACC) (peak MNI coordinates: $x = 10$, $y = 28$, $z = -14$, $P < 0.005$, $t = 10.06$, voxels = 56, corrected by FDR) (**Figure 6C** and **Table 3**).

Correlation analyses revealed that the change of the ALFF values of the left medial prefrontal cortex positively correlated with the improvement of the score of MoCA test ($r = 0.942$, $P = 0.002$) and the reduction of time consumed of VST-C ($r = 0.826$, $P = 0.022$) after rTMS treatments (**Figure 6D**). In addition, positive correlation between the change of the FC values of the right medial prefrontal cortex, vACC, and the improvement of MoCA ($r = 0.826$, $P = 0.022$), VST-C ($r = 0.836$,

TABLE 3 | Changes of ALFF and FC in rTMS group and no-stim control group after 4-week treatments.

Brain regions	Brodmann's area	MNI coordinates			Peak *t*-value	Voxels
		x	y	z		
ALFF						
rTMS (4w > baseline)						
L-MPFC	10	−5	57	−15	5.64	53
No-stim control (4w > baseline)						
R-PPC	6	12	−24	57	−12.75	135
FC						
R-MPFC	10	9	45	−18	7.19	69
R-vACC	25	10	28	−14	10.06	56

ALFF, amplitude of low-frequency fluctuation; FC, functional connectivity; MNI, Montreal Neurological Institute coordinates; L, left; R, right; MPFC, medial prefrontal cortex; PPC, posterior parietal cortex; vACC, right ventral anterior cingulate cortex.

P = 0.019), and MBI test (r = 0.902, P = 0.005) after rTMS treatments were identified (**Figure 6E**).

DISCUSSION

The present study reported the effects of chronic high-frequency rTMS at DLPFC on the improvement of cognitive function and life quality in PSCI patients. These changes accompanied altered activation of local frontal regions and connectivity changes within the frontal network. These results demonstrated that DLPFC rTMS treatment is tolerable, therapeutically effective for PSCI patients, and warrants larger clinical trials in future studies.

We found that rTMS at DLPFC improved executive function for PSCI patients. The results were in accordance with a previous study reporting that TMS improves executive function for patients of cerebrovascular disease with cognitive impairment (Rektorova et al., 2005). In addition, the memory improvement was inconsistent with a previous study using 1-Hz rTMS at the right DLPFC for stroke patients (Lu et al., 2015), in which they reported peripheral brain-derived neurotrophic factor (BDNF) changes as well. It is undetermined if peripheral biomarkers (e.g., BDNF) could predict the clinical improvements for the cognitive function of these patients. One study found that rTMS treatment at DLPFC improves emotion but not cognitive function for PSCI patients (Kim et al., 2010). It is undeniable that rTMS could improve mood disorder for patients with PSCI. However, the study was not sufficiently powered to detect positive effects on cognition and may likely be a result of their incomplete scale, stimulus parameters, and small sample size. Furthermore, cognitive dysfunction had a strong impact on the ADL (Paker et al., 2010). Cognitive functioning early after stroke was found to be an independent predictor of long-term functional outcomes of ADL (McKinney et al., 2002). Our results showed that a higher MoCA score was associated with better performance on MBI score. Irfani et al. (2020) found a positive association between cognitive function and ADL in post-stroke patients and the improvement of ADL may be a result of the recovery of working memory, referring to maintain and manipulate information, which is processed by the frontal lobe. Liu et al. (2020) have also demonstrated that TMS could improve the performance in the ADL and attention function in patients with stroke, which is in line with our study.

The reason we chose DLPFC as a stimulus site is that the DLPFC is related to cognitive function mainly for processing speed, selective attention, working memory, and episodic memory (Gaudeau-Bosma et al., 2013; Parkin et al., 2015; Alcala-Lozano et al., 2017). Besides, DLPFC plays an important part in the central executive network (CEN), which is responsible for high-level cognitive functions, notably the control of attention and working memory (Bressler and Menon, 2010). A meta-analysis has shown that high-frequency rTMS stimulation of DLPFC could improve the cognitive function for healthy people, patients with Alzheimer's disease, depression, executive dysfunction, memory complaints, and Parkinson's disease (Guse et al., 2010). It is recommended that rTMS at 10, 15, or 20 Hz be applied over the left DLPFC within an individual motor threshold of 80–110%, which is most likely to cause significant cognitive improvement (Guse et al., 2010). We did not completely copy the rTMS parameters of previous studies on rTMS treatment of PSCI and made some modifications. The reason why we increased the total number of stimuli to 2,000 was to consider the possibility that increasing the number of stimuli might increase the efficacy and duration of rTMS treatments. A systematic review also concluded that long-term cognitive improvements are likely related to the number of stimulation sessions/days, where more stimulation sessions result in longer-lasting stimulation effects (van Lieshout et al., 2019).

Previous studies reported that patients with PSCI showed less functional connectivity within the brain network (Ding et al., 2014; Dacosta-Aguayo et al., 2015), especially the default-mode network (DMN), which consists of the medial prefrontal cortex (MPFC), posterior cingulate cortex, precuneus, hippocampus, inferior temporal cortex, and inferior parietal lobules (Andrews-Hanna et al., 2010). Stroke patients exhibited decreased functional connectivity in the medial prefrontal, left medial temporal lobe, and posterior cingulate cortex within the DMN, which potentially contributes to the cognitive dysfunction in stroke patients (Tuladhar et al., 2013). PSCI patients showed decreased functional connectivity in the MPFC and hippocampus than stroke patients without cognitive impairment (Ding et al., 2014). Moreover, the increased local activity of MPFC during natural recovery may reflect compensation for loss of cognitive function in stroke patients because MPFC was related to executive functions, task processes, emotional regulation, and social-cognitive processes that are related to the self and others (Ding et al., 2014). It is conceivable that rTMS treatment may facilitate the compensation for cognitive functions after stroke. Besides, Tang et al. (2019) have observed that cognitive training could improve the global cognitive function of patients with subcortical vascular cognitive impairment or dementia and significantly increased the connectivity between the left DLPFC and MPFC, indicating that the connection between DMN

and CEN was important in the recovery of cognitive function. Referring to our study, although the stimulation site was DLPFC, the neural activation was found in MPFC, which could be attributable to the connection of networks.

Our subsequent FC analysis revealed enhanced right MPFC and vACC FC to the left MPFC, which further explained the important role of MPFC in the recovery of cognitive function for stroke patients. The vACC is associated with decision-making, emotion regulation, and self-referential processing and is an important part of the salience network, mediating the conversion of the functional connectivity between the DMN and CEN (Hamilton et al., 2011; van den Heuvel et al., 2013; Yoshimura et al., 2014). Yoshimura et al. (2014) found that cognitive-behavioral therapy influenced MPFC and vACC functioning related to self-referential processing for depression patients. Xue et al. (2017) reported a similar conclusion with our study and found an increased fractional amplitude of low-frequency fluctuation in rostral ACC (one part of vACC) after 20 Hz rTMS on the left DLPFC for healthy participants. Besides, they observed an enhanced rACC/vmPFC FC to frontal, temporal, and hippocampus regions suggesting rACC as a hub region for facilitating the left DLPFC rTMS effects on DMN areas through the frontal-cingulate pathway (Xue et al., 2017). Similar to our study, they also applied high-frequency stimulation of the left DLPFC to observe changes in brain activation and functional connectivity. The differences were that they observed the immediate effects (before and after 48 h after once stimulation) and we observed the cumulative effects (before and after 4 weeks of multiple stimulations). As for our study, we suggested that the left DLPFC rTMS may activate the left MPFC and enhanced the functional connectivity to the contralateral MPFC and vACC to regulate the DMN.

This study has some limitations. First, the sample size was relatively small and only two female patients were included in each group. It is undeniable that the findings were more suitable explaining for male patients. In future studies, we will further expand the sample size to avoid this gender bias. Second, this study applied only one parameter for the rTMS treatments and failed to screen for the optimal stimulation protocol. Third, because of the lack of follow-up assessment, the long-term efficacy and sustained changes in brain function after the cessation of rTMS treatment were not determined.

In summary, our results suggest that high-frequency rTMS applied on the left DLPFC could improve cognitive function for stroke patients with cognitive impairment, with accompanying changes in the left medial prefrontal cortex.

DATA AVAILABILITY STATEMENT

All datasets presented in this study are included in the article/supplementary material.

ETHICS STATEMENT

The studies involving human participants were reviewed and approved by the Institutional Ethics Committee of The Third Affiliated Hospital of Sun Yat-sen University. The patients/participants provided their written informed consent to participate in this study.

AUTHOR CONTRIBUTIONS

All authors listed have made a substantial, direct and intellectual contribution to the work, and approved it for publication.

FUNDING

This work was supported by the National Natural Science Foundation of China (81871847, 81672261, 81601979, 81702232, and 81972151), the Science and Technology Planning Key Project of Guangzhou (201803010119), Guangdong Basic and Applied Basic Research Foundation (2019A1515011106), and the Natural Science Foundation of Guangdong Province of China (2017A030313493).

ACKNOWLEDGMENTS

We would like to thank the clinical research staff in our department for helps during this study.

REFERENCES

Alcala-Lozano, R., Morelos-Santana, E., Cortes-Sotres, J. F., Garza-Villarreal, E. A., Sosa-Ortiz, A. L., and Gonzalez-Olvera, J. J. (2017). Similar clinical improvement and maintenance after rTMS at 5 Hz using a simple vs. complex protocol in Alzheimer's disease. *Brain Stimul.* 11, 625–627. doi: 10.1016/j.brs.2017.12.011

Andrews-Hanna, J. R., Reidler, J. S., Sepulcre, J., Poulin, R., and Buckner, R. L. (2010). Functional-anatomic fractionation of the brain's default network. *Neuron* 65, 550–562. doi: 10.1016/j.neuron.2010.02.005

Bayard, S., Erkes, J., and Moroni, C. (2011). Victoria Stroop Test: normative data in a sample group of older people and the study of their clinical applications in the assessment of inhibition in Alzheimer's disease. *Arch. Clin. Neuropsychol.* 26, 653–661. doi: 10.1093/arclin/acr053

Beristain, X., and Golombievski, E. (2015). Pharmacotherapy to enhance cognitive and motor recovery following stroke. *Drugs Aging* 32, 765–772. doi: 10.1007/s40266-015-0299-0

Bressler, S. L., and Menon, V. (2010). Large-scale brain networks in cognition: emerging methods and principles. *Trends Cogn. Sci.* 14, 277–290. doi: 10.1016/j.tics.2010.04.004

Chao-Gan, Y., and Yu-Feng, Z. (2010). DPARSF: a MATLAB toolbox for "Pipeline" data analysis of resting-state fMRI. *Front. Syst. Neurosci.* 4:13. doi: 10.3389/fnsys.2010.00013

Dacosta-Aguayo, R., Grana, M., Iturria-Medina, Y., Fernandez-Andujar, M., Lopez-Cancio, E., Caceres, C., et al. (2015). Impairment of functional integration of the default mode network correlates with cognitive outcome at three months after stroke. *Hum. Brain Mapp.* 36, 577–590. doi: 10.1002/hbm.22648

Dijkhuizen, R. M., Zaharchuk, G., and Otte, W. M. (2014). Assessment and modulation of resting-state neural networks after stroke. *Curr. Opin. Neurol.* 27, 637–643. doi: 10.1097/wco.0000000000000150

Ding, X., Li, C. Y., Wang, Q. S., Du, F. Z., Ke, Z. W., Peng, F., et al. (2014). Patterns in default-mode network connectivity for determining outcomes in cognitive function in acute stroke patients. *Neuroscience* 277, 637–646. doi: 10.1016/j.neuroscience.2014.07.060

Dionisio, A., Duarte, I. C., Patricio, M., and Castelo-Branco, M. (2018). Transcranial magnetic stimulation as an intervention tool to recover from language, swallowing and attentional deficits after stroke: a systematic review. *Cerebrovasc. Dis.* 46, 178–185. doi: 10.1159/000494213

Gaudeau-Bosma, C., Moulier, V., Allard, A. C., Sidhoumi, D., Bouaziz, N., Braha, S., et al. (2013). Effect of two weeks of rTMS on brain activity in healthy subjects during an n-back task: a randomized double blind study. *Brain Stimul.* 6, 569–575. doi: 10.1016/j.brs.2012.10.009

Guse, B., Falkai, P., and Wobrock, T. (2010). Cognitive effects of high-frequency repetitive transcranial magnetic stimulation: a systematic review. *J. Neural Trans.* 117, 105–122. doi: 10.1007/s00702-009-0333-7

Hamilton, J. P., Glover, G. H., Hsu, J. J., Johnson, R. F., and Gotlib, I. H. (2011). Modulation of subgenual anterior cingulate cortex activity with real-time neurofeedback. *Hum. Brain Mapp.* 32, 22–31. doi: 10.1002/hbm.20997

Iadecola, C., Duering, M., Hachinski, V., Joutel, A., Pendlebury, S. T., Schneider, J. A., et al. (2019). Vascular cognitive impairment and dementia: JACC scientific expert panel. *J. Am. Coll. Cardiol.* 73, 3326–3344.

Irfani Fitri, F., Fithrie, A., and Rambe, A. S. (2020). Association between working memory impairment and activities of daily living in post-stroke patients. *Med. Glasnik* 17, 433–438.

Kim, B. R., Kim, D. Y., Chun, M. H., Yi, J. H., and Kwon, J. S. (2010). Effect of repetitive transcranial magnetic stimulation on cognition and mood in stroke patients: a double-blind, sham-controlled trial. *Am. J. Phys. Med. Rehabil.* 89, 362–368. doi: 10.1097/phm.0b013e3181d8a5b1

Lefaucheur, J. P., Aleman, A., Baeken, C., Benninger, D. H., Brunelin, J., Di Lazzaro, V., et al. (2020). Evidence-based guidelines on the therapeutic use of repetitive transcranial magnetic stimulation (rTMS): an update (2014-2018). *Clin. Neurophysiol.* 131, 474–528.

Lei, X., Zhong, M., Liu, Y., Jin, X., Zhou, Q., Xi, C., et al. (2017). A resting-state fMRI study in borderline personality disorder combining amplitude of low frequency fluctuation, regional homogeneity and seed based functional connectivity. *J. Affect. Disord.* 218, 299–305. doi: 10.1016/j.jad.2017.04.067

Leung, S. O., Chan, C. C., and Shah, S. (2007). Development of a Chinese version of the Modified Barthel Index– validity and reliability. *Clin Rehabil* 21, 912–922. doi: 10.1177/0269215507077286

Leys, D., Henon, H., Mackowiak-Cordoliani, M. A., and Pasquier, F. (2005). Poststroke dementia. *Lancet Neurol.* 4, 752–759.

Liu, J., Qin, W., Wang, H., Zhang, J., Xue, R., Zhang, X., et al. (2014). Altered spontaneous activity in the default-mode network and cognitive decline in chronic subcortical stroke. *J. Neurol. Sci.* 347, 193–198. doi: 10.1016/j.jns.2014.08.049

Liu, Y., Yin, M., Luo, J., Huang, L., Zhang, S., Pan, C., et al. (2020). Effects of transcranial magnetic stimulation on the performance of the activities of daily living and attention function after stroke: a randomized controlled trial. *Clin. Rehabil.* 4:269215520946386.

Lu, H., Zhang, T., Wen, M., and Sun, L. (2015). Impact of repetitive transcranial magnetic stimulation on post-stroke dysmnesia and the role of BDNF Val66Met SNP. *Med. Sci. Monit.* 21, 761–768. doi: 10.12659/msm.892337

McKinney, M., Blake, H., Treece, K. A., Lincoln, N. B., Playford, E. D., and Gladman, J. R. (2002). Evaluation of cognitive assessment in stroke rehabilitation. *Clin. Rehabil.* 16, 129–136. doi: 10.1191/0269215502cr479oa

Nasreddine, Z. S., Phillips, N. A., Bedirian, V., Charbonneau, S., Whitehead, V., Collin, I., et al. (2005). The montreal cognitive assessment, MoCA: a brief screening tool for mild cognitive impairment. *J. Am. Geriatr. Soc.* 53, 695–699. doi: 10.1111/j.1532-5415.2005.53221.x

Paker, N., Buðdaycı, D., Tekdö??, D., Kaya, B., and Dere, C. (2010). Impact of cognitive impairment on functional outcome in stroke. *Stroke Res. Treat.* 2010:652612.

Pan, P., Zhu, L., Yu, T., Shi, H., Zhang, B., Qin, R., et al. (2017). Aberrant spontaneous low-frequency brain activity in amnestic mild cognitive impairment: a meta-analysis of resting-state fMRI studies. *Ageing Res. Rev.* 35, 12–21. doi: 10.1016/j.arr.2016.12.001

Park, I. S., and Yoon, J. G. (2015). The effect of computer-assisted cognitive rehabilitation and repetitive transcranial magnetic stimulation on cognitive function for stroke patients. *J. Phys. Ther. Sci.* 27, 773–776. doi: 10.1589/jpts.27.773

Parkin, B. L., Ekhtiari, H., and Walsh, V. F. (2015). Non-invasive human brain stimulation in cognitive neuroscience: a primer. *Neuron* 87, 932–945. doi: 10.1016/j.neuron.2015.07.032

Rektorova, I., Megova, S., Bares, M., and Rektor, I. (2005). Cognitive functioning after repetitive transcranial magnetic stimulation in patients with cerebrovascular disease without dementia: a pilot study of seven patients. *J. Neurol. Sci.* 229, 157–161. doi: 10.1016/j.jns.2004.11.021

Rossi, S., Hallett, M., Rossini, P. M., Pascual-Leone, A., and The Safety of Tms Consensus Group. (2009). Safety of, Safety, ethical considerations, and application guidelines for the use of transcranial magnetic stimulation in clinical practice and research. *Clin. Neurophys.* 120, 2008–2039. doi: 10.1016/j.clinph.2009.08.016

Sachdev, P. S., Brodaty, H., Valenzuela, M. J., Lorentz, L., Looi, J. C., Berman, K., et al. (2006). Clinical determinants of dementia and mild cognitive impairment following ischaemic stroke: the sydney stroke study. *Dement. Geriatr. Cogn. Disord.* 21, 275–283. doi: 10.1159/000091434

Sun, Y. W., Qin, L. D., Zhou, Y., Xu, Q., Qian, L. J., Tao, J., et al. (2011). Abnormal functional connectivity in patients with vascular cognitive impairment, no dementia: a resting-state functional magnetic resonance imaging study. *Behav. Brain Res.* 223, 388–394. doi: 10.1016/j.bbr.2011.05.006

Tang, Y., Xing, Y., Zhu, Z., He, Y., Li, F., Yang, J., et al. (2019). The effects of 7-week cognitive training in patients with vascular cognitive impairment, no dementia (the Cog-VACCINE study): a randomized controlled trial. *J. Alzheimers Assoc.* 15, 605–614. doi: 10.1016/j.jalz.2019.01.009

Tremblay, M. P., Potvin, O., Belleville, S., Bier, N., Gagnon, L., Blanchet, S., et al. (2016). The victoria stroop test: normative data in quebec-french adults and elderly. *Arch. Clin. Neuropsychol.* 31, 926–933.

Tuladhar, A. M., Snaphaan, L., Shumskaya, E., Rijpkema, M., Fernandez, G., Norris, D. G., et al. (2013). Default mode network connectivity in stroke patients. *PLoS One* 8:e66556. doi: 10.1371/journal.pone.0066556

van den Heuvel, O. A., Van Gorsel, H. C., Veltman, D. J., and Van Der Werf, Y. D. (2013). Impairment of executive performance after transcranial magnetic modulation of the left dorsal frontal-striatal circuit. *Hum. Brain Mapp.* 34, 347–355. doi: 10.1002/hbm.21443

van Lieshout, E. C. C., van Hooijdonk, R. F., Dijkhuizen, R. M., Visser-Meily, J. M. A., and Nijboer, T. C. W. (2019). The effect of noninvasive brain stimulation on poststroke cognitive function: a systematic review. *Neurorehabil. Neural Rep.* 33, 355–374.

Winstein, C. J., Stein, J., Arena, R., Bates, B., Cherney, L. R., Cramer, S. C., et al. (2016). Guidelines for adult stroke rehabilitation and recovery: a guideline for healthcare professionals from the american heart association/american stroke association. *Stroke* 47, e98–e169.

Xue, S. W., Guo, Y., Peng, W., Zhang, J., Chang, D., Zang, Y. F., et al. (2017). Increased low-frequency resting-state brain activity by high-frequency repetitive tms on the left dorsolateral prefrontal cortex. *Front. Psychol.* 8:2266. doi: 10.3389/fpsyg.2017.02266

Yoshimura, S., Okamoto, Y., Onoda, K., Matsunaga, M., Okada, G., Kunisato, Y., et al. (2014). Cognitive behavioral therapy for depression changes medial prefrontal and ventral anterior cingulate cortex activity associated with self-referential processing. *Soc. Cogn. Affect. Neurosci.* 9, 487–493. doi: 10.1093/scan/nst009

Conflict of Interest: The authors declare that the research was conducted in the absence of any commercial or financial relationships that could be construed as a potential conflict of interest.

Copyright © 2020 Yin, Liu, Zhang, Zheng, Peng, Ai, Luo and Hu. This is an open-access article distributed under the terms of the Creative Commons Attribution License (CC BY). The use, distribution or reproduction in other forums is permitted, provided the original author(s) and the copyright owner(s) are credited and that the original publication in this journal is cited, in accordance with accepted academic practice. No use, distribution or reproduction is permitted which does not comply with these terms.

frontiers in Human Neuroscience

ORIGINAL RESEARCH
published: 21 October 2020
doi: 10.3389/fnhum.2020.576171

Convergent Associative Motor Cortical Plasticity Induced by Conditional Somatosensory and Motor Reaction Afferents

Yi Huang[1], *Jui-Cheng Chen*[2,3,4], *Chon-Haw Tsai*[2,3,4] *and Ming-Kuei Lu*[1,2,3,5]*

[1]Graduate Institute of Biomedical Sciences, College of Medicine, China Medical University, Taichung, Taiwan, [2]Department of Neurology, China Medical University Hospital, Taichung, Taiwan, [3]Neuroscience and Brain Disease Center, China Medical University, Taichung, Taiwan, [4]School of Medicine, College of Medicine, China Medical University, Taichung, Taiwan, [5]Ph.D. Program for Translational Medicine, College of Medicine, China Medical University, Taichung, Taiwan

OPEN ACCESS

Edited by:
Ti-Fei Yuan,
Shanghai Jiao Tong University, China

Reviewed by:
Zhishan Hu,
Beijing Normal University, China
Marcello Romano,
Azienda Ospedaliera Ospedali Riuniti Villa Sofia Cervello, Italy

***Correspondence:**
Ming-Kuei Lu
mklu@mail.cmu.edu.tw

Specialty section:
This article was submitted to Brain Imaging and Stimulation, a section of the journal Frontiers in Human Neuroscience

Received: *25 June 2020*
Accepted: *13 August 2020*
Published: *21 October 2020*

Citation:
Huang Y, Chen J-C, Tsai C-H and Lu M-K (2020) Convergent Associative Motor Cortical Plasticity Induced by Conditional Somatosensory and Motor Reaction Afferents. Front. Hum. Neurosci. 14:576171. doi: 10.3389/fnhum.2020.576171

Objective: Associative motor cortical plasticity can be non-invasively induced by paired median nerve electric stimulation and transcranial magnetic stimulation (TMS) of the primary motor cortex (M1). This study investigates whether a simultaneous motor reaction of the other hand advances the associative plasticity in M1.

Methods: Twenty-four right-handed subjects received conventional paired associative stimulation (PAS) and PAS with simultaneous motor reaction (PASmr) with at least a 1-week interval. The PASmr protocol additionally included left abductor pollicis brevis muscle movement responding to a digital sound. The motor reaction time was individually measured. The M1 excitability was examined by the motor evoked potential (MEP), short-interval intracortical inhibition (SICI), and intracortical facilitation (ICF) before and after the PAS protocols.

Results: The conventional PAS protocol significantly facilitated MEP and suppressed SICI. A negative correlation between the reaction time and the MEP change, and a positive correlation between the reaction time and the ICF change were found in the PASmr protocol. By subgrouping analysis, we further found significant facilitation of MEP and a reduction of ICF in the subjects with fast reaction times but not in those with slow reaction times.

Conclusion: Synchronized motor reaction ipsilateral to the stimulated M1 induces associative M1 motor plasticity through the spike-timing dependent principle. MEP and ICF change could represent this kind of plasticity. The current findings provide a novel insight into designing rehabilitation programs concerning motor function.

Keywords: intracortical facilitation (ICF), motor evoked potential (MEP), paired associative stimulation (PAS), primary motor cortex (M1), reaction time, short interval intracortical inhibition (SICI)

INTRODUCTION

The motor cortical plasticity contributes to motor learning and appropriate movements (Sanes and Donoghue, 2000; McKay et al., 2002; Dayan and Cohen, 2011; Kida and Mitsushima, 2018; Kroneberg et al., 2018). A specific type of plasticity following Hebb's theory, or known as the spike-timing dependent principle, has been found existing in the human motor cortex (M1) (Hebb, 1949; Müller-Dahlhaus et al., 2010). Not only has it been observed in the cell level, but also in the systemic and behavioral level (Zhang et al., 1998; Stefan et al., 2000; Bi and Poo, 2001; Dan and Poo, 2004; Cooke and Bliss, 2006; Ziemann et al., 2008). That is, the excitability of M1 can be dependently modulated by repetitive, time-locked pairing stimuli, mostly with one sub-threshold conditioning stimulus and one supra-threshold test stimulus (Müller-Dahlhaus et al., 2010). Paired associative stimulation (PAS) is a non-invasive brain stimulation method commonly applied to modulate M1 excitability (Stefan et al., 2000, 2002). The conventional PAS protocol consists of 90 pairs of electric stimulation at the median nerve and is followed by transcranial magnetic stimulation (TMS) of the M1 contralateral to the stimulated median nerve. The interstimulus interval between the median nerve stimulation and the TMS is a critical factor leading to successful induction of M1 plasticity (Stefan et al., 2000; Müller-Dahlhaus et al., 2010). To induce long-term potentiation (LTP)-like neural activity in M1, the somatosensory afferent from the median nerve stimulation should arrive at the same time with or shortly before the TMS of M1 (Wolters et al., 2003; Ziemann et al., 2004; Byblow et al., 2007; Pötter-Nerger et al., 2009). The somatosensory inputs can be alternative from electric stimulation, passive movement to active movement once the spike-timing dependent principle is followed (Stefan et al., 2000; Thabit et al., 2010; Edwards et al., 2014).

In addition to the ipsilateral somatosensory afferent, the signal from the contralateral M1, probably through the transcallosal pathway, can serve as the conditioning input to induce M1 plasticity (Kobayashi et al., 2003; Koganemaru et al., 2009; Rizzo et al., 2009). It renders the possibility that the sensorimotor activation in the contralateral hemisphere may carry an impact on the induction of M1 plasticity. Nevertheless, the interhemispheric input should promptly arrive in a responsive time window to achieve the induction of M1 plasticity.

This study investigates whether intentional, active movements driven by the contralateral M1 influence the M1 plasticity induced by the conventional PAS protocol. It has been reported that the conventional PAS protocol has a responsive variability (Lahr et al., 2016; Minkova et al., 2019). Since the interval between the median nerve stimulation and the TMS is fixed to 25 milliseconds (ms) in the conventional PAS, one of the possible factors causing individual variability would be dispersed conditioning stimuli at M1 corresponding to the individual timing of the somatosensory afferent. If an additional somatosensory input based on the individual reaction time can be activated, the conjoint conditioning stimuli at M1 may be enhanced and able to decrease the uncertainty of the PAS effect. Therefore, the hypothesis of the current study is that the simultaneous arrival of the sensorimotor afferents from both hemispheres may lead to a convergent influence and enhance the PAS effect on the target M1.

MATERIALS AND METHODS

Subjects

In total, 24 right-handed (Oldfield, 1971) healthy subjects (mean age 24.3 ± 2.9 years, 11 women) participated in this study after giving their written informed consent. They all underwent a motor reaction time measurement (see "Measurement of the Mean Reaction Time to the Auditory Stimulation" section), as well as the PAS protocols including two different motor reacting conditions, respectively (see "Paired Associated Stimulation" and "Paired Associated Stimulation With Simultaneous Motor Reaction at the Contralateral Hand" section). The experimental procedures were in accord with the latest revision of the Declaration of Helsinki. Approval by the local ethics committee of the China Medical University Hospital was obtained (CMUH106-REC2-019).

Procedures

Measurement of Motor Evoked Potentials

TMS was delivered through a focal "figure-of-eight"-shaped stimulating coil (with 70 mm inner diameter of each ring) connected *via* a BiStim moiety to two Magstim 200 magnetic stimulators (Magstim Co., Carmarthenshire, Wales, UK). The optimal coil position ("hot spot"; $M1_{HAND}$) was determined as the site on the left primary motor cortex where the TMS at a supra-threshold intensity consistently produced the largest MEPs in the right APB. The test intensity of the TMS, which was adjusted to produce MEPs around 1 mV in peak-to-peak amplitude on average in the resting APB, is defined as the $MEP_{1\ mV}$. The individual resting motor threshold (RMT) and active motor threshold (AMT) of each subject was respectively determined over the left $M1_{HAND}$. The method we applied for individual RMT and AMT determination has been described in the previous literature (Lu et al., 2012). In the measurement of MEPs, 20 stimuli were recorded at the test intensity level. The inter-stimulus interval (ISI) was determined as 10 s with a 25% variance to limit the anticipation effect.

Short-Interval Intracortical Inhibition (SICI)/Intracortical Facilitation (ICF)

Short-interval intracortical inhibition (SICI) and intracortical facilitation (ICF) were studied with the application of the paired-pulse TMS protocol, which had been well-established in the previous literature (Kujirai et al., 1993; Ziemann et al., 1996). In brief, through using the same "figure-of-eight" stimulating coil over the left $M1_{HAND}$, the two magnetic stimuli were given in order to investigate the effect of the sub-threshold conditioning stimulus (Antal et al., 2000) on the test motor evoked potential (MEP) provoked by the supra-threshold test

stimulus (TS). SICI was assessed at an ISI of 2.0 ms owing to the results of previous literature that the SICI at this level is not interfered by short-interval intra-ortical facilitation (SICF; Peurala et al., 2008). At the baseline recording, the CS intensity was adjusted to produce approximately 50% inhibition in order to provide the highest sensitivity for the detection of changes in SICI after PAS. AMT had been determined over the left M1 prior to the baseline recording, and 95% AMT was set as the CS intensity, which was kept constant throughout the SICI and ICF measurements. In total twelve single and twelve paired TMS were delivered with a pseudorandomized order to measure the SICI and ICF. The ISI was 10 s with a 25% variance.

Measurement of the Mean Reaction Time to the Auditory Stimulation

The reaction time of all subjects was measured by the following equipment and process. Through a pair of earphones connected to the speaker (MDR-XD150, Sony Taiwan Limited) digitally triggered by a computer-based interface (Signal for Windows, Version 3.10, CED, UK), a digital sound with the volume set as 64 dB, the duration as 50 ms, and the frequency as 100 Hz, was transmitted to the subject. The sound was repeated 10 times with an interval of 5 ± 25% seconds (i.e., 3.75–6.25 s). When hearing the sound through the abovementioned settings, every subject was requested to perform the contraction of the left abductor pollicis brevis (APB) muscle as quickly as possible. Surface electromyography (SEMG) was recorded from the left APB muscle to measure each "motor reaction time" span, which was calculated as the period from the starting time of the sound to the onset of the APB muscle activity. The mean reaction time was obtained by averaging ten total measurements of the single reaction time value for each subject.

Paired Associated Stimulation (PAS)

The PAS protocol consists of 90 pairs of a cutaneous electric stimulation of the median nerve at the right wrist followed by a single TMS at the contralateral $M1_{HAND}$ (Stefan et al., 2000). Every single electric stimulation over the median nerve was set 45 ms after an occurrence of a digital sound with the volume set as 64 dB, duration as 50 ms, and frequency as 100 Hz in control, with all subjects keeping their left abductor pollicis brevis (APB) in a relaxed condition through the protocol. The interstimulus interval between the electric stimulation of the median nerve and the TMS is 25 ms, as the method of PAS originally been applied in the pioneered study (Stefan et al., 2000). The intensity of TMS was the $MEP_{1\ mV}$. In total 90 pairs of PAS were delivered at a rate of 0.05 Hz (i.e., duration of 30 min, **Figure 1**).

Paired Associated Stimulation With Simultaneous Motor Reaction at the Contralateral Hand (PASmr)

The PAS with simultaneous motor reaction (PASmr) protocol consists of 90 "triads" of stimuli, which were each composed of: an instant volitional left APB motor reaction to an auditory stimulation, a cutaneous electric stimulation of the median nerve at the right wrist, and a single TMS at the contralateral M1. Throughout the PASmr protocol, a digital sound with the volume set as 64 dB, the duration as 50 ms, and the frequency as 100 Hz

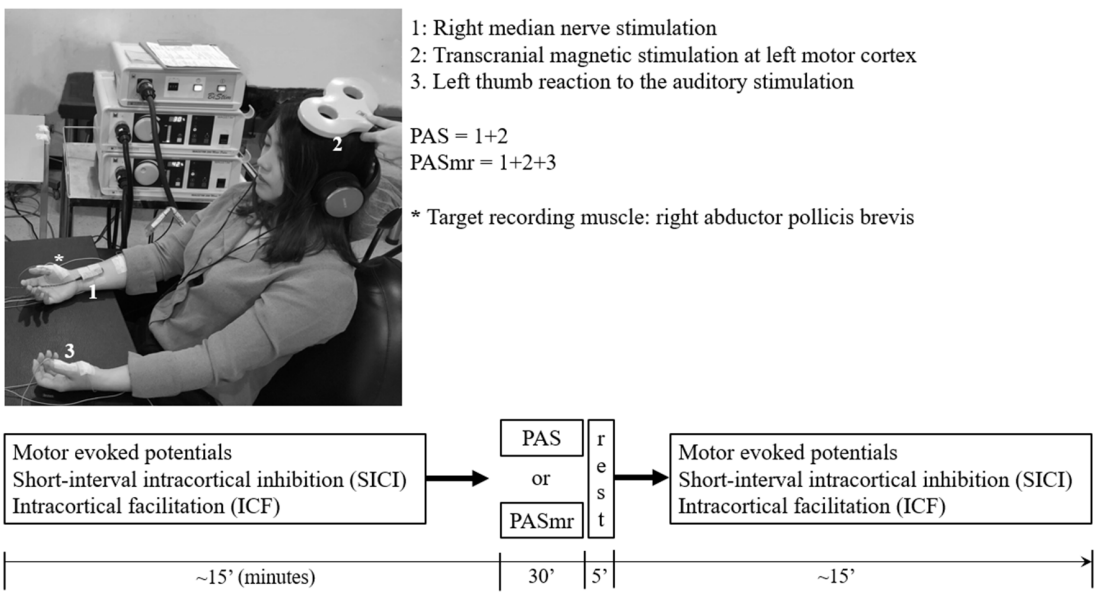

FIGURE 1 | The experimental setup demonstrated by the authors. The subject sat on a chair with his or her arms relaxed and in a supination position. In the "paired associative stimulation (PAS)" protocol, 90 pairs of the transcranial magnetic stimulation (TMS) was delivered to the left motor cortex, 25 ms following the electric stimulation at the right wrist (1 + 2). The motor response was monitored by the surface electromyography at bilateral abductor pollicis brevis (APB) muscles. The earphone was used to receive the sound command triggered from the software in the computer. In the "paired associated stimulation with simultaneous motor reaction at the contralateral hand (PASmr)" protocol, the subjects were requested to move their left APB muscle as quickly as they could (1 + 2 + 3). The experimental design and time flow are shown in the lower panel. All subjects completed the PAS and the PASmr protocols with an interval of at least 1 week.

was transmitted through a pair of earphones connected to the speaker (MDR-XD150, Sony Taiwan Ltd.), digitally triggered by a computer-based interface (Signal for Windows, Version 3.10, CED, UK). In the meanwhile, 45 ms after every auditory stimulation of digital sound, which our subject should instantly react to and perform the left APB muscle contraction as quickly as possible, a pair of PAS (see "Paired Associated Stimulation" section) followed. The intensity of TMS was adjusted to the $MEP_{1\,mV}$. In total 90 "triads" of PASmr were delivered at a rate of 0.05 Hz (i.e., duration of 30 min). All participants received the PAS and the PASmr protocols with a pseudorandomized order and with an interval of at least 1 week. The experiment setup and design are demonstrated in **Figure 1**.

Statistical Analysis

Repeated measures analysis of variance (rmANOVA) was applied to test the intervention effects on the MEP, SICI, and ICF. The within-subject effects were time (pre vs. post) and protocol (PAS vs. PASmr). Conditional on a significant *F*-value, *post hoc* comparisons were performed using paired-sample *t*-tests with Bonferroni's correction. Violation of sphericity was checked with Mauchly's test and degrees of freedom were adjusted whenever Mauchly's $W < 0.05$ using the Greenhouse-Geisser correction (SPSS 22.0). The relationship between reaction time and change of MEP, SICI, and ICF following PAS and PASmr was examined with simple linear regression. Data are reported as means ± SD if not stated otherwise.

RESULTS

All the 24 subjects completed the whole sessions of experimental procedures without any adverse effects during or after the study.

The mean RMT and AMT of the 24 participants were 53 ± 6.9% and 42 ± 5.8%, respectively. The mean $MEP_{1\,mv}$ was 59 ± 8.2%. The intensities applied for measuring SICI and ICF are listed in **Table 1**. We analyzed the data of the 24 subjects for two main effects (i.e., protocol and time). RmANOVA of the MEP amplitude revealed a significant effect of time ($F_{(1,23)} = 6.21$, $P = 0.02$; **Table 2**). A significant effect of time was also found for the analysis of SICI ($F_{(1,23)} = 6.09$, $P = 0.02$). RmANOVA of the ICF did not show any significant effect (all $P > 0.08$). The statistical power reached 0.96 with the effect size of 0.4 for the two-way rmANOVA.

Post hoc comparisons of MEP showed a significant MEP amplitude increase after PAS (pre/post: 0.99 ± 0.15/1.19 ± 0.40 mV, $P = 0.016$ by paired *t*-test) but not PASmr (**Figure 2**). The SICI also showed a significant decrease after PAS (pre/post: 29.6 ± 15.8/37.3 ± 25.5%, $P = 0.045$ by paired *t*-test) but not PASmr (**Figure 3A**). There was no significant difference from the *post hoc* comparisons on ICF (**Figure 3B**). The simple linear regression test showed a significant negative correlation between the reaction time and the MEP change in PASmr ($R^2 = 0.32$, $P = 0.004$) but not PAS (**Figure 4A**). There was a positive correlation between the reaction time and the change of ICF in PASmr ($R^2 = 0.46$, $P < 0.001$) but not PAS (**Figure 4B**). Considering the two subjects with a long reaction time, as this might interfere with the current correlation findings, we re-analyzed the correlations without the two subjects. The correlation between the reaction time and the MEP change did not reach a statistical significance despite a weak trend remaining ($R^2 = 0.09$, $P = 0.18$). The positive correlation between the reaction time and the change of ICF in PASmr was not affected ($R^2 = 0.39$, $P = 0.0019$).

Since there were certain relationships between the reaction time and the measured electrophysiological parameters, we compared the MEP, SICI, and ICF by classifying the results of all 24 subjects into two groups, based on their motor reaction time (see "Measurement of the Mean Reaction Time to the Auditory Stimulation" section), with one group having an average reaction time of less than 110 ms and the other group more than 110 ms. There were twelve subjects in each group. In the group with a reaction time of more than 110 ms, there was no significant change of MEP, SICI, and ICF following the PAS and PASmr. Nevertheless, in the group with a reaction time of less than 110 ms, the comparisons on MEP amplitude showed a significant increase in PASmr (pre/post: 1.03 ± 0.29/1.24 ± 0.34 mV, $P = 0.035$ by paired *t*-test, **Figure 5A**). The ICF showed a significant reduction in PASmr (pre/post: 148.9 ± 60.0/111.1 ± 38.5%, $P = 0.021$ by paired *t*-test, **Figure 5B**). The timing relationship among sensorimotor cortex activation, PAS, and reaction time in this study is demonstrated in **Figure 6**.

TABLE 1 | Transcranial magnetic stimulation (TMS) stimulation parameters.

	MEP	SICI	ICF
Conditioning intensity*		40 ± 5	40 ± 5
Test intensity*	59 ± 8	59 ± 8	59 ± 8

*Presented as percentage of maximal stimulator output.

TABLE 2 | Repeated measures analysis of variance (rmANOVA) of the paired associated stimulation with simultaneous motor reaction at the contralateral hand effect.

		MEP		SICI		ICF	
	d.f.	*F*	*P*	*F*	*P*	*F*	*P*
Protocol[a]	1.23	1.966	0.174	0.259	0.616	0.031	0.863
Time[b]	1.23	**6.210***	**0.020***	**6.090***	**0.021***	1.087	0.308
Protocol X Time	1.23	1.850	0.187	1.314	0.263	1.006	0.326

*$P < 0.05$. [a]2 levels (PAS and PASmr). [b]2 levels (pre and post). Abbreviations: d.f., degrees of freedom; ICF, intracortical facilitation; MEP, motor evoked potential; SICI, short-interval intracortical inhibition. The bold values mean statistical significance.

DISCUSSION

PAS can facilitate MEP with the interstimulus interval of 25 ms between the electrical median nerve stimulation and the TMS of M1, which follows the spike-timing dependent principle (Stefan et al., 2000). In addition to electrical stimulation, intentional hand or foot movement paired with TMS in a specific time interval can alter M1 excitability as well, probably through another somatosensory afferent (Koeneke et al., 2006; Thabit et al., 2010; Mrachacz-Kersting et al., 2012). In principle, the input sensory information should simultaneously or precedingly

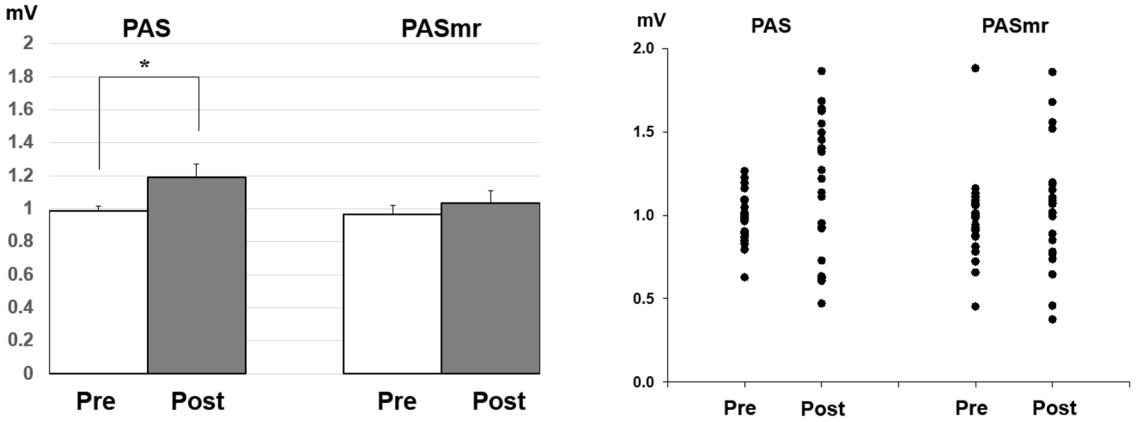

FIGURE 2 | *Post hoc* comparisons of the motor evoked potential (MEP) and the data plots. The MEP showed a significant facilitation following the PAS protocol instead of the PASmr protocol (*$P < 0.05$ by paired *t*-test with Bonferroni's correction).

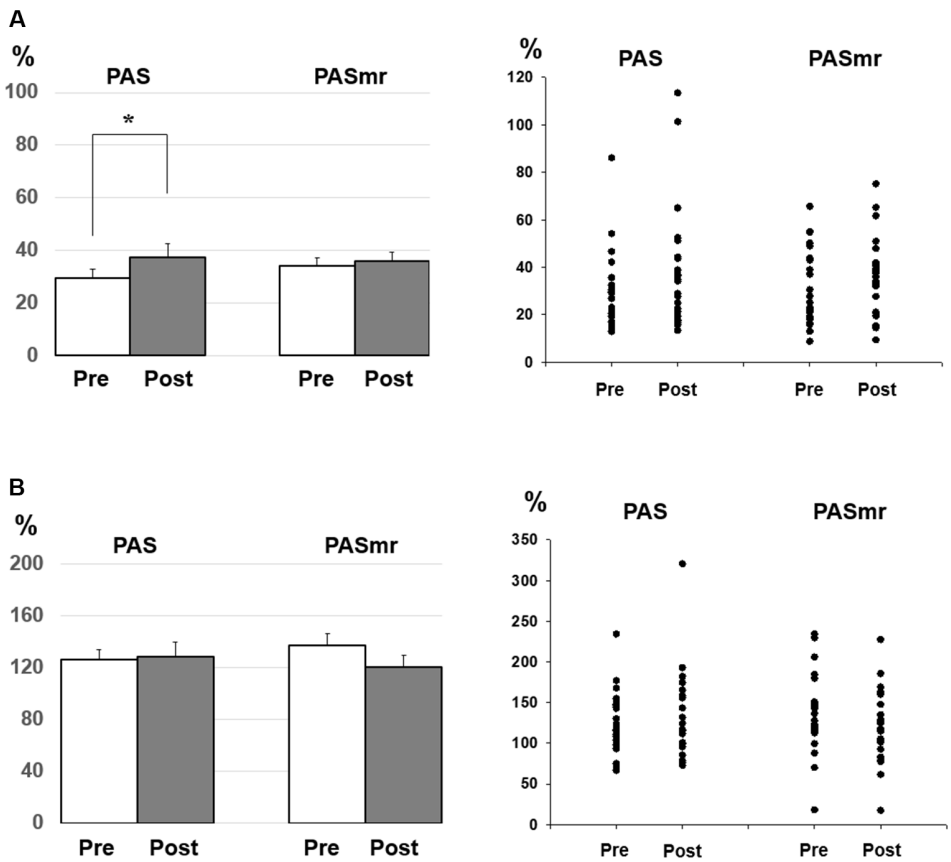

FIGURE 3 | (A) *Post hoc* comparisons of the short-interval intracortical inhibition (SICI) and the data plots. The SICI showed a significant reduction following the PAS protocol but not the PASmr protocol (*$P < 0.05$ by paired *t*-test with Bonferroni's correction). **(B)** *Post hoc* comparisons of the intracortical facilitation (ICF) and the data plots. There was no significant change following the PAS and the PASmr protocol.

arrive at M1 while the paired supra-threshold TMS is delivered so the STDP can be generated in M1. In case the sensory afferent is accomplished through complex pathways such as electroacupuncture, the long-term plasticity-like effect cannot be observed (Huang et al., 2019). The current findings support the notion that the spike-timing dependent principle remains following conditions with multiple sensory afferents if the individual difference of the sensory afferents is carefully

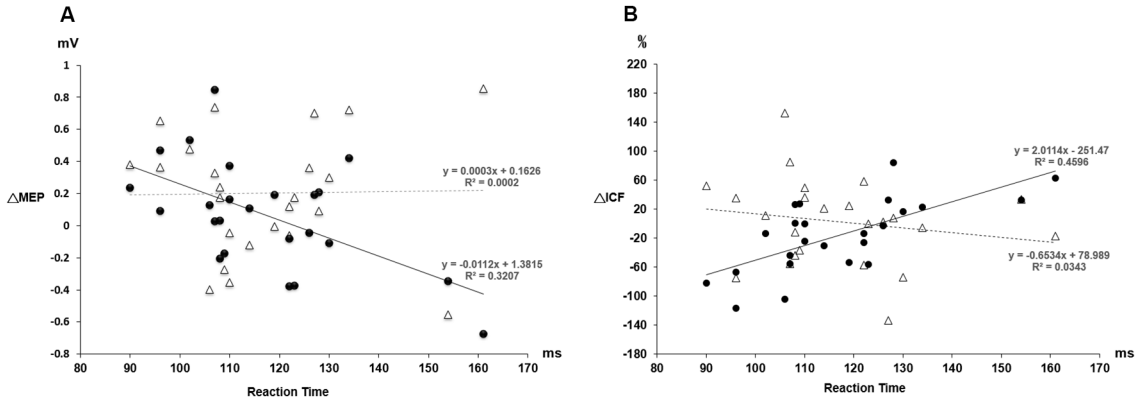

FIGURE 4 | (A) The relationship between the MEP change and the individual reaction time. The triangle values with the dot line were measured from the PAS protocol and the black dot values with the solid line were obtained from the PASmr protocol. There shows a significant negative correlation between the MEP change and the reaction time in the PASmr protocol (R^2 = 0.32, P = 0.004). **(B)** The relationship between the ICF change and the individual reaction time. There is a significant positive correlation between the ICF change and the reaction time in the PASmr protocol (R^2 = 0.46, P < 0.001).

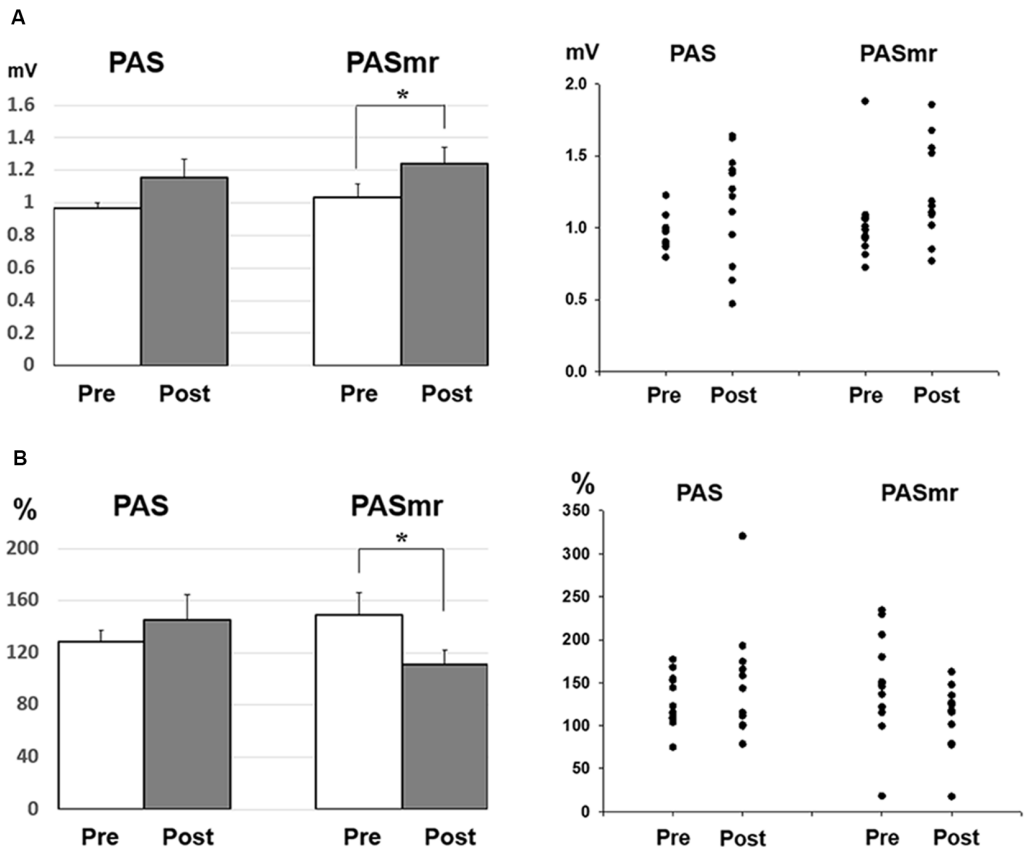

FIGURE 5 | (A) *Post hoc* comparisons of the MEP obtained from the subjects with a reaction time of less than 110 ms (N = 12) and the data plots. The MEP shows a significant facilitation following the PASmr protocol but not the PAS protocol (P = 0.035 by paired t-test with Bonferroni's correction). **(B)** *Post hoc* comparisons of the ICF obtained from the subjects with a reaction time of less than 110 ms (N = 12) and the data plots. The ICF shows a significant reduction following the PASmr protocol but not the PAS protocol (P = 0.021 by paired t-test with Bonferroni's correction *P < 0.05).

considered. In this study, the LTP-like MEP facilitation was found in the PAS protocol but not in the PASmr protocol when all subjects were grouped and analyzed together. Since the reaction time played an important role in the arrival of the second sensory input to M1, the grouped analysis with heterogeneous reaction time may average out and conceal the

real response (see **Figure 2**). The fact that the MEP change was significantly correlated with the individual reaction time in the PASmr protocol but not in the PAS protocol suggests the importance of the reaction time on the measured aftereffects in a group level, although our interpretation is inevitably constrained by the limited number of subjects including two cases with a significantly long reaction time (see **Figures 4A**, **5A**).

The MEP was significantly facilitated after the PASmr protocol in whose reaction time was less than 110 ms. For the subjects with a reaction time of 110 ms or less, their right M1 needs to be activated less than 85 ms after the sound was heard (i.e., 110 ms minus 25 ms, a maximal latency of somatosensory input from left APB muscle). At the same time, the left M1 needs to disinhibit right M1 by forwarding a disinhibition signal, probably through the transcallosal pathway mediating interhemispheric inhibition (Ferbert et al., 1992; Meyer et al., 1995, 1998; Kobayashi et al., 2003; Ni et al., 2009). It will take around 10–15 ms for a signal transmitting through the corpus callosum (Brown et al., 1991; Meyer et al., 1995). Therefore, the left M1 is activated about 70 ms after the sound was heard, 15 ms prior to the right M1 activation. The 15 ms interval is the same as the interval reported to be able to induce LTP-like phenomenon with paired TMS at bilateral M1 in humans (Koganemaru et al., 2009). In the left M1, the somatosensory input from the right median nerve electric stimulation and the transcallosal signal for disinhibiting right M1 are convergent almost at the same time in those subjects with a reaction time of less or equal to 110 ms (see **Figure 6**). The findings suggest that multiple convergent sensory inputs can induce long-term plasticity-like effects if the spike-timing dependent principle for each sensory input is fit.

The SICI was reduced in the PAS protocol (see **Figure 3A**). It has been reported that the excitability-enhancing PAS protocol (i.e., PAS with an interstimulus interval of 25 ms) may reduce SICI in the condition of a high baseline SICI (Russmann et al., 2009; Lu et al., 2016, 2017). In the current study the baseline SICI reached 29.6 ± 15.8%, it would be ranged within a high level of SICI. It is intriguing that the SICI findings were inconsistent between the PAS protocol and the PASmr protocol. There is no significant difference of SICI in the PASmr protocol. In addition to the somatosensory afferent, the transcallosal afferent may be engaged in the PASmr protocol. Previous studies have shown that interhemispheric inhibition (Hatta et al., 2003) interferes with SICI and long-latency afferent inhibition in the target hemisphere (Kukaswadia et al., 2005; Reis et al., 2008). It is possible that a complex interaction between the IHI, SICI, and corticospinal pathways erases the SICI reduction observed in the PAS protocol.

ICF is thought to be mediated by distinct mechanisms from SICI and corticospinal excitability (Chen et al., 1998; Pyndt and Ridding, 2004). The fact that the change of ICF is significantly correlated with the reaction time in the PASmr protocol indicates that ICF is associated with the motor task performed ipsilateral to the tested M1 (see **Figures 3B**, **4B**, **5B**). The previous study has shown that not only the MEP but also the ICF was significantly enhanced during the time the subjects were executing a simple motor task with direct and mirror visual feedback at the same side (Maeda et al., 2002; Garry et al., 2005; Nojima et al., 2012; Kumru et al., 2016). The discrepancy of the ICF change between the previous and the current study can be attributed to the different time period while measuring ICF, during the motor task in the previous study and after the motor task in this study. In addition, the frequency of the motor task (2–3 Hz vs. 0.05 Hz) may also play a role in mediating distinct ICF change. It is noted that the ICF change was only found at the M1 controlling the specific muscle mirror to the contralateral movement side (Kumru et al., 2016). Since the PAS effect is also reported with a topographic specificity (Stefan et al., 2000; Wolters et al., 2003; Michou et al., 2013), the subjects were requested to move their APB muscle mirror to the measured site in this study. A further study investigating the relationship between ICF and motor response is anticipated.

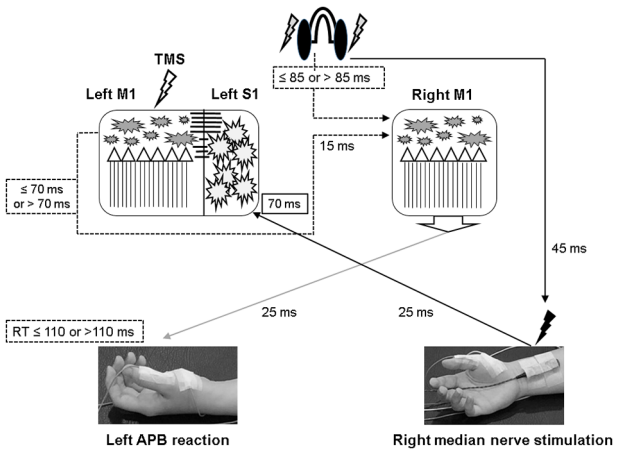

FIGURE 6 | Illustration of the proposed timing flow in bilateral M1. The solid line represents the accurate time period and the dot line indicates the assumed time period. In the PASmr protocol, the somatosensory afferent coming from the right median nerve stimulation arrives at the left somatosensory cortex (S1) approximately 70 ms after the digital sound (shown by the earphones). During the same period, the subjects have to move their left abductor pollicis brevis (APB) muscle to respond to the sound. Since the latency of right M1 to left APB is maximally around 25 ms, a reaction time of 110 ms indicates that the right M1 has to activate corticospinal neurons in 85 ms following the digital sound (that is, 110–25 = 85). Considering that the left M1 needs to disinhibit right M1 through the transcallosal pathway which takes around 15 ms, the left M1 in those subjects with a reaction time of less than 110 ms is supposed to be activated about 70 ms or less following the digital sound (85–15 = 70). Therefore, convergent sensorimotor commands occur almost at the same time when TMS is delivered to the left M1, which takes place in 70 ms following the digital sound.

CONCLUSIONS

The findings suggest that simultaneous somatosensory afferents from the contralateral hemisphere induce STDP in M1. This kind of plasticity can be represented by MEP and ICF. Furthermore, the individual motor reaction time is found significantly

correlated with the degree of the plasticity. Findings provide evidence for designing novel rehabilitation programs concerning motor function.

DATA AVAILABILITY STATEMENT

All datasets presented in this study are included in the article.

ETHICS STATEMENT

The studies involving human participants were reviewed and approved by the local ethics committee of the China Medical University Hospital (CMUH106-REC2-019). The patients/participants provided their written informed consent to participate in this study. Written informed consent was obtained from the individual(s) for the publication of any potentially identifiable images or data included in this article.

AUTHOR CONTRIBUTIONS

YH: subject recruitment, acquisition of data, and writing the first draft. J-CC: experimental design, critical review of the manuscript, and revision of the first draft. C-HT: experimental design, critical review of the manuscript, and comments on the manuscript. M-KL: study concept and experimental design, data analysis and interpretation, and critical revision of the manuscript. All authors contributed to the article and approved the submitted version.

FUNDING

This study was supported in part by grants from the Ministry of Science and Technology (MOST105-2815-C-039-059-B and MOST107-2632-B-039-001) and China Medical University Hospital (DMR-109-230, CRS-108-042), Taichung, Taiwan.

REFERENCES

Antal, A., Dibo, G., Keri, S., Gabor, K., Janka, Z., Vecsei, L., et al. (2000). P300 component of visual event-related potentials distinguishes patients with idiopathic Parkinson's disease from patients with essential tremor. *J. Neural Transm.* 107, 787–797. doi: 10.1007/s007020070059

Bi, G., and Poo, M. (2001). Synaptic modification by correlated activity: Hebb's postulate revisited. *Annu. Rev. Neurosci.* 24, 139–166. doi: 10.1146/annurev.neuro.24.1.139

Brown, P., Day, B. L., Rothwell, J. C., Thompson, P. D., and Marsden, C. D. (1991). Intrahemispheric and interhemispheric spread of cerebral cortical myoclonic activity and its relevance to epilepsy. *Brain* 114, 2333–2351. doi: 10.1093/brain/114.5.2333

Byblow, W. D., Coxon, J. P., Stinear, C. M., Fleming, M. K., Williams, G., Muller, J. F., et al. (2007). Functional connectivity between secondary and primary motor areas underlying hand-foot coordination. *J. Neurophysiol.* 98, 414–422. doi: 10.1152/jn.00325.2007

Chen, R., Tam, A., Butefisch, C., Corwell, B., Ziemann, U., Rothwell, J. C., et al. (1998). Intracortical inhibition and facilitation in different representations of the human motor cortex. *J. Neurophysiol.* 80, 2870–2881. doi: 10.1152/jn.1998.80.6.2870

Cooke, S. F., and Bliss, T. V. (2006). Plasticity in the human central nervous system. *Brain* 129, 1659–1673. doi: 10.1093/brain/awl082

Dan, Y., and Poo, M. M. (2004). Spike timing-dependent plasticity of neural circuits. *Neuron* 44, 23–30. doi: 10.1016/j.neuron.2004.09.007

Dayan, E., and Cohen, L. G. (2011). Neuroplasticity subserving motor skill learning. *Neuron* 72, 443–454. doi: 10.1016/j.neuron.2011.10.008

Edwards, D. J., Dipietro, L., Demirtas-Tatlidede, A., Medeiros, A. H., Thickbroom, G. W., Mastaglia, F. L., et al. (2014). Movement-generated afference paired with transcranial magnetic stimulation: an associative stimulation paradigm. *J. Neuroeng. Rehabil.* 11:31. doi: 10.1186/1743-0003-11-31

Ferbert, A., Priori, A., Rothwell, J. C., Day, B. L., Colebatch, J. G., and Marsden, C. D. (1992). Interhemispheric inhibition of the human motor cortex. *J. Physiol.* 453, 525–546. doi: 10.1113/jphysiol.1992.sp019243

Garry, M. I., Loftus, A., and Summers, J. J. (2005). Mirror, mirror on the wall: viewing a mirror reflection of unilateral hand movements facilitates ipsilateral M1 excitability. *Exp. Brain Res.* 163, 118–122. doi: 10.1007/s00221-005-2226-9

Hatta, A., Nishihira, Y., Kaneda, T., Wasaka, T., Kida, T., Kuroiwa, K., et al. (2003). Somatosensory event-related potentials (ERPs) associated with stopping ongoing movement. *Percept. Mot. Skills* 97, 895–904. doi: 10.2466/pms.2003.97.3.895

Hebb, D. O. (1949). *The Organization of Behavior; a Neuropsychological Theory.* New York, NY: Wiley.

Huang, Y., Chen, J. C., Chen, C. M., Tsai, C. H., and Lu, M. K. (2019). Paired associative electroacupuncture and transcranial magnetic stimulation in humans. *Front. Hum. Neurosci.* 13:49. doi: 10.3389/fnhum.2019.00049

Kida, H., and Mitsushima, D. (2018). Mechanisms of motor learning mediated by synaptic plasticity in rat primary motor cortex. *Neurosci. Res.* 128, 14–18. doi: 10.1016/j.neures.2017.09.008

Kobayashi, M., Hutchinson, S., Schlaug, G., and Pascual-Leone, A. (2003). Ipsilateral motor cortex activation on functional magnetic resonance imaging during unilateral hand movements is related to interhemispheric interactions. *NeuroImage* 20, 2259–2270. doi: 10.1016/s1053-8119(03)00220-9

Koeneke, S., Lutz, K., Herwig, U., Ziemann, U., and Jancke, L. (2006). Extensive training of elementary finger tapping movements changes the pattern of motor cortex excitability. *Exp. Brain Res.* 174, 199–209. doi: 10.1007/s00221-006-0440-8

Koganemaru, S., Mima, T., Nakatsuka, M., Ueki, Y., Fukuyama, H., and Domen, K. (2009). Human motor associative plasticity induced by paired bihemispheric stimulation. *J. Physiol.* 587, 4629–4644. doi: 10.1113/jphysiol.2009.174342

Kroneberg, D., Plettig, P., Schneider, G. H., and Kuhn, A. A. (2018). Motor cortical plasticity relates to symptom severity and clinical benefit from deep brain stimulation in cervical dystonia. *Neuromodulation* 21, 735–740. doi: 10.1111/ner.12690

Kujirai, T., Caramia, M. D., Rothwell, J. C., Day, B. L., Thompson, P. D., Ferbert, A., et al. (1993). Corticocortical inhibition in human motor cortex. *J. Physiol.* 471, 501–519. doi: 10.1113/jphysiol.1993.sp019912

Kukaswadia, S., Wagle-Shukla, A., Morgante, F., Gunraj, C., and Chen, R. (2005). Interactions between long latency afferent inhibition and interhemispheric inhibitions in the human motor cortex. *J. Physiol.* 563, 915–924. doi: 10.1113/jphysiol.2004.080010

Kumru, H., Albu, S., Pelayo, R., Rothwell, J., Opisso, E., Leon, D., et al. (2016). Motor cortex plasticity during unilateral finger movement with mirror visual feedback. *Neural Plast.* 2016:6087896. doi: 10.1155/2016/6087896

Lahr, J., Passmann, S., List, J., Vach, W., Floel, A., and Kloppel, S. (2016). Effects of different analysis strategies on paired associative stimulation. A pooled data analysis from three research labs. *PLoS One* 11:e0154880. doi: 10.1371/journal.pone.0154880

Lu, M. K., Chen, J. C., Chen, C. M., Duann, J. R., Ziemann, U., and Tsai, C. H. (2017). Impaired cerebellum to primary motor cortex associative plasticity in

Parkinson's disease and spinocerebellar ataxia type 3. *Front. Neurol.* 8:445. doi: 10.3389/fneur.2017.00445

Lu, M. K., Chen, C. M., Duann, J. R., Ziemann, U., Chen, J. C., Chiou, S. M., et al. (2016). Investigation of motor cortical plasticity and corticospinal tract diffusion tensor imaging in patients with parkinsons disease and essential tremor. *PLoS One* 11:e0162265. doi: 10.1371/journal.pone.0162265

Lu, M. K., Tsai, C. H., and Ziemann, U. (2012). Cerebellum to motor cortex paired associative stimulation induces bidirectional STDP-like plasticity in human motor cortex. *Front. Hum. Neurosci.* 6:260. doi: 10.3389/fnhum.2012.00260

Maeda, F., Kleiner-Fisman, G., and Pascual-Leone, A. (2002). Motor facilitation while observing hand actions: specificity of the effect and role of observer's orientation. *J. Neurophysiol.* 87, 1329–1335. doi: 10.1152/jn.00773.2000

McKay, D. R., Ridding, M. C., Thompson, P. D., and Miles, T. S. (2002). Induction of persistent changes in the organisation of the human motor cortex. *Exp. Brain Res.* 143, 342–349. doi: 10.1007/s00221-001-0995-3

Meyer, B. U., Röricht, S., Grafin von Einsiedel, H., Kruggel, F., and Weindl, A. (1995). Inhibitory and excitatory interhemispheric transfers between motor cortical areas in normal humans and patients with abnormalities of the corpus callosum. *Brain* 118, 429–440. doi: 10.1093/brain/118.2.429

Meyer, B. U., Röricht, S., and Woiciechowsky, C. (1998). Topography of fibers in the human corpus callosum mediating interhemispheric inhibition between the motor cortices. *Ann. Neurol.* 43, 360–369. doi: 10.1002/ana.410430314

Michou, E., Mistry, S., Rothwell, J., and Hamdy, S. (2013). Priming pharyngeal motor cortex by repeated paired associative stimulation: implications for dysphagia neurorehabilitation. *Neurorehabil. Neural Repair* 27, 355–362. doi: 10.1177/1545968312469837

Minkova, L., Peter, J., Abdulkadir, A., Schumacher, L. V., Kaller, C. P., Nissen, C., et al. (2019). Determinants of inter-individual variability in corticomotor excitability induced by paired associative stimulation. *Front. Neurosci.* 13:841. doi: 10.3389/fnins.2019.00841

Mrachacz-Kersting, N., Kristensen, S. R., Niazi, I. K., and Farina, D. (2012). Precise temporal association between cortical potentials evoked by motor imagination and afference induces cortical plasticity. *J. Physiol.* 590, 1669–1682. doi: 10.1113/jphysiol.2011.222851

Müller-Dahlhaus, F., Ziemann, U., and Classen, J. (2010). Plasticity resembling spike-timing dependent synaptic plasticity: the evidence in human cortex. *Front. Synaptic Neurosci.* 2:34. doi: 10.3389/fnsyn.2010.00034

Ni, Z., Gunraj, C., Nelson, A. J., Yeh, I. J., Castillo, G., Hoque, T., et al. (2009). Two phases of interhemispheric inhibition between motor related cortical areas and the primary motor cortex in human. *Cereb. Cortex* 19, 1654–1665. doi: 10.1093/cercor/bhn201

Nojima, I., Mima, T., Koganemaru, S., Thabit, M. N., Fukuyama, H., and Kawamata, T. (2012). Human motor plasticity induced by mirror visual feedback. *J. Neurosci.* 32, 1293–1300. doi: 10.1523/JNEUROSCI.5364-11.2012

Oldfield, R. C. (1971). The assessment and analysis of handedness: the Edinburgh inventory. *Neuropsychologia* 9, 97–113. doi: 10.1016/0028-3932(71)90067-4

Peurala, S. H., Muller-Dahlhaus, J. F., Arai, N., and Ziemann, U. (2008). Interference of short-interval intracortical inhibition (SICI) and short-interval intracortical facilitation (SICF). *Clin. Neurophysiol.* 119, 2291–2297. doi: 10.1016/j.clinph.2008.05.031

Pötter-Nerger, M., Fischer, S., Mastroeni, C., Groppa, S., Deuschl, G., Volkmann, J., et al. (2009). Inducing homeostatic-like plasticity in human motor cortex through converging corticocortical inputs. *J. Neurophysiol.* 102, 3180–3190. doi: 10.1152/jn.91046.2008

Pyndt, H. S., and Ridding, M. C. (2004). Modification of the human motor cortex by associative stimulation. *Exp. Brain Res.* 159, 123–128. doi: 10.1007/s00221-004-1943-9

Reis, J., Swayne, O. B., Vandermeeren, Y., Camus, M., Dimyan, M. A., Harris-Love, M., et al. (2008). Contribution of transcranial magnetic stimulation to the understanding of cortical mechanisms involved in motor control. *J. Physiol.* 586, 325–351. doi: 10.1113/jphysiol.2007.144824

Rizzo, V., Siebner, H. S., Morgante, F., Mastroeni, C., Girlanda, P., and Quartarone, A. (2009). Paired associative stimulation of left and right human motor cortex shapes interhemispheric motor inhibition based on a Hebbian mechanism. *Cereb. Cortex* 19, 907–915. doi: 10.1093/cercor/bhn144

Russmann, H., Lamy, J. C., Shamim, E. A., Meunier, S., and Hallett, M. (2009). Associative plasticity in intracortical inhibitory circuits in human motor cortex. *Clin. Neurophysiol.* 120, 1204–1212. doi: 10.1016/j.clinph.2009.04.005

Sanes, J. N., and Donoghue, J. P. (2000). Plasticity and primary motor cortex. *Annu. Rev. Neurosci.* 23, 393–415. doi: 10.1146/annurev.neuro.23.1.393

Stefan, K., Kunesch, E., Benecke, R., Cohen, L. G., and Classen, J. (2002). Mechanisms of enhancement of human motor cortex excitability induced by interventional paired associative stimulation. *J. Physiol.* 543, 699–708. doi: 10.1113/jphysiol.2002.023317

Stefan, K., Kunesch, E., Cohen, L. G., Benecke, R., and Classen, J. (2000). Induction of plasticity in the human motor cortex by paired associative stimulation. *Brain* 123, 572–584. doi: 10.1093/brain/123.3.572

Thabit, M. N., Ueki, Y., Koganemaru, S., Fawi, G., Fukuyama, H., and Mima, T. (2010). Movement-related cortical stimulation can induce human motor plasticity. *J. Neurosci.* 30, 11529–11536. doi: 10.1523/JNEUROSCI.1829-10.2010

Wolters, A., Sandbrink, F., Schlottmann, A., Kunesch, E., Stefan, K., Cohen, L. G., et al. (2003). A temporally asymmetric Hebbian rule governing plasticity in the human motor cortex. *J. Neurophysiol.* 89, 2339–2345. doi: 10.1152/jn.00900.2002

Zhang, L. I., Tao, H. W., Holt, C. E., Harris, W. A., and Poo, M. (1998). A critical window for cooperation and competition among developing retinotectal synapses. *Nature* 395, 37–44. doi: 10.1038/25665

Ziemann, U., Ilic, T. V., Pauli, C., Meintzschel, F., and Ruge, D. (2004). Learning modifies subsequent induction of long-term potentiation-like and long-term depression-like plasticity in human motor cortex. *J. Neurosci.* 24, 1666–1672. doi: 10.1523/JNEUROSCI.5016-03.2004

Ziemann, U., Paulus, W., Nitsche, M. A., Pascual-Leone, A., Byblow, W. D., Berardelli, A., et al. (2008). Consensus: motor cortex plasticity protocols. *Brain Stimul.* 1, 164–182. doi: 10.1016/j.brs.2008.06.006

Ziemann, U., Rothwell, J. C., and Ridding, M. C. (1996). Interaction between intracortical inhibition and facilitation in human motor cortex. *J. Physiol.* 496, 873–881. doi: 10.1113/jphysiol.1996.sp021734

Conflict of Interest: The authors declare that the research was conducted in the absence of any commercial or financial relationships that could be construed as a potential conflict of interest.

Copyright © 2020 Huang, Chen, Tsai and Lu. This is an open-access article distributed under the terms of the Creative Commons Attribution License (CC BY). The use, distribution or reproduction in other forums is permitted, provided the original author(s) and the copyright owner(s) are credited and that the original publication in this journal is cited, in accordance with accepted academic practice. No use, distribution or reproduction is permitted which does not comply with these terms.

frontiers in Neural Circuits

ORIGINAL RESEARCH
published: 18 March 2021
doi: 10.3389/fncir.2021.616084

Modulation of the Corticomotor Excitability by Repetitive Peripheral Magnetic Stimulation on the Median Nerve in Healthy Subjects

Yanbing Jia[1†], Xiaoyan Liu[1†], Jing Wei[1], Duo Li[1], Chun Wang[1], Xueqiang Wang[2] and Hao Liu[2,3*]*

[1]Neuro-Rehabilitation Center, JORU Rehabilitation Hospital, Yixing, China, [2]Department of Sport Rehabilitation, Shanghai University of Sport, Shanghai, China, [3]Department of Rehabilitation, JORU Rehabilitation Hospital, Yixing, China

Objective: We aimed to examine the effects of repetitive peripheral nerve magnetic stimulation (rPNMS) on the excitability of the contralateral motor cortex and motor function of the upper limb in healthy subjects.

Methods: Forty-six healthy subjects were randomly assigned to either a repetitive peripheral nerve magnetic stimulation group (n = 23) or a sham group (n = 23). The repetitive peripheral nerve magnetic stimulation group received stimulation using magnetic pulses at 20 Hz, which were applied on the median nerve of the non-dominant hand, whereas the sham group underwent the same protocol without the stimulation output. The primary outcome was contralateral transcranial magnetic stimulation (TMS)-induced corticomotor excitability for the abductor pollicis brevis of the stimulated hand in terms of resting motor threshold (rMT), the slope of recruitment curve, and peak amplitude of motor evoked potential (MEP), which were measured at baseline and immediately after each session. The secondary outcomes were motor hand function including dexterity and grip strength of the non-dominant hand assessed at baseline, immediately after stimulation, and 24 h post-stimulation.

Results: Compared with the sham stimulation, repetitive peripheral nerve magnetic stimulation increased the peak motor evoked potential amplitude immediately after the intervention. The repetitive peripheral nerve magnetic stimulation also increased the slope of the recruitment curve immediately after intervention and enhanced hand dexterity after 24 h. However, the between-group difference for the changes was not significant. The significant changes in hand dexterity and peak amplitude of motor evoked potential after repetitive peripheral nerve magnetic stimulation were associated with their baseline value.

Conclusions: Repetitive peripheral nerve magnetic stimulation may modulate the corticomotor excitability together with a possible lasting improvement in hand dexterity, indicating that it might be helpful for clinical rehabilitation.

Keywords: repetitive peripheral nerve magnetic stimulation, corticomotor excitability, transcranial magnetic stimulation, motor function, brain plasticity

OPEN ACCESS

Edited by:
Ti-Fei Yuan,
Shanghai Jiao Tong University, China

Reviewed by:
Qiang Gao,
Sichuan University, China
He Xiaokuo,
Xiamen Fifth Hospital, China

***Correspondence:**
Hao Liu
liuhao0909@163.com
Xueqiang Wang
wangxueqiang@sus.edu.cn

[†]These authors have contributed equally to this work

Received: *11 October 2020*
Accepted: *01 March 2021*
Published: *18 March 2021*

Citation:
Jia Y, Liu X, Wei J, Li D, Wang C, Wang X and Liu H (2021) Modulation of the Corticomotor Excitability by Repetitive Peripheral Magnetic Stimulation on Median Nerve in Healthy Subjects. Front. Neural Circuits 15:616084. doi: 10.3389/fncir.2021.616084

INTRODUCTION

Repetitive peripheral magnetic stimulation (rPMS) is a safe, non-invasive treatment method for motor impairment and pain in people with neural or musculoskeletal disorders because it can penetrate deeper structures with painless stimulation and can produce muscle contractions and sensory afferents (Beaulieu and Schneider, 2015). With the coil (pulse generator) applied to the muscles, previous studies have demonstrated that rPMS can reduce spasticity and improve motor control of paretic limbs in individuals with stroke (Struppler et al., 2003, 2007; Beaulieu et al., 2015). The underlying mechanism of such clinical improvement is associated with cortical plastic effects. For instance, using neuroimaging tools and transcranial magnetic stimulation (TMS) in stroke, researchers have shown that rPMS on paretic limb muscle can induce the activation of the frontoparietal loops (Struppler et al., 2007; Gallasch et al., 2015) and increase corticomotor excitability (Gallasch et al., 2015; Beaulieu et al., 2017) in the lesioned hemisphere. Such neurophysiological changes can explain the improvement of motor function after rPMS.

Transcutaneous electrical stimulation to the peripheral nerves (PNS) is a common intervention used to treat motor impairment for clinical rehabilitation. In humans, evidence suggests that PNS enhances the excitability of the motor cortex. In our previous study, we applied PNS to the radial and ulnar nerves in the paretic upper limb and showed that PNS for 1 h increased the corticomotor excitability, which was assessed by TMS in both hemispheres, and improved the dexterity performance of the affected upper limb in people with chronic stroke (Liu and Au-Yeung, 2017). When the stimulation is performed over the median nerve, PNS upregulated cortical excitability in both healthy subjects and patients with central nervous system lesions (Farias da Guarda and Conforto, 2014; Chen et al., 2015). To compare with PNS, stimulating the peripheral nerves with magnetic pulses, in a process called repetitive peripheral nerve magnetic stimulation (rPNMS), preferentially activates the lower motor nerves with minimal activation of cutaneous fibers so that is considered as a painless method (Szecsi et al., 2014; Beaulieu and Schneider, 2015). Furthermore, rPNMS does not need skin preparation and the patient can remain clothed. These advantages of magnetic stimulation might allow rPNMS to be used more widely in clinical practice. In terms of clinical effects, few studies demonstrated rPNMS could reduce the muscle spasticity in children with cerebral palsy (Flamand et al., 2012) and improve motor function in healthy people (Kremenic et al., 2004). However, whether rPNMS can induce modulatory effects within the motor cortex is not known. The aim of the present study was therefore to investigate if rPNMS can induce corticomotor excitability changes in normal subjects. We hypothesized that one session of rPNMS to the arm could enhance corticomotor excitability in the contralateral hemisphere together with motor function improvement of the ipsilateral upper limb. Understanding the corticomotor effects of rPNMS in healthy subjects might aid in the use of rPNMS as an evidence-based treatment for clinical rehabilitation.

MATERIALS AND METHODS

Subjects and Study Design

Forty-six young physiotherapy interns in JORU Rehabilitation Hospital were recruited in the study after providing written informed consent. This sample size was based on the data from our pilot study by assuming a type I error of 5% and power of 80%. All subjects were randomly assigned to either an rPNMS group (n = 23, 14 males, nine females; age = 21.17 $\pm$ 1.27 years; right-handed, 21 subjects) or a sham group (n = 23, 12 males, 11 females; age = 21.30 $\pm$ 1.22 years; right-handed, 21 subjects) according to a coded lot picked by them. The inclusion criteria were normal physical status, uneventful past and present medical conditions on the non-dominant upper extremity. Subjects were excluded if they had a history of musculoskeletal or neurological pathology affecting the non-dominant upper limb, signs of cognitive impairments, or contraindications for TMS including a history of epilepsy and presence of metal in the head region or a cardiac pacemaker (Rossi et al., 2009).

All subjects underwent one session of intervention according to the protocol for the specific group (rPNMS or sham). TMS-induced corticomotor excitability and motor function of the non-dominant hand were evaluated at baseline and immediately after the intervention. To examine the lasting effects, motor hand function was also assessed 24 h after the intervention. The assessment and intervention were delivered by specific but different physical therapists to realize the allocation concealment. **Figure 1** presents the experimental procedure for this study. The study protocol was approved by the Research Ethics Committee of the JORU Rehabilitation Hospital (No.: 20190702A01) and was conducted as per the Declaration of Helsinki (World Medical Association, 2013).

Application of Magnetic Stimulation: rPNMS and rPNMS-Sham

Subjects were seated, and their non-dominant forearm, in a supine position, was placed on a pillow at rest on the table in front of them. Magnetic stimulation was applied on the median nerve of the non-dominant hand over the volar side of the forearm at 3–4 cm apart from the distal wrist crease using the Magneuro100 stimulator (VISHEE Company Limited, Nanjing, China) and a figure-of-eight coil (outer diameter of each wing: 80 mm). The coil was positioned such that the handle was perpendicular to the arm (Gallasch et al., 2015).

The stimulation consisted of 60 trains with a pulse frequency of 20 Hz at a train duration of 2 s and an inter-train interval of 8 s. Thus, a total of 2,400 pulses were delivered in the whole session over 10 min. This specific protocol selected in the current study was based on previous literature that reported the longer lasting effects of motor control with 20 Hz peripheral magnetic stimulation and 2,000–4,000 stimuli with OFF/ON ratio at the vicinity of 4 was most used for sensorimotor impairments (Gallasch et al., 2015). The intensity of stimulation was set at 150% threshold intensity which was defined as the lowest output intensity for inducing visible contractions, such as thenar apposition and flexion of the index and middle fingers with a single magnetic pulse on the median

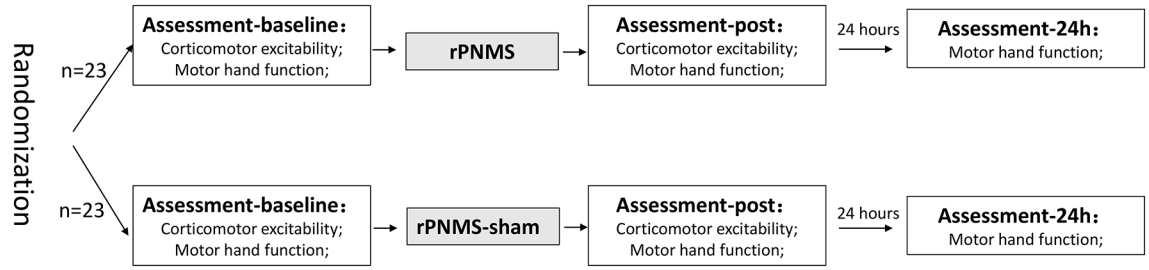

FIGURE 1 | Flowchart of the experimental procedure.

nerve (Gallasch et al., 2015). The mean threshold intensity was 10.35 ± 2.25% of the maximum stimulator output for the rPNMS group and 10.65 ± 2.03% for the sham group. Therefore, the applied mean stimulation intensity was 15.75 ± 3.45% for the rPNMS group and 16.25 ± 3.01% for the sham group. For the sham group, the reverse side of the coil contacted the arm so that no magnetic output was given to the target median nerve with the same noise generated from the stimulator as the rPNMS group.

Outcome Measures

Corticomotor Excitability

Changes in corticomotor excitability for the abductor pollicis brevis muscle (APB) of the non-dominant hand were assessed using the Magneuro 100 stimulator connected with the matching motor evoked potential (MEP) detection module (bandpass: 20–500 Hz) and figure-of-eight coil (VISHEE Company Limited, Nanjing, China). The EMG signals were captured by a pair of self-adhesive surface electrodes placed over the tendon and belly of the APB muscle, with the ground electrode placed over the ulnar styloid process of the arm. The MEP detection module then recorded and processed the signals, and MEP data were output on the computer screen. The corticomotor excitability was evaluated using three parameters: resting motor threshold (rMT), the slope of the MEP recruitment curve (RC slope), and the peak amplitude of MEP (peak MEP). All three parameters have been shown to have good test-retest reliability (intraclass correlation coefficient ≥ 0.75) in our previous study (Liu and Au-Yeung, 2014).

During the TMS assessment, subjects sat on a high-back chair with their arms, legs, neck, and back supported. The examiner placed the coil tangentially on the scalp over the hand representation area of the primary motor cortex (M1) contralateral to the non-dominant hand, with the coil handle pointed backward and at 45° from the midline sagittal plane of the skull. A single magnetic pulse was generated for assessment. The optimal site which is called a "hotspot" was located such that it consistently elicited the largest MEP with the lowest TMS intensity by moving the TMS coil in 1 cm steps over the M1 contralateral to the target APB with a TMS intensity above 60% of the maximum output (Liu and Au-Yeung, 2014). After the hotspot was identified, the rMT was defined as the lowest TMS intensity which could produce MEP amplitudes of at least 50 μV for the relaxed APB muscle in at least 5 out of 10 consecutive TMS stimuli (Darling et al., 2006). Afterward, the MEPs were recorded at stimulation intensities at 1.0, 1.1, 1.2, 1.3, 1.4, and 1.5 of rMT for every five stimuli (Liu and Au-Yeung, 2014). After a resting period of 1 min, the same procedure was repeated. Therefore, the RC in the present study was plotted with the average MEP amplitude of 10 stimuli against the corresponding TMS intensities from 1.0 to 1.5 rMT. With rMT above 72% maximum stimulation output, RC of two subjects were plotted using the intensity from 1.0 to 1.3 of rMT. The RC slope was calculated as the linear slope of this stimulus-response curve. The peak MEP amplitude was identified as the maximum mean MEP evoked by the TMS stimuli in examining the recruiting curve.

Motor Hand Function

Grip Strength

The maximal grip strength of the non-dominant hand was measured using the Jamar dynamometer (Sammons Preston, Rolyon, Bolingbrook, IL, USA) while the subjects were sitting, with the elbow kept at 90° flexion and the forearm in neutral pronation. Three trials of maximal grip force were recorded, and the mean value was calculated.

Hand Dexterity

The dexterity of the non-dominant upper extremity was evaluated using the Purdue pegboard. During the assessment, subjects were required to pick up small pins using the non-dominant hand and insert the pins into holes of the board along the column ipsilateral to the tested hand consecutively. The hand dexterity score was the mean value of the number of pins inserted into the holes in 30 s for three trials.

Data Analysis

The SPSS statistical software package (Version 20.0) was used for data analysis. The demographic characteristics of the subjects and all outcome measures are represented by the calculations of means and standard deviations (SDs). Assumption of normality for all outcomes data was validated using the Shapiro–Wilk test. An independent sample *t*-test was conducted to examine the differences in baseline measurements between the two groups. The corticomotor excitability in terms of rMT, RC slope, and peak MEP amplitude and motor hand function outcomes of grip strength and dexterity function were examined with two-way repeated-measures analysis of variance (ANOVA) with within-subject factor for time (two levels on corticomotor

excitability: baseline, post-stimulation; three levels on motor hand function: baseline, post-stimulation, 24 h afterward) and between-subject factor for the groups (rPNMS and sham). In case of significant or potentially significant time*group interaction effect, *post hoc* comparisons were performed using one-way repeated measures ANOVAs for each group with factor time (two levels on corticomotor excitability: baseline, post-stimulation; three levels on motor hand function: baseline, post-stimulation, 24 h afterward) with the Bonferroni correction. The significance threshold was set at 0.05.

For any significant changes in each outcome measure after rPNMS, the Pearson correlation coefficient was used to examine its relationship with its baseline value. The level of significance was set at 0.05.

RESULTS

Valid data were obtained for all 46 participants of the two groups. None of the subjects reported any feeling of pain or discomfort during either rPNMS or sham stimulation. The demographic characteristics of the subjects in the two groups were comparable (**Table 1**).

The MEP recruitment curves plotted with MEP amplitude against the intensity of the TMS stimulus for the two groups were shown in **Figure 2**. The statistical analysis of all outcomes at baseline with an independent *t*-test showed that there were no significant differences between the two groups ($p > 0.05$). rPNMS resulted in a significant increase in peak MEP amplitude than the sham stimulation. Two-way repeated-measures ANOVA revealed a significant effect of time ($F = 7.458$, $p = 0.009$) and a significant effect of time *group interaction ($F = 5.261$, $p = 0.027$) with no significant effect of group ($F = 0.043$, $p = 0.838$). *Post hoc* comparison showed a significant difference in peak MEP amplitude in the rPNMS group ($p = 0.002$) but not in the sham group ($p = 0.762$) at post-stimulation compared with baseline (**Figure 3**).

rMT and RC slope were respectively decreased and increased in all participants over time: two-way repeated-measures ANOVA demonstrated a significant effect of time ($F = 4.085$, $p = 0.049$ for rMT; $F = 8.205$, $p = 0.006$ for RC slope) but no significant effects of group ($F = 0.030$, $p = 0.863$ for rMT; $F = 0.056$, $p = 0.814$ for RC slope) or group * time interaction ($F = 1.673$, $p = 0.203$ for rMT; $F = 1.735$, $p = 0.195$ for RC slope). *Post hoc* comparison revealed a significant increase in the RC slope ($p = 0.006$; **Figure 4**), whereas the change in rMT was not significant but showed a trend toward reduction ($p = 0.055$) after rPNMS (**Figure 5**). Both rMT and RC slope for corticomotor excitability remained unaltered after sham stimulation.

TABLE 1 | Demographic characteristics of the subjects assigned into two groups.

	rPNMS (n = 23)	Sham (n = 23)
Age (years), mean ± SD	21.17 ± 1.27	21.30 ± 1.22
Male (n)	14	12
Female (n)	9	11
Right-handed (n)	21	21
Left-handed (n)	2	2

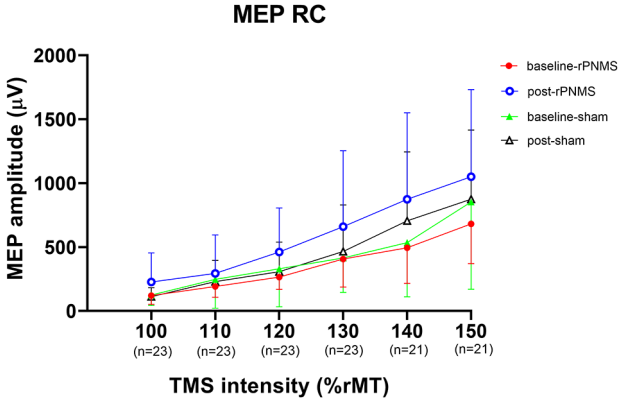

FIGURE 2 | The motor evoked potential (MEP) recruitment curves plotted with MEP amplitude (μV) against the intensity of the transcranial magnetic stimulation (TMS) stimulus (%rMT) for two groups at baseline and post-stimulation. The solid dots (red) and open circles (blue) represent the MEP values for repetitive peripheral nerve magnetic stimulation (rPNMS) at baseline and post-stimulation respectively; the solid (green) and open (black) triangles were for that of sham stimulation at baseline and post-stimulation, respectively.

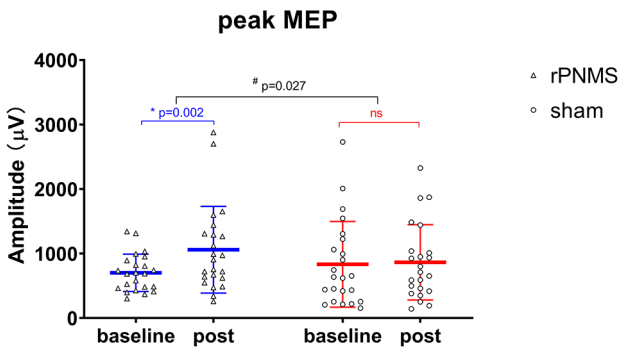

FIGURE 3 | The peak MEP amplitude (μV) was assessed at baseline and immediately after intervention: rPNMS (blue line) and sham (red line). The open triangles and circles represent the individual data in the rPNMS and sham group respectively. The change after rPNMS was different from that after sham stimulation (two-way repeated-measures ANOVA, time*group interaction effect; $^{\#}p = 0.027$). *Post hoc* analysis showed significant improvement in peak MEP amplitude after rPNMS ($^{*}p = 0.002$) but not sham stimulation. ns, not significant.

Regarding the motor hand function, the dexterity of the upper extremity evaluated using the Purdue pegboard was significantly improved after two stimulations over time: two-way repeated-measures ANOVA revealed a significant effect of time ($F = 10.081$, $p = 0.000$) but no significant effects of group ($F = 0.132$, $p = 0.719$) or group * time interaction ($F = 1.577$, $p = 0.212$). The *post hoc* comparison showed the dexterity of the upper extremity evaluated using the Purdue pegboard was significantly improved after rPNMS ($F = 8.851$, $p = 0.001$) but not after sham stimulation ($F = 2.088$, $p = 0.136$). For rPNMS group, the pairwise comparisons revealed that the improvement in Purdue pegboard score was significant at 24 h afterwards compared with baseline ($p = 0.003$) and immediately after

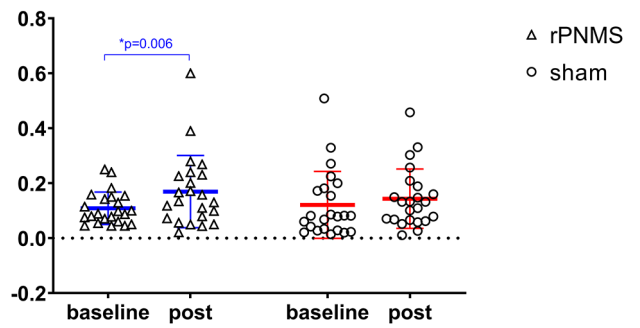

FIGURE 4 | The slope of the MEP recruit curve was assessed at baseline and immediately after intervention: rPNMS (blue line) and sham (red line). The open triangles and circles represent the individual data in the rPNMS and sham group respectively. There was no significant difference in RC slope change between the two groups. The significant change after rPNMS is presented as $^*p = 0.006$.

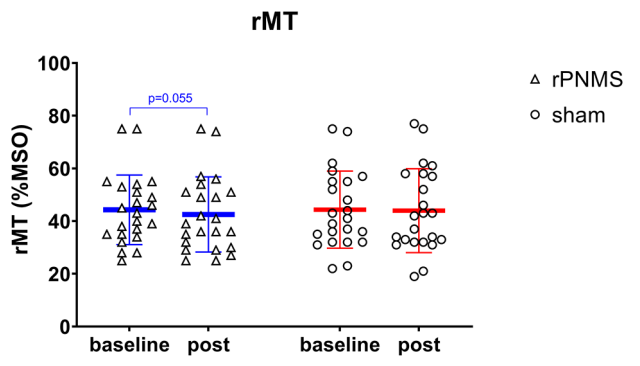

FIGURE 5 | The rMT (%MSO) was assessed at baseline and immediately after intervention: rPNMS (blue line) and sham (red line). The open triangles and circles represent the individual data in the rPNMS and sham group respectively. There was no significant difference in rMT change between the two groups. The change after rPNMS was showed a trend toward reduction as $p = 0.055$.

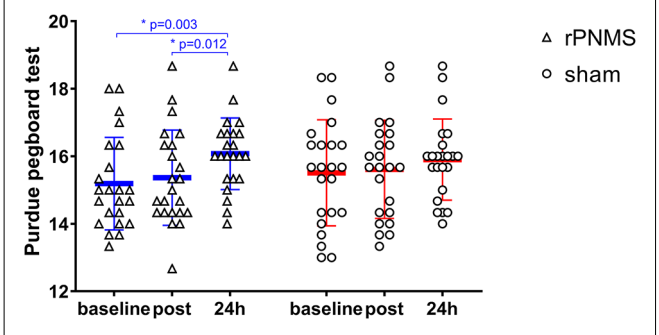

FIGURE 6 | The hand dexterity function in the Purdue pegboard test was assessed at baseline, immediately after the intervention, and 24 h after interventions: rPNMS (blue line) and sham (red line). The open triangles and circles represent the individual data in the rPNMS and sham group respectively. There was no significant difference in hand dexterity change between the two groups. *Post hoc* pairwise comparison with Bonferroni correction revealed that the improvement in Purdue pegboard score was significant at 24 h afterward compared with baseline ($^*p = 0.003$) and immediately after rPNMS ($^*p = 0.012$).

rPNMS ($p = 0.012$; **Figure 6**). There were no significant effects of time ($F = 1.014$, $p = 0.344$), group ($F = 0.040$, $p = 0.842$) or group∗time interaction ($F = 0.168$, $p = 0.765$) regarding grip strength.

The correlation analysis demonstrated that the improvement in Purdue pegboard score (0.88 ± 1.10) and peak MEP amplitude ($357.08 \pm 478.99\ \mu V$) after rPNMS were negatively and positively correlated with their baseline value respectively ($r = -0.651$, $p = 0.001$ and $r = 0.498$, $p = 0.016$; **Figures 7A,B**), whereas the correlation of the change in RC slope with its baseline value was not significant ($r = 0.392$, $p = 0.065$; **Figure 7C**; **Table 2**).

DISCUSSION

The present study aimed to investigate the changes in corticomotor excitability and motor hand function induced by repetitive stimulation using magnetic pulses instead of conventional electrical current, and which was applied on peripheral nerves rather than on muscles as in other previous rPMS studies. This study newly showed that one session of rPNMS applied to the median nerve of the non-dominant upper extremity modestly increased the corticomotor excitability in contralateral M1 and may associate improved hand dexterity in healthy young individuals.

Gallasch et al. (2015) applied repetitive magnetic stimulation with 15,000 pulses delivered at 25 Hz for 20 min on the volar side of the right forearm to stimulate finger and wrist flexor muscles in normal subjects and showed a significant increase in the MEP amplitudes recorded at right flexors carpi radialis. Such upregulation of MEP amplitudes was associated with a decreased short-interval intracortical inhibition (SICI) and increased intracortical facilitation (ICF), which were assessed by paired-pulse TMS, as well as enhanced activation in left precentral/postcentral gyrus, as shown by fMRI scans. Similarly, the present study showed that repetitive magnetic stimulation to the median nerve of the non-dominant hand with 2,400 pulses, delivered at a slightly lower frequency of 20 Hz over 10 min, increased the RC slope and peak MEP amplitudes in the contralateral hemisphere. This observation agreed with the results of studies that demonstrated that the induction of corticomotor excitability changes after an external electrical stimulation was applied to the muscles or peripheral nerves (Charlton et al., 2003; Chipchase et al., 2011). The underlying mechanism may be that the repetitive magnetic stimulation applied on either muscle or the peripheral nerve may have induced the proprioceptive input by the direct action of the sensorimotor nerve fibers and the indirect activation of mechanoreceptors during a rhythmical contraction–relaxation and muscle vibration (Struppler et al., 2004; Momosaki et al., 2017). Such proprioceptive afferent input to the S1 along the ascending sensory pathway then

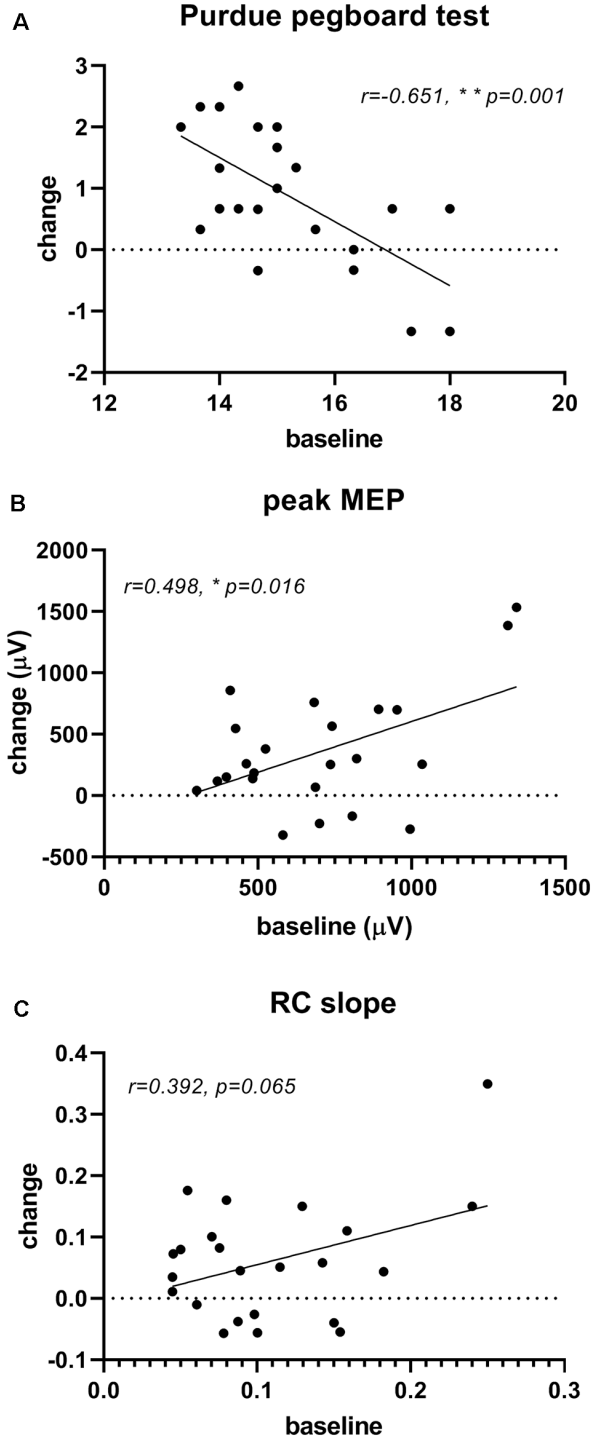

FIGURE 7 | Correlation of significant changes in outcome measures after rPNMS with their baseline value: Purdue pegboard score **(A)**, peak MEP amplitude (μV; **B**) and RC slope **(C)**. The significant correlation was found for Purdue pegboard score (r = −0.651, p = 0.001) and peak MEP amplitude (r = 0.498, p = 0.016) but not for RC slope (r = 0.392, p = 0.065).

might drive reorganization in M1 through the structural and functional connections between S1 and M1 (Schabrun et al., 2013). This neural circuit would play a vital role in modulatory effects of corticomotor excitability from rPNMS in the current study.

The RC represents the growth of MEP amplitudes as a function of TMS output intensity; thus, the slope reflected the neurophysiological strength of intracortical and corticospinal connections (Liu and Au-Yeung, 2014). The peak MEP during the RC assessment revealed the extent of maximal excitation caused by the recruitment of the corticospinal pathways responding to TMS (Liu and Au-Yeung, 2014). Therefore, the increase in the RC slope and peak MEP amplitudes after rPNMS in the present study might indicate the enhanced activation of corticomotor synaptic connections and the corticospinal pathways to the non-dominant APB muscle in contralateral M1. This rapid cortical plasticity was suggested to be associated with the unmasking of latent synapses and the modification of synaptic strength, which are known to be involved in the reduction of GABAergic inhibition (Chipchase et al., 2011; Beaulieu et al., 2017). The downregulation of GABAergic inhibition is the mechanism underlying peripheral electrical nerve (Kaelin-Lang et al., 2002) and magnetic muscle stimulation (Gallasch et al., 2015; Beaulieu et al., 2017). Kaelin-Lang et al. (2002) showed that the MEP amplitudes of contralateral abductor digiti minimi muscle were increased after a 2-h ulnar stimulation. However, this excitatory effect of PNS was blocked by lorazepam, which is a GABA receptor agonist. In contrast, Gallasch et al. (2015) and Beaulieu et al. (2017) demonstrated decreased SICI, which was more likely mediated by GABA-A receptors after one or multiple sessions of rPMS which were applied to stimulate the muscles in the upper limb of normal subjects and the lower limb of chronic stroke patients, respectively. Hence, it remains to be verified whether an increase in RC slope and peak MEP amplitudes after the rPNMS in this study are the after-effects of decreased GABAergic intracortical inhibition.

Gallasch et al. (2015) showed that rPMS applied to muscles could not alter the rMT in healthy subjects, whereas rMT showed non-significant changes but tended to decrease after rPNMS in the present study. As another aspect of corticomotor excitability, the motor threshold is known to depend on the voltage-gated sodium channels and reflects the membrane excitability of the corticomotor neurons in the cortical motor representation region for the target muscle (Liu and Au-Yeung, 2014; Ziemann et al., 2015). Hence, the results of the present study might indicate insufficient changes of ionotropic channels for membrane excitability enhancement of motor neurons contralateral to the APB muscle induced by a single session of rPNMS applied to the median nerve based on the current protocol and healthy sample.

Nevertheless, to take a more rigorous data analysis, the peak MEP amplitude and RC slope after rPNMS were not significantly different from their values in the sham group at baseline and immediately after stimulation even the significant group difference was found for peak MEP amplitude and statistical pre-post change for these two corticomotor excitability outcomes after rPNMS. This may indicate that the corticomotor excitability induced by peripheral magnetic stimulation applied to the median nerve with current protocol in one single session

TABLE 2 | Correlation between changes in outcome measures after repetitive peripheral nerve magnetic stimulation (rPNMS) and their baseline value.

Outcome measures	Baseline (mean ± SD)	Changes (mean ± SD)	Pearson's *r*	*p*
Purdue	15.19 ± 1.37	0.88 ± 1.10	−0.651	0.001**
RC slope	0.11 ± 0.06	0.06 ± 0.10	0.392	0.065
peak MEP	702.09 ± 288.71	357.08 ± 478.99	0.498	0.016*

*Correlation is significant and $p < 0.05$; **correlation is significant and $p < 0.05$.

might not be robust enough. On the other hand, individual data points of peak MEP amplitude and RC slope showed two subjects had a relatively larger response for rPNMS. If these two subjects were excluded, the statistical analysis revealed non-significant group differences (time * group interaction: $F = 2.983$, $p = 0.092$) for peak MEP amplitude with the pre-post change were still significant ($p = 0.003$ for peak MEP amplitude and $p = 0.014$ for RC slope respectively). Hence, the up-regulation effects of corticomotor excitability induced by rPNMS in the present study should be treated with caution. Using repetitive sessions of stimulation, well-designed research with a larger sample and good homogeneity, and healthy subjects should be conducted attempting to elicit more robust modulatory effects of rPNMS.

Previous studies have shown that the rPMS to the muscles could increase dexterity function in stroke patients. Struppler et al. (2003, 2007) demonstrated that the velocity and amplitude of finger movements were significantly enhanced after 15 min of rPMS applied to the hand extensor muscles, and such improvement in dexterity was associated with a reduction in spasticity, which might be the main interference factor of the movements of paretic extremities in patients with spastic paresis. When rPMS is applied to the peripheral nerves, similar effects were also observed in healthy people. Using a pre-post design in normal subjects, Okudera et al. (2015) applied 600 magnetic pulses at a frequency of 20 Hz on the radial nerve of the non-dominant hand and showed that the upper limb dexterity performance was improved, which was measured with the Box and Block Test, and this improvement was sustained for at least 15 min. For hand dexterity function change in the present study, the performance of the subjects for the Purdue pegboard improved after one session of rPNMS on the median nerve of the non-dominant hand, and this improvement was exhibited as a latent effect 24 h afterward. This was in line with the results of a previous study on healthy subjects which showed that rPMS applied to the forearm flexor muscles increased the degree of elbow stabilization (Struppler et al., 2004). This augment of stabilization of the elbow joint is required and important for fine skilled movements such as grasping and manipulation during the Purdue pegboard test. Although such benefits in hand dexterity were observed after rPNMS, the between-group difference was not significant in the statistical analysis. Based on the effect size of 0.19, we deemed that the small sample size ($n = 46$) of the present study might have accounted for the non-significant difference between the two groups. To calculate with a sample size software, a sample of at least 74 (37 per group) would be required to validate the positive effects of rPNMS in improving hand dexterity function beyond that of sham intervention. On the other hand, a notable correlation was found between the amount of change of hand dexterity performance after rPNMS and their baseline values. The good performance of the Purdue pegboard test at baseline was negatively related to its improvement 24 h after rPNMS might indicate the inherent limitation of hand dexterity in healthy people. Moreover, it was noted that the baseline values of the Purdue pegboard score were slightly higher in the sham group (15.50 ± 1.57) than in the rPNMS group (15.19 ± 1.37) even the difference was not significant. Further analysis showed that the Purdue pegboard score of subjects with lower baseline values (<15.50, $n = 11$) in the sham group was also increased at 24 h after the sham stimulation (15.15 ± 0.81) compared with baseline (14.12 ± 0.82; $p = 0.003$) and immediately after sham stimulation (14.42 ± 0.87; $p = 0.024$). This could be explained that the relative inflexible upper extremity in healthy subjects might present better responsiveness to the process of the Purdue pegboard test which *per se* can be seen as a practice. However, this might raise the question of whether the improvement in hand dexterity after rPNMS was attributed to the magnetic nerve stimulation or was due to the lower baseline itself. To address this, a future study with a larger sample would show a more comparable baseline of motor hand function for different groups and should be able to respond to this argument.

A few studies have demonstrated that using multiple sessions of rPMS to stimulate limb muscles could enhance muscle strength. With the coil placed over the anterior aspect of the thigh, Yang et al. (2017) showed that both isometric and isokinetic maximum/average peak torque of quadriceps were increased significantly after 15 min of rPMS applied three times per week for five consecutive weeks, while the quadriceps strength was not changed in the control group, which performed normal activities of daily living during the 5 weeks. Musarò et al. (2019) applied the 10 sessions of daily magnetic stimulation to the forearm flexor muscles in patients with amyotrophic lateral sclerosis and showed significant improvement in the MRC-score of the flexor carpi radialis muscle and muscle strength, which was measured using a handgrip dynamometer. By contrast, no significant improvement in muscle strength was observed in the other untreated muscles and in the opposite arm which received sham stimulation. Besides, rPMS applied to certain muscles for 15–24 sessions in a period of 3–8 weeks also enhanced the muscle strength for several other conditions that may lead to muscle weakness such as COPD (Bustamante et al., 2010) as well as post-operation muscle weakness (Baek et al., 2018). The lack of improvement in handgrip strength after rPNMS on the median nerve in the present study might be due to the minimum dose administered in one single session.

Although rPNMS did not show the superior effects in motor hand function to sham stimulation in the present study,

the up-regulation of corticomotor excitability, even the effects were modest, would allow it to serve as a primer delivered ahead of other interventions and may bring the possible benefits for function enhancement in clinical rehabilitation. On the other hand, the rPNMS-induced increase in peak MEP amplitude was positively related to its value before stimulation might reveal that the people with less exciting motor cortex could be more responsive to rPNMS. Hence, peak MEP amplitude may be used as a TMS outcome to predict the cortical effects when rPNMS is delivered to priming the motor cortex in clinical practice, for example, the sports training of athletes and other conditioning patients without neural system lesion.

Note that the interpretation of the results of this study might be confined to some limitations. First, a small healthy sample was recruited so that the neuromodulation and motor effects of rPNMS would not be generalized to patients with neurological diseases such as stroke. Second, the effects of rPNMS were investigated after only one session. Whether multiple sessions applied more frequently for clinical rehabilitative intervention would lead to more pronounced effects is unknown. Moreover, the corticomotor effects of rPNMS might involve the faciliatory and inhibitory modulation from the intracortical neurons. Single-pulse TMS adopted in the present study could not reveal such neurophysiological processes. Therefore, further studies using paired-pulse TMS and fMRI can examine if repeated rPNMS can induce up-regulation of corticomotor excitability and can enhance motor function as well as the associated neurophysiological processes in a larger sample of healthy subjects and heterogeneous patient populations.

To conclude, one single session of rPNMS applied to the median nerve may increase the corticomotor excitability in contralateral M1, together with a possible improvement in dexterity function of the stimulated upper extremity in healthy people. This shows that rPNMS may be applied as an intervention method for clinical rehabilitation.

DATA AVAILABILITY STATEMENT

The original contributions presented in the study are included in the article, further inquiries can be directed to the corresponding author/s.

ETHICS STATEMENT

The studies involving human participants were reviewed and approved by Research Ethics Committee of the JORU Rehabilitation Hospital. The patients/participants provided their written informed consent to participate in this study.

AUTHOR CONTRIBUTIONS

YJ: study concept, subject recruitment, acquisition of data, and writing the first draft. XL: subject recruitment, acquisition of data, and data analysis. JW, DL, and CW: subject recruitment and acquisition of data. XW: experimental design, data analysis, and comments on the manuscript. HL: study concept and experimental design, data analysis and interpretation, critical revision of the manuscript, and research funding. All authors contributed to the article and approved the submitted version.

FUNDING

This work was supported by a special fund project for science and technology innovation (Social Development) in Yixing (Grant No. 2019SF01) and the fund project of JORU Rehabilitation Hospital (Grant No. JY-2018001A).

ACKNOWLEDGMENTS

The authors thank all the subjects and the staff at the JORU Rehabilitation Hospital for their kind participation and support in this research study.

REFERENCES

Baek, J., Park, N., Lee, B., Jee, S., Yang, S., and Kang, S. (2018). Effects of repetitive peripheral magnetic stimulation over vastus lateralis in patients after hip replacement surgery. *Ann. Rehabil. Med.* 42, 67–75. doi: 10.5535/arm.2018.42.1.67

Beaulieu, L. D., Massé-Alarie, H., Brouwer, B., and Schneider, C. (2015). Noninvasive neurostimulation in chronic stroke: a double-blind randomized sham-controlled testing of clinical and corticomotor effects. *Top. Stroke Rehabil.* 22, 8–17. doi: 10.1179/1074935714Z.0000000032

Beaulieu, L. D., Massé-Alarie, H., Camiré-Bernier, S., Ribot-Ciscar, E., and Schneider, C. (2017). After-effects of peripheral neurostimulation on brain plasticity and ankle function in chronic stroke: the role of afferents recruited. *Clin. Neurophysiol.* 17, 275–291. doi: 10.1016/j.neucli.2017.02.003

Beaulieu, L. D., and Schneider, C. (2015). Repetitive peripheral magnetic stimulation to reduce pain or improve sensorimotor impairments: a literature review on parameters of application and afferents recruitment. *Clin. Neurophysiol.* 45, 223–237. doi: 10.1016/j.neucli.2015.08.002

Bustamante, V., López de Santa María, E., Gorostiza, A., Jiménez, U., and Gáldiz, J. B. (2010). Muscle training with repetitive magnetic stimulation of the quadriceps in severe COPD patients. *Respir. Med.* 104, 237–245. doi: 10.1016/j.rmed.2009.10.001

Charlton, C. S., Ridding, M. C., Thompson, P. D., and Miles, T. S. (2003). Prolonged peripheral nerve stimulation induces persistent changes in excitability of human motor cortex. *J. Neurol. Sci.* 208, 79–85. doi: 10.1016/s0022-510x(02)00443-4

Chen, C. C., Chuang, Y. F., Yang, H. C., Hsu, M. J., Huang, Y. Z., Chang, Y. J., et al. (2015). Neuromuscular electrical stimulation of the median nerve facilitates low motor cortex excitability in patients with spinocerebellar ataxia. *J. Electromyogr. Kinesiol.* 25, 143–150. doi: 10.1016/j.jelekin.2014.10.009

Chipchase, L. S., Schabrun, S. M., and Hodges, P. W. (2011). Peripheral electrical stimulation to induce cortical plasticity: a systematic review of stimulus parameters. *Clin. Neurophysiol.* 122, 456–463. doi: 10.1016/j.clinph.2010.07.025

Darling, W. G., Wolf, S. L., and Butler, A. J. (2006). Variability of motor potentials evoked by transcranial magnetic stimulation depends on muscle activation. *Exp. Brain Res.* 174, 376–385. doi: 10.1007/s00221-006-0468-9

Farias da Guarda, S. N., and Conforto, A. B. (2014). Effects of somatosensory stimulation on corticomotor excitability in patients with unilateral cerebellar infarcts and healthy subjects—preliminary results. *Cerebellum Ataxias* 1:16. doi: 10.1186/s40673-014-0016-5

Flamand, V. H., Beaulieu, L. D., Nadeau, L., and Schneider, C. (2012). Peripheral magnetic stimulation to decrease spasticity in cerebral palsy. *Pediatr. Neurol.* 47, 345–348. doi: 10.1016/j.pediatrneurol.2012.07.005

Gallasch, E., Christova, M., Kunz, A., Rafolt, D., and Golaszewski, S. (2015). Modulation of sensorimotor cortex by repetitive peripheral magnetic stimulation. *Front. Hum. Neurosci.* 9:407. doi: 10.3389/fnhum.2015.00407

Kaelin-Lang, A., Luft, A. R., Sawaki, L., Burstein, A. H., Sohn, Y. H., Cohen, L. G., et al. (2002). Modulation of human corticomotor excitability by somatosensory input. *J. Physiol.* 540, 623–633. doi: 10.1113/jphysiol.2001.012801

Kremenic, I. J., Ben-Avi, S. S., Leonhardt, D., and McHugh, M. P. (2004). Transcutaneous magnetic stimulation of the quadriceps *via* the femoral nerve. *Muscle Nerve* 30, 379–381. doi: 10.1002/mus.20091

Liu, H., and Au-Yeung, S. S. (2014). Reliability of transcranial magnetic stimulation induced corticomotor excitability measurements for a hand muscle in healthy and chronic stroke subjects. *J. Neurol. Sci.* 341, 105–109. doi: 10.1016/j.jns.2014.04.012

Liu, H., and Au-Yeung, S. S. (2017). Corticomotor excitability effects of peripheral nerve electrical stimulation to the paretic arm in stroke. *Am. J. Phys. Med. Rehabil.* 96, 687–693. doi: 10.1097/PHM.0000000000000748

Momosaki, R., Yamada, N., Ota, E., and Abo, M. (2017). Repetitive peripheral magnetic stimulation for activities of daily living and functional ability in people after stroke. *Cochrane Database Syst. Rev.* 6:CD011968. doi: 10.1002/14651858.CD011968.pub2

Musarò, A., Dobrowolny, G., Cambieri, C., Onesti, E., Ceccanti, M., Frasca, V., et al. (2019). Neuromuscular magnetic stimulation counteracts muscle decline in ALS patients: results of a randomized, double-blind, controlled study. *Sci. Rep.* 9:2837. doi: 10.1038/s41598-019-39313-z

Okudera, Y., Yoshihiko, T., Sato, M., Chida, S., Hatakeyama, K., Watanabe, M., et al. (2015). The impact of high-frequency magnetic stimulation of peripheral nerves: muscle hardness, venous blood flow and motor function of upper extremity in healthy subjects. *Biomed. Res.* 36, 81–87. doi: 10.2220/biomedres.36.81

Rossi, S., Hallett, M., Rossini, P. M., and Pascual-Leone, A., and The Safety of TMS Consensus Group (2009). Safety, ethical considerations and application guidelines for the use of transcranial magnetic stimulation in clinical practice and research. *Clin. Neurophysiol.* 120, 2008–2039. doi: 10.1016/j.clinph.2009.08.016

Schabrun, S. M., Ridding, M. C., Galea, M. P., Hodges, P. W., and Chipchase, L. S. (2013). Primary sensory and motor cortex excitability are co-modulated in response to peripheral electrical nerve stimulation. *PLoS One* 7:e51298. doi: 10.1371/journal.pone.0051298

Struppler, A., Angerer, B., Gündisch, C., and Havel, P. (2004). Modulatory effect of repetitive peripheral magnetic stimulation on skeletal muscle tone in healthy subjects: stabilization of the elbow joint. *Exp. Brain. Res.* 157, 59–66. doi: 10.1007/s00221-003-1817-6

Struppler, A., Binkofski, F., Angerer, B., Bernhardt, M., Spiegel, S., Drzezga, A., et al. (2007). A fronto-parietal network is mediating improvement of motor function related to repetitive peripheral magnetic stimulation: a PET-H2O15 study. *NeuroImage* 36, t174–t186. doi: 10.1016/j.neuroimage.2007.03.033

Struppler, A., Havel, P., and Müller-Barna, P. (2003). Facilitation of skilled finger movements by repetitive peripheral magnetic stimulation (RPMS)—A new approach in central paresis. *Neurorehabilitation* 18, 69–82. doi: 10.3233/nre-2003-18108

Szecsi, J., Straube, A., and Fornusek, C. (2014). Comparison of the pedalling performance induced by magnetic and electrical stimulation cycle ergometry in able-bodied subjects. *Med. Eng. Phys.* 36, 484–489. doi: 10.1016/j.medengphy.2013.09.010

World Medical Association (2013). World Medical Association Declaration of Helsinki: ethical principles for medical research involving human subjects. *JAMA* 310, 2191–2194. doi: 10.1001/jama.2013.281053

Yang, S. S., Jee, S., Hwang, S. L., and Sohn, M. K. (2017). Strengthening of quadriceps by neuromuscular magnetic stimulation in healthy subjects. *PMR* 9, 767–773. doi: 10.1016/j.pmrj.2016.12.002

Ziemann, U., Reis, J., Schwenkreis, P., Rosanova, M., Strafella, A., Badawy, R., et al. (2015). TMS and drugs revisited 2014. *Clin. Neurophysiol.* 126, 1847–1868. doi: 10.1016/j.clinph.2014.08.028

Conflict of Interest: The authors declare that the research was conducted in the absence of any commercial or financial relationships that could be construed as a potential conflict of interest.

Copyright © 2021 Jia, Liu, Wei, Li, Wang, Wang and Liu. This is an open-access article distributed under the terms of the Creative Commons Attribution License (CC BY). The use, distribution or reproduction in other forums is permitted, provided the original author(s) and the copyright owner(s) are credited and that the original publication in this journal is cited, in accordance with accepted academic practice. No use, distribution or reproduction is permitted which does not comply with these terms.

frontiers in Neural Circuits

ORIGINAL RESEARCH
published: 09 April 2021
doi: 10.3389/fncir.2021.670189

Blockade of Motor Cortical Long-Term Potentiation Induction by Glutamatergic Dysfunction Causes Abnormal Neurobehavior in an Experimental Subarachnoid Hemorrhage Model

Minoru Fujiki[1], Kazuhiro Kuga[2], Harushige Ozaki[2], Yukari Kawasaki[1] and Hirotaka Fudaba[1]*

[1]*Department of Neurosurgery, School of Medicine, Oita University, Oita, Japan,* [2]*Drug Safety Research and Evaluation, Takeda Pharmaceutical Company Limited, Fujisawa, Japan*

Subarachnoid hemorrhage (SAH) is a life-threatening condition that can also lead to permanent paralysis. However, the mechanisms that underlying neurobehavioral deficits after SAH have not been fully elucidated. As theta burst stimulation (TBS) can induce long-term potentiation (LTP) in the motor cortex, we tested its potential as a functional evaluation tool after experimentally induced SAH. Motor cortical inter-neuronal excitability was evaluated in anesthetized rats after 200 Hz-quadripulse TBS (QTS5), 200 Hz-quadripulse stimulation (QPS5), and 400 Hz-octapulse stimulation (OPS2.5). Furthermore, correlation between motor cortical LTP and N-methyl-D-aspartate-receptor activation was evaluated using MK-801, a NMDA-receptor antagonist. We evaluated inhibition-facilitation configurations [interstimulus interval: 3 ms; short-latency intracortical inhibition (SICI) and 11 ms; intracortical facilitation (ICF)] with paired electrical stimulation protocols and the effect of TBS paradigm on continuous recording of motor-evoked potentials (MEPs) for quantitative parameters. SAH and MK-801 completely blocked ICF, while SICI was preserved. QTS5, QPS5, and OPS2.5 facilitated continuous MEPs, persisting for 180 min. Both SAH and MK-801 completely blocked MEP facilitations after QPS5 and OPS2.5, while MEP facilitations after QTS5 were preserved. Significant correlations were found among neurological scores and 3 ms-SICI rates, 11 ms-ICF rates, and MEP facilitation rates after 200 Hz-QTS5, 7 days after SAH (R^2 = 0.6236; r = −0.79, R^2 = 0.6053; r = −0.77 and R^2 = 0.9071; r = 0.95, $p < 0.05$, respectively). Although these findings need to be verified in humans, our study demonstrates that the neurophysiological parameters 3 ms-SICI, 11 ms-ICF, and 200 Hz-QTS5-MEPs may be useful surrogate quantitative biomarkers for assessing inter-neuronal function after SAH.

Keywords: electrical stimulation, theta burst stimulation, long-term potentiation, neurobehavior, subarachnoid hemorrhage, motor-evoked potential

OPEN ACCESS

Edited by:
Ti-Fei Yuan,
Shanghai Jiao Tong University, China

Reviewed by:
Antonio Suppa,
Sapienza University of Rome, Italy
Yasuo Terao,
Kyorin University, Japan

****Correspondence:***
Minoru Fujiki
fujiki@oita-u.ac.jp

Received: *20 February 2021*
Accepted: *17 March 2021*
Published: *09 April 2021*

Citation:
Fujiki M, Kuga K, Ozaki H, Kawasaki Y and Fudaba H (2021) Blockade of Motor Cortical Long-Term Potentiation Induction by Glutamatergic Dysfunction Causes Abnormal Neurobehavior in an Experimental Subarachnoid Hemorrhage Model. Front. Neural Circuits 15:670189. doi: 10.3389/fncir.2021.670189

INTRODUCTION

Survivors of subarachnoid hemorrhage (SAH) are confronted with a variety of long-term problems, including focal neurological deficits, cognitive declines, and higher brain dysfunction, which can be difficult to evaluate (Hackett and Anderson, 2000; Kreiter et al., 2002; Jeon et al., 2010; Sherchan et al., 2011). An objective evaluation of cognitive-neurophysiological function is important for clinical translation, since direct links between quantitative biomarker and clinical symptoms in SAH patients have not been fully established (Kreiter et al., 2002; Sherchan et al., 2011). Furthermore, there are few functional evaluation studies on neurobehavioral and morphological changes following SAH in animals (Thal et al., 2008; Silasi and Colbourne, 2009; Sherchan et al., 2011). Therefore, we intended to perform electrophysiological investigation of cortical excitability, which is potentially related to inter-neuronal functions and might be a possible quantitative biomarker reflecting pathophysiological conditions after SAH.

Theta burst stimulation (TBS) of the hippocampus (3–5 pulses at a frequency of 100 Hz-burst, repeated at 5 Hz) was first shown to facilitate hippocampal-evoked potentials for several hours, on the basis of long-term potentiation (LTP) in animal models (Hess and Donoghue, 1996). TBS stimulation has subsequently been translated to humans using non-invasive transcranial magnetic stimulation (TMS) of the motor cortex (three pulses at a frequency of 50 Hz-burst, repeated at 5 Hz, total, 600 pulses; Huang et al., 2005). It has been used either in intermittent and facilitatory or continuous and inhibitory TBS (iTBS and cTBS, respectively) paradigms for motor-evoked potentials (MEPs) with repetitive TMS (rTMS; Huang et al., 2005). TBS has widespread applications as a non-invasive methodology to evaluate and modify neural-networks within the human brain (Huang et al., 2005; Jung et al., 2016). Therefore, to replicate these human findings, we explored inter-neuronal function in the motor cortex of a rat SAH model after TBS by comparing two standard LTP protocols. Because methodological standardization for LTP induction on the motor cortex remains controversial both in humans and animals, comparison between facilitatory TBS protocol and those for hippocampal LTP induction in experimental condition is informative. Therefore, we designed experimental protocols with a consistent number of total pulses of 1,440 between each condition, at different pulse (200 or 400 Hz) and different burst frequencies [every 200 ms (5 Hz; theta-rhythm), 5 and 10 s]. Hence, total duration of stimulation differed among the TBS and two standard LTP protocol groups (usual durations of each group; 72 s and 30 min, respectively). We also tested the effects of an N-methyl-D-aspartate (NMDA)-receptor antagonist (MK-801) on MEPs after TBS.

MATERIALS AND METHODS

Animals

All experimental protocols were performed in accordance with the Japanese National Institute of Health Guide for the Care and Use of Laboratory Animals and approved by the Oita University Ethical Review Committee (protocol number 192302). Following a sample size calculation, we conducted our experiments on a total of 50 adult, male Sprague–Dawley rats (body weight, 295–377 g, aged 8.2 $\pm$ 0.2 weeks old) that were housed in a controlled environment with room temperature (24.5–25.0°C), 12/12-h light/dark cycle, and constant humidity. Rat food pellets and tap water were provided *ad libitum* between experimental procedures. The study was composed of three different experimental sessions involving 50 animals: [A] continuous MEP recording after 200 Hz-quadripulse TBS, 200 Hz-QPS, and 400 Hz-OPS (QTS5, QPS5, and OPS2.5, respectively, n = 5, each condition); [B] the same procedure as in [A], but with NMDA-receptor antagonist MK-810 (1 mg/kg) administration to explore the correlation between MEP modification and NMDA activation (n = 5, each condition); [C] same procedure as in [A], but 7 days after SAH to explore the underlying functional consequences and pathophysiology (n = 5, each condition; **Figure 1**).

Induction of Cisterna Magna SAH Model

Seven days before testing, the rats were deeply intraperitoneally anesthetized with a combination of medetomidine/midazolam/butorphanol anesthesia (0.15/2.0/5.0 mg/kg, respectively). The anesthetic conditions were continuously verified through the experiment (maintained during electrode implantation, SAH induction and during data recording 7 days after) in all animals (Fujiki et al., 2004, 2020a,b; Qin et al., 2015; Mishra et al., 2017). Briefly, the absence of pedal withdrawal (“toe-pinch”) reflex was used for assessment of anesthesia and analgesia depth, and the body temperature was maintained at 37°C intra- and postoperatively with a temperature-controlled heating pad.

Autologousblood (300 μl) was injected into the subarachnoid space over a 3-min time frame from a catheter within the cisterna magna. The injection was repeated 48 h after first injection (Qin et al., 2015).

Continuous Recording of MEPs

MEPs were continuously recorded from the contralateral right biceps brachii muscle *via* wire-electrodes, as per previously described methods (Fujiki et al., 2004, 2020a,b; Mishra et al., 2017). Electrode setting and base-MEP recordings were performed before the induction of SAH. During MEP measurements, rats were anesthetized with amedetomidine/midazolam/butorphanol combination to preserve the motor responses in the same manner with SAH induction.

Paired Motor Cortex Electrical Stimulation for Inhibition-Facilitation Configurations

Intracortical inhibition or facilitation [short-latency intracortical inhibition (SICI) and intracortical facilitation (ICF)] were tested using a paired electrical and subthreshold conditioning stimulus (CS) preceding a suprathreshold test stimulus (TS) after resting motor threshold (RMT) determination (Kujirai et al., 1993; Rothwell, 1997; Fujiki et al., 2020a). The RMT was measured by varying the stimulator output by 0.1-mA-step until six stable peak-to-peak-50 μV-MEP elicitations were obtained for every

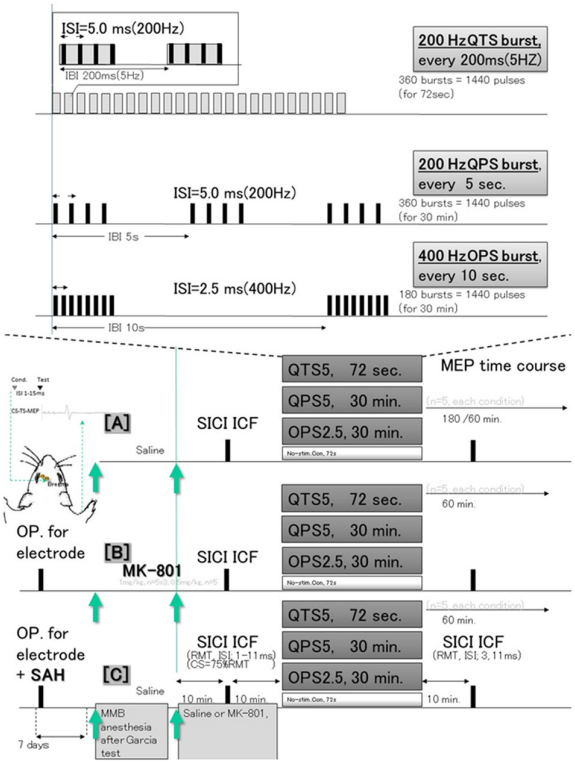

FIGURE 1 | Schematic illustration of the experimental protocol and stimulus configurations. In **(A)**, epidural electrodes [Plastics One with 1.19 mm diameter with a flat tip on two locations: 1.0 mm rostral and 2.0 mm lateral (1R, 2L) and 3.0 mm rostral and 4.0 mm lateral from bregma (3R, 4L); orange circles in **(B)**] were placed 7 days before testing under MMB anesthesia. The screw electrodes were attached in advance to a head connector (Plastics One) such that they were secured with skull screws and dental acrylic for repeated measurements. Motor cortex stimulation for motor-evoked potential (MEP) recording: a train of three biphasic square wave pulses was delivered with an isolated pulse stimulator to achieve temporal summation for selective activation of the motor cortex (0.2 ms per pulse for each polarity; interstimulus interval of 3 ms; refer Fujiki et al., 2020a for detail). QTS5 consists of a burst of four monophasic pulses, 0.2 ms pulse duration at 200 Hz, repeated at 5 Hz, and delivered for 72 s continuously (Jung et al., 2016). QPS5 consisted of the same burst, repeated every 5 s for 30 min, a total 360 bursts based on original reports of QPS of the human motor cortex by Hamada et al. (2008). OPS2.5 consisted of a burst of eight pulses at 400 Hz, repeated every 10 s for 30 min, total 180 bursts, both consisting of 1,440 pulses (Steward et al., 2020). No-stimulation condition was instead produced by unplugging the electrodes at the stimulator while the high frequency stimulation protocol was carried out. Subthreshold CS was set at 75% RMT, while the intensity of TS was adjusted to evoke an MEP of approximately 300 μV (peak-to-peak) in the right BB muscle. Interstimulus intervals (ISIs) of 1, 2, 3, 5, 7, 11, 13, and 15 ms were utilized to test intracortical inhibitions or facilitations. Full ISIs were tested 10 min before QTS5, QPS5 and OPS2.5, while ISIs of 3 and 11 ms were tested 10 min after each stimulation in controls under MMB anesthesia, under MK-801 and 7 days after Subarachnoid Hemorrhage (SAH). Three different experimental sessions [no-Theta Burst Stimulation (TBS) control **(A)**, under MK-801 **(B)**, and 7 days after SAH induction **(C)**] were tested at least 7 days after electrode settings (SAH induction). MMB, medetomidine/midazolam/butorphanol anesthesia (0.15/2.0/5.0 mg/kg, respectively; intraperitoneally. SICI, short latency intracortical inhibition; ICF, intracortical facilitation; QTS5, quadripulse TBS (QTS5 ms; 200 Hz); QPS5, quadripulse stimulation (QPS5; 200 Hz); OPS2.5, octapulse stimulation (OPS2.5; 400 Hz, n = 5 each); conditioning stimulus (CS); resting motor threshold (RMT); test stimulus (TS).

12 trials. Two isolated stimulators connected with acustom-made single-stimulus-electrode switching unit were controlled for appropriate stimulus intervals (1, 2, 3, 5, 7, 11, 13, and 15 ms) and intensity (0.5–1.2 mA) in a similar manner as paired TMS (Vahabzadeh-Hagh et al., 2011; Hsieh et al., 2012; Fujiki et al., 2020a).

Motor Cortex Electrical Stimulation: 200 Hz-Quadripulse TBS, 200 Hz-Quadripulse and 400 Hz-Octapulse Stimulation for LTP Induction

A 200 Hz-quadripulse TBS (QTS5 ms), 200 Hz-quadripulse stimulation (QPS5), 400 Hz-Octapulse stimulation (OPS2.5; n = 5 each) or an absent (no-) stimulation was applied for 72 s. Three different experimental sessions (no-TBS [A], treated with MK-801[B] and 7 days after SAH induction [C]) were tested for at least 7 days after electrode settings (SAH induction; **Figure 1**).

The animals were humanely sacrificed after data collection with an overdose of anesthetic prior to decapitation. The brains were then prepared for verification of electrode position and histological evaluation after SAH. High-frequency stimulation (QTS5, QPS5, and OPS2.5) was delivered at an intensity of 75%-RMT (0.5–1.2 mA; Yang et al., 2019; Fujiki et al., 2020a) for 1,440 pulses and post stimulus-continuous MEPs were recorded at 0.1 Hz for 60 or 180 min. The no-stimulation condition was produced by unplugging the electrodes while the high-frequency stimulation protocol was carried out.

Effects of MK-801

A separate group of animals were prepared to explore the correlation between motor cortical LTP induction after QTS5, QPS5, and OPS2.5 and NMDA-receptor activation, with rats receiving an NMDA-receptor antagonist, MK-801 (1 mg/kg, intraperitoneally; FUJIFILM Wako Pure Chemical Corporation, Japan; [B] in **Figure 1**, n = 15). Low-dose MK-801 (0.5 mg/kg) was tested only for MEPs and CS preceding TS-MEP recording (n = 5). Based on the previously reported pharmacokinetic and pharmacodynamic properties of MK-801 in rats, we adjusted motor cortical LTP induction periods to make them comparable with the bet time window (Wegener et al., 2011). Furthermore, to confirm whether MK-801 was at a steady state during the induction of motor cortical LTP by QTS5, QPS5, and OPS2.5, the pharmacodynamics of MK-801 were tested by means of functional observation battery (FOB) using eight separate group of animals. We verified the positive steady symptoms during 1-h-post-dose periods (see **Supplementary Material** for detail). Thus, we could confirm that MK-801 doses were steady during the induction of LTP, but interaction with anesthetic combination was not confirmed.

Neurological and Histological Evaluation After Experimental SAH

The SAH grading of animals at 7 days was determined according to previously described methods (Sugawara et al., 2008). Modified Garcia's neurological scores (consisting of six tests; scored 3–18) were evaluated at 7 days after SAH by a blinded investigator (Garcia et al., 1995). Animals that survived for 7 days

after SAH were evaluated for histological analysis (hematoxylin and eosin and silver stain) immediately after MEP evaluations (Fujiki et al., 2004).

Data Analysis

The MEP data were analyzed offline, as per previous reports (Sykes et al., 2016; Fujiki et al., 2020a). MEP amplitudes were measured in a peak-to-peak manner, with 120% RMT stimulus intensity used for MEP recording with a 10-s interval, six individual sweeps run each minute (except for the initial 30 min in which a 10-s interval, three sweeps protocol was run every 5 min). This allowed us to record MEP development during QPS5 and OPS2.5. Amplitude was normalized to the final 5-min baseline amplitude and expressed as percentage-change, allowing for between-subject comparisons and grouping into 5 min bins.

Different groups of animals were compared using analysis of variance (ANOVA) with a Student–Newman–Keul *post-hoc* analysis (SPSS, Cary, NC, USA). Data are presented as mean ± standard error of the mean. For QTS5, QPS5, and OPS2.5 effects, statistical significance of group differences was analyzed by ANOVA with time (TIME) as within-subject factor and group (GROUP) as between-subjects factor. This was followed by *post-hoc* Holm test. To investigate whether the time effect differed among groups, we confirmed the TIME × GROUP interaction. Differences were considered significant at $P \leq 0.05$.

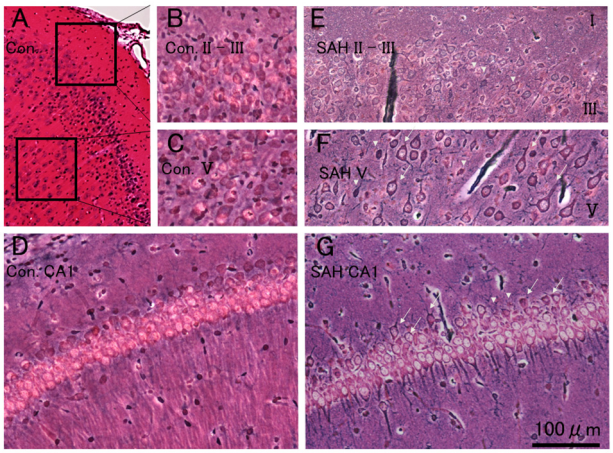

FIGURE 2 | Histopathological results at 7 days after SAH. Photomicrograph indicating neuronal density in the motor cortical layers I-III, V, and CA1 region of the hippocampus in a rat 7 days after no-TBS control **(A,B,C,D)** and SAH **(E,F,G)**. Note that the prominent cell damages in the motor cortical layers III and V area in the rat subjected to SAH [showing transition between healthy cells (arrows) and with dead or dying cells (arrowheads)] and the relative absence of neuron loss in the hippocampal CA1 area (showing a mixture of some dying cells in healthy cells). Panel **(C)** illustrates cell density in a control case. Bars = 200 μm **(A)** and 100 μm (**B,C,D,E,F** and **G**). Areas in panels **(B,C)** correspond to the inset area in Panel **(A)**.

RESULTS

General Condition and Histopathology 7 Days After SAH

Physiological parameters were within the normal range before induction of SAH [pH, 7.45 ± 0.01; pO_2 (mmHg), 75.2 ± 1.8; pCO_2 (mmHg), 47.1 ± 2.1; and Hematocrit (%), 51 ± 0.8]. All control MEPs were abolished immediately after SAH induction on the day which became nil. There was no mortality in either no-TBSor SAH animals during the 7 days. The average SAH grade was 3.2 ± 1.1. **Figure 2** illustrates the characteristic pattern of neuronal morphology in the rat motor cortical layers I-III, V, and CA1 region of the hippocampus after 7 days in the no-TBS control (A, B, C, D) and SAH (E, F, G) conditions.

As previously documented (Ostrowski et al., 2005), there was extensive neuronal damage, predominantly in motor cortical layers III and V area in rats, subjected to SAH (compare **Figures 2B,C** controls with **Figures 2E,F**). Notably, the neurons in the hippocampal CA1 area were relatively preserved. Moreover, rather than having drastic cell loss, rats subjected to SAH displayed morphological abnormalities in their cortical neurons. However, whether there were any quantitative differences in cell number between the SAH and no-TBS control animals were not investigated.

MEP Basic Waveforms

The final 5 min of MEP baseline parameters, including RMT, latency, and amplitudes, in no-TBS controls, MK-801, and SAH groups are summarized in **Table 1**. No qualitative differences were found among the groups. In addition, there was no statistically significant effect of MK-801 administration and SAH on RMT, latency, or amplitude (**Figures 3A,B**).

Inhibition-Facilitation Configurations With Paired-Stimulation Protocol-MEPs

Paired-stimulation protocol-MEPs showed inhibition (ISIs, 1–3 ms; SICI) and facilitation (ISI, 11 ms; ICF) patterns (left graph, **Figure 3B**). While MK-801 completely blocked 11 ms-ICF, 3 ms-SICI was preserved [low dose (0.5 mg/kg); orange-dotted lines and high dose (1.0 mg/kg); red-lines, respectively; asterisk (*) indicate significance; $P < 0.05$; **Figures 3A,B**]. One-way ANOVA revealed that significant difference at an ISI of 9 ($F_{(1,28)} = 16.36$, $P = 0.00037$), 11 ($F_{(1,28)} = 45.51$, $P < 0.0001$), 13 ($F_{(1,28)} = 7.86$, $P = 0.0096$; 1 mg/kg), and ISI of 9 ($F_{(1,18)} = 8.69$, $P = 0.0082$), 11 ($F_{(1,18)} = 18.62$, $P = 0.00037$), and 13 ms ($F_{(1,18)} = 5.05$, $P = 0.038$; 0.5 mg/kg), respectively.

LTP of MEPs After 200 Hz-QTS5 in No-TBS-Control Rats

Motor cortical QTS5 continuously facilitated MEPs immediately after stimulation (**Figure 4A**), lasting for 180 min ($P < 0.05$; **Figure 4B**). Both QPS5 and OPS2.5 facilitated MEPs during 30 min stimulation periods, also lasting 180 min ($P < 0.05$; **Figures 4A,B**). ANOVA revealed that significant main effect of group on MEP in normalized MEP amplitude over time, while *post-hoc* comparison indicated that MEP amplitudes were significantly higher than those in the no-TBS group ($P < 0.001$; **Figure 4**). QTS5, QPS5, and OPS2.5 significantly facilitated 11 ms-ICF (QTS5: $F_{(1,18)} = 7.99$, $P = 0.011$; QPS5: $F_{(1,18)} = 22.08$, $P = 0.00018$; OPS2.5: $F_{(1,18)} = 21.51$, $P = 0.0002 < 0.05$; values

TABLE 1 | MEP baseline parameters.

		Control (n = 15)	MK-801 (n = 15)	SAH (n = 15)	F	P
Baseline	RMT (mA)	1.05 ± 0.04	1.04 ± 0.04	1.04 ± 0.03	$F_{(2,42)}$ = 0.035	0.97
	latency (ms)	14.2 ± 0.31	13.6 ± 0.32	13.5 ± 0.34	$F_{(2,42)}$ = 1.466	0.24
	amplitude (μV)	280 ± 9.72	291 ± 18.64	312 ± 9.18	$F_{(2,42)}$ = 1.485	0.24

MEP, motor evoked potential; RMT, resting motor threshold; SAH, subarachnoid hemorrhage.

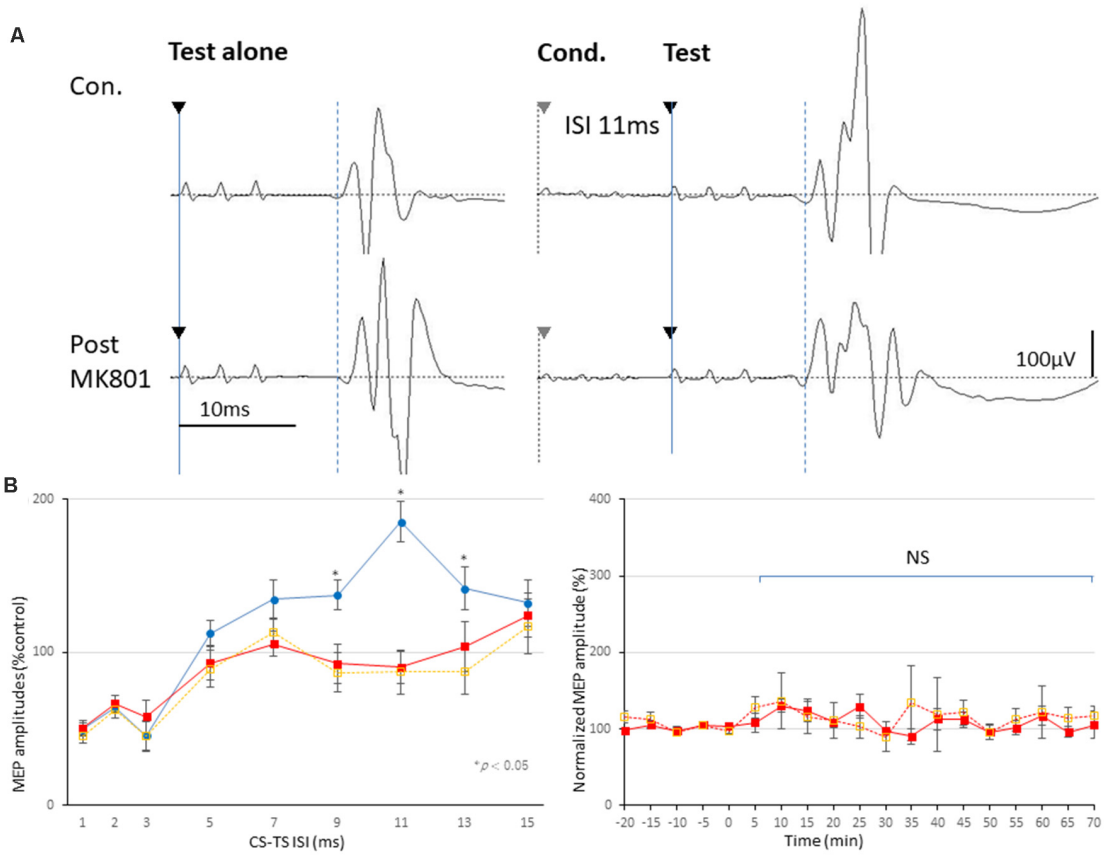

FIGURE 3 | Effects of MK-801 on MEPs and 3 ms-inhibition and 11 ms-facilitation patterns. **(A,B)** Basic waveform of MEPs recorded from the biceps muscle is composed of short-latency (approximately 14 ms) biphasic waves. Inhibition and facilitation patterns of MEPs at ISIs of 3 and 11 ms under medetomidine/midazolam/butorphanol (MMB) anesthesia (**A,B**; Circle). This phenomenon is reminiscent of the SICI and ICF in the human motor cortex using paired pulse TMS. Rats with MK-801 injection (1 mg and 0.5 mg/kg, i.p.) demonstrated significant suppression at 11 ms-facilitation but consistent amplitudes of test MEPs. Analysis of Variance (ANOVA) revealed that the values were significantly smaller in the MK-801 groups at an ISI of 11 ms. *P < 0.05 (**B**; square, solid and dotted line, respectively). Note that an absence of statistically significant effects of MK-801 administrations on parameters RMT, latency, or amplitude was found **(B)**. NS, statistically not significant.

between groups: $F_{(2,13)}$ = 3.47, P = 0.65; **Figure 5D**, left graph), whereas 3 ms-SICI was not affected in controls.

SICI, ICF, and 200 Hz-QTS5 Induced TLP Effect on SAH-Rat MEPs

Both 3 ms-inhibition and 11 ms-facilitation configurations were suppressed after SAH (P < 0.05; **Figures 6A,B**). One-way ANOVA revealed a significant difference at an ISI of 5 ($F_{(1,28)}$: 8.740, P = 0.0062) 7 ($F_{(1,28)}$: 5.43, P = 0.027), 9 ($F_{(1,28)}$: 23.10, P < 0.0001), 11 ($F_{(1,28)}$ = 56.02, P < 0.0001), 13 ($F_{(1,28)}$ = 17.25, P < 0.001), 15 ($F_{(1,28)}$ = 8.64, P = 0.0065) ms, respectively. There was a tendency for the 3 ms-SICI to be suppressed, although the change was not statically significant (**Figure 6B**). Therefore, intracortical inhibition and facilitation profiles 7 days after SAH in this study, were entirely different than normal controls.

It should be noted that CS preceding TS-MEP amplitudes (% control) at both 3 ms-inhibitory and 11 ms-facilitatory phases were suppressed approximately 25% compared to TS-alone base-MEP amplitudes (**Figure 6B**, red-line). All MEP facilitations after QPS5, OPS2.5-stimulations were completely suppressed, while those after QTS5 were preserved both with MK-801 and 7 days after SAH (compare **Figures 5B,C** with **Figure 5A**).

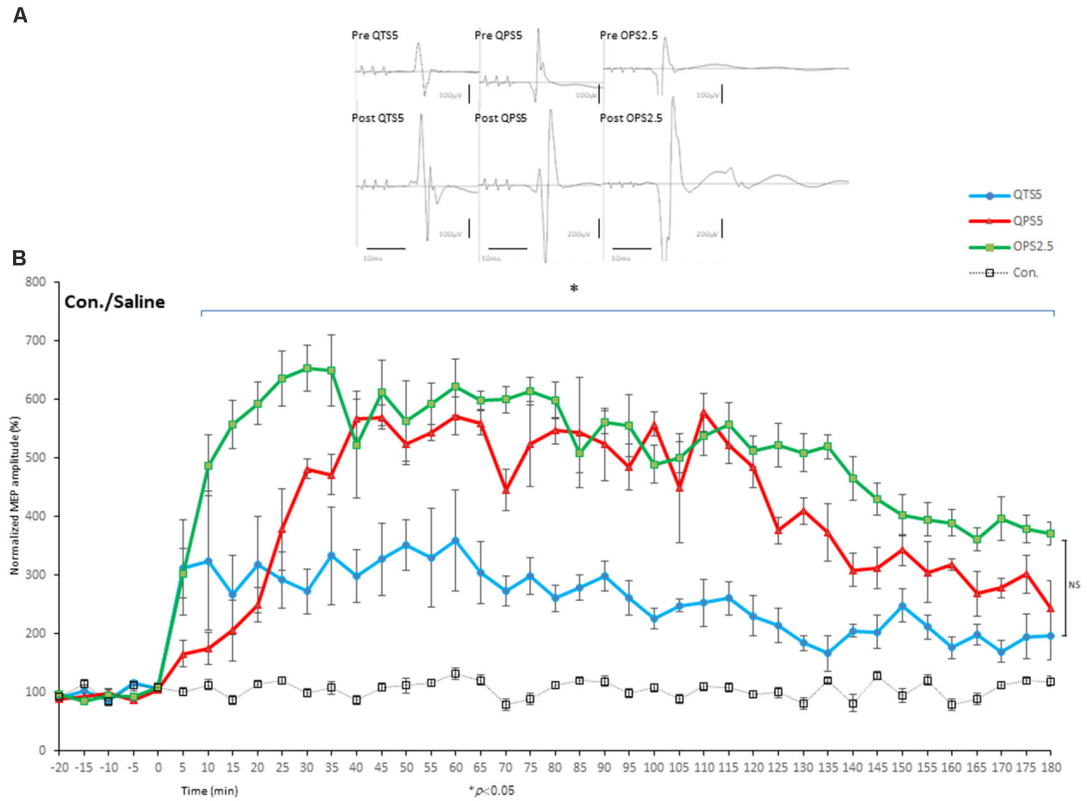

FIGURE 4 | Quantitative evaluation of the MEPs after 200 and 400 Hz high-frequency stimulation in control animals. Time course of MEPs after QTS5, QPS5, and OPS2.5 in no-TBS controls. MEP facilitation after OTS5, QPS5, and OPS2.5 stimulation in control animals **(A,B)**. Note that 10 ms of horizontal calibration bar and 100 μV vertical bar in pre-stimulation and QTS5, whereas 200 μV vertical bar in post-QPS5 and OPS2.5. MEPs were strongly facilitated immediately after motor cortical QTS5 (blue-line), lasting upto 180 min under MMB anesthesia. Both QPS5 and OPS2.5 also facilitated MEPs lasting up to 180 min under MMB anesthesia (red- and green-line, respectively). ANOVA revealed a significant main effect of group on MEP, whereby the effects of stimulation differed among the four groups (main effect of GROUP, $F_{(3,55)} = 148.23$, $P < 0.001$; main effect of TIME, $F_{(13,224)} = 18.56$, $P < 0.001$; interaction of GROUP × TIME, $F_{(39,224)} = 4.55$, $P < 0.001$). A *post-hoc* analysis indicated significant increases, compared to the no-TBS group, in the MEP amplitudes after the stimulation in the QTS5, QPS5, and OPS2.5 groups ($P < 0.001$). Multiple comparisons between the QTS5 and no-TBS groups were conducted at each time point. Our results indicated the MEP amplitudes in the QTS5 group were significantly increased compared with those in the no-TBS group at several time points ($P < 0.001$, respectively). Differences in the increase of MEP amplitudes were observed immediately following stimulation and persisted for more than 3 h (data not shown) following stimulation, suggesting persistent TBS effects on the MEP amplitudes. Both QPS5 and OPS2.5 appeared to induce stronger facilitation than QTS5 during stimulation for the first 30 min (statistically not significant), but there were no significant differences between the three groups in the final 30 min ($P > 0.05$). NS, statistically not significant. *$P < 0.05$.

ANOVA revealed that significant main effect of group on MEP after QTS5 under MK-801, whereby the effects of stimulation differed among the four groups (main effect of GROUP, $F_{(3,55)} = 8.42$, $P < 0.001$; main effect of TIME, $F_{(13,224)} = 4.52$, $P < 0.001$; interaction of GROUP × TIME, $F_{(39,224)} = 3.07$, $P < 0.001$; **Figure 5B**).

A *post-hoc* analysis indicated that significant main effect group increases in the MEP amplitudes compared to those in the no-TBS group, after stimulation in the QTS5 and MK-801 groups ($P = 0.015$). Multiple comparisons between the QTS5 and no-TBS groups were conducted at each time point. Our results indicated that the MEP amplitudes in the QTS5 group were significantly higher than those in the (no-TBS) stimulation control sham group at transient initial time points (5, 10 min following stimulation: $P = 0.01$, respectively; compare **Figure 5B** with **Figure 5A**).

ANOVA revealed that significant main effect of group on MEP after QTS5 7 days after SAH, whereby the effects of stimulation differed among the four groups (main effect of GROUP, $F_{(3,55)} = 24.37$, $P < 0.001$; main effect of TIME, $F_{(13,224)} = 0.858$, $P = 0.5979$; interaction of GROUP × TIME, $F_{(39,224)} = 0.57$, $P = 0.98$; **Figure 5C**).

A *post-hoc* analysis indicated that significant main effect group increases in the MEP amplitudes compared to those in the no-TBS group, after the stimulation in the QTS5 and SAH group ($P < 0.001$). Multiple comparisons between the QTS5 and no-TBS groups were conducted at each time point. Our results indicated that the MEP amplitudes in the QTS5 group were significantly higher than those in the no-TBS group at two time points (10, 25 min following stimulation: $P = 0.048$, 0.044, respectively; compare **Figure 5C** with **Figure 5A**).

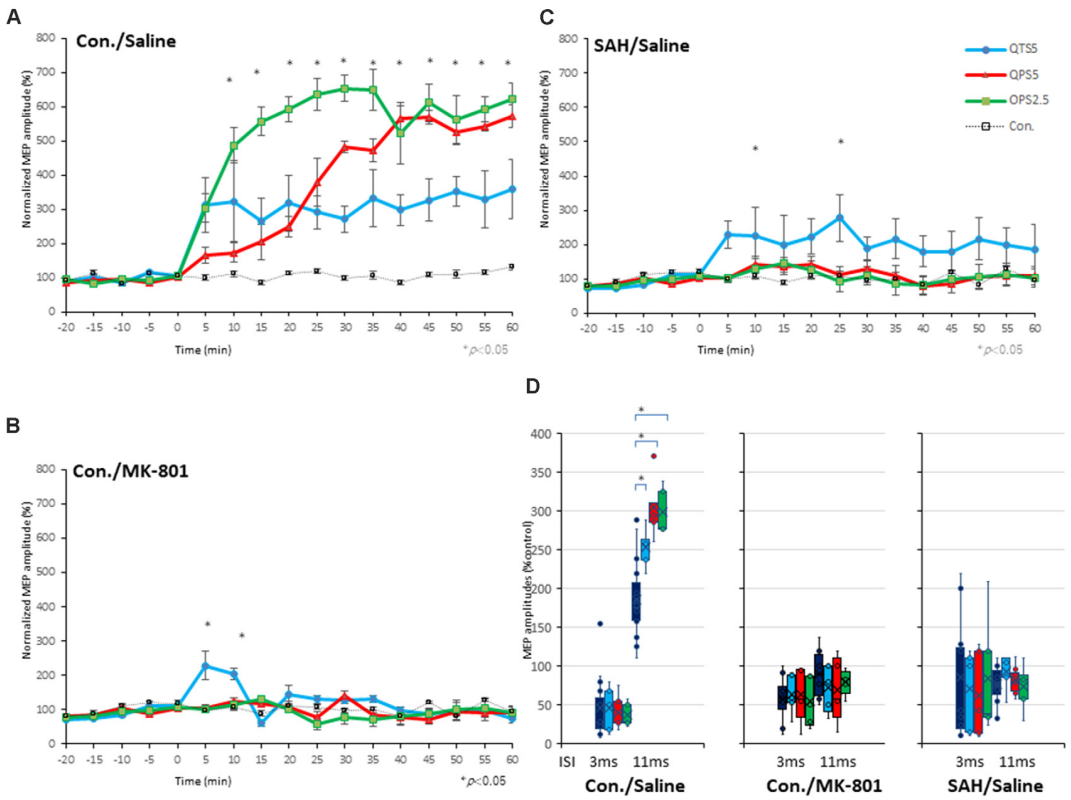

FIGURE 5 | Quantitative evaluation of the MEPs after 200 Hz, 400 Hz high-frequency stimulation in control, MK-801 treated, and SAH animals. Time course of MEPs after QTS5, QPS5, and OPS2.5 in no-TBS controls, animals under MK-801, and SAH models. **(A)** MEP amplitudes in the QTS5 (blue-line), QPS5 (red-line), and OPS2.5 (green-line) groups were significantly increased compared with those in the no-TBS group at several time points. **(B)** MEP amplitudes in the QTS5 under MK-801 group were significantly increased compared with those in the no-TBS group at transient time points (5 min and 10 min post-stimulation, $^*P < 0.05$). **(C)** MEP amplitudes in the QTS5 after SAH group were increased compared with those in the no-TBS group at several time points (10 min and 25 min post-stimulation, $^*P < 0.05$). Note an absence of statistically significant effects of SAH on parametersRMT, latency, or amplitude was found. **(D)** ICF at ISI of 11 ms were significantly facilitated after QTS5, QPS5, and OPS2.5, whereas SICI at an ISI of 3 ms was not affected under MMB anesthesia in controls (left graph). Facilitations after stimulation in MMB controls were suppressed both under MK-801 and 7 days after SAH (middle and right graph).

All 11 ms-ICF facilitations after QTS5, QPS5, and OPS2.5 stimulations were suppressed both under MK-801 and 7 days after SAH (**Figure 5D**, middle and right graph).

Correlation Between Neurological Score and 3 ms-SICI, 11 ms-ICF, and 200 Hz-QTS5-MEPs After SAH

The mean neurological scores for the control and SAH groups are compared in **Figure 6C** (statistical significance was found at 7 days after SAH onset; $P < 0.001$). Garcia's neurological scores and 3 ms-SICI rates and 11 ms-ICF rates were significantly correlated ($R^2 = 0.6236$; $r = -0.79$; $P = 0.00046$ and $R^2 = 0.6053$; $r = -0.77$; $P = 0.00063$, respectively; **Figure 6D**).

No statistical difference was found in the neurological scores among pre-QTS5, pre-QPS5, and pre-OPS2.5 groups (scores between groups; $F_{(2, 12)} = 0.077$, $P = 0.93$; 12.6 ± 1.08, 12.8 ± 1.15, 13.2 ± 1.07, respectively).

Garcia's neurological scores and normalized MEP amplitudes at 25 min, only after QTS5, were significantly correlated ($R^2 = 0.9071$; $r = 0.95$; $P = 0.012$; blue solid line in **Figure 6E**), but not after QPS5 and OPS2.5 ($R^2 = 0.4303$; $r = -0.65$; $P = 0.23$; red dashed line and $R^2 = 0.0236$; $r = 0.15$; $P = 0.81$; green dashed line, respectively; **Figure 6E**).

DISCUSSION

We verified the pattern of MEP facilitation, as a consequence of three different LTP-inducing, high-frequency electrical stimulations of the motor cortex in control and SAH model rats. For our study, we used the same pattern of stimulation for MEP facilitation in the motor cortex as shown in previous human and animal studies (QTS5; Jung et al., 2016, QPS5; Hamada et al., 2008, OPS2.5; Steward et al., 2020, respectively). Four or eight pulses at high frequency (200 or 400 Hz-burst), repeated at 5 Hz (four pulses at 5 ms inter-pulse interval; QTS5), every 5 s (four pulses at 5 ms inter-pulse interval; QPS5) or every 10 s (eight pulses at 2.5 ms inter-pulse interval; OPS2.5), under a constant number of 1,440 pulses, were consistent between each condition.

Using continuous MEP recording, we found that high-frequency repetitive electrical stimulation at 200 and

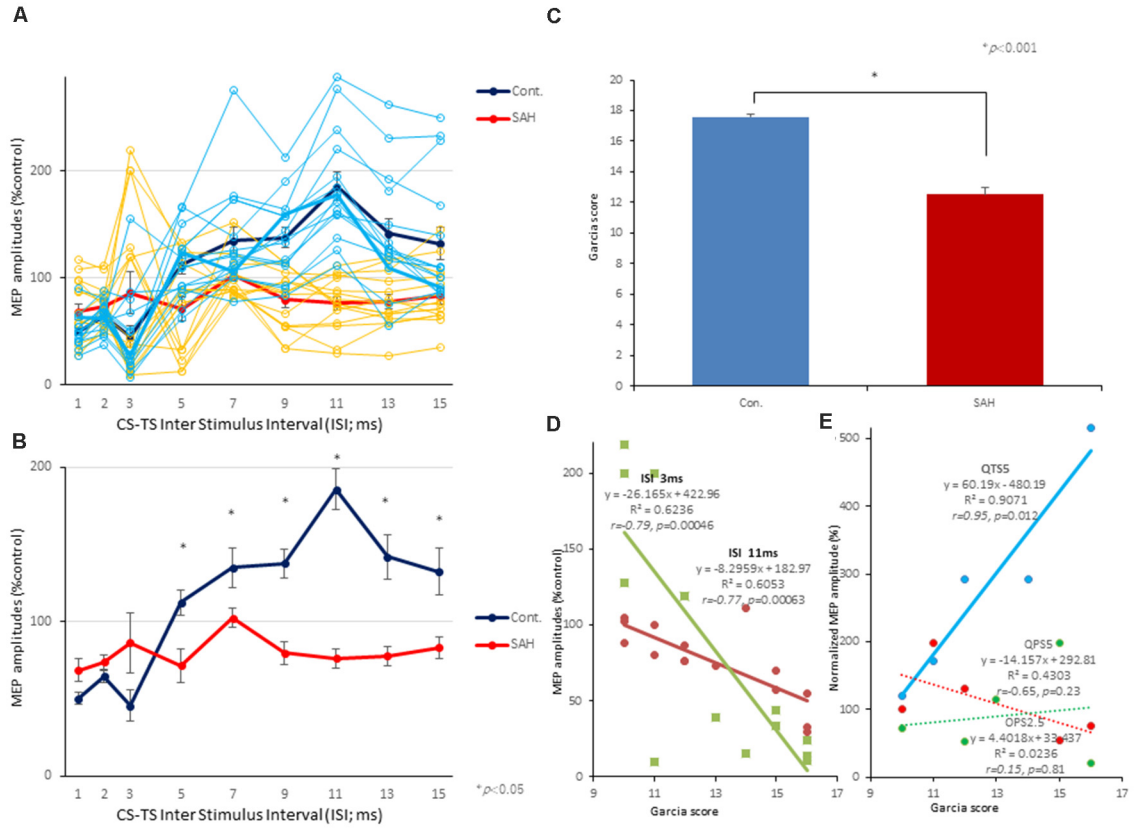

FIGURE 6 | Effects of SAH on 3 ms-inhibition (SICI) and 11 ms-facilitation (ICF) patterns, neurological scores, and correlations between parameters for SICI/ICF and MEP amplitudes after 200 Hz-QTS5. Individual profiles of normalized MEPs in each ISI in controls and SAH animals under MMB anesthesia **(A,B)**. Averaged normalized MEPs under SAH (red) and control (blue) at CS at 75% RMT preceding TS-MEPs **(A,B)**. No-TBS control-MMB-anesthetized rats demonstrated the significant inhibition at ISIs of 3 ms and facilitation at 11 ms, whereas SAH rats demonstrated the significant suppression at 11 ms-facilitation at 75% RMT-CS. Inhibition at an ISI of 3 ms were slightly preserved (statistically not significant; **A,B**). ANOVA revealed that the values were significantly greater in the control group than in the SAH group at an ISI of 11 ms. $^*P < 0.05$. Neurological scores of rats after SAH were significantly lower than those of the control group at 7 days after onset ($P < 0.001$; **C**). There were significant correlations between Garcia's neurological scores and 3 ms-inhibition rates (light green solid line) and 11 ms-facilitation rates (brown solid line; **D**). There were significant correlations between Garcia's neurological scores and normalized MEP amplitudes at 25 min, only after 200 Hz-QTS5 ($P = 0.012$; blue solid line) but not after QPS5 ($P = 0.23$; red dashed line) and OPS2.5 ($P = 0.81$; green dashed line; **E**).

400 Hz strongly activated MEPs, persisting for 180 min under anesthesia. SAH and MK-801, the NMDA-receptor antagonist, completely blocked MEP facilitation, while it was preserved after QTS5 treatment.

Correlation Between Morphological and Neurophysiological Changes After SAH

Morphological damages following SAH, demonstrating substantial neuronal damages in the motor cortical layers III and V were similar to those reported in previous study (Ostrowski et al., 2005). Careful correlational interpretation should be done between morphological changes and present neurophysiological results. The final output neuronal cells in layer V contributing to generate MEPs are affected both by corticospinal neurons and by surrounding GABAergic and glutamatergic interneurons, which connect with corticospinal neurons. Thus, our results are based on cortical excitability and potentially summarize the overall inter-neuronal functions.

SICI, ICF, and Motor Cortical LTP for Surrogate Quantitative Biomarker for SAH

The three neurophysiological parameters (3 ms-SICI, 11 ms-ICF, and 200 Hz-QTS5-MEPs) that were found to correlate with behavioral scores could be useful as surrogate quantitative biomarkers. However, we did not use direct measurements and therefore these findings do not reflect the degree of GABAergic and glutamatergic deficiency and/or plasticity 7 days after SAH.

We attempted to determine whether CS preceding 3 ms-SICI, 11 ms-ICF, and LTP-like MEP responses after high-frequency stimulations could provide an accurate correlation with the clinical symptoms observed in patients with SAH.

200 Hz-QTS of the Rat Motor Cortex Facilitates MEP; Rationale for Glutamatergic Mechanisms

Considering the difference between electrical stimulation and TMS (while current density close to the electrodes is higher

than that in between electrodes, it is more uniform with TMS), stimulus parameters of electrical stimulation as in TMS may not always induce the same neuroplasticity. Furthermore, stimulus parameters for experimental hippocampal LTP induction have never been applied for motor cortical LTP induction both in human and animals. To understand the underlying mechanisms and verify compatibility with human and animal results, experiments comparing with other patterns of stimulation will be informative. The fact that both QPS5 and OPS2.5 appeared to induce stronger facilitation than QTS5 during stimulation for the first 30 min on control animals, but there were no significant differences among the three groups in the final 30 min, is of interest. Longer stimulus duration providing stronger developing phases in QPS5 and OPS2.5 (QTS5; 72 s vs. 30 min) is one possibility (Nakamura et al., 2016). Future studies in this regard are warranted.

The present results re-confirmed 11 ms-ICF as glutamatergic inter-neuronal hypothesis within the motor cortex, depending on NMDA-receptor activation both in humans and rats (Di Lazzaro and Rothwell, 2014; Di Lazzaro et al., 2018; Fujiki et al., 2020a). Indeed, the facilitatory effect of QPS5 is proposed to be glutaminergic receptor-mediated, because ICF is facilitated after TMS-QPS5 in the human motor cortex (Hamada et al., 2008). Furthermore, a 200 Hz-burst pattern (ISI of 5 ms) is considered optimal for inducing sufficient-maximal postsynaptic Ca^{2+} influx, triggering intra- and/or inter-neuronal signaling cascades for the LTP induction *via* activity dependent NMDA-receptor activation (Kenney and Manahan-Vaughan, 2013). The OPS2.5 facilitatory effect that produces a 400 Hz-burst (ISI of 2.5 ms) has been considered a glutaminergic receptor-mediatedgold standard in the animal hippocampal LTP induction model, which has been recently applied a motor cortical electrical stimulation induced-LTP model (Steward et al., 2020).

Transient MEP facilitation after QTS5 under MK-801 suggests different underlying mechanisms between QPS5, OPS2.5, and QTS5. The importance of an "inter-burst interval of 5 Hz in TBS" has been proposed, with GABAergic inhibition in intracortical interneurons preventing the decay in burst efficiency and facilitating long-term MEP and hippocampal LTP (Kenney and Manahan-Vaughan, 2013; Jung et al., 2016). All these observations in relation to NMDA receptor-dependent synaptic plasticity are distinctly correlated with frequency-dependency (Kenney and Manahan-Vaughan, 2013; Jung et al., 2016; Fujiki et al., 2020b). Although there is evidence that LTP-like MEP facilitation after high-frequency stimulation of the motor cortex, which may be the part of the common mechanisms for hippocampal LTP induction (Kelleher et al., 2004), 3 ms-SICI, 11 ms-ICF, and 200 Hz-QTS5-MEPs are more broadly applicable, as sensitive-quantitative surrogate markers of NMDA-receptor activation that underly synaptic plasticity after SAH.

Our results expand the current consensus of inter-neuronal profiles affected by high-frequency stimulation (200 Hz-TBS, 200 and 400 Hz) of the rat hippocampus to the motor cortex in the experimental settings. We further demonstrated that these stimulation paradigms activate NMDA receptors, and that NMDA-receptor mediated glutamatergic inter-neuronal dysfunction correlates with neurobehavioral deficits after SAH. However, these results need to be verified in humans.

Limitations and Future Work

First, considering that the animals in the present study were under stable anesthetic conditions, it should be noted that RMT and all altered parameters in MEPs, SICIs, ICFs, and MEP facilitations after LTP-inducing high-frequency stimulations through the experiments may have been affected by midazolam, a GABA-A agonist-based anesthetic combination. However, in contrast to urethane, a compound commonly used for synaptic plasticity studies for non-survival single session (Sykes et al., 2016), the present combination (applicable for repeated survival experiments) is also favorable for multi-synaptic MEP studies (Fujiki et al., 2020a). Second, the relationship between pathophysiological cascades of SAH and NMDA glutamatergic inter-neuronal dysfunction remains unclear. In this regard, further careful and detailed studies are required to elucidate the links between neuro-biological effects at the molecular level to address safety issues with stimulation of the motor cortex, as well as high-frequency stimulation, and induction of LTP in the human brain. This is consistent with the current consensus that even non-invasive-TMS in both humans and animals can induce LTP/LTD and alter synaptic plasticity with cellular and/or molecular mechanisms (Carmel et al., 2010; Müller-Dahlhaus and Vlachos, 2013; Rodger and Sherrard, 2015; Fujiki et al., 2020a,b). Therefore, non-invasive-brain stimulation-based therapies may be beneficial for treating neurobehavioral deficits after SAH.

CONCLUSION

QTS5, QPS5, and OPS2.5 strongly facilitated MEPs. MK-801 and SAH completely blocked these MEP facilitations, while MEP facilitation after QTS5 was preserved. Garcia's neurological scores and 3 ms-SICI rates, 11 ms-ICF rates, and MEP facilitations after 200 Hz-QTS5-MEPs were significantly correlated. Neurophysiological evaluation of 3 ms-SICI, 11 ms-ICF, and 200 Hz-QTS5-MEPs may be useful surrogate quantitative biomarkers for inter-neuronal functional evaluation after SAH.

DATA AVAILABILITY STATEMENT

The raw data supporting the conclusions of this article will be made available by the authors, without undue reservation.

ETHICS STATEMENT

The animal study was reviewed and approved by Oita University Ethical Review Committee.

AUTHOR CONTRIBUTIONS

MF, KK, HO, and YK designed the research and wrote the article. MF, HF, and YK performed experiments. MF, KK, HO, and HF

analyzed data. All authors contributed to the article and approved the submitted version.

FUNDING

This work was supported in part by Grants-in-Aid for Scientific Research (C) (MF, YK, and HF), a medical research grant on traffic accidents by The General Insurance Association of Japan (MF), and Co-Create Knowledge for Pharma Innovation with Takeda (COCKPI-T; MF).

ACKNOWLEDGMENTS

We thank Dr. Kenji Sugita for technical assistance.

SUPPLEMENTARY MATERIAL

The Supplementary Material for this article can be found online at: https://www.frontiersin.org/articles/10.3389/fncir.2021.670189/full#supplementary-material.

REFERENCES

Carmel, J. B., Berrol, L. J., Brus-Ramer, M., and Martin, J. H. (2010). Chronic electrical stimulation of the intact corticospinal system after unilateral injury restores skilled locomotor control and promotes spinal axon outgrowth. *J. Neurosci.* 30, 10918–10926. doi: 10.1523/JNEUROSCI.1435-10.2010

Di Lazzaro, V., and Rothwell, J. C. (2014). Corticospinal activity evoked and modulated by non-invasive stimulation of the intact human motor cortex. *J. Physiol.* 592, 4115–4128. doi: 10.1113/jphysiol.2014.274316

Di Lazzaro, V., Rothwell, J., and Capogna, M. (2018). Noninvasive stimulation of the human brain: activation of multiple cortical circuits. *Neuroscientist* 24, 246–260. doi: 10.1177/1073858417717660

Fujiki, M., Kobayashi, H., Inoue, R., and Ishii, K. (2004). Immediate plasticity in the motor pathways after spinal cord hemisection: implications for transcranial magnetic motor-evoked potentials. *Exp. Neurol.* 187, 468–477. doi: 10.1016/j.expneurol.2004.03.009

Fujiki, M., Kawasaki, Y., and Fudaba, H. (2020a). Continuous theta-burst stimulation intensity dependently facilitates motor-evoked potentials following focal electrical stimulation of the rat motor cortex. *Front. Neural Circuits* 14:585624. doi: 10.3389/fncir.2020.585624

Fujiki, M., Yee, K. M., and Steward, O. (2020b). Non-invasive high frequency repetitive transcranial magnetic stimulation (hfrTMS) robustly activates molecular pathways implicated in neuronal growth and synaptic plasticity in select populations of neurons. *Front. Neurosci.* 14:558. doi: 10.3389/fnins.2020.00558

Garcia, J. H., Wagner, S., Liu, K. F., and Hu, X. J. (1995). Neurological deficit and extent of neuronal necrosis attributable to middle cerebral artery occlusion in rats: statistical validation. *Stroke* 26, 627–634. doi: 10.1161/01.str.26.4.627

Hackett, M. L., and Anderson, C. S. (2000). Health outcomes 1 year after subarachnoid hemorrhage: an international population-based study. The Australian cooperative research on subarachnoid hemorrhage study group. *Neurology* 55, 658–662. doi: 10.1212/wnl.55.5.658

Hamada, M., Terao, Y., Hanajima, R., Shirota, Y., Nakatani-Enomoto, S., Furubayashi, T., et al. (2008). Bidirectional long-term motor cortical plasticity and metaplasticity induced by quadripulse transcranial magnetic stimulation. *J. Physiol.* 586, 3927–3947. doi: 10.1113/jphysiol.2008.152793

Hess, G., and Donoghue, J. P. (1996). Long-term potentiation and long-term depression of horizontal connections in rat motor cortex. *Acta Neurobiol. Exp.* 56, 397–405.

Hsieh, T. H., Dhamne, S. C., Chen, J. J., Pascual-Leone, A., Jensen, F. E., and Rotenberg, A. (2012). A new measure of cortical inhibition by mechanomyography and paired-pulse transcranial magnetic stimulation in unanesthetized rats. *J. Neurophysiol.* 107, 966–972. doi: 10.1152/jn.00690.2011

Huang, Y. Z., Edwards, M. J., Rounis, E., Bhatia, K. P., and Rothwell, J. C. (2005). Theta burst stimulation of the human motor cortex. *Neuron* 45, 201–206. doi: 10.1016/j.neuron.2004.12.033

Jeon, H., Ai, J., Sabri, M., Tariq, A., and Macdonald, R. L. (2010). Learning deficits after experimental subarachnoid hemorrhage in rats. *Neuroscience* 169, 1805–1814. doi: 10.1016/j.neuroscience.2010.06.039

Jung, N. H., Gleich, B., Gattinger, N., Hoess, C., Haug, C., Siebner, H. R., et al. (2016). Quadri-pulse theta burst stimulation using ultra-high frequency bursts—a new protocol to induce changes in cortico-spinal excitability in human motor cortex. *PLoS One* 11:e0168410. doi: 10.1371/journal.pone.0168410

Kelleher, R. J., 3rd, Govindarajan, A., and Tonegawa, S. (2004). Translational regulatory mechanisms in persistent forms of synaptic plasticity. *Neuron* 44, 59–73. doi: 10.1016/j.neuron.2004.09.013

Kenney, J., and Manahan-Vaughan, D. (2013). NMDA receptor-dependent synaptic plasticity in dorsal and intermediate hippocampus exhibits distinct frequency-dependent profiles. *Neuropharmacology* 74, 108–118. doi: 10.1016/j.neuropharm.2013.02.017

Kreiter, K. T., Copeland, D., Bernardini, G. L., Bates, J. E., Peery, S., Claassen, J., et al. (2002). Predictors of cognitive dysfunction after subarachnoid hemorrhage. *Stroke* 33, 200–209. doi: 10.1161/hs0102.101080

Kujirai, T., Caramia, M. D., Rothwell, J. C., Day, B. L., Thompson, P. D., Ferbert, A., et al. (1993). Corticocortical inhibition in humanmotor cortex. *J. Physiol.* 471, 501–519. doi: 10.1113/jphysiol.1993.sp019912

Mishra, A. M., Pal, A., Gupta, D., and Carmel, J. B. (2017). Paired motor cortex and cervical epidural electrical stimulation timed to converge in the spinal cord promotes lasting increases in motor responses. *J. Physiol.* 595, 6953–6968. doi: 10.1113/JP274663

Müller-Dahlhaus, F., and Vlachos, A. (2013). Unraveling the cellular and molecular mechanisms of repetitive magnetic stimulation. *Front. Mol. Neurosci.* 6:50. doi: 10.3389/fnmol.2013.00050

Nakamura, K., Groiss, S. J., Hamada, M., Enomoto, H., Kadowaki, S., Abe, M., et al. (2016). Variability in response to quadripulse stimulation of the motor cortex. *Brain Stimul.* 9, 859–866. doi: 10.1016/j.brs.2016.01.008

Ostrowski, R. P., Colohan, A. R. T., and Zhang, J. H. (2005). Mechanisms of hyperbaric oxygen-induced neuroprotection in a rat model of subarachnoid hemorrhage. *J. Cereb. Blood Flow Metab.* 25, 554–571. doi: 10.1038/sj.jcbfm.9600048

Qin, Y., Gu, J. W., Li, G. L., Xu, X. H., Yu, K., and Gao, F. B. (2015). Cerebral vasospasm and corticospinal tract injury induced by a modified rat model of subarachnoid hemorrhage. *J. Neurol. Sci.* 358, 193–200. doi: 10.1016/j.jns.2015.08.1536

Rodger, J., and Sherrard, R. M. (2015). Optimising repetitive transcranial magnetic stimulation for neural circuit repair following traumatic brain injury. *Neural Regen. Res.* 10, 357–359. doi: 10.4103/1673-5374.153676

Rothwell, J. C. (1997). Techniques and mechanisms of action of transcranial stimulation of the human motor cortex. *J. Neurosci. Methods* 74, 113–122. doi: 10.1016/s0165-0270(97)02242-5

Sherchan, P., Lekic, T., Suzuki, H., Hasegawa, Y., Rolland, W., Duris, K., et al. (2011). Minocycline improves functional outcomes, memory deficits and histopathology after endovascular perforation-induced sub arachnoid hemorrhage in rats. *J. Neurotrauma* 28, 2503–2512. doi: 10.1089/neu.2011.1864

Silasi, G., and Colbourne, F. (2009). Long-term assessment of motor and cognitive behaviours in the intraluminal perforation model of subarachnoid hemorrhage in rats. *Behav. Brain Res.* 198, 380–387. doi: 10.1016/j.bbr.2008.11.019

Steward, O., Coulibaly, A. M., Metcalfe, M., Yonan, J. M., and Yee, K. M. (2020). AAVshRNA-mediated PTEN knockdown in adult neurons attenuates activity-dependent immediate early gene induction. *Exp. Neurol.* 326:113098. doi: 10.1016/j.expneurol.2019.113098

Sugawara, T., Ayer, R., Jadhav, V., and Zhang, J. H. (2008). A new grading system evaluating bleeding scale in filament perforation subarachnoid hemorrhage rat model. *J. Neurosci. Methods* 167, 327–334. doi: 10.1016/j.jneumeth.2007.08.004

Sykes, M., Matheson, N. A., Brownjohn, P. W., Tang, A. D., Rodger, J., Shemmell, J. B., et al. (2016). Differences in motor evoked potentials induced in rats by transcranial magnetic stimulation under two separate

anesthetics: implications for plasticity studies. *Front. Neural Circuits* 10:80. doi: 10.3389/fncir.2016.00080

Thal, S. C., Mebmer, K., Elsaesser, R. S., and Zausinger, S. (2008). Neurological impairment in rats after subarachnoid hemorrhage—a comparison of functional tests. *J. Neurol. Sci.* 268, 150–159. doi: 10.1016/j.jns.2007.12.002

Vahabzadeh-Hagh, A. M., Muller, P. A., Pascual-Leone, A., Jensen, F. E., and Rotenberg, A. (2011). Measures of cortical inhibition by paired-pulse transcranial magnetic stimulation in anesthetized rats. *J. Neurophysiol.* 105, 615–624. doi: 10.1152/jn.00660.2010

Wegener, N., Nagel, J., Gross, R., Chambon, C., Greco, S., Pietraszek, M., et al. (2011). Evaluation of brain pharmacokinetics of (+)MK-801 in relation to behaviour. *Neurosci. Lett.* 503, 68–72. doi: 10.1016/j.neulet.2011.08.012

Yang, Q., Ramamurthy, A., Lall, S., Santos, J., Ratnadurai-Giridharan, S., Lopane, M., et al. (2019). Independent replication of motor cortex and cervical spinal cord electrical stimulation to promote forelimb motor function after spinal cord injury in rats. *Exp. Neurol.* 320:112962. doi: 10.1016/j.expneurol.2019.112962

Conflict of Interest: KK and HO were employed by the Takeda Pharmaceutical Company Limited.

The remaining authors declare that the research was conducted in the absence of any commercial or financial relationships that could be construed as a potential conflict of interest.

Copyright © 2021 Fujiki, Kuga, Ozaki, Kawasaki and Fudaba. This is an open-access article distributed under the terms of the Creative Commons Attribution License (CC BY). The use, distribution or reproduction in other forums is permitted, provided the original author(s) and the copyright owner(s) are credited and that the original publication in this journal is cited, in accordance with accepted academic practice. No use, distribution or reproduction is permitted which does not comply with these terms.

frontiers in Human Neuroscience

ORIGINAL RESEARCH
published: 23 April 2021
doi: 10.3389/fnhum.2021.620958

Short-Term High-Intensity Interval Exercise Promotes Motor Cortex Plasticity and Executive Function in Sedentary Females

Min Hu[1†], Ningning Zeng[2†], Zhongke Gu[3†], Yuqing Zheng[1], Kai Xu[3], Lian Xue[4], Lu Leng[5], Xi Lu[6], Ying Shen[7] and Junhao Huang[1]**

[1] Guangdong Provincial Key Laboratory of Sports and Health Promotion, Scientific Research Center, Guangzhou Sport University, Guangzhou, China, [2] Shenzhen Key Laboratory of Affective and Neuroscience, Center for Brain Disorders and Cognitive Sciences, Shenzhen University, Shenzhen, China, [3] Department of Sport and Health Sciences, Nanjing Sport Institute, Nanjing, China, [4] Scientific Laboratory Center, Nanjing Sport Institute, Nanjing, China, [5] College of Foreign Languages, Jinan University, Guangzhou, China, [6] Department of Rehabilitation Medicine, China-Japan Friendship Hospital, Beijing, China, [7] Rehabilitation Medicine Center, The First Affiliated Hospital of Nanjing Medical University, Nanjing, China

OPEN ACCESS

Edited by:
Charlotte A. Boettiger, University of North Carolina at Chapel Hill, United States

Reviewed by:
Maxciel Zortea, Federal University of Rio Grande do Sul, Brazil
Yudai Yamazaki, University of Tsukuba, Japan

***Correspondence:**
Ying Shen
shenying_1981@hotmail.com
Junhao Huang
junhaohuang2006@hotmail.com

[†] These authors have contributed equally to this work

Specialty section:
This article was submitted to Brain Imaging and Stimulation, a section of the journal Frontiers in Human Neuroscience

Received: 24 October 2020
Accepted: 31 March 2021
Published: 23 April 2021

Citation:
Hu M, Zeng N, Gu Z, Zheng Y, Xu K, Xue L, Leng L, Lu X, Shen Y and Huang J (2021) Short-Term High-Intensity Interval Exercise Promotes Motor Cortex Plasticity and Executive Function in Sedentary Females. Front. Hum. Neurosci. 15:620958. doi: 10.3389/fnhum.2021.620958

Previous research has demonstrated that regular exercise modulates motor cortical plasticity and cognitive function, but the influence of short-term high-intensity interval training (HIIT) remains unclear. In the present study, the effect of short-term HIIT on neuroplasticity and executive function was assessed in 32 sedentary females. Half of the participants undertook 2 weeks of HIIT. Paired-pulse transcranial magnetic stimulation (ppTMS) was used to measure motor cortical plasticity via short intracortical inhibition (SICI) and intracortical facilitation (ICF). We further adapted the Stroop task using functional near-infrared spectroscopy (fNIRS) to evaluate executive function in the participants. The results indicated that, compared with the control group, the HIIT group exhibited decreased ICF. In the Stroop task, the HIIT group displayed greater activation in the left dorsolateral prefrontal cortex (DLPFC) and left orbitofrontal cortex (OFC) even though no significant difference in task performance was observed. These findings indicate that short-term HIIT may modulate motor cortical plasticity and executive function at the neural level.

Keywords: short intracortical inhibition, intracortical facilitation, high-intensity interval training, executive function, sedentary females

INTRODUCTION

Synaptic plasticity refers to the ability of the nervous system to modify the strength of communication between neurons (Citri and Malenka, 2008). There is plentiful evidence that engaging in regular exercise enhances synaptic plasticity, thus having a positive effect on brain cognitive function (Cotman and Berchtold, 2002; Bramham and Messaoudi, 2005). Despite numerous studies highlighting the importance of exercise in maintaining brain function and health, exercise-induced cortical and functional changes in the brain remain largely unelucidated.

Transcranial magnetic stimulation (TMS) provides a distinct opportunity to non-invasively assess neuroplasticity. Numerous studies have used TMS to assess neuroplasticity after exercise

in healthy individuals (Rossi and Rossini, 2004; Mellow et al., 2020). Short intracortical inhibition (SICI) decreases following sessions of high-intensity exercise (Smith et al., 2014; Opie and Semmler, 2019). Acute aerobic exercise has also been shown to induce a change in intracortical facilitation (ICF) (Singh et al., 2014; Nicolini et al., 2019). Both SICI and ICF are involved in cortical plasticity in the motor cortex. SICI is mediated by the inhibitory neurotransmitter $GABA_a$ receptor (Kujirai et al., 1993; Paulus et al., 2008), while ICF is thought to reflect the numbers of glutamate neurons and n-methyl-aspartic acid (NMDA) receptors (Liepert et al., 1997; Paulus et al., 2008).

Exercise not only changes cortical plasticity but also has a positive effect on cognitive function. Previous studies have found that, compared with a control group, attention (Bherer, 2015), memory (Stroth et al., 2009), motor performance (Fisher et al., 2008; Ellen et al., 2017) and executive function (Smiley-Oyen et al., 2008) in the exercise group were significantly greater after aerobic training. Likewise, neuroimaging studies using fMRI and fNIRS have found that the prefrontal brain region involving these cognitive functions displayed greater activity after exercise (Derrfuss et al., 2004; Yanagisawa et al., 2010). For example, older adults who performed six months' aerobic exercise exhibited greater activation in frontal brain regions, and those functional changes were associated with better cognitive performance (Colcombe et al., 2004; Szcs et al., 2012; Bherer, 2015). Similar findings were observed even after a single session of moderate exercise (Yanagisawa et al., 2010).

High-intensity interval training (HIIT), a form of exercise characterized by repeated short and intensive workouts combined with short recovery intervals, has become popular in sedentary individuals (El-Sayes et al., 2019; Nicolini et al., 2019). HIIT not only improves physiological function but also promotes executive function (Kujach et al., 2018). However, the effect of short-term HIIT on neuroplasticity requires further investigation. Elucidating the mechanisms by which HIIT modulates motor cortical excitability is necessary in order that exercise protocols can be used as an intervention in neurorehabilitation. In the present study, the effect of short-term HIIT on neuroplasticity and executive function in sedentary individuals was assessed. Paired-pulse TMS was used to measure SICI and ICF, and the Stroop task was adopted to assess executive function, in combination with fNIRS. We hypothesized that short-term HIIT would induce changes in SICI and ICF, accompanied by increased executive function.

METHODS

Subjects

Thirty two healthy female subjects were selected for participation in the study. The inclusion criteria were: (1) age 18-30 years; (2) individuals that were sedentary (no regular exercise, fewer than 3 times per week and less than 20 min on each occasion); (3) no contraindication to exercise (assessed by a physical activity preparation questionnaire, PAR-Q); (4) no contraindication to TMS according to the TMS safety guidelines (Rossi et al., 2009). Subjects that had a history of seizures, were currently prescribed psychoactive medication or with a history of cardiovascular disease were excluded from the study. All subjects were right-handed and had normal vision. Signed informed consent was provided in every case. The ethics of the study were approved by the Guangzhou Sport Institute.

Design

The 32 subjects were randomly divided into two groups: a high-intensity interval training (HIIT) group and a control group. All subjects participated in three periods: a pre-training period, training period, and a post-training period. As illustrated in **Figure 1**, prior to the pre-training session, subjects reported demographic information, including age, education, body mass index (BMI), physical activity preparation (PAR-Q), Physical activity level measured by the international physical activity questionnaire (IPAQ). The training protocol was similar to that of previous studies (Babraj et al., 2009; Ellen et al., 2017). During the period of training, the HIIT group completed 8 high-intensity interval training sessions, 25 min each in length, 4 times per week, lasting for 2 weeks. Participants in the control group maintained their normal lifestyle without training. During pre-training and post-training periods, the physiological and cognitive function of each subject, and cortical plasticity (assessed by TMS) and neuropsychological tests were evaluated.

Ethics and Dissemination

This study was approved by the Ethics Committee of Guangzhou Sport University (2019LCLL-10) and conducted in accordance with the Declaration of Helsinki. The trial was registered in the China Clinical Trial Registration Center (ChiCTR1900028645). All participants signed an informed consent form before they were randomly assigned into their respective groups.

Exercise Protocol

The exercise procedure was same as that of previous studies (Ellen et al., 2017). High-intensity interval training was conducted using a stationary power bike (BikeReha, Netherlands). The intensity of training for each subject was selected based on their heart rate reserve (HRR). We used age-predicted HRpeak to calculate HRR (Tanaka et al., 2001). Resting heart rate (RHR) was recorded while seated. The training program consisted of alternating on 4 occasions between a 50% HRR cycle for 3 min and 90% HRR cycle for 2 min, for a total duration of 20 min. Subjects completed a 2-min warm-up and a 2-min relaxation session by cycling at very low intensity both prior to and following training. Subjects' heart rates were monitored continuously during the entire training session. The Borg perceived fatigue scale was used after training to assess each subject's feelings of fatigue, ranging from 6 (no exertion at all) to 20 (maximal exertion). HIIT parameters detailed in **Supplementary Table 1**.

Physiological Function Evaluation

Blood pressure measurement: The blood pressure of each subject was measured from 08:00 to 10:00 in the morning while fasting using an Omron HEM-7124 electronic sphygmomanometer (Omron, Dalian). Subjects sat quietly for 10 min prior to measurement.

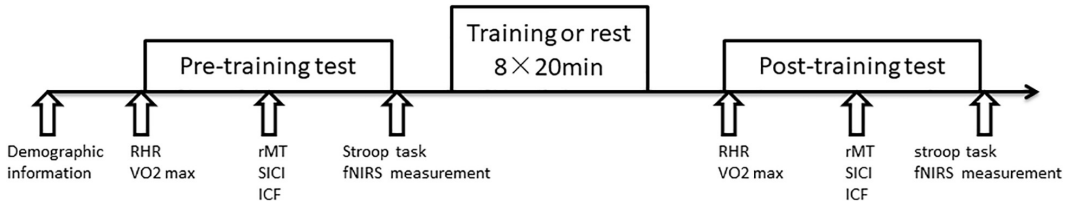

FIGURE 1 | Study timeline. Firstly participants reported demographic information. RHR, $VO2_{peak}$, motor cortical plasticity (rMT, SICI, ICF), Stroop task were then measured before and after HIIT. During the training period, the HIIT group received 2 weeks of training consisting of 8 sessions lasting 20 min each.

Peak oxygen consumption (VO_2peak) measurement: VO_2peak was measured using a respiratory portable gas analyzer (Cosmed K5, Rome, Italy) during running in a treadmill (hpCosmus,Germany). Heart rate was measured and recorded using a Polar heart rate monitor (Polar, Finland). For the test, a 3-min warm-up was performed at a constant running speed of 2.7 km/h, followed by increased speed and gradient every 3 min. The criteria for recording VO_2peak measurements ensured that the heart rate reached 180 beats /min, with a respiratory quotient greater than 1.15.

Neuropsychological Measurement

All subjects were assessed using the Pittsburgh Sleep Quality Index (PSQI), Beck Depression Inventory (BDI), Beck Anxiety Inventory (BAI), and Barratt Impulsivity Scale (BIS). The BIS consists of 30 items assessing three sub-dimensions of impulsivity, including attentional impulsivity (BIS-attention), motor impulsivity (BIS-motor), and no plan (BIS-no plan).

Stroop Task

The Stroop task referred to the previous studies (Plenger et al., 2016). The stimulus was presented on a black screen. In the center of the screen, a white "+" fixation point was first presented for 500 ms, and then a stimulus was randomly presented for 200 ms. The stimulus consisted of four words, including "red", "blue", "green", and "yellow", with font colors including red, blue, green, and yellow. Subjects were asked to respond to the color of the stimulus by pressing the key on the keyboard ("D" for "red", "F" for "blue", "J" for "green" and "K" for "yellow") corresponding to the color of the stimulus as quickly and accurately as possible, rather than from the actual words. The task consisted of six blocks. Two task conditions were in the block sequence ABBABA. In condition A (congruent condition), the color of the stimulus matched the word. In condition B (incongruent condition), the color of the stimulus did not correspond with the word. For each block, 12 stimuli were presented over 30 s.

Functional Near-Infrared Spectroscopy Test

Functional near-infrared spectroscopy (fNIRS) was used during the Stroop task. A continuous wave near infrared spectroscopy (CW-NIRS) system (NIRSIT, OBELAB, South Korea) was used to measure changes in light intensity at a sampling rate of 8.13 Hz. The light probe consisted of 24 light sources and 32 detectors. A total of 48 predefined channels were measured, with intervals of 3 cm between light source-detectors. Measurements were obtained from the prefrontal cortex, where the center of the lowest optical probe was aligned with the frontal pole zero (FPz) position of the 10-20 electrode EEG system to eliminate positional uncertainty between subjects. The modified Beer Lambert Law (MBLL) was used to convert raw light intensities into concentration changes in oxygenated hemoglobin (ΔHbO2). The region of interest (ROI) was selected based on previous study (Zhang et al., 2020; Jang et al., 2021). The MNI coordinates for each channel were defined base on the equipment coordinates.

Transcranial Magnetic Stimulation

Subjects were seated in an upright armchair with the instruction to relax their right arm entirely. Surface electromyography (EMG) was recorded from the abductor pollicis brevis (APB) muscle of the right hand via electrodes placed 2 cm apart in a belly-tendon montage. Single monophasic TMS was used via a figure of eight coil (outer diameter of each loop: 70 mm) connected to a Neuro-MS/D stimulator (Neurosoft, Russia). The coil was held tangentially to the skull, with the handle pointing posteriorly and laterally at an angle of approximately 45°to the sagittal plane over the left primary motor cortex (M1) hand region. The resting motor threshold (RMT) was then measured by determining the TMS intensity required to obtain a motor evoked potential (MEP) in the APB $>$ 50 μV in five out of 10 consecutive trials, expressed as the percentage of maximum stimulator output (MSO). The SICI and ICF were measured using paired-pulse TMS paradigms. The intensity of the conditioning stimulus (CS) was 90% of RMT and that of the test stimulus (TS) was 120% RMT. TS and CS were separated by an interstimulus interval (ISI) of 2.5 ms for SICI and 12 ms for ICF. 10 consecutive trials were delivered with TMS pulse given every 5 s. SICI and ICF were assessed by calculating the peak-to-peak amplitude of the MEP_{TS} and MEP_{CS-TS}. Then the SICI and ICF were computed as the ratio of MEP_{CS-TS} and MEP_{TS} (MEP_{CS-TS} / MEP_{TS}).

Statistical Analysis

Statistical analysis of the cognitive and TMS test data was conducted using SPSS Statistics version 21 software. Any values failing to meet assumptions of normality were transformed into log values. Two-way repeated-measures analysis of variance was used for the group and training periods (recording means and standard deviations). P-values <0.05 were considered significant. Bonferroni-adjusted pairwise comparisons were used.

fNIRS data were analyzed by NIRSIT Analysis Tool v2.2 software. Oxygenated hemoglobin concentration (HbO) was analyzed by the peak value of oxy-Hb in the present study. Spline interpolation was used in preprocessing to eliminate the effects of head movements. Components with frequencies greater than 0.1 Hz and less than 0.01 Hz were filtered to eliminate the effects of high-frequency physiological signals and low-frequency baseline drift. The data in the first 10 s of each condition was used as a baseline for HbO, which was then subtracted from the HbO values of each task condition to obtain final HbO data. According to the previous studies (Zhang et al., 2020; Jang et al., 2021), a total of 8 regions of interest (ROI) were defined: right dorsolateral prefrontal cortex (right DLPFC), right ventrolateral prefrontal cortex (right VLPFC), right frontopolar prefrontal cortex (right FPA), right orbitofrontal cortex (right OFC), left dorsolateral prefrontal cortex (left DLPFC), left ventrolateral prefrontal cortex (left VLPFC), left frontopolar prefrontal cortex (left FPA), and left orbitofrontal cortex (left OFC). The mean HbO value for each ROI was calculated.

RESULTS

Demographic Results

There were no differences in the HIIT and Control groups in terms of their demographic characteristics (age, education, BMI, and physical activity level), neuropsychological characteristics (sleep quality, depression, anxiety), pre-training physiological function (DBP, SBP, RHR, and VO_2peak) impulsivity, and TMS parameters in the pre-training period (**Table 1**). We also used 2-way ANOVA for RMT and MEP: groups: (HIIT, Control) × training periods (pre-training, post training). The results showed that there was no significant main effect of groups or training periods for RMT, $F_{group(1,30)} = 1.01$, $p = 0.377$, $\eta^2 = 0.063$; $F_{training(1,30)} = 0.03$, $p = 0.872$, $\eta^2 = 0.001$. The interaction effect was significant, $F_{interaction(1,30)} = 5.15$, $p = 0.012$, $\eta^2 = 0.256$. Simple t test found RMT of CON group was significantly higher in post-training than in pre-training, $t = 3.31$, $p = 0.005$, Cohen's d = 0.516, while no difference for HIIT group, $t = 0.70$, $p = 0.494$, Cohen's d = 0.109. Group difference was not significant both in pre-training and post-training, $t = 0.41$, $p = 0.685$, Cohen's d = 0.141, $t = 1.287$, $p = 0.208$, Cohen's d = 0.229. There was no significant main effect or interaction effect for MEP, $F_{training(1,30)} = 1.453$, $p = 0.237$, $\eta^2 = 0.046$; $F_{group(1,30)} = 0.17$, $p = 0.680$, $\eta^2 = 0.008$; $F_{interaction(1,30)} = 1.68$, $p = 0.205$, $\eta^2 = 0.053$.

Short-Interval intracortical Inhibition and Intracortical Facilitation

We first compared the TMS parameters between HIIT group and control group. Independent t test was adapted. As shown in Table1, there was no significant difference on RMT, MEP,

TABLE 1 | Demographic information and Baseline TMS parameters (X ± SD).

	CON (n = 16)	HIIT (n = 16)	t	p
Age(year)	19.31 ± 0.60	19.13 ± 0.62	0.868	0.392
Education(year)	13.69 ± 0.79	13.44 ± 0.51	1.059	0.298
BMI(kg/m^2)	21.04 ± 2.48	21.31 ± 2.08	−0.330	0.744
IPAQ(MET-min/w)	1111 ± 930	1655 ± 1136	−1.488	0.147
PSQI	7.25 ± 2.52	7.19 ± 2.34	0.073	0.943
BDI	6.50 ± 6.71	5.73 ± 7.92	0.280	0.782
BAI	6.60 ± 6.47	5.73 ± 7.93	0.987	0.330
BIS-noplan	53.57 ± 12.16	62.50 ± 13.69	−1.876	0.071
BIS-motor	34.82 ± 11.54	31.41 ± 11.79	0.799	0.431
BIS-attention	66.43 ± 9.84	69.53 ± 8.86	−0.909	0.371
BIS-total	51.07 ± 5.52	54.47 ± 6.18	−1.334	0.193
RHR (bpm)	77.56 ± 7.68	80.50 ± 6.40	1.213	0.211
VO_2 peak(ml/kg/min)	35.57 ± 2.83	35.28 ± 4.82	0.211	0.834
RMT_{pre}(%MSO)	65.12 ± 9.69	68.19 ± 11.44	0.409	0.685
RMT_{post}(%MSO)	63.63 ± 10.91	63.14 ± 10.74	1.287	0.208
MEP_{pre}(μv)	716.52 ± 215.81	765.91 ± 203.65	−0.666	0.511
MEP_{post}(μv)	717.90 ± 229.05	727.88 ± 170.77	−0.140	0.890
TS(%MSO)	77.27 ± 11.25	74.87 ± 13.44	0.572	0.600
CS(%MSO)	57.84 ± 8.45	56.28 ± 10.28	0.414	0.653
SICI(%TS)	29.18 ± 8.54	30.63 ± 9.89	−0.347	0.670
ICF(%TS)	143.61 ± 21.78	138.82 ± 25.63	−0.514	0.611

BMI = body mass index; IPAQ = International Physical Activity Questionnaire; PSQI = Pittsburgh sleep quality scores; BDI = Beck depression scores; BAI = Beck anxiety scores; BIS-noplan = no planning impulsiveness scores; BIS-motor = motor impulsiveness scores; BIS-attention = attention impulsiveness scores; BIS-total = Barratt impulsiveness total scores; RHR = resting heart rate; VO2peak = peak oxygen uptake; RMT_{pre} = resting motor threshold in pre-training session; RMT_{post} = resting motor threshold in post-training session; MEP: motor evoked potential; MSO = maximum stimulus output; TS = test stimulus; CS = conditional stimulus; SICI = short intracortical inhibition; ICF = intracortical facilitation.

CS, TS, SICI, and ICF amplitude between two groups in pre-training session.

A two-factor repeated measures ANOVA was adopted with 2 groups: (HIIT, Control) × 2 training periods (pre-training, post training). As displayed in **Figure 2**, for SICI, the results indicate that neither the principal effect of group or training period nor the interaction between group and training period were significant, with the group main effect: $F_{(1,30)} = 0.88$, $p = 0.356$, $\eta^2 = 0.028$; training main effect: $F_{(1,30)} = 0.152$, $p = 0.701$, $\eta^2 = 0.007$; interaction effect: $F_{(1,30)} = 2.576$, $p = 0.123$, $\eta^2 = 0.109$. For ICF, the results suggest a marginally significant interaction between the group and training periods, $F_{(1,30)} = 4.17$, $p = 0.054$, $\eta^2 = 0.167$. Post-hoc comparison indicated that ICF declined significantly after training in the HIIT group, $t = 2.76$, $p = 0.015$, Cohen's $d = 0.690$, but not in the Control group, $t = 0.54$, $p = 0.597$, Cohen's $d = 0.135$. The main effect of the group and training periods were not significant, $F_{(1,30)} = 0.21$, $p = 0.65$, $\eta^2 = 0.001$; $F_{(1,30)} = 0.35$, $p = 0.561$, $\eta^2 = 0.016$.

Stroop Task Performance

We first calculated the Stroop effect for accuracy (ACC) and response time (RT) by subtracting ACC (or RT) in the congruent condition from the incongruent condition.

Stroop effects were significant in both the pre-training and post-training periods for the two groups: the ACC in the congruent condition was higher than in the incongruent condition, $p_s < 0.001$. The RT in the congruent condition was significantly shorter than that of the incongruent condition, $p_s < 0.001$. Repeated measures ANOVA (2 group (HIIT, Control) × 2 training periods (pre-training, post-training)) indicates a significant main effect from the training period in terms of RT, $F_{(1,30)} = 4.61$, $p = 0.041$, $\eta^2 = 0.141$. The Stroop effect of RT in the post-training period was shorter than in the pre-training period. But other effects or interactions were not significant, $p_s > 0.05$ (see **Table 2**).

fNIRS Outcomes

For the outcome of fNIRS analysis, we focused on the neural response of 8 ROIs during the congruent and incongruent conditions and used the difference (incongruent-congruent) to represent the hemodynamic response due to Stroop interference. Furthermore, a 2 group (HIIT, Control) × 2 training periods (pre-training, post-training) repeated measures ANOVA was used for the Stroop effect for HbO in the 8 ROIs. As shown in **Figure 3**, Group × training period indicated a significant interaction effect in the left DLPFC, $F_{(1,30)} = 5.60$, $p = 0.025$, $\eta^2 = 0.157$. The simple effect indicated that HbO was higher in the post-training period ($M_{post} = 1.55^{*}10^{-4}$, $SD_{post} = 2.53^{*}10^{-4}$) than in the pre-training period ($M_{pre} = 2.29^{*}10^{-5}$, $SD_{pre} = 1.58^{*}10^{-4}$) for the HIIT group, $t = 2.09$, $p = 0.045$, Cohen's $d = 0.52$, but with no difference for the Control group ($M_{pre} = 8.45^{*}10^{-5}$, $SD_{pre} = 1.56^{*}10^{-4}$; $M_{post} = 1.11^{*}10^{-6}$, $SD_{post} = 1.30^{*}10^{-4}$), $t = 1.19$, $p = 0.250$, Cohen's d = 0.29. A similar result was found in the left OFC: the interaction between the group and training periods was marginally significant, $F_{(1,30)} = 4.00$,

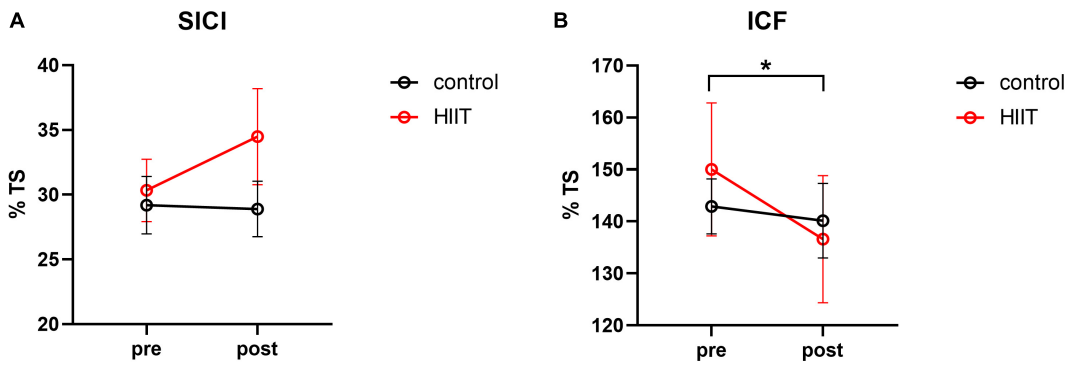

FIGURE 2 | (A) Mean short intracortical inhibition value calculated from the percentage of the test stimulus in the pre-training period compared with the post-training periods of the control and HIIT groups. **(B)** Mean intracortical facilitation value calculated from the percentage of the test stimulus in the pre-training and post-training periods of the control and HIIT groups. The hollow circles represent the raw values of each participant. *$p < 0.05$.

TABLE 2 | Accuracy and response time in stroop task of HIIT group and Control group (X ± SE).

		CON		HIIT	
		pre-test	**post-test**	**pre-test**	**post-test**
RT(ms)	congruent	441.02 ± 24.30	430.09 ± 22.37	459.59 ± 18.25	438.35 ± 20.63
	incongruent	581.73 ± 27.53	552.25 ± 25.62	603.41 ± 18.05	585.82 ± 24.78
ACC(%)	congruent	97.22 ± 0.77	96.83 ± 0.64	98.21 ± 0.69	98.02 ± 0.68
	incongruent	94.84 ± 1.08	96.03 ± 0.91	96.23 ± 1.22	95.44 ± 0.85

HIIT, high intensity interval training; RT, response time; ACC, accuracy.

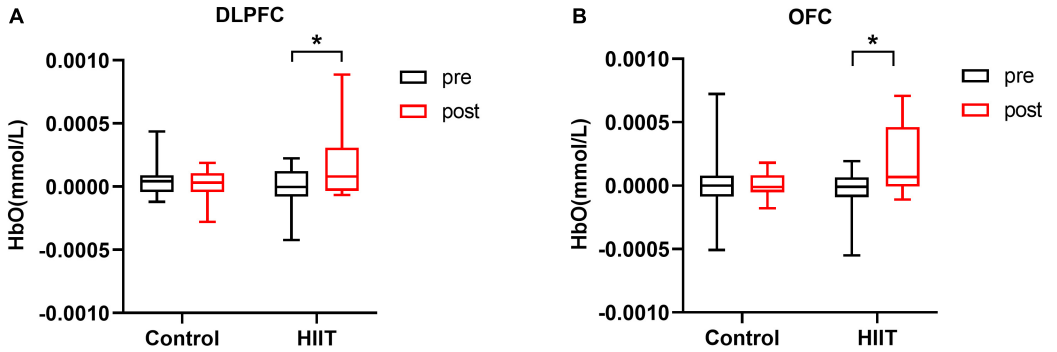

FIGURE 3 | (A) Mean oxygenated hemoglobin concentration in the left DLPFC in the pre-training and post-training periods of the control and HIIT groups. **(B)** Mean oxygenated hemoglobin concentration in the left OFC in the pre-training and post-training periods of the control and HIIT groups. Error bars represent standard deviations. *$p < 0.05$.

$p = 0.046$, $\eta^2 = 0.118$. Post-hoc comparison demonstrated that HbO was significantly higher in the post-training period ($M_{post} = 1.64*10^{-4}$, $SD_{post} = 2.76*10^{-4}$) than in the pre-training period ($M_{pre} = 7.32*10^{-5}$, $SD_{pre} = 1.95*10^{-4}$) for the HIIT group, $t = 2.95$, $p = 0.010$, Cohen's $d = 0.74$, but with no difference for the Control group ($M_{pre} = 2.46*10^{-6}$, $SD_{pre} = 2.65*10^{-4}$; $M_{post} = 1.16*10^{-5}$, $SD_{post} = 1.19*10^{-4}$), $t = 0.18$, $p = 0.859$, Cohen's d = 0.045.

DISCUSSION

The present study targeted in sedentary female individuals, examined the effect of short-term, high-intensity interval exercise on motor cortex plasticity and executive function. We found that, compared with the Control group, those individuals who received 2 weeks of HIIT exhibited an exercise-mediated reduction of intracortical facilitation. The brain activation related to Stroop interference was also significantly enhanced in the left dorsolateral prefrontal cortex and the left orbitofrontal cortex following training. These findings provide evidence that short-term HIIT effectively enhances motor cortical plasticity and modulates the prefrontal cortical activation. It emphasizes the importance of the effect of short-term physical training on improvements in neuroplasticity.

To date, various HIIT protocols has been conducted to improve the motor or cognitive functions. Nicolini et al. (2019) carried out 6 weeks HIIT over sedentary young males, to evaluate their corticospinal excitability and working memory. They found ICF was significantly reduced while no change of working memory. Similarily, in our findings, short-term HIIT can also reduce ICF which indicates that short-term exercise is effective and adequate to improve fitness for healthy young adults. What is different is that our study found short-term HIIT can also modulate the executive-related cortical activations though no changes in behavioural performance. Previous study demonstrated that acute HIIT can improve executive performance in association with dorsolateral prefrontal activation (Kujach et al., 2018). These findings combined may suggest that HIIT specifically enhances the specific executive functions. it needs further investigate simultaneously in the future.

Previous studies have demonstrated that acute aerobic exercise modulates motor cortical excitability, suggesting that acute exercise might promote short-term plasticity within the motor region (Singh et al., 2014; Hendrikse et al., 2017; Andrews et al., 2020). In the present study, we found that ICF declined after 2 weeks of HIIT in sedentary females. This finding is similar to that of a previous study in which appeared in sedentary males after 6 weeks of HIIT (Nicolini et al., 2019). These findings suggest that short-term and chronic exercise possibly affect the modulation of ICF comparably. ICF is thought to reflect the activation of glutamatergic interneurons and NMDA receptors (Liepert et al., 1997; Paulus et al., 2008). Suppression of ICF after short-term training might help maintain excitability and prime the release of GABAergic inhibition. As with ICF, previous research suggests that the inhibitory after-effects of cTBS are modulated by NMDA receptors (Huang et al., 2007). Consequently, the results of the present study add to the evidence that short-term HIIT can modulate cortical excitability in a facilitative manner (Nicolini et al., 2019).

High intensity interval training modulates the executive-related brain activations. In the previous studies, 4 weeks of light intensity exercise in sedentary individuals improved performance of the Stroop task (Gomes-Osman et al., 2017) and acute high intenrsity interval training can improve stroop performance with related dorsolateral prefrontal activation (Kujach et al., 2018). Similarily, the present study utilized the Stroop task to reflect the performance of executive function of sedentary females and investigated potential mechanisms using fNIRS. Although HIIT did not have a measurable effect on executive performance, increased activation of the Stroop effect on the left DLPFC and on the left OFC was observed. Greater activation was observed in the incongruent condition following HIIT, consistent with previous studies (Kujach et al., 2018; Ji et al., 2019). The DLPFC is a crucial region of the brain that monitors and processes Stroop cognitive conflict, essential for executive function (Yanagisawa et al., 2010). The OFC and its functional connectivity with the DLPFC are also important for inhibitory control (Kronhaus et al., 2006;

Darnai et al., 2019). Recent study demonstrated that optimal cognitive control performance are associated with the functional interactions of specific cortical structures belonging to both the cognitive control network and the default mode network, not to the cognitive control network alone (Herbet and Duffau, 2020). Thus, our findings may reflect improvements in executive control processes at the macro neural level and need explore the whole brain activation in the future study.

There are a number of limitations to the present study. Firstly, we did not monitor the menstrual cycle, which is specific to females and has a significant impact on the activity of the central nervous system (Farage et al., 2008; Andreano and Cahill, 2010). Additionally, significant changes in SICI were not observed in the present study which may be due to the selected population or specific exercise protocol. Further investigation is required to explain this. Furthermore, cortical plasticity was measured on the musculus abductor pollicis brevis but training mostly focused on the muscles of the lower limb, which may indicate an indirect relationship.

In conclusion, the current study demonstrates that 2 weeks of high-intensity interval training in sedentary females decreased Intracortical facilitation and induced greater activation in the left DLPFC and OFC during executive tasks. The results provide evidence that short-term high-intensity interval training can modulate cortex plasticity and executive-related cortical activations.

DATA AVAILABILITY STATEMENT

The original contributions presented in the study are included in the article/**Supplementary Material**, further inquiries can be directed to the corresponding author/s.

ETHICS STATEMENT

The studies involving human participants were reviewed and approved by the Guangzhou Sport Institute. The patients/participants provided their written informed consent to participate in this study.

AUTHOR CONTRIBUTIONS

YS, JH, and MH designed, organized the study and provided the financial support for the study. ZG carried out literature search and collected the data of the experiment. YZ took part in the data collection and data analysis. KX, LX, and LL provided the assistance for data acquisition and data analysis. XL provided significant suggestions and modifications of the data analysis and manuscript revision. NZ analyzed the data and wrote the main manuscript. All authors have read and approved the content of the manuscript.

FUNDING

This work was supported by National Natural Science Foundation of China (31971105, 81902294, and 81702230), the National Key R&D Program of China (2018YFC2001600 and 2018YFC2001603) and the Humanities and Social Science Foundation of Ministry of Education of China (18YJC880035).

ACKNOWLEDGMENTS

The authors thank Prof. Ti-Fei Yuan for advice on experimental design.

SUPPLEMENTARY MATERIAL

The Supplementary Material for this article can be found online at: https://www.frontiersin.org/articles/10.3389/fnhum.2021.620958/full#supplementary-material

REFERENCES

Andreano, J. M., and Cahill, L. (2010). Menstrual cycle modulation of medial temporal activity evoked by negative emotion. *NeuroImage* 53, 1286–1293. doi: 10.1016/j.neuroimage.2010.07.011

Andrews, S. C., Curtin, D., Hawi, Z., Wongtrakun, J., Stout, J. C., and Coxon, J. P. (2020). Intensity matters: high-intensity interval exercise enhances motor cortex plasticity more than moderate exercise. *Cerebral Cortex* 30, 101–112. doi: 10.1093/cercor/bhz075

Babraj, J. A., Vollaard, N. B. J., Keast, C., Guppy, F. M., Cottrell, G., and Timmons, J. A. (2009). Extremely short duration high intensity interval training substantially improves insulin action in young healthy males. *BMC Endocrine Disord.* 9:3. doi: 10.1186/1472-6823-9-3

Bherer, L. (2015). Cognitive plasticity in older adults: effects of cognitive training and physical exercise. *Ann. N. Y. Acad. Sci.* 1337, 1–6. doi: 10.1111/nyas.12682

Bramham, C. R., and Messaoudi, E. (2005). BDNF function in adult synaptic plasticity: the synaptic consolidation hypothesis. *Prog. Neurobiol.* 76, 99–125. doi: 10.1016/j.pneurobio.2005.06.003

Citri, A., and Malenka, R. C. (2008). Synaptic plasticity: multiple forms, functions, and mechanisms. *Neuropsychopharmacology* 33, 18–41. doi: 10.1038/sj.npp.1301559

Colcombe, S. J., Kramer, A. F., Erickson, K. I., Scalf, P., McAuley, E., Cohen, N. J., et al. (2004). Cardiovascular fitness, cortical plasticity, and aging. *Proc. Natl. Acad. Sci. U.S.A.* 101, 3316–3321. doi: 10.1073/pnas.0400266101

Cotman, C. W., and Berchtold, N. C. (2002). Exercise: a behavioral intervention to enhance brain health and plasticity. *Trends Neurosci.* 25, 295–301. doi: 10.1016/S0166-2236(02)02143-4

Darnai, G., Perlaki, G., Zsidó, A. N., Inhóf, O., Orsi, G., Horváth, R., et al. (2019). Internet addiction and functional brain networks: task-related fMRI study. *Sci. Rep.* 9:15777. doi: 10.1038/s41598-019-52296-1

Derrfuss, J., Brass, M., and Yves Von Cramon, D. (2004). Cognitive control in the posterior frontolateral cortex: evidence from common activations in task coordination, interference control, and working memory. *NeuroImage* 23, 604–612. doi: 10.1016/j.neuroimage.2004.06.007

Ellen, L., Stavrinos, and James, C. (2017). High-intensity interval exercise promotes motor cortex disinhibition and early motor skill consolidation. *J. Cogn. Neurosci.* 29, 593–604. doi: 10.1162/jocn

El-Sayes, J., Turco, C. V., Skelly, L. E., Nicolini, C., Fahnestock, M., Gibala, M. J., et al. (2019). The effects of biological sex and ovarian hormones on exercise-induced neuroplasticity. *Neuroscience* 410, 29–40. doi: 10.1016/j.neuroscience.2019.04.054

Farage, M. A., Osborn, T. W., and MacLean, A. B. (2008). Cognitive, sensory, and emotional changes associated with the menstrual cycle: a review. *Arch. Gynecol. Obstetr.* 278, 299–307. doi: 10.1007/s00404-008-0708-2

Fisher, B. E., Wu, A. D., Salem, G. J., Song, J. E., Lin, J., Yip, J., et al. (2008). The effect of exercise training in improving motor performance and corticomotor excitability in persons with early parkinson's disease. *Arch. Phys. Med. Rehabil.* 89, 1221–1229. doi: 10.1016/j.apmr.2008.01.013

Gomes-Osman, J., Cabral, D., Hinchman, C., Jannati, A., Morris, T., and Pascual-Leone, A. (2017). The effects of exercise on cognitive function and brain plasticity-a feasibility trial. *Restor. Neurol. Neurosci.* 35, 547–556. doi: 10.1016/j.physbeh.2017.03.040

Hendrikse, J., Kandola, A., Coxon, J., Rogasch, N., and Yücel, M. (2017). Combining aerobic exercise and repetitive transcranial magnetic stimulation to improve brain function in health and disease. *Neurosci. Biobehav. Rev.* 83, 11–20. doi: 10.1016/j.neubiorev.2017.09.023

Herbet, G., and Duffau, H. (2020). Revisiting the functional anatomy of the human brain: toward a meta-networking theory of cerebral functions. *Physiol. Rev.* 100, 1181–1228. doi: 10.1152/physrev.00033.2019

Huang, Y. Z., Chen, R. S., Rothwell, J. C., and Wen, H. Y. (2007). The after-effect of human theta burst stimulation is NMDA receptor dependent. *Clin. Neurophysiol.* 118, 1028–1032. doi: 10.1016/j.clinph.2007.01.021

Jang, S., Choi, J., Oh, J., Yeom, J., Hong, N., Lee, N., et al. (2021). Use of virtual reality working memory task and functional near-infrared spectroscopy to assess brain hemodynamic responses to methylphenidate in ADHD children. *Front. Psychiatry* 11:564618. doi: 10.3389/fpsyt.2020.564618

Ji, Z., Feng, T., Mei, L., Li, A., and Zhang, C. (2019). Influence of acute combined physical and cognitive exercise on cognitive function: an NIRS study. *PeerJ* 2019, 1–16. doi: 10.7717/peerj.7418

Kronhaus, D. M., Lawrence, N. S., Williams, A. M., Frangou, S., Brammer, M. J., Williams, S. C. R., et al. (2006). Stroop performance in bipolar disorder: further evidence for abnormalities in the ventral prefrontal cortex. *Bipol. Disord.* 8, 28–39. doi: 10.1111/j.1399-5618.2006.00282.x

Kujach, S., Byun, K., Hyodo, K., Suwabe, K., Fukuie, T., Laskowski, R., et al. (2018). A transferable high-intensity intermittent exercise improves executive performance in association with dorsolateral prefrontal activation in young adults. *NeuroImage* 169, 117–125. doi: 10.1016/j.neuroimage.2017.12.003

Kujirai, T., Caramia, M. D., Rothwell, J. C., Day, B. L., Thompson, P. D., Ferbert, A., et al. (1993). Corticocortical inhibition in human motor cortex. *J. Physiol.* 471, 501–519. doi: 10.1113/jphysiol.1993.sp019912

Liepert, J., Schwenkreis, P., Tegenthoff, M., and Malin, J. P. (1997). The glutamate antagonist Riluzole suppresses intracortical facilitation. *J. Neural Trans.* 104, 1207–1214. doi: 10.1007/BF01294721

Mellow, M. L., Goldsworthy, M. R., Coussens, S., and Smith, A. E. (2020). Acute aerobic exercise and neuroplasticity of the motor cortex: a systematic review. *J. Sci. Med. Sport* 23, 408–414. doi: 10.1016/j.jsams.2019.10.015

Nicolini, C., Toepp, S., Harasym, D., Michalski, B., Fahnestock, M., Gibala, M. J., et al. (2019). No changes in corticospinal excitability, biochemical markers, and working memory after six weeks of high-intensity interval training in sedentary males. *Physiol. Rep.* 7, 1–15. doi: 10.14814/phy2.14140

Opie, G. M., and Semmler, J. G. (2019). Acute exercise at different intensities influences corticomotor excitability and performance of a ballistic thumb training task. *Neuroscience* 412, 29–39. doi: 10.1016/j.neuroscience.2019.05.049

Paulus, W., Classen, J., Cohen, L. G., Large, C. H., Di Lazzaro, V., Nitsche, M., et al. (2008). State of the art: pharmacologic effects on cortical excitability measures tested by transcranial magnetic stimulation. *Brain Stimul.* 1, 151–163. doi: 10.1016/j.brs.2008.06.002

Plenger, P., Krishnan, K., Cloud, M., Bosworth, C., Qualls, D., and Carlos, M. D. L. P. (2016). Fnirs-based investigation of the stroop task after tbi. *Brain Imaging Behav.* 10, 357–366. doi: 10.1007/s11682-015-9401-9

Rossi, S., Hallett, M., Rossini, P. M., Pascual-Leone, A., Avanzini, G., Bestmann, S., et al. (2009). Safety, ethical considerations, and application guidelines for the use of transcranial magnetic stimulation in clinical practice and research. *Clin. Neurophysiol.* 120, 2008–2039. doi: 10.1016/j.clinph.2009.08.016

Rossi, S., and Rossini, P. M. (2004). TMS in cognitive plasticity and the potential for rehabilitation. *Trends Cogn. Sci.* 8, 273–279. doi: 10.1016/j.tics.2004.04.012

Singh, A. M., Duncan, R. E., Neva, J. L., and Staines, W. R. (2014). Aerobic exercise modulates intracortical inhibition and facilitation in a nonexercised upper limb muscle. *BMC Sports Sci. Med. Rehabil.* 6:23. doi: 10.1186/2052-1847-6-23

Smiley-Oyen, A. L., Lowry, K. A., Francois, S. J., Kohut, M. L., and Ekkekakis, P. (2008). Exercise, fitness, and neurocognitive function in older adults. *Ann. Behav. Med.* 36, 280–291. doi: 10.1007/s12160-008-9064-5.Exercise

Smith, A. E., Goldsworthy, M. R., Garside, T., Wood, F. M., and Ridding, M. C. (2014). The influence of a single bout of aerobic exercise on short-interval intracortical excitability. *Exp. Brain Res.* 232, 1875–1882. doi: 10.1007/s00221-014-3879-z

Stroth, S., Hille, K., Spitzer, M., and Reinhardt, R. (2009). Aerobic endurance exercise benefits memory and affect in young adults. *Neuropsychol. Rehabil.* 19, 223–243. doi: 10.1080/09602010802091183

Szcs, D., Killikelly, C., and Cutini, S. (2012). Event-related near-infrared spectroscopy detects conflict in the motor cortex in a Stroop task. *Brain Res.* 1477, 27–36. doi: 10.1016/j.brainres.2012.08.023

Tanaka, H., Monahan, K. D., and Seals, D. R. (2001). Age-predicted maximal heart rate revisited. *J. Am. Coll. Cardiol.* 37, 153–156. doi: 10.1016/S0735-1097(00)01054-8

Yanagisawa, H., Dan, I., Tsuzuki, D., Kato, M., Okamoto, M., Kyutoku, Y., et al. (2010). Acute moderate exercise elicits increased dorsolateral prefrontal activation and improves cognitive performance with Stroop test. *NeuroImage* 50, 1702–1710. doi: 10.1016/j.neuroimage.2009.12.023

Zhang, Z., Olszewska-Guizzo, A., Husain, S. F., Bose, J., Choi, J., Tan, W., et al. (2020). Brief relaxation practice induces significantly more prefrontal cortex activation during arithmetic tasks comparing to viewing greenery images as revealed by functional near-infrared spectroscopy (fNIRS). *Int. J. Environ. Res. Public Health* 17:8366. doi: 10.3390/ijerph17228366

Conflict of Interest: The authors declare that the research was conducted in the absence of any commercial or financial relationships that could be construed as a potential conflict of interest.

Copyright © 2021 Hu, Zeng, Gu, Zheng, Xu, Xue, Leng, Lu, Shen and Huang. This is an open-access article distributed under the terms of the Creative Commons Attribution License (CC BY). The use, distribution or reproduction in other forums is permitted, provided the original author(s) and the copyright owner(s) are credited and that the original publication in this journal is cited, in accordance with accepted academic practice. No use, distribution or reproduction is permitted which does not comply with these terms.

frontiers in Neural Circuits

ORIGINAL RESEARCH
published: 28 April 2021
doi: 10.3389/fncir.2021. 675365

Subsequent Acupuncture Reverses the Aftereffects of Intermittent Theta-Burst Stimulation

Xiao-Kuo He[1,2†], Hui-Hua Liu[3†], Shan-Jia Chen[1†], Qian-Qian Sun[2], Guo Yu[1], Lei Lei[1], Zhen-Yuan Niu[1], Li-Dian Chen[2] and Tsung-Hsun Hsieh[4,5,6*]*

[1] Fifth Hospital of XiaMen, Xiamen, China, [2] Fujian University of Traditional Chinese Medicine, Fuzhou, China, [3] Sun Yat-sen Memorial Hospital, Sun Yat-sen University, Guangzhou, China, [4] School of Physical Therapy, Graduate Institute of Rehabilitation Science, Chang Gung University, Taoyuan, Taiwan, [5] Neuroscience Research Center, Chang Gung Memorial Hospital, Taoyuan, Taiwan, [6] Healthy Aging Research Center, Chang Gung University, Taoyuan, Taiwan

Objective: This study explored whether acupuncture affects the maintenance of long-term potentiation (LTP)-like plasticity induced by transcranial magnetic stimulation (TMS) and the acquisition of motor skills following repetitive sequential visual isometric pinch task (SVIPT) training.

Methods: Thirty-six participants were recruited. The changes in the aftereffects induced by intermittent theta-burst stimulation (iTBS) and followed acupuncture were tested by the amplitude motor evoked potential (MEP) at pre-and-post-iTBS for 30 min and at acupuncture-in and -off for 30 min. Secondly, the effects of acupuncture on SVIPT movement in inducing error rate and learning skill index were tested.

Results: Following one session of iTBS, the MEP amplitude was increased and maintained at a high level for 30 min. The facilitation of MEP was gradually decreased to the baseline level during acupuncture-in and did not return to a high level after needle extraction. The SVIPT-acupuncture group had a lower learning skill index than those in the SVIPT group, indicating that acupuncture intervention after SVIPT training may restrain the acquisition ability of one's learning skills.

Conclusion: Acupuncture could reverse the LTP-like plasticity of the contralateral motor cortex induced by iTBS. Subsequent acupuncture may negatively affect the efficacy of the acquisition of learned skills in repetitive exercise training.

Keywords: acupuncture, cortical excitably, long-term potentiation, acquisition of learned skills, sequential visual isometric index finger abduction task

OPEN ACCESS

Edited by:
Ti-Fei Yuan,
Shanghai Jiao Tong University, China

Reviewed by:
Chong Leong Lao,
Rehabilitation Medicine Clinic, Kiang Wu Hospital, China
Ying Shen,
The First Affiliated Hospital of Nanjing Medical University, China
Chuyan Yang,
The First Affiliated Hospital of Nanchang University, China

***Correspondence:**
Li-Dian Chen
cld@fjtcm.edu.cn
Tsung-Hsun Hsieh
hsiehth@mail.cgu.edu.tw

† These authors have contributed equally to this work

Received: *03 March 2021*
Accepted: *29 March 2021*
Published: *28 April 2021*

Citation:
He X-K, Liu H-H, Chen S-J, Sun Q-Q, Yu G, Lei L, Niu Z-Y, Chen L-D and Hsieh T-H (2021) Subsequent Acupuncture Reverses the Aftereffects of Intermittent Theta-Burst Stimulation. Front. Neural Circuits 15:675365. doi: 10.3389/fncir.2021. 675365

INTRODUCTION

Motor learning is the process of acquiring motor skills in repetitive training, in which the execution of actions is improved by goal-oriented training (Roth et al., 2020). When given a series of varying motor learning items, subsequent movements may interfere with the imprinted memory stimulated by previous motor learning (Hulme et al., 2013). In order to learn the different motor skills in sequential order, the acquired memory for the previous motor skill would be inhibited by the later movement (Hulme et al., 2013). Several preclinical studies have found that skill learning

in the previous movement can be influenced by subsequent behavioral activity. For example, in a rat model, when stimulated by differing frequencies of electric stimulation, the hippocampal trisynaptic loop demonstrated the efficiency of frequency-dependent synaptic transmission, known as long-term potentiation (LTP) and long-term depression (LTD)-like plasticity (Huang and Kandel, 2005). Several studies have supported the hypothesis that LTP is critical in memory formation and consolidation (Kramar and Lynch, 2003). The presence of LTP could be reversed by subsequent electrical stimulation or depotentiation. This was demonstrated by Dong et al., 2020, who applied low-frequency electrical stimulation and found a form-and time-dependent effect on the maintenance of LTP of the hippocampus (Dong et al., 2020). Similarly, LTP of hippocampal synapses in adult rats was reversed as rats entered a novel environment (Xu et al., 1998).

Acupuncture is a traditional Chinese therapeutic method and is widely used in clinical practice to treat diseases such as hemiplegia, stroke, and Alzheimer's disease (Wang et al., 2018; Zheng et al., 2018). Previous research has suggested that electroacupuncture could restore hippocampal LTP in rats (He et al., 2012). Clinical data also indicated that acupuncture could modulate corticomotoneuronal excitability in healthy adults and post-stroke patients (Yi et al., 2017; He et al., 2019).

In the first part of the present study, to investigate the effects of acupoint acupuncture on LTP-like plasticity changes, we applied the intermittent theta-burst stimulation (iTBS) over the motor cortex of the upper extremities to induce LTP-like plasticity and then investigated the neuromodulation effect induced by acupuncture. In the second portion, we explored whether acupuncture could affect the acquisition of motor skills following repetitive exercise training.

MATERIALS AND METHODS

Patients

A total of 37 healthy participants were recruited from Taihe Hospital in Shiyan City, and one withdrew due to illness. All healthy right-handed subjects had no history of head trauma, neurological disease, or other medical problems. Exclusion criteria included left-handedness, contraindications to TMS (e.g., metal residues, menstruating or pregnant women, etc.), taking any medication on a regular basis, and a positive history of psychiatric or neurologic diseases. Before the experiment, all participants were required to sign a written informed consent. The protocols were approved by the Ethics Committee of Taihe Hospital (Affiliated Hospital of the Hubei University of Medicine in China; approval number: 2014001-2).

Experimental Design

The present study was divided into two parts (**Figure 1**). In the first experiment, the participants were randomly divided into iTBS (control group, $n = 18$) and iTBS-acupuncture (acupuncture group, $n = 18$) groups. The effects of TMS with the iTBS scheme on motor cortical excitability were verified (**Figure 1A**). Next, to observe the neuromodulation of aftereffects induced by the iTBS and the subsequent intervention of acupuncture, acupuncture was performed 10 min after iTBS, and the needle was *in-situ* for 30 min. The measurements of motor cortical excitability were assessed before iTBS and every 5 min for up to 70 min after the end of iTBS (**Figure 1A**).

In the second part (**Figure 1B**), to observe the effect of acupuncture on the acquisition of motor skills following repetitive exercise training, 36 participants were randomly divided into the sequential visual isometric pinch task (SVIPT) and SVIPT-acupuncture equal groups. The SVIPT training was conducted for 5 days on the left upper limb. The motor skill proficiency was assessed after each SVIPT training for five successive days. In the SVIPT-acupuncture group, with the same motor skill proficiency evaluation for five consecutive days, the SVIPT-acupuncture group received extra acupuncture with Quchi and Waiguan acupoints for 30 min on the same left upper limb after SVIPT repetitive training for four consecutive days. However, on the fifth day, the subjects only received the SVIPT training but not given the acupuncture. Under this experimental design, the immediate effect of acupuncture on the ability of motor skill acquisition can be observed for four successive days. In addition, with the avoidance of the immediate or short effect of acupuncture, the long-term effect of SVIPT combined with acupuncture on the acquisition of motor skills was assessed on the fifth day after 4 days of SVIPT-acupuncture intervention. All the above trial protocols have been registered with the China Clinical Trial Registry (registration no. ChiCTR-IPR-17010490).

Assessment of Motor Cortical LTP-Like Plasticity

Motor cortical plasticity was evaluated by changes in MEP amplitude following iTBS. All TMS and TMS-iTBS interventions were performed using a transcranial magnetic stimulator (YRD-1, maximum magnetic field intensity = 2.2 T; Wuhan Yiruide Medical Equipment New Technology Co., Ltd., Wuhan, China) and a figure of eight coils (YRD, diameter = 9 cm; Wuhan Yiruide Medical Equipment New Technology Co., Ltd.). To determine the level of MEP amplitude, electromyographic (EMG) activity was obtained with disposable adhesive electrodes on the belly of the first dorsal interosseous (FDI) muscle and the metacarpophalangeal joint (Yahagi and Kasai, 1998). The EMG activity was amplified with (gain = 1000) and filtered using 50-Hz notches prior to digitization at 1 kHz (MP30, BIOPAC System, CA, United States).

To properly induce the MEP elicited by a single pulse of TMS, the center of TMS coils was focused on the right motor cortex corresponding to the left FDI muscle. The optimal scalp location, known as the hot spot, was determined by the scalp location at which MEPs could be elicited in the FDI muscle at the lowest stimulus strength. Once the hot spot was found, the coil was securely fixed in place with a mechanical device.

The resting motor threshold (rMT) was defined as the minimum stimulus intensity at which five of the 10 consecutive single stimuli at the hot spot elicited an MEP amplitude of at least 50 μV in the relaxed muscle (Rossini et al., 2015). The single pulse of the TMS intensity to elicit MEP during the

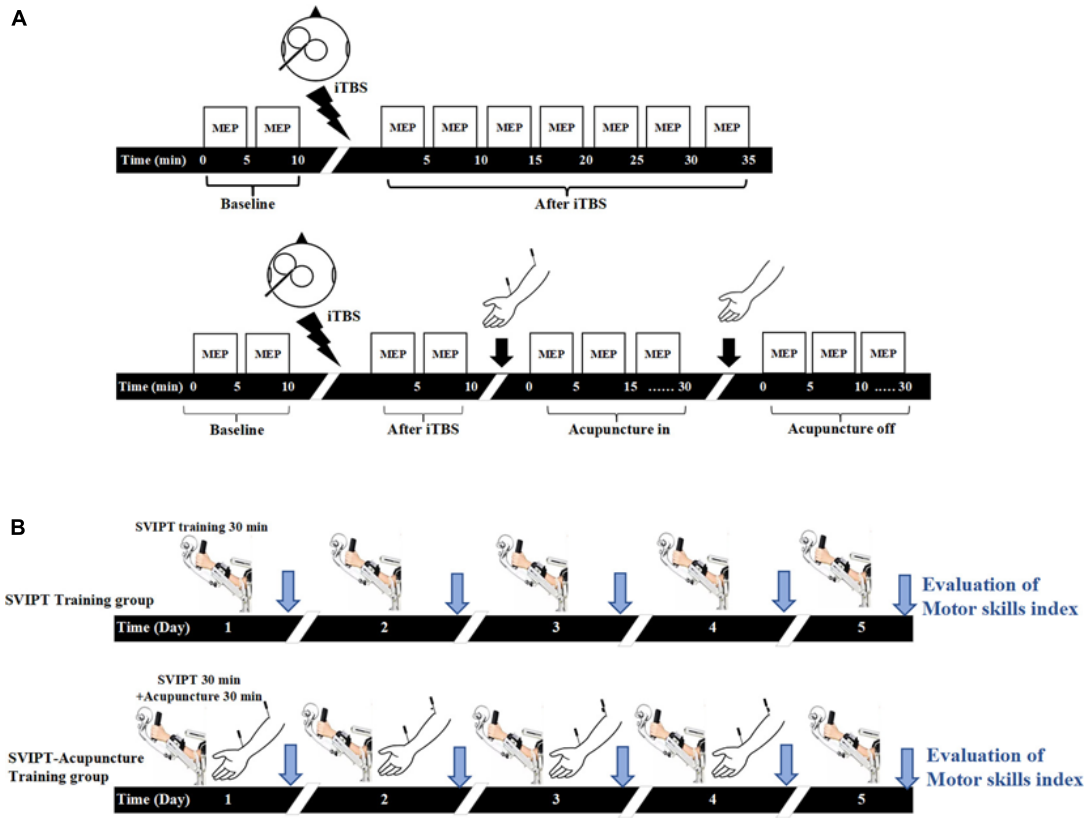

FIGURE 1 | Experimental design. **(A)** In the intermittent theta-burst stimulation (iTBS) group, the baseline of motor evoked potential (MEP) amplitudes induced by transcranial magnetic stimulation (TMS) with the iTBS scheme over the primary motor cortex (M1) under resting conditions was measured for 10 min, then the LTP-like plasticity induced by iTBS was measured by TMS elicited MEP for 35 min. In the iTBS-acupuncture group, the changes of MEP were tested at pre- and post-iTBS for 10 min, then measured under acupuncture-in and off for 30 min after iTBS intervention. **(B)** Both groups carried on sequential visual isometric pinch task (SVIPT) training for 30 min, but the SVIPT-acupuncture group was given additional acupuncture after SVIPT training. After 10 min of SVIPT intervention, two needles were inserted into the Quchi and Waiguan acupoints and kept in the upper limb of the training side for 30 min and then extracted. The learning skill index was evaluated by video recorder continuously over 5 consecutive days.

entire stimulation paradigm was set at 120% rMT of the FDI. In the single iTBS group, the MEPs were measured "before" (10 min before iTBS, referred to as $iTBS_{pre}$) and "after" (30 min after iTBS, referred to as $iTBS_{post-5\ min}$, $iTBS_{post-15\ min}$, and $iTBS_{post-30\ min}$). In the iTBS-acupuncture group, the MEP was measured "before" (10 min before iTBS, referred to $iTBS'_{pre}$) and "after" (10 min after iTBS, referred to $iTBS'_{post-5}$ and $iTBS'_{post-10}$), as well as "in" (30 min with the needle *in situ*, referred to as $acupuncture_{in-5\ min}$, $acupuncture_{in-15\ min}$, and $acupuncture_{in-30\ min}$) and "off" (30 min after needle removal, referred to as $acupuncture_{post-5\ min}$, $acupuncture_{post-15\ min}$, and $acupuncture_{post-30\ min}$) (**Figure 1A**). The mean MEP amplitude was calculated as the average of the MEPs at each time point and then normalized to the 15-min pre-iTBS baseline.

Intermittent Theta-Burst Stimulation and Acupuncture Intervention

To induce LTP-like plasticity, the intervention mode of iTBS was utilized in both groups over the right motor cortex corresponding to the left hand. The stimulus parameter of iTBS was a series of stimuli strings at 80% aMT of output intensity with a total of 600 TMS stimuli for 190 s. The iTBS protocol, containing 3-pulse bursts at 50 Hz repeated at 5 Hz, was performed with a 2-s train and repeated every 10 s for 20 repetitions (Franca et al., 2006; Hsieh et al., 2015). For acupuncture in-off, the iTBS-acupuncture group was under aseptic conditions and received extra acupuncture by experienced acupuncturists after 10 min of iTBS stimulation. The acupuncture needles were 0.3 × 40 mm (Huatuo; Suzhou Medical Supplies Factory, Suzhou City, China). The Quchi (LI-11) and Waiguan (TB-5) acupoints on the left hand are two of the most frequently explored points in Chinese acupuncture to treat poststroke motor dysfunction (Gao et al., 2011). To ensure that the patients felt De Qi (sensations of aching and tingling), proper techniques such as "lifting and thrusting" and no "rotating" were conducted at each point, and then the needles were kept *in situ* for 30 min without further stimulation.

Motor Skills Training and Evaluation

In the second part, the intelligent feedback training system (IFTS, SV3.8, Guangzhou Yikang Medical Equipment Industry Co., Ltd.,

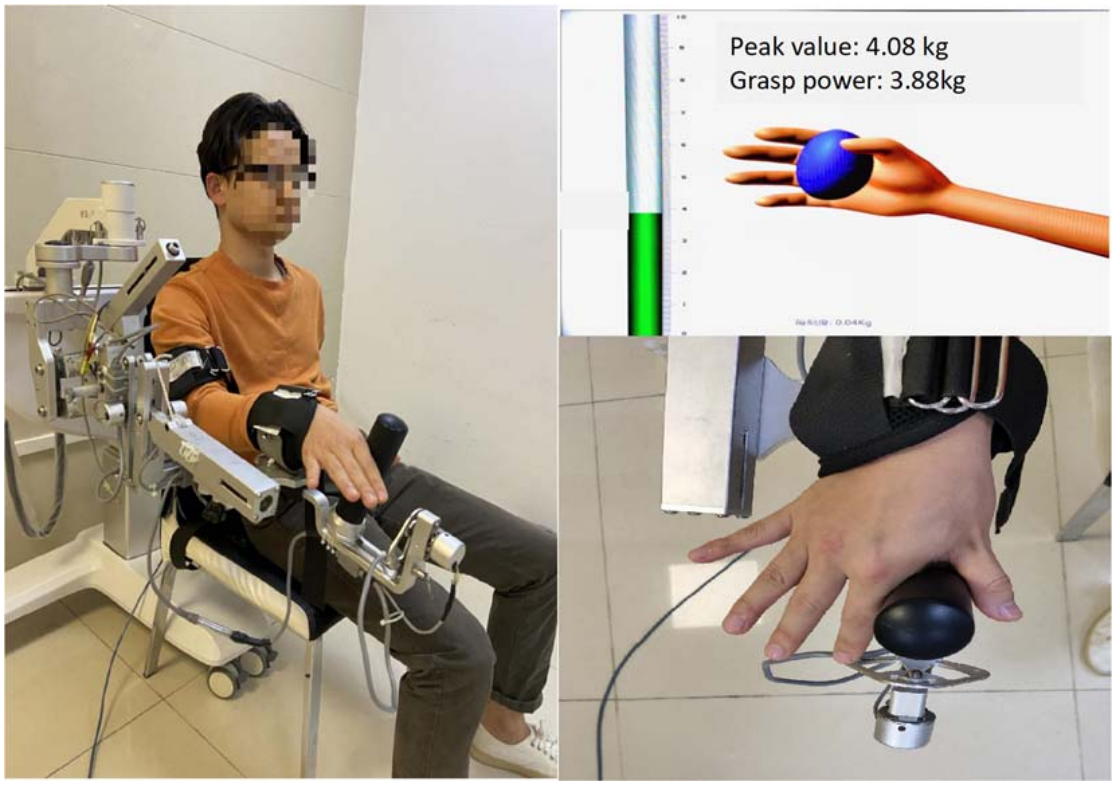

FIGURE 2 | The SVIPT program. Participants were seated with the left shoulder and elbow flexed and the forearm in a neutral position and fixed on the upper limb exoskeleton of the intelligent feedback training system (IFTS). The radial side of the index finger and thumb was tightly attached to the columnar sensor. Participants learned to control column pressure to reach the target number range.

Guangzhou, China) was used for motor skills training. For the starting position, participants were seated with the left shoulder and elbow flexed and the forearm in a neutral position and fixed on the upper limb exoskeleton of the IFTS. The wrist and finger joints were unrestricted, and the radial side of the index finger was tightly attached to the columnar sensor to receive pressure when the index finger was abducted. A 40-inch monitor was placed 1.5 m in front of the participants, where the height could be adjusted to the height of the participants' eyes (**Figure 2**).

The motor skill proficiency was calculated using the SVIPT speed and error rates. Before implementing the SVIPT program, the maximum abducting force of each participant's index finger was measured to ensure that the maximum pinching would not exceed the top of the column. The 0–50% range of the maximum abducting force of each participant's index finger was marked on the pressure column and was divided into ten equal parts. The participants were able to control the pressure in the range of the marked number by abducting the index finger. Seven metronomes with different speeds (30, 45, 60, 75, 90, 105, and 120 bpm) were used to remind the participants to complete the action/movement/motion within each beat following the starting instructions and that at every beat, action/motion should be accomplished. Control of the cursor rose from 0 point to the corresponding number, and once it reached the target, the participant had control over the cursor to return to the 0 point as soon as possible. Participants repeated the above procedure in the order of 0–6–0–3–0–1–0–7–0–2–0–9–0–5–0–8–0–4–0. Finally, the cursor returned to the 0 point, with a total of nine target points in the order of: 6/3/1/7/2/9/5/8/4. Seven metronomes beats appeared randomly, and each beat was repeated three times with a 1 min rest between each task. We used a camera to monitor the entire process. Finally, the SVIPT-acupuncture group was given additional acupuncture by experienced acupuncturists. The needles' Quchi and Waiguan acupoints were kept in the training side upper limb for 30 min and then extracted. Proper techniques such as "lifting and thrusting" and no "rotating" were conducted to make the patients experience De Qi. The acupuncture stimulus was repeated consecutively for 4 days, and no acupuncture was given after the fifth day of SVIPT training.

The hand performance of movement speed and errors were recorded by a video recorder continuously over five consecutive days after SVIPT training. SVIPT speed was the average time to complete three learning tasks in a row under each beat. Accuracy was defined as the number of times the cursor reached the serial number in three consecutive learnings at each metronome beat. The error rates were calculated as a 1 – accurate rate. The speed–accuracy tradeoff function (SAF) of each day quantified the acquisition ability of motor skills, calculated as the time of completion speed under each metronome beat as the abscissa and

the corresponding error rate as the ordinate. The motor skills index was the change in SAF value using the following formula:

$$(\text{Skill index, SI}) = \frac{1 - \text{Error rate}}{\text{Error rate } (\text{In}(\text{Duration})^b)}, \quad b = 5.424 \tag{1}$$

Statistical Analysis

STATA software was used to conduct statistical analyses (version 14.0; StataCorp, College Station, TX, United States). The MEP amplitude was calculated by the electromyogram software automatically. Three MEPs amplitudes every 5 min were measured to calculate the average amplitude and the average of the first three amplitudes (15 min) before the acupuncture were considered baseline. The average MEP amplitude in every 5 min divided by the baseline equaled the rate of change with the time as the abscissa and the change rate as the ordinate. The double factor variance analysis method was used to compare the changes in the skill index of the two groups over time. The *Q*-test was applied to intra-group and inter-group comparisons. The significance level was set at $P < 0\ 05$. Unless otherwise stated, values are reported as mean ± standard deviation.

RESULTS

Motor Evoked Potential Amplitudes Were Consistently Higher After iTBS$_{post-30\ min}$ Stimulation

During iTBS intervention, subjects had no muscle contractions but felt scalp constrictions. The constrictions disappeared when the iTBS stimulation was stopped. The data showed that MEP amplitudes began to increase after iTBS stimulation. Representative changes in MEPs recorded at the iTBS$_{pre}$ baseline, iTBS$_{post-5\ min}$, iTBS$_{post-15\ min}$, and iTBS$_{post-30\ min}$ are presented in **Figure 3A**. The MEP amplitudes after 10 min increased to 1.547 ± 0.454 mV, 1.5 times higher than the baseline value ($P < 0.05$). Next, MEP gradually decreased and flattened, but it was statistically higher than the baseline lasting for 30 min ($P = 0.046$). The MEP amplitude ratio after iTBS$_{post-30\ min}$ was 139 ± 16.89%, indicating that iTBS facilitated cortical excitability and induced LTP-like plasticity (**Figures 3A**, **4**).

Inhibition of MEP Amplitudes After iTBS-Acupuncture (In-Off) Stimulation

Representative changes in MEPs recorded at iTBS$_{pre}$, iTBS$_{post-5}$, iTBS$_{post-10}$, acupuncture$_{in-5\ min}$, acupuncture$_{in-10\ min}$, acupuncture$_{off-5\ min}$, and acupuncture$_{off-10\ min}$ are presented in **Figure 3B**. Under acupuncture-in stimulation, the amplitude of MEP in a V-shaped change, as it first decreased and then increased, was always below the iTBS level (**Figure 4**).

After needling in the Quchi and Waiguan acupoints, the averaged normalized MEP amplitude decreased approximately to the baseline level (1.03 ± 0.34) during acupuncture$_{in-5\ min}$ and continued to drop to its lowest point (0.84 ± 0.39) during acupuncture$_{in-10\ min}$, and then began to increase to the baseline level during acupuncture$_{in-15-25\ min}$. During acupuncture-off stimulation, MEPs showed progressive enhancement for up to 25 min when compared with the baseline MEPs (**Figure 4**). This pattern demonstrates that acupuncture may suppress MEP amplitudes and disturb the maintenance of LTP-like plasticity induced by iTBS.

Acupuncture Restrained the Learning Skill Index After Movement Practice

The SVIPT training effect was evaluated using the acquired learning skill index. A learning curve is defined as "the rate of skills or knowledge acquired over a period of time." The learning curve consisted of the time abscissa of action completion and the error rate ordinate at each metronome velocity. The acquisition ability of motor skills after every day of training was assessed by SAF. As shown in **Table 1** and **Figure 5**, both the SVIPT and SVIPT-acupuncture groups demonstrated that all participants had higher error rates while speed increased, especially during the first 2 days of training. As the training time increased, the

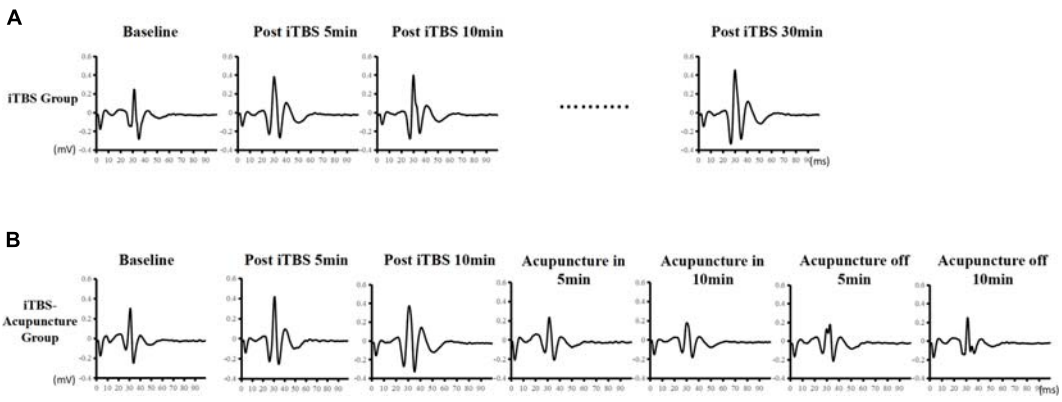

FIGURE 3 | Effect of iTBS and acupuncture on MEPs. Time-course changes of MEPs following iTBS in panel **(A)** and iTBS and subsequent acupuncture intervention in panel **(B)**. Representative MEP traces following iTBS present an apparent increase, whereas there are traces of a decrease in MEP amplitude after subsequent acupuncture intervention.

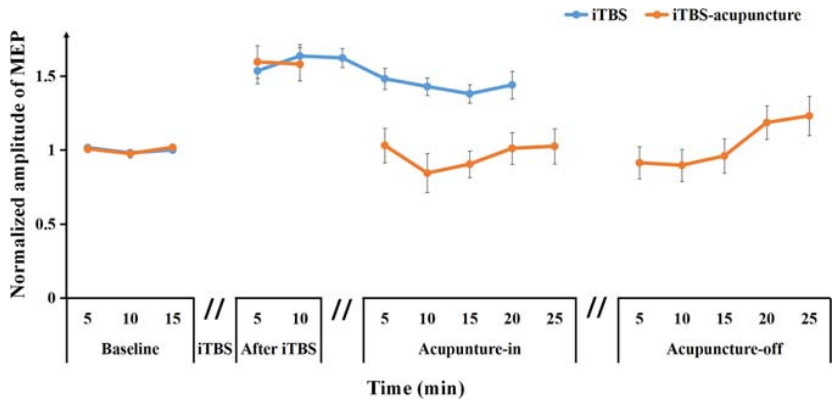

FIGURE 4 | Averaged changes in the MEP amplitude at pre and after iTBS, as well as iTBS with subsequent acupuncture in-off intervention are presented. Data are shown as the mean ± SEM.

TABLE 1 | Learning skills index in sequential visual isometric pinch task (SVIPT) and SVIPT-acupuncture groups.

			120 bpm	105 bpm	90 bpm	75 bpm	60 bpm	45 bpm	30 bpm
SVIPT group	D1	Error rate	73.33	70.00	66.67	66.11	65.56	57.78	50.00
		Time	5.63	6.21	6.79	8.05	9.31	13.59	17.87
	D2	Error rate	57.78	55.00	52.22	48.33	44.44	39.44	34.44
		Time	5.72	6.31	6.90	7.94	8.99	13.58	18.16
	D3	Error rate	48.56	42.11	36.67	37.11	37.56	32.22	28.89
		Time	5.41	6.25	7.10	8.20	9.31	13.88	18.45
	D4	Error rate	43.33	39.89	32.44	30.44	28.44	30.00	25.56
		Time	5.67	6.42	7.16	9.30	8.84	13.72	17.99
	D5	Error rate	41.33	31.89	26.44	24.94	24.44	25.00	21.56
		Time	5.57	6.32	7.06	8.30	9.54	13.27	16.99
SVIPT-acupuncture group	D1	Error rate	71.11	69.89	68.89	67.64	63.78	58.65	49.56
		Time	5.78	6.23	6.78	8.12	9.33	13.50	17.61
	D2	Error rate	65.56	60.30	56.67	53.40	51.11	46.70	34.67
		Time	5.82	6.01	6.44	8.05	9.89	12.80	17.67
	D3	Error rate	62.22	58.40	55.56	47.90	40.00	36.80	33.33
		Time	5.69	6.20	6.30	8.07	9.44	13.10	17.78
	D4	Error rate	56.67	55.80	55.56	42.80	36.67	32.20	29.56
		Time	5.58	6.15	6.00	7.68	9.44	13.00	16.81
	D5	Error rate	55.89	54.21	54.28	40.79	32.60	27.87	21.93
		Time	5.61	6.20	5.98	7.58	9.33	12.98	17.01

subjects in the SVIPT group showed a noticeable decrease in error rates with either fast or slow metronome velocity. As seen in the SAF curve, when compared with the SVIPT group, the error rate in the SVIPT-acupuncture group was still maintained at a higher level with an increase in number of training days, especially at the higher speed (**Figure 5**).

The learning skill index in the SVIPT group was higher than that of the SVIPT-acupuncture group. The result of two-factor ANOVA showed a statistically significant difference between the two groups ($F = 50.68$, $P < 0.01$). The learning skill indices had a cumulative effect on time and training. Alternatively, with the accumulation of time and quantity of training, the participants engaged in SVIPT motor practice without acupuncture demonstrated a better average learning skill index than participants with additional acupuncture (**Table 1**). No significant differences were found in the first 2 practice days ($q = 0.001$, $P = 0.68$; $q = 0.022$, $P = 0.743$). Over time, the SVIPT group demonstrated a progressively higher index than the SVIPT-acupuncture group on the third ($q = 0.035$, $P = 0.058$), fourth ($q = 0.083$, $P < 0.01$), and fifth days ($q = 0.088$, $P < 0.01$) (**Table 2**). These results suggest that acupuncture intervention may restrain the subjects' learning skill index after movement practice and could inhibit the cortical plasticity induced by the SVIPT practice.

DISCUSSION

Several notable results were demonstrated in the present study. First, iTBS facilitated cortical excitability and

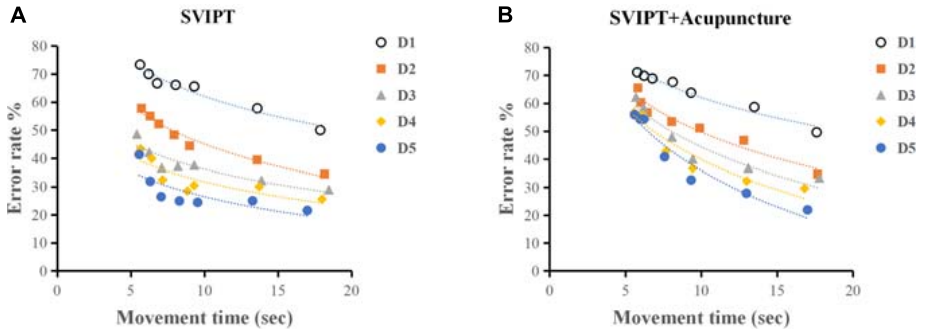

FIGURE 5 | (A) As practice continued, participants in SVIPT groups obtained an apparent decrease in error rates with either fast or slow metronome velocity. **(B)** Acupuncture restrained the learning skill index after movement practice. The SVIPT-acupuncture group obtained higher error rates when the test speed was increased.

induced LTP-like plasticity over the M1 cortex. Second, unilateral acupuncture in off stimulation reversed the maintenance of LTP-like plasticity induced by iTBS. Third, these results suggested that subsequent acupuncture intervention after movement practice may inhibit learning skill indices following repetitive exercise training, indicating that subsequent acupuncture in the contralateral upper limb had a negative impact on the behavioral outcomes of motor learning.

In the present study, we measured cortical plasticity as reflected by MEP changes. iTBS over the M1 region was proven to initiate a long-term increase in MEP amplitude that was higher than the baseline (139 ± 16.89%, $P = 0.046$) and LTP-like plasticity had a duration longer than 30 min. This is consistent with the literature and it is believed that LTP-like plasticity is produced over the stimulus cortical side. Preclinical and clinical studies have confirmed that the induction of LTP is related to the intensity and time-dependent on stimuli (Fino et al., 2010; Zhang et al., 2010), regulates the magnitude and direction of MEP induction (He et al., 2019), and is involved in two mechanisms of homeostatic plasticity or gating mechanisms (Karabanov et al., 2015; Yee et al., 2017). Recently, several studies have reported that homeostatic plasticity plays an important role in the control of synaptic plasticity. In accord with the Bienenstock–Cooper–Munro (BCM) rule contribute to regulating plasticity (Bienenstock et al., 1982), the plasticity induced by motor skill training, transcranial direct current stimulation (tDCS) or paired associative stimulation (PAS) changed the synaptic modification threshold or regulated excitability in the motor cortex (Rioult-Pedotti et al., 2000; Siebner et al., 2004). In the current study, the changes of LTP-like plasticity induced by iTBS or acupuncture could be expected from a homeostatic mechanism that controls the motor cortical excitability. Gating mechanisms could also be involved in the changes of LTP-like plasticity induced by iTBS or acupuncture. The gating mechanisms, including transiently suppressing the efficacy of intracortical inhibitory circuits, shifting intrinsic excitability of the targeted neurons or increasing net calcium influx into the targeted cortical neurons, may promote the induction of LTP-like plasticity in neural circuits targeted by iTBS, physical training or acupuncture (Ziemann and Siebner, 2008; Karabanov et al., 2015).

The present study concluded that acupuncture at the Quchi and Waiguan acupoints reversed the LTP induced by iTBS, indicating that high MEP gradually reduced to the baseline level after acupuncture-in and did not return to the iTBS level after needle extraction. This suggests a time-dependent reversal of LTP by unilateral acupuncture in-off stimulation, considered as "depotentiation" (Huang and Hsu, 2011). Concurrent with previous studies (Kramar and Lynch, 2003), subsequent low-frequency afferent stimulations (LFS), such as brief periods of hypoxia, application of receptor, and brief cooling shock reversal of the depotentiation (Kulla and Manahanvaughan, 2000; Huang and Hsu, 2011; Park et al., 2019), were introduced after TBS completely reversed LTP. As we adopted acupoint acupuncture as the subsequent spike, in the phase of acupuncture-in, the MEP amplitude demonstrated a V-shaped change, as it decreased after acupuncture$_{in-5\ min}$ administration, until it reached the lowest point (0.90 ± 0.25) after acupuncture$_{in-15\ min}$, and then slowly recovered to the equivalent baseline level (1.01 ± 0.36) after acupuncture$_{in-30\ min}$. In acupuncture-off, the MEP continued to reach the lowest point (0.91 ± 0.42) after acupuncture$_{off-5\ min}$, and slowly increased to approximately 1.18 times of the

TABLE 2 | Learning skill index for 5 days in the SVIPT and SVIPT-acupuncture groups.

	SVIPT group	SVIPT-acupuncture group	*q*	*P*
D1	0.082 ± 0.013	0.083 ± 0.014$^{\#}$	0.00104	0.68
D2	0.107 ± 0.015	0.090 ± 0.022$^{\#}$	0.02202	0.743
D3	0.189 ± 0.019	0.098 ± 0.022$^{\#}$	0.03545	0.058
D4	0.187 ± 0.016	0.104 ± 0.020**	0.08276	<0.01
D5	0.213 ± 0.019	0.126 ± 0.027**	0.08777	<0.01

$^{\#}$*Represents P > 0.05.*
***Represents P < 0.01.*

baseline (1.18 ± 0.40) after acupuncture$_{off-20\ min}$. These results indicated that the depotentiation effects of the motor cortex-corticospinal tract comprised a reversal of iTBS induced LTP, which occurred following acupuncture. This potentiation may provide a mechanism for preventing the saturation of synaptic potentiation and increase the efficiency and capacity of the information storage of the neuronal network (Kulla and Manahanvaughan, 2000; Chen et al., 2001; Huang and Hsu, 2011; Park et al., 2019).

The mechanisms responsible for the depotentiation effect of acupuncture following LTP induction are unclear, and metaplasticity does not explain the results. Our previous study demonstrated that the MEP amplitude after simple acupuncture-in gradually decreased and slowly recovered in the shape of a "V," immediately rose, and then continued to slowly rise after extraction of the needle. Both simple acupuncture processes did not exceed 20 min, which may be a short-term inhibition or potentiation, in accordance with the results of simple acupuncture examinations of the modulatory effect on cortical plasticity (Chen et al., 2006; He et al., 2019). Researchers have suggested that simple acupuncture needling or LFS (Huang et al., 2001) that affects cortical excitability may be related to the plasticity processes mediated by *N*-methyl-D-aspartic (NMDA) receptors. To a certain extent, we suggest that the functional state of $GABA_b$ receptors involved in acupuncture may be partially interpreted as decreased cortex excitability during the acupuncture-in state reversed by iTBS induction. However, the mechanisms of decreased cortex excitability during the acupuncture-off state persistently reversed iTBS induction, although this was unclear due to the increased MEP after needle extraction. Some researchers have also found that LTP stabilization requires protein synthesis in the consolidation of long-term memory (Abraham and Williams, 2008), and that the pharmacological inhibition of proteasome-dependent protein degradation would disrupt the expression of late (L-) LTP (Fonseca et al., 2006). Researchers have also emphasized that brain-derived neurotrophic factors (BDNFs) can sustain L-LTP through PKM when protein synthesis is inhibited fluence the subsequent induction ability of the latter stimulus (Abraham, 2008). Depotentiation effects have shown that synaptic modifications can be reversed by subsequent stimuli, which inhibit the maintenance of LTP instead of reversing LTP into LTD; however, these effects do not demonstrate a long-term change. This finding has been demonstrated previously, as LTP of hippocampal synapses in adult rats was reversed as the rats entered a novel environment (Zhou and Poo, 2004; Abraham, 2008). Previous studies have revealed that acupuncture mainly comes with short-term potentiation/depression and that it modulates an opposite effect on MEP change with slight depression after needling-in and significant facilitation after needling-off (Zhou and Poo, 2004; He et al., 2019). We found that iTBS-induced LTP-like plasticity can be inhibited by either needle in or needle off, which indicates that depotentiation, rather than metaplasticity, occurs in motor cortical circuits; however, little is known about its molecular mechanisms.

Recently, considerable interest has been generated by the possibility that the activity-dependent persistent reversal of previously established synaptic LTP (depotentiation) may be important in the time- and state-dependent erasure of memory. We used the experimental scheme of SVIPT (Abraham, 2008; Reis et al., 2009) and acupuncture to explore whether SVIPT-acupuncture can affect the acquisition ability of learning skills. The SAF curve showed that the SVIPT group without acupuncture demonstrated a more satisfactory performance than the SVIPT-acupuncture group with an acupoint needle, especially as practice time continued, in reducing error rates with either the fast or slow metronome. Simultaneously, the learning skill index in the SVIPT group was significantly higher than that of the SVIPT-acupuncture group ($F = 50.68$, $P < 0.01$). These results suggest that subsequent acupoint acupuncture after motor skill training inhibited the maintenance of LTP-like plasticity and restrained the subjects' learning ability, which was consistent with this electrophysiological results. The present and previous studies are concordant because they both demonstrated that abnormal maintenance of LTP/LTD would lead to difficulty in the reconstruction of the normal motor in learning ability in preclinical Parkinson's models (Picconi et al., 2003). Exercise training is closely related to cortical motor regions, and how depotentiation affects motor skill acquisition needs further research. This behavioral data showed that the learning skill indices in the SVIPT-acupuncture group were lower than those of the SVIPT group, but a small amount of skill improvement could still be achieved through daily training. The underlying reasons for this difference require further analysis.

In this study, we first observed the effects of acupuncture on the left upper limb area corresponding to contralateral motor cortical excitability. In the secondary objective, we further investigated the interaction between acupuncture and the acquisition of learned skills. In addition, many existing studies on the interaction of non-invasive brain stimulation technologies such as repetitive TMS and transcranial direct current stimulation have verified synaptic metaplasticity (Hamada et al., 2008; Pötter-Nerger et al., 2009), while this research was focused on depotentiation. We propose that subsequent acupuncture may negatively affect the efficacy of learned skills after iTBS or rehabilitation training.

CONCLUSION

The repetitive TMS Evidence-based guidelines recommend the use of HF-rTMS or iTBS over the M1 area on the affected side, which can facilitate the M1 excitability and LTP effect and improve recovery of upper limb function in stroke patients (Lefaucheur et al., 2020). Acupuncture can specifically modulate the excitability of the contralateral primary motor cortex (M1) (Ferbert et al., 1992). However, these two different therapies were dependent on the therapist's schedule in clinical practice. It has not been reported whether the order of application of iTBS and acupuncture affects the therapeutic effect and the mechanism is unclear. This research attempts to explore this relationship and contribute to this regard. The results of the present study indicate that unilateral acupuncture in-off can reverse LTP-like plasticity of the contralateral motor cortex induced by iTBS, namely

acupuncture electrically induced synaptic depotentiation. Subsequent continuous acupuncture on the upper limbs of the training side may inhibit the acquisition of learned skills during repetitive exercise training. Understanding the neurophysiological or cellular basis of motor cortical plasticity may help gain insight into the long-term synaptic plasticity involved in rehabilitation therapy and neuromodulatory technologies (such as iTBS and acupuncture), thereby revealing potential therapeutic targets for neurological diseases.

DATA AVAILABILITY STATEMENT

The raw data supporting the conclusion of this article will be made available by the authors, without undue reservation.

ETHICS STATEMENT

The trial protocols have been registered with the China Clinical Trial Registry (Registration No. ChiCTR-IPR-17010490). The protocols were approved by the Ethics Committee of Taihe Hospital (Affiliated Hospital of Hubei University of Medicine in China; Approval Number: 2014001-2). The patients/participants provided their written informed consent to participate in this study.

AUTHOR CONTRIBUTIONS

X-KH and H-HL designed the study. LL, GY, and Z-YN conducted the study, including patient recruitment and data collection. X-KH and L-DC contributed to data analysis. H-HL and S-JC prepared the manuscript draft with important intellectual input from X-KH and T-HH. All authors approved the final manuscript. All authors listed have made a substantial, direct and intellectual contribution to the work, and approved it for publication.

FUNDING

This research was funded by the Sun Yat-sen Memorial Hospital, and the Sun Yat-sen University (National Natural Science Foundation of China, Grant No. 81902286 to H-HL), the Ministry of Science and Technology of Taiwan (Grant No. MOST 109-2314-B-182-029-MY3 to T-HH), and The Chang Gung Memorial Hospital (Grant Nos. CMRPD1H0463 and CMRPD1K0671 to T-HH).

REFERENCES

Abraham, W. C. (2008). Metaplasticity: tuning synapses and networks for plasticity. *Nature Reviews Neuroscience* 9, 387. doi: 10.1038/nrn2356

Abraham, W. C., and Williams, J. M. (2008). LTP maintenance and its protein synthesis-dependence. *Neurobiology of Learning & Memory* 89, 260–268.

Bienenstock, E. L., Cooper, L. N., and Munro, P. W. (1982). Theory for the development of neuron selectivity: orientation specificity and binocular interaction in visual cortex. *J Neurosci* 2, 32–48.

Chen, A. C., Liu, F. J., Wang, L., and Arendt-Nielsen, L. (2006). Mode and site of acupuncture modulation in the human brain: 3D (124-ch) EEG power spectrum mapping and source imaging. [Controlled Clinical Trial; Journal Article; Research Support, Non-U.S. Gov't]. *Neuroimage* 29, 1080–1091. doi: 10.1016/j.neuroimage.2005.08.066

Chen, Y. L., Huang, C. C., and Hsu, K. S. (2001). Time-dependent reversal of long-term potentiation by low-frequency stimulation at the hippocampal mossy fiber-CA3 synapses. [Journal Article; Research Support, Non-U.S. Gov't]. *J Neurosci* 21, 3705–3714.

Dong, L., Li, G., Gao, Y., Lin, L., Zheng, Y., and Cao, X. B. (2020). Exploring the form− And time−dependent effect of low−frequency electromagnetic fields on maintenance of hippocampal long−term potentiation. [Journal Article]. *European Journal of Neuroscience* 00, 1–15. doi: 10.1111/ejn.14705

Ferbert, A., Vielhaber, S., Meincke, U., and Buchner, H. (1992). Transcranial magnetic stimulation in pontine infarction: correlation to degree of paresis. *J Neurol Neurosurg Psychiatry* 55, 294–299.

Fino, E., Paille, V., Cui, Y., Morera-Herreras, T., Deniau, J. M., and Venance, L. (2010). Distinct coincidence detectors govern the corticostriatal spike timing-dependent plasticity. [Journal Article]. *J Physiol* 588(Pt 16), 3045–3062. doi: 10.1113/jphysiol.2010.188466

Fonseca, R., Vabulas, R. M., Hartl, F. U., Bonhoeffer, T., and Nägerl, U. V. (2006). A Balance of Protein Synthesis and Proteasome-Dependent Degradation Determines the Maintenance of LTP. *Neuron* 52, 239–245.

Franca, M., Koch, G., Mochizuki, H., Huang, Y. Z., and Rothwell, J. C. (2006). Effects of theta burst stimulation protocols on phosphene threshold. [Comparative Study; Journal Article]. *Clin Neurophysiol* 117, 1808–1813. doi: 10.1016/j.clinph.2006.03.019

Gao, J., Wang, S., Wang, X., and Zhu, C. (2011). Electroacupuncture enhances cell proliferation and neuronal differentiation in young rat brains. [Journal Article; Research Support, Non-U.S. Gov't]. *Neurol Sci* 32, 369–374. doi: 10.1007/s10072-010-0402-6

Hamada, M., Terao, Y., Hanajima, R., Shirota, Y., Nakatani-Enomoto, S., Furubayashi, T., et al. (2008). Bidirectional long-term motor cortical plasticity and metaplasticity induced by quadripulse transcranial magnetic stimulation. [Journal Article; Research Support, Non-U.S. Gov't]. *J Physiol* 586, 3927–3947. doi: 10.1113/jphysiol.2008.152793

He, X., Yan, T., Chen, R., and Ran, D. (2012). Acute effects of electro-acupuncture (EA) on hippocampal long term potentiation (LTP) of perforant path-dentate gyrus granule cells synapse related to memory. [Journal Article; Research Support, Non-U.S. Gov't]. *Acupunct Electrother Res* 37, 89–101. doi: 10.3727/036012912x13831831256168

He, X. K., Sun, Q. Q., Liu, H. H., Guo, X. Y., Chen, C., and Chen, L. D. (2019). Timing of Acupuncture during LTP-Like Plasticity Induced by Paired-Associative Stimulation. [Journal Article; Randomized Controlled Trial]. *Behav Neurol* 2019, 9278270. doi: 10.1155/2019/9278270

Hsieh, T. H., Huang, Y. Z., Rotenberg, A., Pascual-Leone, A., Chiang, Y. H., Wang, J. Y., et al. (2015). Functional Dopaminergic Neurons in Substantia Nigra are Required for Transcranial Magnetic Stimulation-Induced Motor Plasticity. [Journal Article; Research Support, Non-U.S. Gov't]. *Cereb Cortex* 25, 1806–1814. doi: 10.1093/cercor/bht421

Huang, C. C., and Hsu, K. S. (2011). Progress in Understanding the Factors Regulating Reversibility of Long-term Potentiation. *Reviews in the Neurosciences* 12, 51–68.

Huang, C. C., Liang, Y. C., and Hsu, K. S. (2001). Characterization of the mechanism underlying the reversal of long term potentiation by low frequency stimulation at hippocampal CA1 synapses. [Journal Article; Research Support, Non-U.S. Gov't]. *J Biol Chem* 276, 48108–48117. doi: 10.1074/jbc.M106388200

Huang, Y. Y., and Kandel, E. R. (2005). Theta frequency stimulation induces a local form of late phase LTP in the CA1 region of the hippocampus. *Learning & Memory* 12, 587–593.

Hulme, S. R., Jones, O. D., and Abraham, W. C. (2013). Emerging roles of metaplasticity in behaviour and disease. [Journal Article; Research Support,

Non-U.S. Gov't; Review]. *Trends Neurosci* 36, 353–362. doi: 10.1016/j.tins.2013.03.007

Karabanov, A., Ziemann, U., Hamada, M., George, M. S., Quartarone, A., Classen, J., et al. (2015). Consensus Paper: Probing Homeostatic Plasticity of Human Cortex With Non-invasive Transcranial Brain Stimulation. *Brain Stimul* 8, 993–1006.

Kramar, E. A., and Lynch, G. (2003). Developmental and regional differences in the consolidation of long-term potentiation. [Comparative Study; Journal Article]. *Neuroscience* 118, 387–398. doi: 10.1016/s0306-4522(02)00916-8

Kulla, A., and Manahanvaughan, D. (2000). Depotentiation in the Dentate Gyrus of Freely Moving Rats is Modulated by D1/D5 Dopamine Receptors. *Cereb. Cortex* 10, 614–620.

Lefaucheur, J. P., Aleman, A., Baeken, C., Benninger, D. H., Brunelin, J., Di Lazzaro, V., et al. (2020). Evidence-based guidelines on the therapeutic use of repetitive transcranial magnetic stimulation (rTMS): An update (2014-2018). [Journal Article; Research Support, Non-U.S. Gov't; Review]. *Clin Neurophysiol* 131, 474–528. doi: 10.1016/j.clinph.2019.11.002

Park, P., Sanderson, T. M., Bortolotto, Z. A., Georgiou, J., Zhuo, M., Kaang, B. K., et al. (2019). Differential sensitivity of three forms of hippocampal synaptic potentiation to depotentiation. [Journal Article; Research Support, Non-U.S. Gov't]. *Mol Brain* 12, 30. doi: 10.1186/s13041-019-0451-6

Picconi, B., Centonze, D., Håkansson, K., Bernardi, G., and Calabresi, P. (2003). Loss of bidirectional striatal synaptic plasticity in L-DOPA-induced dyskinesia. *Nature Neuroscience* 6, 501–506.

Pötter-Nerger, M., Fischer, S., Mastroeni, C., Groppa, S., and Siebner, H. R. (2009). Inducing Homeostatic-Like Plasticity in Human Motor Cortex Through Converging Corticocortical Inputs. *Journal of Neurophysiology* 102, 3180–3190.

Reis, J., Schambra, H. M., Cohen, L. G., Buch, E. R., and Krakauer, J. W. (2009). Noninvasive cortical stimulation enhances motor skill acquisition over multiple days through an effect on consolidation. *Proc Natl Acad Sci U S A* 106, 1590–1595.

Rioult-Pedotti, M. S., Friedman, D., and Donoghue, J. P. (2000). Learning-induced LTP in neocortex. *Science* 290, 533–536.

Rossini, P. M., Burke, D., Chen, R., Cohen, L. G., Daskalakis, Z., Di, Iorio R, et al. (2015). Non-invasive electrical and magnetic stimulation of the brain, spinal cord, roots and peripheral nerves: Basic principles and procedures for routine clinical and research application. An updated report from an I.F.C.N. Committee. *Clinical Neurophysiology* 126, 1071–1107.

Roth, R. H., Cudmore, R. H., Tan, H. L., Hong, I., Zhang, Y., and Huganir, R. L. (2020). Cortical Synaptic AMPA Receptor Plasticity during Motor Learning. [Journal Article]. *Neuron* 105, 895–908. doi: 10.1016/j.neuron.2019.12.005

Siebner, H. R., Lang, N., Rizzo, V., Nitsche, M. A., Paulus, W., Lemon, R. N., et al. (2004). Preconditioning of low-frequency repetitive transcranial magnetic stimulation with transcranial direct current stimulation: evidence for homeostatic plasticity in the human motor cortex. *J Neurosci* 24, 3379–3385.

Wang, X., Zhang, Q., Cui, B., Huang, L., Wang, D., Ye, L., et al. (2018). Scalp-cluster acupuncture with electrical stimulation can improve motor and living ability in convalescent patients with post-stroke hemiplegia. [Journal Article]. *J Tradit Chin Med* 38, 452–456.

Xu, L., Anwyl, R., and Rowan, M. J. (1998). Spatial exploration induces a persistent reversal of long-term potentiation in rat hippocampus. *Nature* 394, 891–894.

Yahagi, S., and Kasai, T. (1998). Facilitation of motor evoked potentials (MEPs) in first dorsal interosseous (FDI) muscle is dependent on different motor images. *Electroencephalography & Clinical Neurophysiology* 109, 409–417.

Yee, A. X., Hsu, Y. T., and Lu, C. (2017). A metaplasticity view of the interaction between homeostatic and Hebbian plasticity. *Philosophical Transactions of the Royal Society B Biological Sciences* 372, 20160155.

Yi, Y., Ines, E., Siqi, C., Shaosong, W., Fan, Z., and Linpeng, W. (2017). Neuroplasticity Changes on Human Motor Cortex Induced by Acupuncture Therapy: A Preliminary Study. *Neural Plasticity* 2017, 1–8.

Zhang, Y., Cai, G. E., Yang, Q., Lu, Q. C., and Ju, G. (2010). Time-dependent changes in learning ability and induction of long-term potentiation in the lithium-pilocarpine-induced epileptic mouse model. *Epilepsy & Behavior* 17, 448–454.

Zheng, W., Su, Z., Liu, X., Zhang, H., Han, Y., Song, H., et al. (2018). Modulation of functional activity and connectivity by acupuncture in patients with Alzheimer disease as measured by resting-state fMRI. [Clinical Trial; Journal Article; Research Support, Non-U.S. Gov't]. *PLoS One* 13:e196933. doi: 10.1371/journal.pone.0196933

Zhou, Q., and Poo, M. M. (2004). Reversal and consolidation of activity-induced synaptic modifications. [Journal Article; Review]. *Trends Neurosci* 27, 378–383. doi: 10.1016/j.tins.2004.05.006

Ziemann, U., and Siebner, H. R. (2008). Modifying motor learning through gating and homeostatic metaplasticity. [Journal Article; Review]. *Brain Stimul* 1, 60–66. doi: 10.1016/j.brs.2007.08.003

Conflict of Interest: The authors declare that the research was conducted in the absence of any commercial or financial relationships that could be construed as a potential conflict of interest.

Copyright © 2021 He, Liu, Chen, Sun, Yu, Lei, Niu, Chen and Hsieh. This is an open-access article distributed under the terms of the Creative Commons Attribution License (CC BY). The use, distribution or reproduction in other forums is permitted, provided the original author(s) and the copyright owner(s) are credited and that the original publication in this journal is cited, in accordance with accepted academic practice. No use, distribution or reproduction is permitted which does not comply with these terms.

frontiers in Neural Circuits

ORIGINAL RESEARCH
published: 29 April 2021
doi: 10.3389/fncir.2021.548299

The Modulatory Effects of Intermittent Theta Burst Stimulation in Combination With Mirror Hand Motor Training on Functional Connectivity: A Proof-of-Concept Study

*Jack Jiaqi Zhang and Kenneth N. K. Fong**

Department of Rehabilitation Sciences, The Hong Kong Polytechnic University, Hung Hom, Hong Kong

Mirror training (MT) is an observation-based motor learning strategy. Intermittent theta burst stimulation (iTBS) is an accelerated form of excitatory repetitive transcranial magnetic stimulation (rTMS) that has been used to enhance the cortical excitability of the motor cortices. This study aims to investigate the combined effects of iTBS with MT on the resting state functional connectivity at alpha frequency band in healthy adults. Eighteen healthy adults were randomized into one of three groups—Group 1: iTBS plus MT, Group 2: iTBS plus sham MT, and Group 3: sham iTBS plus MT. Participants in Groups 1 and 3 observed the mirror illusion of the moving (right) hand in a plain mirror for four consecutive sessions, one session/day, while participants in Group 2 received the same training with a covered mirror. Real or sham iTBS was applied daily over right motor cortex prior to the training. Resting state electroencephalography (EEG) at baseline and post-training was recorded when participants closed their eyes. The mixed-effects model demonstrated a significant interaction effect in the coherence between FC4 and C4 channels, favoring participants in Group 1 over Group 3 ($\Delta\beta = -0.84$, $p = 0.048$). A similar effect was also found in the coherence between FC3 and FC4 channels favoring Group 1 over Group 3 ($\Delta\beta = -0.43$, $p = 0.049$). In contrast to sham iTBS combined with MT, iTBS combined with MT may strengthen the functional connectivity between bilateral premotor cortices and ipsilaterally within the motor cortex of the stimulated hemisphere. In contrast to sham MT, real MT, when combined with iTBS, might diminish the connectivity among the contralateral parietal–frontal areas.

Keywords: theta burst stimulation, mirror training, mirror visual feedback, coherence, electroencephalogram

OPEN ACCESS

Edited by:
Oscar Arias-Carrion, Hospital General Dr. Manuel Gea Gonzalez, Mexico

Reviewed by:
Alexey Brazhe, Lomonosov Moscow State University, Russia
Jessica Cantillo-Negrete, National Institute of Rehabilitation Luis Guillermo Ibarra Ibarra, Mexico

***Correspondence:**
Kenneth N. K. Fong
rsnkfong@polyu.edu.hk

Received: *02 April 2020*
Accepted: *06 April 2021*
Published: *29 April 2021*

Citation:
Zhang JJ and Fong KNK (2021) The Modulatory Effects of Intermittent Theta Burst Stimulation in Combination With Mirror Hand Motor Training on Functional Connectivity: A Proof-of-Concept Study. Front. Neural Circuits 15:548299. doi: 10.3389/fncir.2021.548299

INTRODUCTION

Mirror training (MT), in which participants are required to move one side of their hand while simultaneously observing the mirror visual feedback (MVF) from a mirror placed in the mid-sagittal plane, has been investigated with healthy adults to study the process of observation-based motor learning (Zult et al., 2016; Chen et al., 2019) and also applied in stroke rehabilitation to

improve the upper extremity motor relearning in patients with hemiplegia (Fong et al., 2019). The neural correlates underlying the MT are still under exploration, and there has been evidence that MVF can activate the parietal–frontal areas across bilateral hemispheres as well as the ipsilateral sensorimotor area (ipsilateral to the training hand and contralateral to the static hand behind the mirror) (Zhang et al., 2018). A possible explanation is that the parietal–frontal area encompasses the so-called human mirror neuron system (MNS), which can be activated during both observation and execution of movements (Rizzolatti and Craighero, 2004). In humans, it is believed that mirror neurons are located in the inferior frontal gyrus and adjacent premotor cortex, and in the rostral part of the inferior parietal lobule (Iacoboni and Dapretto, 2006). The role of the MNS is to facilitate the sensorimotor area in order to prepare the brain to be more receptive and ready to acquire new motor skills, in either healthy individuals (Bahr et al., 2018) or patients with stroke (Ding et al., 2018; Bai et al., 2019b).

Some studies have used non-invasive brain stimulation (NIBS)—most commonly repetitive transcranial magnetic stimulation (rTMS) and transcranial direct current stimulation (tDCS), to modulate the brain response to MT (von Rein et al., 2015; Kim and Yim, 2018; Jin et al., 2019). Facilitating the motor cortex by excitatory NIBS, including high-frequency rTMS or anodal tDCS, prior or concurrently to MT showed a greater effect on enhancing motor performance (measured using a two-ball rotation task) in healthy adults (von Rein et al., 2015) and motor recovery (measured using the box and block test or the action research arm test) in patients with stroke (Kim and Yim, 2018; Jin et al., 2019), indicating a synergistic effect when combining these two treatment modalities. Intermittent theta burst stimulation (iTBS) is an accelerated form of excitatory rTMS as it can yield a similar effect with high-frequency rTMS by using a very short conditioning time (i.e., 600 pulses a session, delivered in 3 min) (Huang and Rothwell, 2004). There is evidence to support that iTBS delivered to the motor cortex could enhance the efficacy of motor training in healthy individuals (Platz et al., 2018) and patients with stroke (Ackerley et al., 2016). However, it is still unclear whether iTBS could enhance observation-based motor learning via MT, and what its underpinning neural correlates are.

Brain activation during MVF training has been investigated in previous studies. Studies have shown the activation of the ipsilateral motor cortex (ipsilateral to the training hand and contralateral to the MVF) caused by MT (Saleh et al., 2017; Bai et al., 2019a). The activation of frontal regions, for example, premotor area, and parietal regions, has been also reported in previous literature (Hamzei et al., 2012; Saleh et al., 2017; Bai et al., 2019a; Ding et al., 2019). However, the intercortical functional connectivity when receiving MT is seldom investigated, which is of importance to understand the role of MNS in MT-related neural networks. Coherence-based connectivity analysis using electroencephalography (EEG) has been used to study the focal and remote effects of NIBS (Jing and Takigawa, 2000; Jin et al., 2017). Previously, an EEG experiment has shown that observation-induced neurophysiological changes over frontal, central, and parietal areas are primarily evident in the alpha frequency band (Frenkel-Toledo et al., 2013). This finding indicated the alpha rhythm might be associated with the function of the MNS network. Therefore, the alpha frequency band has been used as the outcome to explore the neuromodulatory effects of rTMS (Jin et al., 2017) and MT (Rosipal et al., 2019) in healthy adults.

To the best of our knowledge, no study to date has explored the functional connectivity for combined effect of iTBS with MT; in existing studies, they have been applied alone. The aim of this study was to explore the combined effect of iTBS with right-hand motor training with MVF on modulating the functional connectivity at alpha frequency band during the eye closed resting state in a group of healthy adults, compared with either iTBS or MT alone. This proof-of-concept experiment would help clarify the neural network in both ipsilateral (ipsilateral to the training hand in MT) and contralateral (contralateral to the training hand in MT) hemispheres of this combined intervention and lead to future studies in the stroke population.

MATERIALS AND METHODS

Participants

Potential participants were students enrolled from a local university via convenience sampling. Participants were invited to join the study if they could fulfill all the following inclusion criteria: (1) aged between 18 and 30; (2) right-handed, assessed by Edinburgh handedness inventory (Oldfield, 1971); and (3) normal or correct-to-normal vision. Participants were excluded if they met any of the following exclusion criteria: (1) any contraindication of NIBS (e.g., history of seizure, metal implant, current use of psychoactive drugs, etc.); (2) any known neurological or psychiatric disease; (3) any form of upper limb or hand injury in the past 3 months; and (4) upper limb or hand deformities. Written informed consent was obtained before their participation. The ethical approval for the current study was obtained from the Human Ethics Sub-Committee, University Research Committee of The Hong Kong Polytechnic University (Reference number: HSEARS20180120003). The study was designed as a controlled experiment with three parallel groups.

Experimental Procedure

Participants were randomly allocated to one of the three groups: (1) iTBS plus MT, (2) iTBS plus sham MT, and (3) sham iTBS plus MT, by drawing lots. **Figure 1** demonstrates the procedure of study and the intervention setup. All participants had to attend two EEG assessment sessions and four consecutive training sessions, one session per day.

EEG Acquisition

Electroencephalography was captured with a 64-channel cap (64-channel Quik-Cap, Compumedics Neuroscan, United States) using a Digital DC EEG Amplifier and Neuroscan Curry 7 (Compumedics Neuroscan, United States). Electrode impedance was kept below 10 kohm, and signal was sampled at 1,024 Hz. A ground electrode was positioned on the forehead in front of the Cz electrode, and two reference electrodes were placed

A

	Baseline EEG measurement		Posttraining EEG measurement
Group 1	Resting state (Eye closed)	iTBS plus mirror training 15 minutes/day, 4 days	Resting state (Eye closed)
Group 2	Resting state (Eye closed)	iTBS plus sham mirror training 15 minutes/day, 4 days	Resting state (Eye closed)
Group 3	Resting state (Eye closed)	Sham iTBS plus mirror training 15 minutes/day, 4 days	Resting state (Eye closed)

B

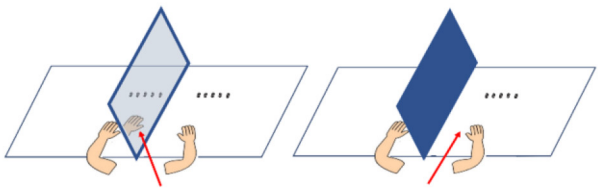

FIGURE 1 | The demonstration of study design and intervention. **(A)** The study procedure. **(B)** Demonstration of mirror training (left-side) and sham mirror training (right-side). The red arrow denotes the visual direction during the training.

on the left and right mastoids. All channels were used during recording, although our analysis was limited to a few channels of interest. Task-designed EEG recording and corresponding results were reported in another article (Zhang and Fong, 2019). In this article, we focus on the resting state functional connectivity. Resting state EEG was recorded for approximately 2 min and 50 s at each assessment session, when the participants closed their eyes. Participants were seated upright in an electromagnetic shielded room and required to minimize any body movement during the recording. EEG data were collected by the same experimenter who performed the TBS and motor training.

Transcranial Magnetic Stimulation Session

Standard 600-pulse iTBS protocol proposed by Huang and Rothwell (2004) (i.e., 20 trains of 10 bursts given with 8-s intervals, with a total of 600 pulses, 192 s per session) was delivered daily by MagPro stimulators (MagVenture, Denmark) with a butterfly-shape coil (C-B60), over the right motor cortex for four consecutive days. The coil was positioned at an angle of 45° to the mid-sagittal plane of the participants' heads. The stimulation target (i.e., right motor cortex) was identified as the area in which the most consistent and largest motor-evoked potential (MEP) output was found. The positioning of the coil was maintained by means of Vicra optical tracking using the Localite neuro-navigation system based on a data set of a standard head (Localite, Bonn, Germany). The intensity of stimulation of iTBS was set at 80% of individual active motor threshold (Huang and Rothwell, 2004). Active motor threshold is defined as the minimum intensity over the motor cortex that could elicit an MEP of no less than 200 μv in five out of 10 trials during a slightly voluntary contraction (20% of the maximal voluntary contraction) of the contralateral first dorsal interosseous muscle. Sham stimulation was delivered using the same coil that delivers only 20% of the individual active motor threshold.

Motor Training Session

Immediately after each TBS session, participants underwent right-hand motor training with a mirror or a covered mirror. We followed the previous studies using four-day MT in healthy adults (Hamzei et al., 2012; Lappchen et al., 2015). The participants in Groups 1 and 3 were required to look at the MVF reflected in the mirror when performing the right-hand motor training, with the left hand behind the mirror remaining static. Participants in Group 2 were asked to perform the same training with the mirror covered and looking directly at their moving (right) hand, the aim of which was to control the cross-education effect from the right hand motor training to the static left hand (Zult et al., 2014). Our training tasks were modified from the Nine-hole peg test, Minnesota dexterity test, Purdue Pegboard test, and two-ball rotation task, lasting for approximately 15 min per session, including picking up, placing and displacing pegs, making an assembly with a pin, a washer, and a collar, placing, displacing, and turning plastic disks, and in-hand rotation of two wooden balls. Behavioral motor performance was also assessed before and after the intervention, by using these four assessments. The results of behavioral motor performance have been reported in another article (Zhang and Fong, 2019).

EEG Data Pre-processing

Raw EEG signals were band-pass filtered between 1 and 30 Hz, by using *pop_eegfiltnew* function in EEGLab. The data were filtered using a Hamming windowed sinc FIR filter. The filter orders were 3,300 and 440, respectively. Then the data were down-sampled at 250 Hz. By visual inspection, we rejected bad channels with abnormally high-amplitude signals and time periods containing significant movement artifacts. Channel's data were then re-referenced to the common average. An independent component

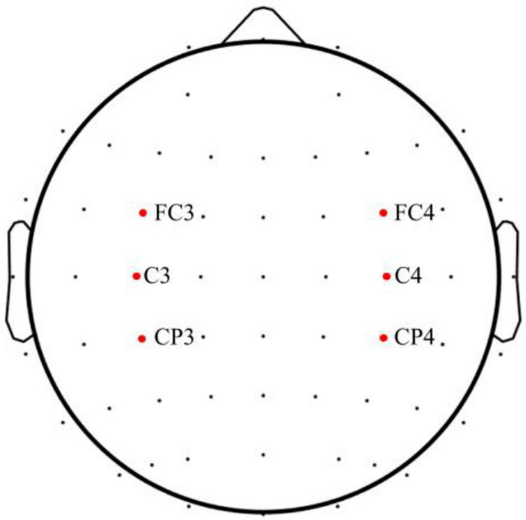

Channel pairs	Connectivity
FC3-FC4	Interhemispheric, premotor-premotor
FC3-C3	Intrahemispheric, premotor-motor
FC3-C4	Interhemispheric, premotor-motor
FC3-CP3	Intrahemispheric, premotor-parietal
FC4-C3	Interhemispheric, premotor-motor
FC4-CP4	Intrahemispheric, premotor-parietal
FC4-C4	Intrahemispheric, premotor-motor
C3-C4	Interhemispheric, motor-motor
C3-CP3	Intrahemispheric, motor-parietal
C3-CP4	Interhemispheric, motor-parietal
C4-CP3	Interhemispheric, motor-parietal
C4-CP4	Intrahemispheric, motor-parietal
CP3-CP4	Interhemispheric, parietal-parietal

FIGURE 2 | Channel pairs of interest.

analysis algorithm was used to identify any ocular component that was further rejected (Delorme and Makeig, 2004).

Surface Laplacian transformation was carried out in order to minimize volume conduction effects from real connectivity among brain areas, *via* the current source density toolbox (Tenke and Kayser, 2005). The continuous data were segmented into several 2-s epochs before the surface Laplacian. We first generated two transformation matrices terms. The two matrices were used for the spherical spline interpolation of surface potentials (G) and current source densities (H), respectively (Perrin et al., 1989). The following parameters were used in the calculation, i.e., smoothing constant (lambda) = 10^{-5}, the number of iterations = 50, $m = 4$ (the constant which affected the flexibility of the spherical splines). Then, we applied the CSD transform to EEG data with the two transformation matrices (Kayser and Tenke, 2006).

Coherence Analysis

Based on the previous hypothesis of MNS, we focused on the intrahemispheric connectivity within premotor, motor, and parietal areas in either left (contralateral to the training hand) or right (ipsilateral to the training hand) hemisphere, and interhemispheric connectivity among bilateral premotor, motor, and parietal areas (Zhang et al., 2018). As there is evidence showing the connectivity between ipsilateral MNS to the contralateral motor area (Hamzei et al., 2012; Saleh et al., 2017), we also explored the functional linkage of the premotor or parietal area on one side of the hemisphere with the motor area on another side of the hemisphere. Therefore, 13 pairs of channels were investigated (see **Figure 2** for the selected channel pairs). Channels FC3, FC4, C3, C4, CP3, and CP4 were selected to represent the left and right premotor areas, left and right motor areas, and left and right parietal areas, respectively, according to a previous report (Jin et al., 2017). Coherence-based measure was used in the present study to probe the functional connectivity among the cortical areas (Guevara and Corsi-Cabrera, 1996). Coherence represents the normalized covariance of two time series in the frequency band. The coherence at a frequency f for signal x and y is computed by the normalization of cross spectrum as follows (Guevara and Corsi-Cabrera, 1996):

$$Coherence\ (f)\ \frac{\left|\langle Pxy\ (f)\rangle\right|^2}{(Pxx\ \times\ Pyy)}$$

where Pxx and Pyy refer to the auto-spectrum of signal x and y, respectively, and Pxy refers to the cross-spectral spectrum. The estimated coherence ranges from 0 to 1, in which 0 means that there is no linear dependence between the two channels at frequency f. A higher level of coherence suggests higher statistical dependence between the two signals, and vice versa. Frequency band was set at between 8 and 12 Hz, as the alpha rhythm is the dominant frequency during the eye closed resting state (Jin et al., 2017) and previous literature also shows the potential correlation between alpha rhythm and MNS activities (Frenkel-Toledo et al., 2013). Coherence was further transformed to z scores by using the following formula:

$$Z = 0.5 \times \log((1 + \text{coherence})/(1-\text{coherence}))$$

Statistical Analysis

Statistical analysis was performed with IBM Statistical Product and Service Solutions (SPSS) version 23.0. Baseline characteristics were compared by one-way ANOVA or Fisher's exact test.

TABLE 1 | Results of coherence differences across three groups.

		Within-group differences		Between-group differences			
		Z	***p***	**Comparisons**	**Δβ**	**SE**	***p***
Pair 1: FC3-FC4	Group 1	−1.75	0.080	Group 3 *vs.* Group 1	−0.43	0.21	0.049*
	Group 2	−0.52	0.600	Group 2 *vs.* Group 1	−0.13	0.19	0.513
	Group 3	−1.21	0.225				
Pair 2: FC3-C3	Group 1	−0.67	0.500	Group 3 *vs.* Group 1	−0.19	0.50	0.715
	Group 2	−0.73	0.463	Group 2 *vs.* Group 1	0.43	0.48	0.386
	Group 3	−0.135	0.893				
Pair 3: FC3-C4	Group 1	−1.21	0.225	Group 3 *vs.* Group 1	−0.32	0.21	0.143
	Group 2	−0.94	0.345	Group 2 *vs.* Group 1	0.02	0.20	0.911
	Group 3	−0.94	0.345				
Pair 4: FC3-CP3	Group 1	−0.41	0.686	Group 3 *vs.* Group 1	−0.09	0.28	0.745
	Group 2	−1.78	0.075	Group 2 *vs.* Group 1	0.63	0.27	0.033*
	Group 3	−1.21	0.225				
Pair 5: FC4-C3	Group 1	−1.21	0.225	Group 3 *vs.* Group 1	−0.23	0.20	0.251
	Group 2	−0.11	0.917	Group 2 *vs.* Group 1	−0.21	0.19	0.277
	Group 3	−0.14	0.893				
Pair 6: FC4-C4	Group 1	−2.02	0.043*	Group 3 *vs.* Group 1	−0.84	0.39	0.048*
	Group 2	−1.36	0.173	Group 2 *vs.* Group 1	−0.10	0.38	0.784
	Group 3	−0.94	0.345				
Pair 7: FC4-CP4	Group 1	−1.21	0.225	Group 3 *vs.* Group 1	−0.25	0.18	0.170
	Group 2	−0.94	0.345	Group 2 *vs.* Group 1	−0.34	0.17	0.057
	Group 3	−0.14	0.893				
Pair 8: C3-C4	Group 1	−2.02	0.043*	Group 3 *vs.* Group 1	−0.21	0.25	0.425
	Group 2	−0.94	0.345	Group 2 *vs.* Group 1	−0.08	0.24	0.759
	Group 3	−0.41	0.686				
Pair 9: C3-CP3	Group 1	−1.48	0.138	Group 3 *vs.* Group 1	0.40	0.28	0.173
	Group 2	−1.992	0.046*	Group 2 *vs.* Group 1	0.59	0.27	0.045*
	Group 3	−0.674	0.500				
Pair 10: C3-CP4	Group 1	−0.67	0.500	Group 3 *vs.* Group 1	−0.01	0.21	1.000
	Group 2	−0.94	0.345	Group 2 *vs.* Group 1	−0.25	0.20	1.000
	Group 3	−0.41	0.686				
Pair 11: C4-CP3	Group 1	−0.41	0.686	Group 3 *vs.* Group 1	0.11	0.17	0.522
	Group 2	−1.36	0.173	Group 2 *vs.* Group 1	0.11	0.16	0.513
	Group 3	−1.75	0.080				
Pair 12: C4-CP4	Group 1	−0.67	0.500	Group 3 *vs.* Group 1	0.16	0.18	0.380
	Group 2	−1.15	0.249	Group 2 *vs.* Group 1	−0.01	0.17	0.935
	Group 3	−1.48	0.138				
Pair 13: CP3-CP4	Group 1	−1.75	0.080	Group 3 vs. Group 1	0.05	0.12	0.688
	Group 2	−1.15	0.249	Group 2 vs. Group 1	0.05	0.12	0.688
	Group 3	−1.75	0.080				

*$P < 0.05$.

A mixed-effects regression model with random intercepts and slopes was used to detect any significant difference in the change of coherence, using the z score after log transformation, among the three groups, because of its superiority in analyzing the repeated measures data (Gueorguieva and Krystal, 2004). We included group allocation, time, and interaction of group and time as fixed-effects. The random intercept and random slope of change in dependent variables over time were included as random-effects, i.e., the model assumed that individuals differed at baseline and in the rate of change over time, which accounted for the uncontrollable variability within the sample and hence achieved greater power (Gueorguieva and Krystal, 2004). Group was labeled as 1, 2, and 3, which represented our three experimental groups. Time was coded as baseline and post-training, represented as values of 1 and 2. Maximum likelihood was chosen as the estimation method, and the heterogeneous first−order autoregressive covariance structure was selected to estimate the model parameters. Between-group differences were investigated in terms of group by time interaction effects, i.e., the difference in slope reflected the difference in change of coherence between-group (Lewthwaite et al., 2018). According to our objective, we compared

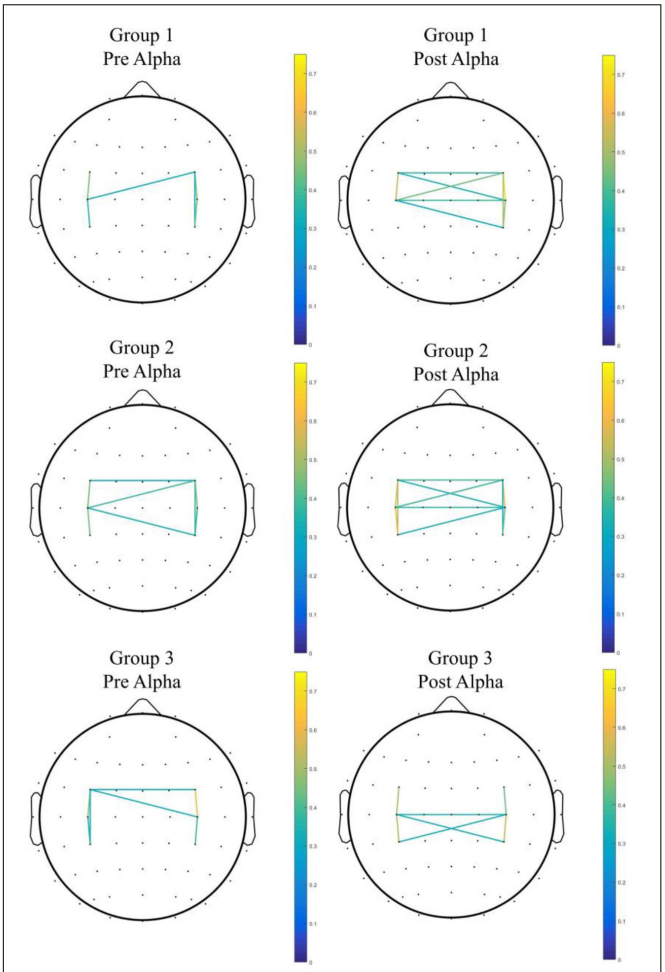

FIGURE 3 | The pre–post comparison of coherence in each group. Only pairs with coherence > 0.3 were shown.

the potential differences between Group 1 (iTBS plus MT) with Group 2 (iTBS plus sham MT), and Group 1 (iTBS plus MT) with Group 3 (sham iTBS plus MT). Within-group differences were examined by separated related-sample Wilcoxon signed rank tests. The level of significance was set at $p < 0.05$.

RESULTS

Characteristics of Participants

We received 19 applications for participation, of which one participant was excluded due to the history of childhood epilepsy. Therefore, 18 participants were recruited for our experiment. There was no significant between-group difference in age (25.30 ± 2.00 *vs.* 26.50 ± 2.17 *vs.* 26.33 ± 2.25, $p = 0.602$) and gender (three females *vs.* two females *vs.* four females, $p = 0.835$). From the 18 participants, one case's baseline EEG data and another case's post-training EEG data were removed from data analysis due to significant noise. Therefore, the pre–post comparison of EEG analysis was conducted on 16 cases (Group 1 = 5 *vs.* Group 2 = 6 *vs.* Group 3 = 5). On average, 2.59 ± 2.08 channels were labeled as bad channels and thus rejected after the data preprocessing. No channel of interest was labeled as bad channels among our sample. The mean length of data that were used in the final analysis was 149.89 ± 15.57 s.

Coherence Analysis

The results of statistical comparisons across the three groups are reported in **Table 1**. When comparing Group 3 and Group 1, the mixed-effect model demonstrated a significant interaction effect in the coherence between FC4 and C4 (Group 3 *vs.* Group 1, difference in slope = −0.84; SE = 0.39, $p = 0.048$), and between FC3 and FC4 (Group 3 *vs.* Group 1, difference in slope = −0.43; SE = 0.21, $p = 0.049$). The results indicated enhanced connectivity between right premotor and motor areas and bilateral premotor areas in participants from Group 1, in contrast to those in Group 3. Within-group comparison showed that there were significant differences in coherence between FC4 and C4 channels, and between C3 and C4 channels in Group 1 ($Z = -2.02$, $p = 0.043$).

When comparing Group 2 and Group 1, the mixed-effect model demonstrated a significant interaction effect in the coherence between C3 and CP3 (Group 2 *vs.* Group 1, difference in slope = 0.59; SE = 0.27, $p = 0.045$), as well as the coherence between FC3 and CP3 (Group 2 *vs.* Group 1, difference in slope = 0.63; SE = 0.27, $p = 0.033$), which indicated enhanced connectivity among premotor, motor, and parietal areas over the contralateral hemisphere (contralateral to the moving hand and ipsilateral to the MVF) in Group 2, in contrast to Group 1. Within-group differences were found in coherence between C3 and CP3 ($Z = -2.00$, $p = 0.046$) in Group 2, but there was no significant interaction effect among the groups observed (see **Figure 3** for the pre–post comparisons of coherence in each group and see **Figure 4** for the channel pairs with significant interaction effects).

DISCUSSION

The present study investigated the combined effect of iTBS with MT on modulating the resting state functional connectivity at alpha frequency band, in healthy adults. Our experiment found that the combination of iTBS with MT strengthened intrahemispheric connectivity between premotor and motor areas in the ipsilateral (right) side, as indicated by the increased coherence between FC4 and C4 channels, as well as the interhemispheric connectivity of bilateral premotor cortices, as indicated by the increased coherence between FC3 and FC4 channels. Compared with participants who received iTBS with MT, those who received iTBS with sham MT showed an increase of functional connectivity between contralateral (left) premotor and parietal areas, as well as the connectivity between left premotor and motor areas, as indicated by increased coherence between FC3, C3, and CP3 channels.

The change of cortical connectivity induced by MT has been investigated in previous studies. Bai et al. (2019a) investigated the

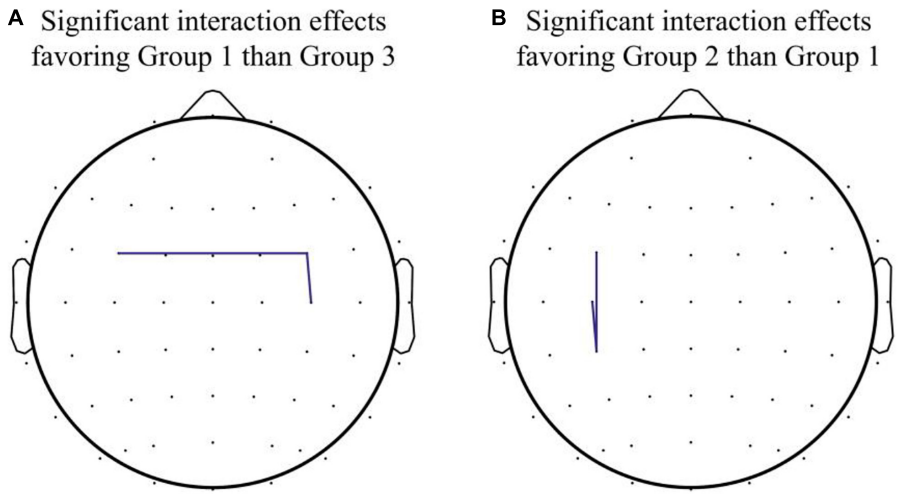

FIGURE 4 | Significant interaction effects in channel pairs. **(A)** Significant interaction effects favoring Group 1 over Group 3 were noted in coherence between FC3 and FC4 and between FC4 and C4. **(B)** Significant interaction effects favoring Group 2 over Group 1 were noted in coherence between FC3 and CP3 and between C3 and CP3.

instant effect of MVF on healthy adults, using functional near-infrared spectroscopy (fNIRS) and they reported a strengthened functional correlation between the supplementary motor area and the sensorimotor area over the ipsilateral (right) hemisphere (ipsilateral to the training hand and contralateral to the MVF) when participants were viewing the MVF. Saleh et al. studied the instant effect of MVF on patients with stroke using functional magnetic resonance imaging (fMRI). Increased connectivity between contralesional inferior parietal lobule and ipsilesional primary motor cortex induced by MVF was then reported (Saleh et al., 2017). Those findings were in line with the hypothesis of MNS, which postulates that the activation of both the parietal–frontal area and the sensorimotor area could be elicited by MVF. The training effect of multiple-session MT on functional connectivity was only investigated in one previous study by Hamzei et al. (2012), which demonstrated the strengthened functional connectivity between the bilateral premotor areas and the motor area in healthy adults after four daily sessions of MT.

The effect of MT on functional connectivity in healthy adults has only been investigated by using hemodynamic signals (Hamzei et al., 2012; Bai et al., 2019a). Thus, our study probes functional connectivity in response to these two treatment modalities by EEG. The advantage of EEG is its excellent temporal resolution, which is likely to enable the detection of subtle neuroplastic changes. Compared with participants who received sham iTBS with MT, those who received iTBS with MT showed enhanced connectivity between premotor (FC4) and motor (C4) areas in the ipsilateral hemisphere as well as interhemispheric connectivity between bilateral premotor areas (i.e., FC3 and FC4). Functionally, the premotor cortex receives sensory input from the parietal cortex and projects to the motor cortex, which plays an important role in motor preparation and planning (Wong et al., 2015). There has been evidence that the premotor cortex has a mirror neuron-like property that can be activated during the observation of movement (Rizzolatti et al., 1996). A meta-analysis of fMRI experiments showed a bilateral activation of premotor areas in response to the action observation of unilateral hand movement (Caspers et al., 2010). The functional difference of left and right premotor cortices was revealed in an fMRI study, which showed that the left premotor cortex was more involved with the object manipulation during action observation and the right premotor cortex was more involved with the observed movement (Manthey et al., 2003). In a study on stroke patients, the activation of premotor cortex in both ipsilesional and contralesional hemispheres was enhanced after mirror therapy (Bhasin et al., 2012), indicating that the premotor areas on both hemispheres are likely to be part of the MNS. Strengthened connectivity among bilateral premotor and ipsilateral motor areas may indicate that the effect of MVF-based observation motor learning could be enhanced when it is in combination with iTBS over the motor cortex. A previous clinical study about the effects of MT on functional connectivity in patients with stroke, identified significant connectivity enhancement at resting state, over premotor, motor, and parietal areas bilaterally (Ding et al., 2019), in patients who received 10-session MT. Therefore, in order to yield maximal benefits for patients, there needs to be further investigation to determine an optimal dose of MT intervention when it is applied in different clinical populations with suitable priming techniques that can be combined with.

In our previous study (Zhang and Fong, 2019), we did not observe any significant difference in MVF-induced ERD and motor performance between iTBS plus MT and iTBS plus sham MT. However, using coherence analysis, we observed strengthened connectivity between left premotor, motor, and parietal areas in participants who received iTBS plus sham MT, in contrast to those who received iTBS plus MT. This finding may be attributed to the modulatory effect of active hand training with direct observation of the moving hand, which promotes the functional interrelationship among the premotor, motor, and

parietal areas, but the effect was limited within the contralateral hemisphere and was not transferred interhemispherically across the corpus callosum. A previous experimental study showed that MT may have a suppression on the contralateral hemisphere (contralateral to the training hand in MT), compared with sham MT (Bartur et al., 2015). The increase in coherence in contralateral hemisphere after receiving iTBS plus sham MT might also reveal that MT may induce a shift of activation to the ipsilateral hemisphere (ipsilateral to the training hand in MT) and simultaneously suppress the activity of the contralateral hemisphere. We hypothesized that this modulatory effect to the ipsilateral hemisphere (i.e., ipsilesional hemisphere in patients with stroke) associated with MT may therefore be useful to the hemiparetic arm recovery for patients after a unilateral stroke.

LIMITATIONS

This proof-of-concept study has several limitations. First, our current study was limited by its small sample size. Although a multiple-session intervention may stabilize the response, we cannot fully control the confounding effects in association with the inter-subject variability of iTBS. Second, we did not apply multiple comparison corrections with regard to the exploratory nature of this study. Third, EEG has its limitation in spatial resolution, although we had applied spatial filters to improve the spatial precision. Besides, our connectivity analysis was limited to coherence. This measure has been widely used to assess the functional connectivity and its meaning is easy for clinicians to understand. However, there were other novel connectivity indices that we did not use in the current study, such as phase synchronization-based measures and Granger causality-based measures. They may provide additional information about the connectivity. Lastly, we only measured the resting-state functional connectivity; motor task-related functional connectivity may also be very promising to be used as a physiological biomarker for motor recovery. In addition, different stages of movement may influence the dynamics of functional connectivity. An event-related EEG experiment with motion analysis may provide rich information for us to explore the motor task-related functional connectivity. Further study on the stroke population is needed to investigate the potential clinical effects of the combined treatments for hemiparetic arm functions.

CONCLUSION

In contrast to sham iTBS combined with MT, iTBS combined with MT may strengthen the functional connectivity between bilateral premotor cortices and ipsilaterally within the motor cortex of the stimulated hemisphere. In contrast to sham MT, real MT, when combined with iTBS, might diminish the connectivity among the contralateral parietal–frontal–motor circuits, perhaps due to the shift of activation to the ipsilateral hemisphere after MT.

DATA AVAILABILITY STATEMENT

The raw data supporting the conclusions of this article will be made available by the authors, without undue reservation. Requests to access the datasets should be directed to JZ, jack-jq.zhang@connect.polyu.hk.

ETHICS STATEMENT

The studies involving human participants were reviewed and approved by the Human Ethics Sub-Committee, University Research Committee of The Hong Kong Polytechnic University (Reference number: HSEARS20180120003). The patients/participants provided their written informed consent to participate in this study.

AUTHOR CONTRIBUTIONS

JZ and KF were involved in the conception and design of the study. JZ conducted the experiment and wrote up the first draft. KF supervised the progress and reviewed and edited the manuscript. Both authors approved the submission of the final version of the manuscript.

FUNDING

This project was funded by General Research Fund (Grant No. 15105919M), Research Grants Council, University Grants Committee, Hong Kong SAR, awarded to KF.

ACKNOWLEDGMENTS

The authors would like to thank all participants in this study. The authors thank the University Research Facility in Behavioral and Systems Neuroscience at The Hong Kong Polytechnic University for facility support.

REFERENCES

Ackerley, S. J., Byblow, W. D., Barber, P. A., Macdonald, H., Mcintyre-Robinson, A., and Stinear, C. M. (2016). Primed physical therapy enhances recovery of upper limb function in chronic stroke patients. *Neurorehabil. Neural Repair* 30, 339–348. doi: 10.1177/1545968315595285

Bahr, F., Ritter, A., Seidel, G., Puta, C., Gabriel, H. H. W., and Hamzei, F. (2018). Boosting the motor outcome of the untrained hand by action observation: mirror visual feedback, video therapy, or both combined–what is more effective? *Neural Plast.* 2018:8369262.

Bai, Z., Fong, K. N. K., Zhang, J., and Hu, Z. (2019a). Cortical mapping of mirror visual feedback training for unilateral upper extremity:

a functional near-infrared spectroscopy study. *Brain Behav.* 10: e01489.

Bai, Z., Zhang, J., Zhang, Z., Shu, T., and Niu, W. (2019b). Comparison between movement-based and task-based mirror therapies on improving upper limb functions in patients with stroke: a pilot randomized controlled trial. *Front. Neurol.* 10:288. doi: 10.3389/fneur.2019.00288

Bartur, G., Pratt, H., Dickstein, R., Frenkel-Toledo, S., Geva, A., and Soroker, N. (2015). Electrophysiological manifestations of mirror visual feedback during manual movement. *Brain Res.* 1606, 113–124. doi: 10.1016/j.brainres.2015.02.029

Bhasin, A., Padma Srivastava, M. V., Kumaran, S. S., Bhatia, R., and Mohanty, S. (2012). Neural interface of mirror therapy in chronic stroke patients: a functional magnetic resonance imaging study. *Neurol. India* 60, 570–576. doi: 10.4103/0028-3886.105188

Caspers, S., Zilles, K., Laird, A. R., and Eickhoff, S. B. (2010). ALE meta-analysis of action observation and imitation in the human brain. *Neuroimage* 50, 1148–1167. doi: 10.1016/j.neuroimage.2009.12.112

Chen, Y., Wang, P., Bai, Y., and Wang, Y. (2019). Effects of mirror training on motor performance in healthy individuals: a systematic review and meta-analysis. *BMJ Open Sport Exerc. Med.* 5:e000590. doi: 10.1136/bmjsem-2019-000590

Delorme, A., and Makeig, S. (2004). EEGLAB: an open source toolbox for analysis of single-trial EEG dynamics including independent component analysis. *J. Neurosci. Methods* 134, 9–21. doi: 10.1016/j.jneumeth.2003.10.009

Ding, L., Wang, X., Chen, S., Wang, H., Tian, J., Rong, J., et al. (2019). Camera-based mirror visual input for priming promotes motor recovery, daily function, and brain network segregation in subacute stroke patients. *Neurorehabil. Neural Repair* 33, 307–318. doi: 10.1177/1545968319836207

Ding, L., Wang, X., Guo, X., Chen, S., Wang, H., Jiang, N., et al. (2018). Camera-based mirror visual feedback: potential to improve motor preparation in stroke patients. *IEEE Trans. Neural Syst. Rehabil. Eng.* 26, 1897–1905. doi: 10.1109/tnsre.2018.2864990

Fong, K. N., Ting, K. H., Chan, C. C., and Li, L. S. (2019). Mirror therapy with bilateral arm training for hemiplegic upper extremity motor functions in patients with chronic stroke. *Hong Kong Med. J.* 25(Suppl. 3), 30–34.

Frenkel-Toledo, S., Bentin, S., Perry, A., Liebermann, D. G., and Soroker, N. (2013). Dynamics of the EEG power in the frequency and spatial domains during observation and execution of manual movements. *Brain Res.* 1509, 43–57. doi: 10.1016/j.brainres.2013.03.004

Gueorguieva, R., and Krystal, J. H. (2004). Move over ANOVA: progress in analyzing repeated-measures data and its reflection in papers published in the Archives of General Psychiatry. *Arch. Gen. Psychiatry* 61, 310–317. doi: 10.1001/archpsyc.61.3.310

Guevara, M. A., and Corsi-Cabrera, M. (1996). EEG coherence or EEG correlation? *Int. J. Psychophysiol.* 23, 145–153. doi: 10.1016/s0167-8760(96)00038-4

Hamzei, F., Lappchen, C. H., Glauche, V., Mader, I., Rijntjes, M., and Weiller, C. (2012). Functional plasticity induced by mirror training: the mirror as the element connecting both hands to one hemisphere. *Neurorehabil. Neural Repair* 26, 484–496. doi: 10.1177/1545968311427917

Huang, Y. Z., and Rothwell, J. C. (2004). The effect of short-duration bursts of high-frequency, low-intensity transcranial magnetic stimulation on the human motor cortex. *Clin. Neurophysiol.* 115, 1069–1075. doi: 10.1016/j.clinph.2003.12.026

Iacoboni, M., and Dapretto, M. (2006). The mirror neuron system and the consequences of its dysfunction. *Nat. Rev. Neurosci.* 7, 942–951. doi: 10.1038/nrn2024

Jin, J. N., Wang, X., Li, Y., Jin, F., Liu, Z. P., and Yin, T. (2017). The effects of rTMS combined with motor training on functional connectivity in alpha frequency band. *Front. Behav. Neurosci.* 11:234. doi: 10.3389/fnbeh.2017.00234

Jin, M., Zhang, Z., Bai, Z., and Fong, K. N. K. (2019). Timing-dependent interaction effects of tDCS with mirror therapy on upper extremity motor recovery in patients with chronic stroke: a randomized controlled pilot study. *J. Neurol. Sci.* 405:116436. doi: 10.1016/j.jns.2019.116436

Jing, H., and Takigawa, M. (2000). Observation of EEG coherence after repetitive transcranial magnetic stimulation. *Clin. Neurophysiol.* 111, 1620–1631. doi: 10.1016/s1388-2457(00)00357-6

Kayser, J., and Tenke, C. E. (2006). Principal components analysis of Laplacian waveforms as a generic method for identifying ERP generator patterns: I. Evaluation with auditory oddball tasks. *Clin. Neurophysiol.* 117, 348–368. doi: 10.1016/j.clinph.2005.08.034

Kim, J., and Yim, J. (2018). Effects of high-frequency repetitive transcranial magnetic stimulation combined with task-oriented mirror therapy training on hand rehabilitation of acute stroke patients. *Med. Sci. Monit.* 24, 743–750. doi: 10.12659/msm.905636

Lappchen, C. H., Ringer, T., Blessin, J., Schulz, K., Seidel, G., Lange, R., et al. (2015). Daily iTBS worsens hand motor training–a combined TMS, fMRI and mirror training study. *Neuroimage* 107, 257–265. doi: 10.1016/j.neuroimage.2014.12.022

Lewthwaite, R., Winstein, C. J., Lane, C. J., Blanton, S., Wagenheim, B. R., Nelsen, M. A., et al. (2018). Accelerating stroke recovery: body structures and functions, activities, participation, and quality of life outcomes from a large rehabilitation trial. *Neurorehabil. Neural Repair* 32, 150–165. doi: 10.1177/1545968318760726

Manthey, S., Schubotz, R. I., and von Cramon, D. Y. (2003). Premotor cortex in observing erroneous action: an fMRI study. *Cogn. Brain Res.* 15, 296–307. doi: 10.1016/S0926-6410(02)00201-X

Oldfield, R. C. (1971). The assessment and analysis of handedness: the Edinburgh inventory. *Neuropsychologia* 9, 97–113. doi: 10.1016/0028-3932(71)90067-4

Perrin, F., Pernier, J., Bertrand, O., and Echallier, J. F. (1989). Spherical splines for scalp potential and current density mapping. *Electroencephalogr. Clin. Neurophysiol.* 72, 184–187. doi: 10.1016/0013-4694(89)90180-6

Platz, T., Adler-Wiebe, M., Roschka, S., and Lotze, M. (2018). Enhancement of motor learning by focal intermittent theta burst stimulation (iTBS) of either the primary motor (M1) or somatosensory area (S1) in healthy human subjects. *Restor. Neurol. Neurosci.* 36, 117–130. doi: 10.3233/rnn-170774

Rizzolatti, G., and Craighero, L. (2004). The mirror-neuron system. *Annu. Rev. Neurosci.* 27, 169–192.

Rizzolatti, G., Fadiga, L., Gallese, V., and Fogassi, L. (1996). Premotor cortex and the recognition of motor actions. *Brain Res. Cogn. Brain Res.* 3, 131–141. doi: 10.1016/0926-6410(95)00038-0

Rosipal, R., Porubcová, N., Barančok, P., Cimrová, B., Farkaš, I., and Trejo, L. J. (2019). Effects of mirror-box therapy on modulation of sensorimotor EEG oscillatory rhythms: a single-case longitudinal study. *J. Neurophysiol.* 121, 620–633. doi: 10.1152/jn.00599.2018

Saleh, S., Yarossi, M., Manuweera, T., Adamovich, S., and Tunik, E. (2017). Network interactions underlying mirror feedback in stroke: a dynamic causal modeling study. *Neuroimage Clin.* 13, 46–54. doi: 10.1016/j.nicl.2016.11.012

Tenke, C. E., and Kayser, J. (2005). Reference-free quantification of EEG spectra: combining current source density (CSD) and frequency principal components analysis (fPCA). *Clin. Neurophysiol.* 116, 2826–2846. doi: 10.1016/j.clinph.2005.08.007

von Rein, E., Hoff, M., Kaminski, E., Sehm, B., Steele, C. J., Villringer, A., et al. (2015). Improving motor performance without training: the effect of combining mirror visual feedback with transcranial direct current stimulation. *J. Neurophysiol.* 113, 2383–2389. doi: 10.1152/jn.00832.2014

Wong, A. L., Haith, A. M., and Krakauer, J. W. (2015). Motor planning. *Neuroscientist* 21, 385–398.

Zhang, J. J., and Fong, K. N. K. (2019). Enhancing mirror visual feedback with intermittent theta burst stimulation in healthy adults. *Restor. Neurol. Neurosci.* 37, 483–495. doi: 10.3233/rnn-190927

Zhang, J. J. Q., Fong, K. N. K., Welage, N., and Liu, K. P. Y. (2018). The activation of the mirror neuron system during action observation and action

execution with mirror visual feedback in stroke: a systematic review. *Neural Plast.* 2018:2321045.

Zult, T., Goodall, S., Thomas, K., Solnik, S., Hortobagyi, T., and Howatson, G. (2016). Mirror training augments the cross-education of strength and affects inhibitory paths. *Med. Sci. Sports Exerc.* 48, 1001–1013. doi: 10.1249/mss.0000000000000871

Zult, T., Howatson, G., Kadar, E. E., Farthing, J. P., and Hortobagyi, T. (2014). Role of the mirror-neuron system in cross-education. *Sports Med.* 44, 159–178. doi: 10.1007/s40279-013-0105-2

Conflict of Interest: The authors declare that the research was conducted in the absence of any commercial or financial relationships that could be construed as a potential conflict of interest.

Copyright © 2021 Zhang and Fong. This is an open-access article distributed under the terms of the Creative Commons Attribution License (CC BY). The use, distribution or reproduction in other forums is permitted, provided the original author(s) and the copyright owner(s) are credited and that the original publication in this journal is cited, in accordance with accepted academic practice. No use, distribution or reproduction is permitted which does not comply with these terms.

frontiers in Human Neuroscience

ORIGINAL RESEARCH
published: 07 June 2021
doi: 10.3389/fnhum.2021.656975

Brain-Computer Interface Coupled to a Robotic Hand Orthosis for Stroke Patients' Neurorehabilitation: A Crossover Feasibility Study

Jessica Cantillo-Negrete[1], Ruben I. Carino-Escobar[1], Paul Carrillo-Mora[2], Marlene A. Rodriguez-Barragan[3], Claudia Hernandez-Arenas[3], Jimena Quinzaños-Fresnedo[3], Isauro R. Hernandez-Sanchez[3], Marlene A. Galicia-Alvarado[4], Adan Miguel-Puga[5] and Oscar Arias-Carrion[5,6]*

[1] Division of Research in Medical Engineering, Instituto Nacional de Rehabilitación "Luis Guillermo Ibarra Ibarra," Mexico City, Mexico, [2] Neuroscience Division, Instituto Nacional de Rehabilitación "Luis Guillermo Ibarra Ibarra," Mexico City, Mexico, [3] Division of Neurological Rehabilitation, Instituto Nacional de Rehabilitación "Luis Guillermo Ibarra Ibarra," Mexico City, Mexico, [4] Department of Electrodiagnostic, Instituto Nacional de Rehabilitación "Luis Guillermo Ibarra Ibarra," Mexico City, Mexico, [5] Unidad de Trastornos de Movimiento y Sueño (TMS), Hospital General "Dr. Manuel Gea González," Mexico City, Mexico, [6] Centro de Innovación Médica Aplicada (CIMA), Hospital General "Dr. Manuel Gea González," Mexico City, Mexico

OPEN ACCESS

Edited by:
Eduardo Fernandez, Miguel Hernández University of Elche, Spain

Reviewed by:
Faddi Ghassan Saleh Velez, Spaulding Rehabilitation Hospital, United States
Camila Bonin Pinto, Northwestern University, United States

***Correspondence:**
Jessica Cantillo-Negrete
jcantillo@inr.gob.mx

Specialty section:
This article was submitted to Brain Imaging and Stimulation, a section of the journal Frontiers in Human Neuroscience

Received: *08 February 2021*
Accepted: *12 May 2021*
Published: *07 June 2021*

Citation:
Cantillo-Negrete J, Carino-Escobar RI, Carrillo-Mora P, Rodriguez-Barragan MA, Hernandez-Arenas C, Quinzaños-Fresnedo J, Hernandez-Sanchez IR, Galicia-Alvarado MA, Miguel-Puga A and Arias-Carrion O (2021) Brain-Computer Interface Coupled to a Robotic Hand Orthosis for Stroke Patients' Neurorehabilitation: A Crossover Feasibility Study. Front. Hum. Neurosci. 15:656975. doi: 10.3389/fnhum.2021.656975

Brain-Computer Interfaces (BCI) coupled to robotic assistive devices have shown promise for the rehabilitation of stroke patients. However, little has been reported that compares the clinical and physiological effects of a BCI intervention for upper limb stroke rehabilitation with those of conventional therapy. This study assesses the feasibility of an intervention with a BCI based on electroencephalography (EEG) coupled to a robotic hand orthosis for upper limb stroke rehabilitation and compares its outcomes to conventional therapy. Seven subacute and three chronic stroke patients (M = 59.9 ± 12.8) with severe upper limb impairment were recruited in a crossover feasibility study to receive 1 month of BCI therapy and 1 month of conventional therapy in random order. The outcome measures were comprised of: Fugl-Meyer Assessment of the Upper Extremity (FMA-UE), Action Research Arm Test (ARAT), motor evoked potentials elicited by transcranial magnetic stimulation (TMS), hand dynamometry, and EEG. Additionally, BCI performance and user experience were measured. All measurements were acquired before and after each intervention. FMA-UE and ARAT after BCI (23.1 ± 16; 8.4 ± 10) and after conventional therapy (21.9 ± 15; 8.7 ± 11) were significantly higher ($p < 0.017$) compared to baseline (17.5 ± 15; 4.3 ± 6) but were similar between therapies ($p > 0.017$). *Via* TMS, corticospinal tract integrity could be assessed in the affected hemisphere of three patients at baseline, in five after BCI, and four after conventional therapy. While no significant difference ($p > 0.05$) was found in patients' affected hand strength, it was higher after the BCI therapy. EEG cortical activations were significantly higher over motor and non-motor regions after both therapies ($p < 0.017$). System performance increased across BCI sessions, from 54 (50, 70%) to 72% (56, 83%). Patients reported moderate mental workloads and excellent usability with the BCI. Outcome measurements implied that a BCI intervention

using a robotic hand orthosis as feedback has the potential to elicit neuroplasticity-related mechanisms, similar to those observed during conventional therapy, even in a group of severely impaired stroke patients. Therefore, the proposed BCI system could be a suitable therapy option and will be further assessed in clinical trials.

Keywords: electroencephalography, Fugl-Meyer, hemiparesis, motor intention, TMS, ARAT

INTRODUCTION

It is estimated that worldwide, 24.9 million people are living with ischemic stroke sequelae, and there are approximately 11.6 million new cases per year, making stroke one of the leading causes of disability (Benjamin et al., 2018). Stroke sequelae include complete or partial paralysis of one hemibody, known as hemiparesis (Bruce, 2005). Treatment for hemiparesis focuses on motor rehabilitation strategies that aim to enhance neural plasticity, stroke's primary recovery mechanism (Bruce, 2005; Pekna et al., 2012). These strategies are most effective during the acute and subacute phases of stroke (Lee et al., 2015; Branco et al., 2019). Specifically, upper limb motor recovery seems to occur predominantly during these stages (Borschmann and Hayward, 2020). However, it has been reported that motor rehabilitation of the upper limb is difficult to achieve for most patients; 6 months after stroke onset, approximately 65% of patients are unable to use the affected upper limb in their daily activities (Bruce, 2005; Lee et al., 2015). Therefore, assessing the efficacy of new upper limb rehabilitation technologies is currently of interest to research (Hatem et al., 2016; Bertani et al., 2017).

Brain-Computer Interfaces (BCI) is a promising technology for upper limb stroke rehabilitation. These systems allow users to control an external device by decoding their intentions from the central nervous system, typically from electroencephalogram (EEG) recordings (Wolpaw et al., 2002). BCI systems comprise four stages: brain signal acquisition, processing, external device control, and feedback. Mental rehearsal of movement, attempted movement, or motor intention (MI), elicits activations over the sensorimotor cortex (Monge-Pereira et al., 2017). Studies confirm that stroke patients can control a BCI using this MI. MI can elicit increased or decreased alpha (8–13 Hz) and beta (14–32 Hz) oscillations in the EEG with respect to baseline. These cortical activations, known as event-related desynchronization/synchronization (ERD/ERS) (Pfurtscheller and Lopes Da Silva, 1999), are similar to those produced by passive movement and motor execution (Carrillo-de-la-Peña et al., 2008; Kraeutner et al., 2014). There is some evidence that BCI based on MI and coupled to assistive robotic devices promotes neural plasticity by providing somatosensory feedback while the subject executes MI of the paralyzed upper limb (Remsik et al., 2016; Monge-Pereira et al., 2017). This closed-loop somatosensory stimulation has the potential to enhance motor-related cortical activity in healthy subjects (Cantillo-Negrete et al., 2019) and stroke patients (Ono et al., 2014), ultimately aiding in restoring function to the affected upper limb.

Although BCI systems with different feedback types, such as visual, robotic, and functional electrical stimulation (FES) devices, have shown great potential for upper-limb rehabilitation of stroke patients, their efficacy is under evaluation by different research groups. For a review, see López-Larraz et al. (2018) and Cervera et al. (2018). However, most of these studies are on chronic stroke patients (Ramos-Murguialday et al., 2013; Ang et al., 2014; Ono et al., 2014). Few studies of BCI coupled to robotic assistive devices have focused on patients in earlier stroke stages (Frolov et al., 2017). Moreover, to the authors' knowledge, little has been reported that compares the effects of these devices for upper limb motor recovery after stroke to those of conventional therapy. Studies with the largest reported sample sizes have provided conventional therapy simultaneous to the intervention with the BCI coupled to a robotic device, without a direct comparison between them (Ramos-Murguialday et al., 2013; Frolov et al., 2017). Their direct comparison may help define a potential role for BCI interventions in the clinical environment for stroke patients. The implementation of these systems would reduce dependence on the availability of physiotherapists, which could effectively increase the amount of upper limb therapy stroke patients receive in the critical window after injury, thereby lessening the burden of stroke in healthcare systems worldwide.

Therefore, this study assesses the feasibility of an intervention with an MI-based BCI coupled with a robotic hand orthosis for upper limb stroke rehabilitation (referred to as ReHand-BCI) and compares patients' outcomes with those obtained with conventional therapy. For this purpose, subacute and chronic stroke patients were recruited for a crossover pilot study, in which two groups of patients received both BCI and conventional upper limb therapy in a different sequence. The Fugl-Meyer Assessment of Upper Extremity (FMA-UE) and the Action Research Arm Test (ARAT) (Lang et al., 2006) were used for assessing upper limb motor recovery after each treatment. Hand dynamometry, transcranial magnetic stimulation (TMS), BCI performance, quantitative EEG, and user experience were also evaluated to complement the clinical measurements.

MATERIALS AND METHODS

Patients

Patients meeting the following criteria were invited to participate by medical specialists from the stroke rehabilitation service of the medical institution in which this study was conducted. Inclusion criteria: adults (>18 years) diagnosed by a neurologist with ischemic stroke in either hemisphere confirmed by magnetic resonance imaging (MRI) or computed tomography (CT). No less than 2 months and no more than 12 months since the onset of stroke. Study subjects presented mild to severe hand paralysis [Motricity Index = 0, 11 or 19 (Demeurisse et al., 1980)] and

were right-handed before the stroke. Subjects had normal or corrected to normal vision. Most had mild alterations in attention and memory processes according to the neuropsychological test NEUROPSI (Ostrosky et al., 2019) and demonstrated an adequate understanding of instructions according to the Boston Diagnostic Aphasia Examination (BDAE-3) (Goodglass et al., 2005). Exclusion criteria were: severe spasticity (Modified Ashworth Scale score $>$ 2) in finger regions, severe aphasia (severity scale score $\geq$ 2), and history of other previous neurological lesions. Elimination criteria included the patients' determination to withdraw from therapy, pain in the upper limb, epilepsy, seizures, or symptoms of any other neurological disorder during the study.

ReHand-BCI System

The ReHand-BCI is controlled by MI of the stroke patients' paralyzed hand and includes the following stages:

- Acquisition stage: EEG signals were recorded using a cap with 11 active electrodes (g.LadyBird, g.tec). Electrodes were placed on F3, C3, T3, P3, Fz, Cz, Pz, F4, C4, T4, and P4 according to the international 10-20 system. The reference electrode was placed in the right earlobe, and the ground electrode was placed in the AFz position. Each channel was amplified and digitalized with a g.USBamp amplifier from g.tec connected to a PC at a sampling rate of 256 Hz with 24-bit A/D resolution.
- Processing stage: Windows of one-second length were processed following these phases. The first phase consisted of the temporal filtering of the acquired multichannel EEG using subject-specific frequency bands, selected following an offline setup described below. A 30th-order FIR notch filter was also applied to the EEG signals. The second phase comprised spatial filtering using the Common Spatial Pattern (CSP) algorithm (Blankertz et al., 2008). Afterward, in the third phase, Linear Discriminant Analysis (LDA) was used for classification. Spatial filters and LDA coefficients were computed as described below. This processing stage is similar to the Filter-Bank Common Spatial Patterns (FBCSP) algorithm (Ang et al., 2008). The processing stage's algorithms were programmed using the MATLAB 2015b software. A more detailed description of the online processing stage's algorithms can be found in a previous work by Cantillo-Negrete et al. (Cantillo-Negrete et al., 2018).
- Robotic Hand Orthosis Control: If the processing stage detected MI of the stroke patients' paralyzed hand, a Bluetooth wireless command was sent to a robotic hand orthosis fixed to that hand, which then provided passive flexion and extension of their paralyzed fingers (Martinez-Valdes et al., 2014). Patients were shown faces with different degrees of smiling expressions after a defined number of trials had elapsed (a run of the system). This feedback indicated the number of times the system correctly identified MI and activated the robotic hand orthosis.
- Computation of subject-specific parameters: These parameters were computed to set up the online BCI processing stage. First, acquired multichannel EEG were visually inspected to discard trials with excessive artifacts. Afterward, temporal filtering using six 30th-order FIR bandpass filters in the 8–12, 12–16, 16–20, 20–24, 24–28, and 28–32 Hz frequency bands was performed, and a 30th-order FIR notch filter was also applied to the EEG signals. Then, CSP spatial filtering was performed. Spatial filters were calculated by solving the eigenvalue of the covariance matrices of the MI and rest classes, which resulted in 11 spatial filters for each sub-band; thus, 66 features were computed for each trial. Next, the feature selection algorithm using Particle Swarm Optimization (PSO) (Shi and Eberhart, 1998) was applied to select the least number of features for which a higher classification accuracy could be obtained. PSO parameters were set based on previous studies (Cantillo-Negrete et al., 2017, 2018), with the stopping criteria of the algorithm set at either finding a combination of features for which 100% of classification accuracy could be reached or when 50 generations (iterations) had elapsed. Finally, the fourth phase is an LDA classifier, which uses a subset of the 66 features obtained with CSP as input. This combination of temporal and spatial filtering and particle swarm optimization used for feature selection is referred to as FBCSP+PSO. After this process, subject-specific frequency bands, CSP filters, and LDA coefficients were used for the online implementation of the algorithm.

Previous studies had shown that stroke patients could control the ReHand-BCI with the 11 electrode configuration (Cantillo-Negrete et al., 2017, 2018) and that the ReHand-BCI could be set up in less than 10 min. To determine if the robotic hand orthosis was apt for BCI feedback, its capability to promote cortical activations above the sensorimotor cortex was first confirmed in healthy subjects (Cantillo-Negrete et al., 2019). The ReHand-BCI system is depicted in **Figure 1**.

Study Design

A randomized crossover pilot study was planned with a convenience sample of at most 10 subacute and chronic stroke patients, as is recommended in feasibility studies for early clinical evaluation of medical devices (FDA, 2011; Billingham et al., 2013). Patients were randomly allocated to one of two different sequences of therapeutic intervention. The sequence for group 1 (AB) was comprised of 12 sessions of BCI therapy (A) followed by 12 sessions of conventional upper limb therapy (B). While the sequence for group 2 was, first 12 sessions of conventional therapy (B), then 12 sessions of BCI therapy (A). Each therapeutic intervention consisted of three sessions per week for 4 weeks. Standard treatment for stroke sequelae, including lower-limb and speech therapy, was unrestricted for the study subjects. The experimental sessions were added to the patients' standard treatment, with both groups receiving conventional upper limb therapy. Simple randomization was programmed in Microsoft Excel® and was blinded for all study participants, except for the researcher who executed the program. **Figure 2** shows a diagram of the experimental study's design.

Before the group assignment, baseline clinical assessments were obtained for each patient, including FMA-UE and ARAT. Stroke diagnosis was confirmed with an MRI study. Physiological measurements such as hand dynamometry (HD), TMS and EEG, were also assessed at baseline. After each group's first therapy, FMA-UE, ARAT, HD, TMS, and EEG were measured again. Then after the crossover therapy, these same measurements were repeated.

Baseline EEG

Baseline EEG was recorded to obtain the patients' offline performance and rule out exclusion criteria such as other neurological pathologies. EEG acquisition was performed in two sessions to avoid patient fatigue. In each session, patients performed four tasks; affected hand motor imagery, non-affected hand motor imagery, affected hand movement intention, and non-affected hand movement execution (80 trials per task, 320 trials in total). Only the 80 trials of affected hand motor intention were used to compare ERD/ERS at baseline and after therapies. The post-therapy EEGs were acquired in a single session of 60 trials similar to a therapy session. Recordings were done in a sound-attenuated closed room, with a computer screen placed at approximately 1.5 m from patients seated in a comfortable armchair. The electrode positions and recording system were the same as with the ReHand-BCI (see section "ReHand-BCI System"). Visual and auditory cues, based on the Graz paradigm (Pfurtscheller and Neuper, 2001), were shown to patients, instructing them when to perform MI. **Figure 3A** shows the timing of the visual and auditory cues during baseline recordings.

BCI Therapy

Sessions were conducted in the same sound-attenuated room and under the same experimental conditions as those used for baseline EEG (see section "Baseline EEG"). First, an EEG cap with 11 electrodes as mentioned above was adjusted to the patient's head; next, the robotic hand orthosis was fitted to the stroke patients' affected hand. Afterward, visual and auditory cues signaled patients when to initiate MI of their hand, which involved the intention of continuous finger flexion and extension. Each session included three runs of 20 trials each (60 trials, i.e., attempts of MI per session). The time structure of each trial was as follows. The first 3 s were of REST, then an arrow pointing at the stroke patient's affected hand signaled the onset of MI. The arrow was shown for 1.5 s, after which the screen turned black until the 8 s mark of the trial. From 8 to 12 s, feedback was either provided by the robotic hand orthosis, which passively flexed

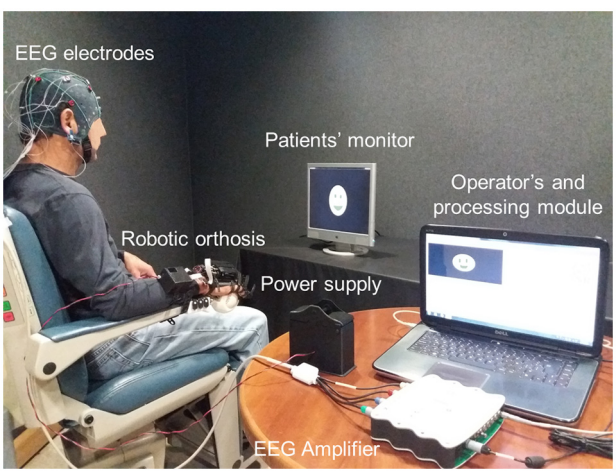

FIGURE 1 | ReHand-BCI system. Acquisition stage comprised of EEG electrodes, amplifier, and A/D converter. The processing module included CSP, PSO, and LDA programmed in a PC, which also has a graphical user interface for setting up therapy parameters. Commands are sent through wireless communication from the PC to the robotic hand orthosis.

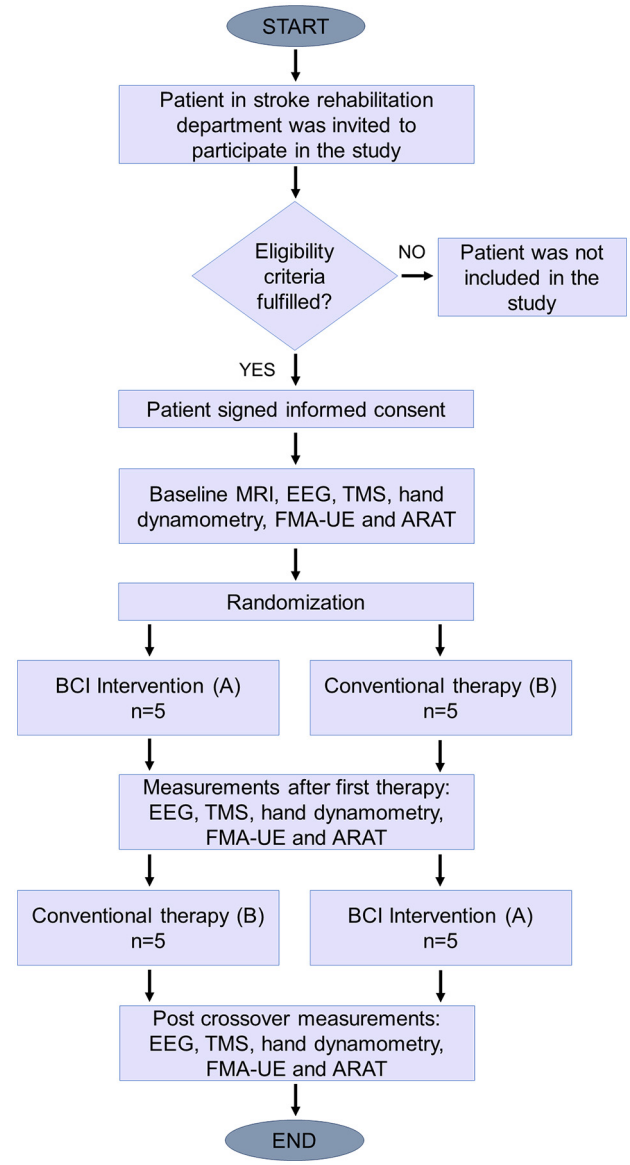

FIGURE 2 | Study design diagram. After eligibility criteria were assessed, patients were assigned randomly to one of the two sequences.

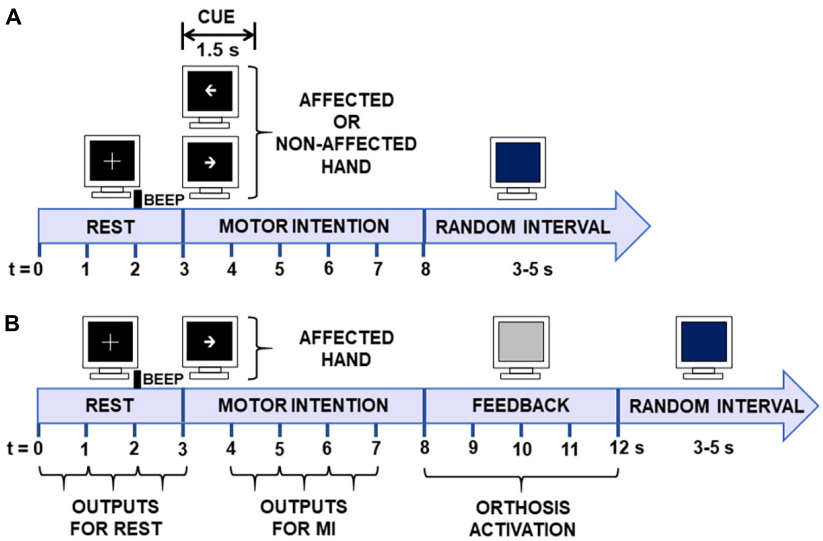

FIGURE 3 | Time diagrams of offline and online trials. **(A)** Baseline EEG recordings. During the first 3 s, patients rested with their eyes open (REST). From 3 to 4.5 s, an arrow signaled them to initiate MI with the affected or unaffected limb. MI was performed from 3 to 8 s. The data from REST (0–3 s) and MI (4–7 s) periods were used for posterior EEG analyses. **(B)** Online BCI trials. The first 3 s was used for classification of the REST condition, and from 4 to 7 s for MI of the affected limb.

then extended the fingers, or by non-activation of the orthosis. During the feedback period, the screen turned gray. From 12 s onward, a blue screen signaled to patients that they could move or relax and lasted for a random interval of 3–5 s to prevent habituation. Following this interval, a new trial started, or if 20 trials had already elapsed, then a resting period of a least 1 min was observed before the next run started. The time structure of the trials is shown in **Figure 3B**. The duration of each session ranged from 30 to 40 min, depending on the time needed to place the electrodes and fit the robotic orthosis.

In the first session, the robotic orthosis was activated in all 60 of the trials to obtain MI and REST data used to set the BCI processing stage of the following session and for patients to get familiarized with the system. From the second session onward, the BCI processing stage was configured (see section "ReHand-BCI System") with data from the previous session, and the robotic orthosis was only activated if at least two 1-s time windows of the MI interval were correctly classified. Patients' online performance was computed for each of the 12 sessions. For each trial, classification accuracy was computed as the percentage of correct classified 1-s windows of REST and MI of each trial (see **Figure 3B**). Then, the classification accuracy of all 60 trials recorded per BCI intervention session was averaged for each patient. Afterward, the grand averaged classification accuracies were computed.

At the end of each patient's last session of BCI, they answered the NASA Task Load Index (NASA-TLX) (Hart and Staveland, 1988) and System Usability Scale (SUS) (Brooke, 1996) questionnaires that assessed the subjective mental workload and the quality of the user experience when interacting with the ReHand-BCI. The raw NASA-TLX was used (the version that does not incorporate a multi-dimensional rating procedure), as evidence suggests that this version might increase experimental validity (Bustamante and Spain, 2012; Hart, 2012).

Conventional Therapy

Conventional therapy was conducted in identical environmental conditions and by the same experienced professional therapist from the brain plasticity service. The intervention consisted of activities aimed at improving function of the affected upper limb, including neurofacilitation techniques for strengthening muscle tone and increasing voluntary movement, sensitivity reeducation, stretching, activities for the improvement of fine and gross grip, mobility arcs, muscle strength, and coordination. The duration of each session ranged from 30 to 40 min, depending on the time it took patients to complete the same exercise routine. **Figure 4** shows a patient's execution of upper-limb rehabilitation exercises during conventional therapy.

Outcome Measurements

Clinical guidelines state that the FMA-UE should be used for sensitivity and motor evaluations of stroke patients and the ARAT for motor assessment of upper-limb function (Winstein et al., 2016). FMA-UE is the primary outcome measure reported by studies aiming to assess BCI efficiency for stroke rehabilitation (Ramos-Murguialday et al., 2013; Ang et al., 2014, 2015; Frolov et al., 2017). The ARAT has also been used as a primary or complementary outcome measure in BCI-based stroke rehabilitation studies (Frolov et al., 2017). Therefore, these two clinical scales were used to assess patient's upper-limb motor recovery. The FMA-UE is a 0–66 item scale, in which a higher score represents less upper-limb motor impairment. The ARAT score ranges from 0–57; 0 is given if no upper-limb movements could be executed. FMA-UE

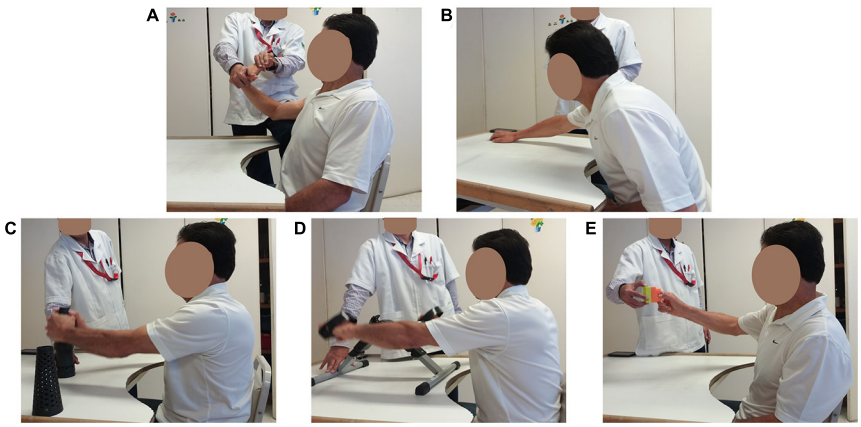

FIGURE 4 | Conventional therapy. **(A)** Finger and wrist stretching exercises. **(B)** Arm stretches. **(C)** Gross pinch and lifting objects. **(D)** Gross pinch and rotating arm exercise. **(E)** Fine pinch grip lifts.

and ARAT measurements were taken three times for each patient, at baseline, after the first therapy, and after the crossover therapy.

For HD, grip and pinch strength of the affected hand were assessed using the Biometrics E-link evaluation system. The dynamometer was placed in the second handle position. First, three measurements of grip strength were taken of the unaffected hand; if the coefficient of variation (Kroemer and Marras, 1980) was above 15%, then the measurements were repeated. Afterward, the affected hand was assessed using the same procedure. Patients had a 1-min rest period between measurements. Pinch strength was assessed using the same procedure but by measuring the force exerted between the index and thumb fingers. These measurements were used to compute the average grip and pinch strength for each hand per session.

For TMS, a baseline MRI was used for the neuronavigation system. It was obtained by acquiring an image sequence using a 64-channel head coil (Siemens Skyra 3.0T, Erlangen, Germany). The anatomical scan collected 192 mm × 1.2 mm thick slices with a voxel size of 1 mm × 1 mm × 1.2 mm, repetition time and echo time (TR/TE) of 2050/2.43 ms, field of view (FOV) 256 × 256 and matrix 256 × 256, and a coronal sequence for neuronavigation.

Single-pulse TMS motor evoked potentials (MEPs) were recorded by a physician trained to use a Rapid2 MAGSTIM device with a figure-of-eight coil. A bipolar EMG with a sampling frequency of 1,500 Hz was placed in the first dorsal interosseous muscle of both affected and unaffected hands. Each TMS session started with an initial mapping of the sensorimotor cortex of the patients' unaffected hemisphere (UH), using MRI-guided stereotaxic neuronavigation, following the relative-frequency method described by Rossini et al. (Rossini et al., 2015) to determine the resting motor threshold (RMT). Then, stimulus intensity was lowered in steps of 1% MSO until MEPs were not detected in less than five out of 10 trials. Next, using this stimulus intensity plus 1 (i.e., the RMT), 30 trials were recorded to compute the MEP amplitude of the UH motor cortex. Afterward, the same procedure was used for the affected hemisphere (AH). It has been reported that at least 20 trials of MEP recordings should be made for reliable assessment of single-pulse MEPs (Biabani et al., 2018). Therefore, each session's MEP peak to peak amplitude was computed using an automatic recognition software that averaged maximum and minimum values from the 20 trials with the fewest artifacts (Tecuapetla-Trejo et al., 2020). MEP amplitude was used to assess the corticospinal tract integrity of patients before and after the interventions.

EEG recordings were first filtered with a 30th-order FIR bandpass filter from 8 to 32 Hz and a 30th-order FIR notch filter from 58 to 62 Hz. Afterward, a common average reference (CAR) spatial filter was applied on each channel to reduce reference placement effects on the EEG signal (Bertrand et al., 1985). Visual inspection of the EEG readouts was performed to identify and reject trials with artifacts. Alpha (8–13 Hz) and beta (14–32 Hz) ERD/ERS (Pfurtscheller and Lopes Da Silva, 1999) were computed for each trial and channel, using Equation 1.

$$\%ERD/ERS = \frac{P_{MI} - P_{rest}}{P_{rest}} * 100 \quad (1)$$

Where P_{MI} is the MI task's power, and P_{rest} is the averaged power during the rest condition. Power was computed using the complex Morlet wavelet transform, as reported by Tallon-Baudry et al. (1999).

For the posterior statistical analysis, 3-s windows, including REST (0–3 s) and MI (4–7 s) intervals were extracted. Grand average topographic maps were computed with the ERD/ERS from baseline, after BCI, and after conventional therapy. To unify the data collected from patients' affected and unaffected hemispheres, ERD/ERS for the left hemisphere's channels (F3, C3, T3, and P3) of patients with right hemisphere lesions were interchanged with right hemisphere channels (F4, C4, T4, and P4). This change allowed all patient's cortical activity of the affected hemisphere to be shown over the left hemisphere's channels (FAH, CAH, TAH, and PAH) and the unaffected

hemisphere's activity to be shown over the right channels (FUH, CUH, TUH, and PUH).

Statistical Analysis

Outcome measures obtained at baseline, after BCI, and after conventional therapy were assessed for Gaussian distribution with a Lilliefors-corrected Kolmogorov-Smirnov test. Differences between groups' baseline clinical measurements were evaluated using non-paired *t*-tests (Wilcoxon rank-sum tests for non-Gaussian distributions). Repeated measurements analysis of variance (ANOVA) was used if data followed a Gaussian distribution; if not, an exact Friedman test was used to assess if significant differences were found between baseline and after both therapies. Multiple comparisons testing with paired *t*-tests (Wilcoxon signed-rank tests for non-Gaussian distributions) was performed with a Bonferroni correction applied. The binary outcome of the TMS results (presence or not of resting motor threshold) was analyzed with the McNemar test to assess differences between the two therapies, and a Cochran's Q test was used to identify differences between repeated measurements. To assess the reliability of the BCI, the practical level of chance, defined by Müller-putz et al. (2008) as the upper confidence interval of a random classifier's accuracy, was computed with a binomial distribution using a significance level of 0.05. For all statistical tests, the significance level (α) was set at 0.05. Statistical analysis was done using the SPSS v.17 software.

RESULTS

Clinical Outcomes

In total, 11 patients were included in this study; patient P2 was eliminated after presenting a mild convulsive episode after the conventional therapy (B) and before the BCI intervention (A). The patient (male, 53 years old, 160 days since stroke onset) did not report previous seizure events at enrollment in the study nor during the baseline TMS session (MEPs were elicited in both hemispheres). His elimination from the study was due to the possibility that another neuropathology triggered the seizure event and could affect his motor recovery. Demographic data for each patient is shown in **Table 1**.

The recruited sample was balanced regarding gender and affected hemisphere. Seven patients were in the subacute (7 days to 6 months) and three in the chronic (>6 months) phase of stroke (Bernhardt et al., 2017). Their age range was between 43 and 85 years at the beginning of the study. Most patients presented subcortical stroke (n = 8), one patient had a cortical stroke (n = 1), and one patient had a cortical-subcortical stroke (n = 1). The patients' age was similar for sequence AB and BA, $t(8) = -0.023$, $p = 0.398$. However, there was a significant difference in time after stroke onset, $t(8) = 2.38$, $p = 0.023$. The baseline clinical and HD data were similar for both sequences (FMA-UE, $p = 0.214$; ARAT, $p = 0.326$; grip strength, $p = 0.167$; pinch strength, $p = 0.683$). **Table 2** shows FMA-UE, ARAT, and HD scores at baseline and after both therapies.

TABLE 1 | Demographic data of stroke patients included in the present study, including therapy sequence allocation.

ID (Sequence)	Gender	Hemiparesis	TSSO (days)	Age (years)	Lesion, type, and location	Baseline FMA-UE, ARAT	Baseline grip, pinch strength (Kgf)	MEPs in AH
P1(AB)	Female	Right	280	54	Subcortical. L. Lentiform Nucleus, L. Internal Capsule, and L. Thalamus.	12, 0	0.6, 0.1	No
P3(BA)	Female	Left	81	85	Subcortical. R. Pontine Tegmentum.	13, 3	1.3, 0.7	Yes
P4(AB)	Female	Right	218	58	Subcortical. L. Lentiform Nucleus, L. Internal Capsule.	9, 5	0.5, 0	Yes
P5(BA)	Female	Left	146	54	Cortical-Subcortical. R. Insula, R. Lentiform Nucleus, R. Internal Capsule.	9, 0	0.5, 0	No
P6(BA)	Male	Left	37	43	Subcortical. R. Pontine Tegmentum.	8, 0	0.2, 0.2	No
P7(AB)	Male	Right	100	48	Subcortical. L. Internal Capsule.	15, 0	1.9,0	No
P8(BA)	Male	Right	97	53	Cortical. L. Insula	14, 3	0.7, 0	No
P9(AB)	Male	Right	260	63	Subcortical. L. Lentiform Nucleus, L. Internal Capsule.	59, 21	9.7, 2.3	Yes
P10(BA)	Male	Left	87	65	Subcortical. R. Internal Capsule. R. Thalamus.	12, 3	0, 0	No
P11(AB)	Female	Left	98	76	Subcortical. R. Internal Capsule.	24, 8	0.8, 0.5	No
Mean (SD)			**140 (83)**	**59.9 (12.8)**		**17.5(15.3), 4.3(6.4)**	**1.62(2.9), 0.38(0.72)**	

TSSO, Time since stroke onset; AH, Affected Hemisphere.
Patients' age and time since stroke onset are relative to the beginning of the study. The presence of Motor Evoked Potentials (MEPs) was assessed with Transcranial Magnetic Stimulation before interventions.
The bold values are the mean and the standard deviation of values of the fourth and fifth columns of the table.

TABLE 2 | Clinical and hand dynamometry (kgf) outcomes.

Outcome Measure	Baseline (BL)		BCI (A)		Conventional (B)		*p*	Pairwise Comparison
	Mean (SD)	Median [IQR]	Mean (SD)	Median [IQR]	Mean (SD)	Median [IQR]		
FMA-UE	17.5 (15.3)	12.5 [9;17]	23.1 (16.1)	**15.5** [13;30]	21.9 (15.5)	15 [12;35]	0.014	BL > A*; BL > B*; A = B
ARAT	4.3 (6.4)	3 [0;6]	8.4 (10.1)	**4.5** [0;16]	8.7 (11.3)	**4.5** [0;16]	0.001	BL > A*; BL > B*; A = B
HD(grip)	1.62 (2.9)	0.65 [0.4;1.5]	2.42 (3.3)	**1.35** [0.3;1.4]	1.58 (2.6)	0.90 [0.7;3.2]	0.682	–
HD(pinch)	0.38 (0.72)	0.05 [0;0.6]	0.45 (0.48)	**0.30** [0.8;0.3]	0.29 (0.48)	0.15 [0.1;0.7]	0.376	–

*HD, Hand Dynamometry; SD, Standard Deviation; IQR, Interquartile Range; *p < .017.*
Highest median values are shown in bold.

An exact Friedman test showed a statistically significant difference between FMA-UE scores measured at baseline, after BCI therapy, and after conventional therapy (**Table 2**). *Post hoc* tests using an exact Wilcoxon signed-rank test with a Bonferroni-adjusted alfa level showed a statistically significant increase in FMA-UE scores after BCI and conventional therapy compared to baseline. However, the scores after BCI and conventional therapy were not significantly different. FMA-UE scores measured before and after BCI therapy indicated an average gain of 2.4 (SD = 3.2), and before and after conventional therapy showed an average gain of 3 (SD = 7.7). Therefore, after completing the interventions, the mean FMA-UE score increased by 5.4 points.

Similarly, an exact Friedman test showed a statistically significant difference in ARAT scores measured at baseline, after BCI therapy, and after conventional therapy (**Table 2**). *Post hoc* tests demonstrated that ARAT scores after BCI and after conventional therapy were significantly higher than baseline. However, BCI and conventional therapy scores were not significantly different. ARAT scores measured before and after BCI therapy indicated an average gain of 2.1 (SD = 3.2), and before and after conventional therapy showed an average gain of 3 (SD = 5.1). So, after completing the interventions, the mean ARAT score increased by 5.1 points. An average FMA-UE gain of 4.6 (SD = 7.5) was observed in patients after the first intervention, while an average FMA-UE gain of 0.8 (SD = 2.5) was observed after the second intervention. An average ARAT gain of 3.4 (SD = 5.1) was observed in patients after the first intervention, followed by a gain of 1.7 (SD = 2.9) after the second intervention.

Hand Dynamometry

The outcomes for grip and pinch strength of each stroke patients' paralyzed hand are presented in **Table 2**. Although an exact Friedman test shows no statistical difference in grip strength measured at baseline, after BCI, and after conventional therapy, median grip strength of the patients' paralyzed hand was higher after BCI. Similarly, there was no statistically significant difference between pinch strength measured at baseline and after both interventions; however, median pinch strength after BCI was higher than after conventional therapy.

TMS Outcomes

Figure 5 shows the MEP amplitudes of each patient before and after each therapy. Patients presented the most pronounced differences in the AH. The highest difference in median MEP amplitude was observed in the AH after the BCI intervention (Δ = 132 μV), while after conventional therapy, this difference was less pronounced (Δ = −52 μV). In the UH, differences of median MEP amplitude were not as pronounced as in the AH (Δ = 3 μV after the BCI and Δ = 66 μV after conventional therapy). Two patients that did not present MEPs in their AH before the BCI presented them after the intervention, whereas one patient that did not present MEPs in the AH before conventional therapy presented them after the intervention.

Median resting motor thresholds in the UH were between 63–66% of the maximum output of the TMS system, while in the AH, they were between 87–100%. As resting motor thresholds and MEPS were not detected in all patients, statistical analyses could not be done on TMS continuous measurements. Therefore, MEPS in the affected hemisphere were analyzed as binary outcomes, considered either detected or not. A McNemar's test determined no statistical difference ($p > 0.05$) between BCI and conventional therapy regarding MEP presence. Besides, a Cochran's test showed that statistically, there was no difference in detection/presence of MEPS between baseline, after BCI, and after conventional therapy ($p > 0.05$).

Quantitative EEG

Figure 6 shows grand averaged ERD/ERS during MI of patients' affected hand at baseline and after interventions. Also, for each band, the results of exact Friedman tests, with Bonferroni correction for comparing channels' ERD/ERS are given. In alpha (8–13 Hz), comparisons with baseline activations showed that after the BCI intervention, patients presented significant ERD/ERS differences in more regions (central, temporal and parietal) than the regions with significant differences observed after conventional therapy (frontal and temporal). The only significant difference noted between BCI and conventional therapies was in the central sagittal area, with more pronounced ERD elicited after the BCI therapy. In beta (14–32 Hz), ERD/ERS differences after the BCI compared to baseline were detected in frontal and parietal regions. After the conventional therapy, significant differences were evident in frontal channels compared to baseline measurements. Differences between ERD/ERS after the BCI and conventional therapies were only significant in the frontal and parietal regions of the AH.

BCI Performance

The grand average percentage of classification accuracy (%CA) during each of the 12 BCI sessions is shown in **Figure 7**. Since the last session's (session 12) percentage of classification accuracy

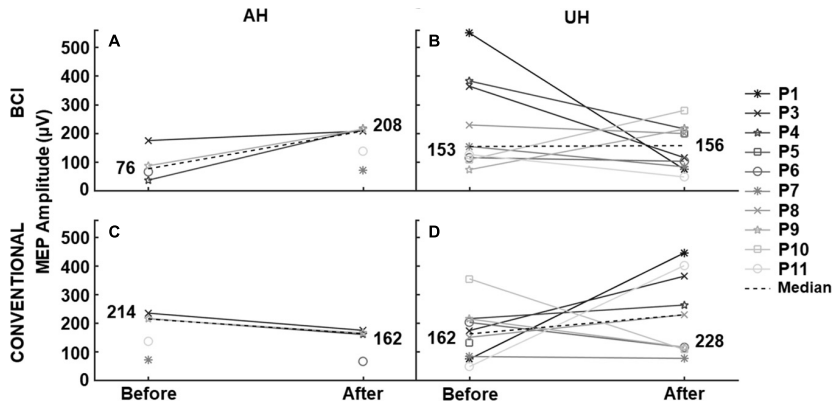

FIGURE 5 | MEP amplitude before and after each intervention. TMS elicited median MEP amplitude in patients' affected (AH) and unaffected (UH) hemispheres, before and after the BCI and conventional therapies. Patients that did not present MEPs are not shown in the measurements.

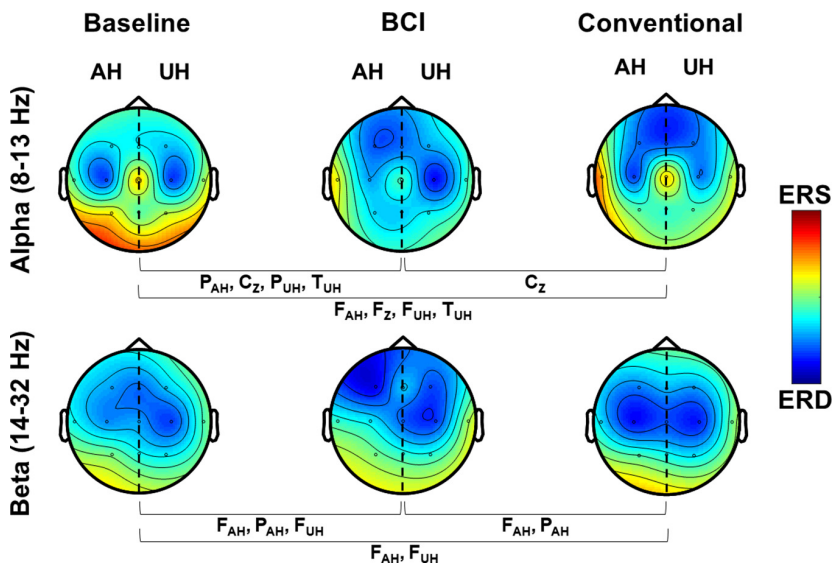

FIGURE 6 | Grand average ERD/ERS maps in alpha and beta. ERD/ERS is shown over affected and unaffected hemispheres during MI (4–7 s). Channels that presented significant differences ($p < 0.017$) between measurements are shown.

(%CA) had the highest median, we only compared this session's %CA with the %CA of the other sessions (session 2 to 11). Session 1 was not compared because it was a calibration session. Therefore, *post hoc* analysis with Wilcoxon signed-rank tests was done with a Bonferroni correction ($p = 0.05/10$) since 10 comparisons were performed. Significant differences were only observed between session 12 with sessions 2 and 4. Only the second session's median %CA was below the practical level of chance (58%). A positive linear trend of 0.61 was computed from %CA and session number using linear regression analysis ($R^2 = 0.47$, $p = 0.002$), which suggests that classification accuracy increased across sessions.

User Experience With the BCI

Figure 8A shows the average SUS scores given by each patient that underwent BCI therapy. For the SUS graph, patients rated different aspects of the system's usability with a descriptive adjective ranging from "best imaginable" to "worst imaginable," per the study of Bangor et al. (2009). Eight patient's assessment of the system was within the best possible range. One patient rated the system in the second-best range (P6), and one patient graded its usability in the acceptable range (P1). **Figure 8B** displays averaged NASA-TLX scores. Adjectives words were added to figure based on the rating scale's endpoints. Their responses indicated high overall performance and low frustration with the system. Also, patients stated that using the system required moderate mental demand and effort and low to moderate physical and temporal demand.

DISCUSSION

While FMA-UE and ARAT measurements showed no significant differences in patients' upper limb motor recovery between the

BCI and conventional therapy, patients were less impaired after either intervention, which suggests both interventions effectively increased upper limb motor function in stroke patients. A relevant point to consider is that the conventional therapy involved gross pinch and different upper-limb movements, unlike the BCI, that only comprised gross pinch. However, clinical outcomes showed that the effects of both interventions were similar. Therefore, although the BCI therapy only targeted finger flexion-extension, it was hypothesized that the ReHand-BCI could also benefit motor recovery due to the closed-loop communication between the patient and their affected upper limb that it provides. This hypothesis is reinforced by other BCI studies that reported lower stroke rehabilitation outcomes of control groups that only received passive movement feedback (Li et al., 2014) or sham feedback (Ramos-Murguialday et al., 2013; Frolov et al., 2017).

In the present study, changes in FMA-UE after BCI were between 2.4 ± 3.2, which is within the range of the study of Ang et al. (Ang et al., 2015) (4.55 ± 6.1) and Ramos-Murguialday et al. (2013) (3.4 ± 2.2). It is important to remark that the mean gain of FMA-UE scores in our study was lower than those reported in the aforementioned studies. However, in the study of Ang et al., mean FMA-UE scores at baseline were 26.3 ± 10.3, while in the present study, they were 17.5 ± 15.3. This difference suggests that our patients had more upper limb motor impairment at baseline, and therefore, as stated in other works, their probability of achieving upper limb motor recovery was lower (Bruce, 2005; Lee et al., 2015). Also, Frolov et al. (2017) reported a median FMA-UE difference of three points in subacute stroke patients after therapy with a BCI, which is within the observed range of 2.4 ± 3.2 in our study. However, these FMA-UE differences were below the range of 7.2 ± 2.3 reported in another study of Ang et al. (2014) after 1.5-months of BCI coupled to a robotic hand knob. Possible explanations for these results could be the longer duration of their BCI therapy and lower baseline upper limb motor impairment (33 ± 16.2). Therefore, the upper limb motor recovery of the patients in this study was similar to what has been reported for other BCI coupled to robotic assistive devices with a comparable duration of therapy and upper limb impairment at baseline, and lower than studies reporting longer BCI interventions, or patients with lower baseline upper limb motor impairments.

To the authors' knowledge, only Frolov et al. (Frolov et al., 2017) have reported stroke patients' ARAT scores after upper limb rehabilitation using a BCI system coupled to a robotic assistive device. In their work, a median difference of two points in the ARAT score was reported after the BCI therapy in subacute stroke patients, which is within the range observed in the present study. This finding implies that the ReHand-BCI could elicit a similar degree of motor recovery as a state-of-the-art BCI system coupled to a robotic assistive device designed for stroke patients' upper limb neurorehabilitation.

After each therapy, mean differences in the FMA-UE were not higher than the minimal clinically important difference (MCID) of 5.25 (Page et al., 2012), nor was the ARAT mean difference for any individual intervention higher than the MCID for ARAT of 5.7 (Van Der Lee et al., 2001). However, the mean gain in the FMA-UE observed in the present study after finalizing the interventions (M = 5.4) was higher than the MCID. Also, the MCID of the ARAT is close to the mean gain observed after completing the interventions in this study (M = 5.1); therefore, even to a small degree, patients' recovery may be noticeable in their daily living activities. It also highlights

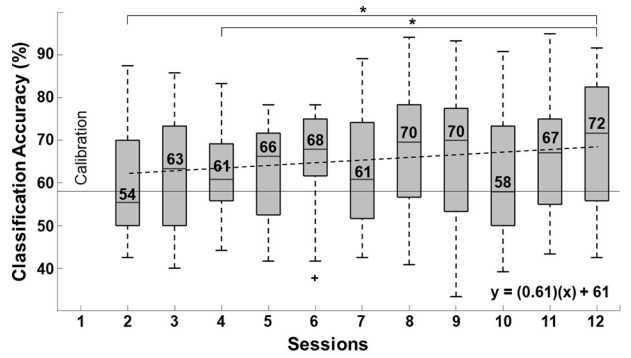

FIGURE 7 | Linear trend of BCI performance measured with the percentage of classification accuracy (%CA). Significant differences ($p < 0.005$) in %CA between consecutive sessions are indicated with (*). Outliers are also marked (+). The practical level of chance is shown as a horizontal broken line.

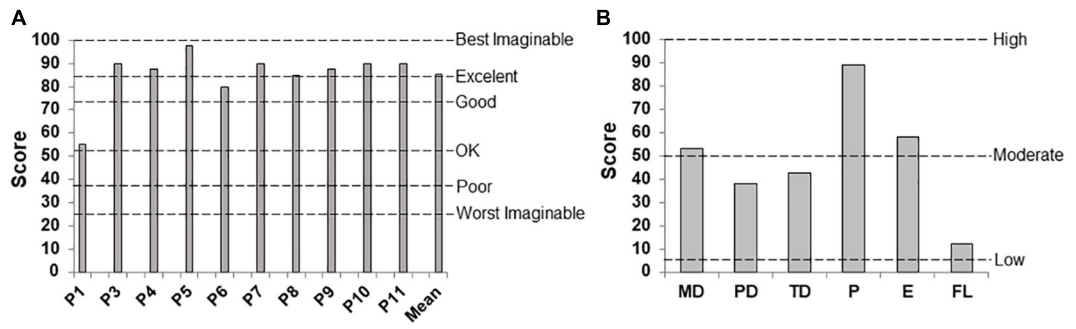

FIGURE 8 | User experience after concluding the BCI intervention. **(A)** System Usability Scale and **(B)** NASA-TLX, showing averaged scores assigned to the factors of Mental Demand (MD), Physical Demand (PD), Temporal Demand (TD), Overall Performance (P), Effort (E), and Frustration Level (FL).

that for stroke patients with severe baseline impairments to achieve clinically relevant gains in upper limb recovery, the duration of treatment should be more than 1-month and include more than 12 sessions. Also worthy of mention is that patients showed a higher average recovery in both FMA-UE and ARAT after the first therapy, compared to the recovery observed after the second therapy. Greater recovery after the first period of intervention, compared to the second, was also reported by Ang et al. (2014) since an average gain of 5.8 points in the FMA-UE score during three intervention weeks was followed by a lower gain of 1.4 after another 3 weeks of intervention in stroke patients. The lower motor recovery gain observed during the second intervention could have been caused by attenuation of treatment-driven functional recovery mechanisms due to less availability of residual neuronal substrate used for compensatory cortical reorganization processes (Stern, 2009; Alawieh et al., 2018). However, the effects of BCI and conventional treatments over time need to be assessed with a larger sample.

Most patients included in the present study were in the subacute stage of stroke, so spontaneous recovery was likely a contributing factor to patients' observed clinical outcomes. However, the magnitude of spontaneous recovery has been reported to be correlated with initial stroke severity (Cassidy and Cramer, 2017; Delavaran et al., 2017), and subacute patients with low scores of FMA-UE have been reported to have a lower degree of spontaneous recovery (Franck et al., 2017). Only one of the seven subacute patients that participated in the present study had moderate impairment (a score of 23 in FMA-UE), while the others had severe impairment (0–22 in FMA-UE) (Woodbury et al., 2013). Furthermore, most subacute patients had severely compromised corticospinal tract integrity, as shown by an absence of MEPs in their AH before interventions; which has been related to lower recovery prognosis (Stinear et al., 2017). Therefore, the recovery observed in the subacute patients of our study was likely to be associated with the effects of the BCI and conventional therapies.

Grasp and pinch dynamometry showed no significant differences between measurements taken at baseline or after either therapy. However, the highest median scores for both grasp and pinch were observed after the BCI. Also, after the BCI intervention, relative changes in median grasp strength were 108% higher than baseline measurements and 20% higher than a study that used an MI-based BCI without an assistive robotic device, reported by Prasad et al. (Prasad et al., 2010). The gain in grip strength after 1 month of the BCI intervention (Mdn = 0.65 kg) amounted to almost half the grip strength gain reported in a sample of severely impaired stroke patients (Mdn = 2 kg) after 12 months of conventional therapy (Franck et al., 2017). These results suggest that the ReHand-BCI may increase grip strength in patients' affected hands.

The majority of patients did not present MEPs when TMS was applied over their AH, which reinforces the statement that most had severe upper limb motor impairment and suggests that the integrity of the AH corticospinal tract of most patients was compromised. It also indicates that most patients in the present study had a poor prognosis. The PREP algorithm proposed by Stinear et al. (Stinear et al., 2017) predicts the potential for upper limb motor recovery after stroke; it shows an association between the absence of MEPs in the AH and adverse prognosis. Interestingly, two patients who did not present MEPs in the AH at baseline presented them after the BCI intervention. Furthermore, higher median MEP amplitudes over the AH after the BCI intervention could imply that neuroplasticity effects led to an increase in these patients' corticospinal integrity. Integrity of the corticospinal tract in the AH, measured with TMS, has been associated with decreased upper limb motor impairment in stroke patients (Delvaux et al., 2003; Stinear et al., 2017). However, due to the low number of patients that presented MEPs in the AH and the difficulty of finding MEPs in the AH of stroke patients overall, these observations must be confirmed in a larger sample.

After the BCI therapy, quantitative EEG showed that in alpha band, ERD was significantly more pronounced in central sagittal regions than at baseline and after conventional therapy. This finding implies that when patients' performed MI of their affected hand during BCI therapy, more areas of the sensorimotor cortex presented enhanced motor-related activity than at baseline or after conventional therapy. A possible explanation for this could be that the passive movement feedback provided by the robotic orthosis reinforced closed-loop communication between the sensorimotor cortex and the affected upper limb. As reported previously by our group (Cantillo-Negrete et al., 2019) and others (Ang et al., 2015), in healthy individuals and stroke patients, respectively, subjects presented more activity in alpha and/or beta after training with the BCI compared to baseline in areas not usually associated with motor tasks, such as frontal, parietal, and temporal regions. Also, frontal regions showed higher activations in beta after the BCI compared to conventional therapy, which could be due to an enlargement of the motor cortex area during motor-related tasks. This compensatory mechanism was observed by Ward et al. (2003) in severely impaired stroke patients using fMRI, in a review by Cassidy and Cramer (Cassidy and Cramer, 2017), and was hypothesized after the preliminary results of a longitudinal analysis of ERD/ERS across therapy sessions (Carino-Escobar et al., 2019). Although some BCI aimed for stroke rehabilitation only use activations from the AH (López-Larraz et al., 2018), the ReHand-BCI (that uses data from both hemispheres) could be enhancing cortical activations usually present in motor-related regions of the cortex and other areas. This enhancement may be associated with the neural plasticity observed during motor-related tasks in patients with severe motor impairment.

Despite variability in patients' BCI system control, a trend toward higher %CA was observed across therapy sessions. Patients' median control was only below the practical level of chance in the second session (which was the first session patients attempted to control the BCI) and was highest in the last session (72%). Increased %CA across sessions with a BCI coupled to robotic assistive devices has been previously reported in stroke patients by Ramos-Murguialday et al. (2013) and Frolov et al. (2017). In the present study, the only significant differences in patients' BCI control were observed between sessions 2 and 4 and the session with the highest median (session 12). This indicates that patients were achieving higher accuracy scores from the

fifth session onward, which is slightly sooner than patients in the study by Ramos-Murguialday et al. (2013), whose degree of control was higher from the seventh session forward. In the 12th session of the present study, patients obtained a median maximum accuracy with the ReHand-BCI of 72% [55.8, 82.5%]. These degrees of control are in the same range as those reported by Ang et al. (2011) of an average of 74% in 46 stroke patients, using a 27-electrode system. However, in the last session with the ReHand-BCI, patients' median accuracy was lower than the maximum accuracy range of 97.5–96.2% reported by Irimia et al. (2018) in five stroke patients controlling a BCI using 64 electrode positions, but within their minimum reported accuracy range (82.5–60%). A possible reason for this difference could be the enhanced spatial resolution of a BCI system with 64 electrode positions, compared to ReHand-BCI with 11. While a higher number of electrode positions has shown to increase %CA in BCI (Edlinger et al., 2015), an association between stroke patients' control accuracy of a BCI system and upper limb motor recovery has not been proven. Therefore, further research is needed to ascertain its relevance for stroke rehabilitation.

Responses to the SUS questionnaire suggest that stroke patients in this study found the ReHand-BCI easy to use. The NASA-TLX results indicate that only moderate mental demand and effort were needed to use the system. This level of effort may have helped maintain patients' motivation throughout the therapy, as it reflects that the task required for system control was neither easy nor too difficult. Patients evaluated their overall performance using the system as excellent. Therefore, the system could be improved by offering different levels of difficulty, which would help sustain their interest level during more extended treatment periods. Also, patients reported low frustration, coupled with low mental and temporal demands while using the ReHand-BCI. A system that is too demanding could make patients feel frustrated and potentially lead to the abandonment of the intervention.

Limitations

The present work has the following limitations. First, a convenience sample of 10 patients is too low to accurately measure the differences in recovery, TMS, EEG, and HD measurements obtained after BCI and after conventional therapy. However, the sample size was adequate to perform an early clinical evaluation and had the advantage that each patient served as his or her own control. Moreover, the sample of this study was homogeneous regarding stroke-induced upper limb sequelae. Therefore, the results of this study support the hypothesis that the ReHand-BCI system has similar effects in stroke upper limb rehabilitation as conventional therapy and invite future clinical trials to assess this hypothesis.

Another limitation is the duration of the therapy since more than 1 month would be ideal for correctly assessing whether a BCI intervention improves the clinical and physiological outcomes of conventional therapy. Also, physiological measurements with a higher spatial resolution such as fMRI would provide additional insights into neuroplasticity-related mechanisms that could better elucidate the ReHand-BCI system's efficacy for neurorehabilitation. Finally, the differences between therapies were calculated with the assumption that carryover effects were equal among groups. Carryover effects are an important limitation in crossover study designs; however, a washout period cannot be implemented without depriving stroke patients of valuable therapy sessions. Therefore, for ethical reasons, patients were provided upper limb rehabilitation therapy for the study duration, and no washout period was implemented. Despite these limitations, the findings support the hypothesis that ReHand-BCI is an effective approach to increase stroke patients' recovery of upper-limb function.

CONCLUSION

The present work assesses the feasibility of an intervention with a BCI system coupled to a robotic hand orthosis for stroke patients' upper limb rehabilitation by comparing outcomes measured after a 12-session intervention using the ReHand-BCI with those obtained after the same number of sessions of conventional therapy. Also, system usability and subjective mental workload metrics were assessed after the BCI. This early clinical evaluation supports the hypothesis that the ReHand-BCI system can promote neuroplasticity and could be as effective as conventional therapy for upper limb recovery, but this still needs to be assessed in clinical trials. Also, future studies should consider interventions with a duration of more than 12 sessions to better assess gains in motor recovery. The measurement of physiological variables such as corticospinal tract integrity to complement clinical outcomes and the integration of user experience surveys that evaluate if the system has an adequate degree of difficulty for stroke patients will further elucidate the efficacy of BCI systems.

Finally, it has been suggested that increasing the frequency of interventions which include movement of patients' paralyzed upper limbs, such as BCI therapies, could enhance stroke patients' motor recovery (López-Larraz et al., 2018). However, the World Health Organization (WHO) has stated that the current rehabilitation workforce is insufficient in several parts of the world (Krug and Cieza, 2017). Therefore, the validation of BCI systems for stroke recovery is relevant as BCI systems could fill this gap by offering an additional tool to healthcare institutions, thereby increasing the number of patients that receive rehabilitation sessions or the frequency of these sessions, even in the early stages of stroke.

DATA AVAILABILITY STATEMENT

The datasets presented in this article are not readily available because of ethical reasons. Requests to access the datasets should be directed to the corresponding author.

ETHICS STATEMENT

The studies involving human participants were reviewed and approved by the National Institute of Rehabilitation Ethics Committee. The patients/participants provided their written

informed consent to participate in this study. Written informed consent was obtained from the individuals for the publication of any potentially identifiable images or data included in this article.

AUTHOR CONTRIBUTIONS

JC-N, RC-E, PC-M, JQ-F, and OA-C conceived and designed the study. JC-N, RC-E, MR-B, CH-A, MG-A, IH-S, and AM-P performed data collection. JC-N, RC-E, PC-M, JQ-F, and OA-C analyzed the data. JC-N, RC-E, PC-M, and OA-C drafted and edited the manuscript. JQ-F, MG-A, MR-B, CH-A, IH-S, and AM-P provided critical revisions. All authors have approved the final version of the manuscript submitted for publication.

FUNDING

This work was supported by Consejo Nacional de Ciencia y Tecnología (CONACYT) (Grants Numbers SALUD-2015-2-262061 and SALUD-2018-02-B-S-45803).

ACKNOWLEDGMENTS

We would like to thank all patients that participated in this study and their primary caregivers. Also, we would like to thank Oscar R. Marrufo-Meléndez and Roberto Galán Galán for performing the MRI studies and Emmanuel Simental Aldaba for assistance with the clinical evaluations.

REFERENCES

Alawieh, A., Zhao, J., and Feng, W. (2018). Factors affecting post-stroke motor recovery: implications on neurotherapy after brain injury. *Behav. Brain Res.* 340, 94–101. doi: 10.1016/j.bbr.2016.08.029

Ang, K. K., Chin, Z. Y., Zhang, H., and Cuntai, G. (2008). "Filter Bank Common Spatial Pattern (FBCSP) in brain-computer interface," in *Proceedings of the 2008 IEEE International Joint Conference on Neural Networks (IEEE World Congress on Computational Intelligence)*. (Hong Kong: IEEE), 2390–2397.

Ang, K. K., Chua, K. S. G., Phua, K. S., Wang, C., Chin, Z. Y., Kuah, C. W. K., et al. (2015). A randomized controlled trial of EEG-based motor imagery brain-computer interface robotic rehabilitation for stroke. *Clin. EEG Neurosci.* 46, 310–320. doi: 10.1177/1550059414522229

Ang, K. K., Guan, C., Chua, K. S. G., Ang, B. T., Kuah, C. W. K., Wang, C., et al. (2011). A large clinical study on the ability of stroke patients to use an EEG-based motor imagery brain-computer interface. *Clin. EEG Neurosci.* 42, 253–258. doi: 10.1177/155005941104200411

Ang, K. K., Guan, C., Phua, K. S., Wang, C., Zhou, L., Tang, K. Y., et al. (2014). Brain-computer interface-based robotic end effector system for wrist and hand rehabilitation: results of a three-armed randomized controlled trial for chronic stroke. *Front. Neuroeng.* 7:30. doi: 10.3389/fneng.2014.00030

Bangor, A., Kortum, P., and Miller, J. (2009). Determining what individual SUS scores mean: adding an adjective rating scale. *J. Usability Stud.* 4, 114–123.

Benjamin, E. J., Virani, S. S., Callaway, C. W., Chamberlain, A. M., Chang, A. R., Cheng, S., et al. (2018). Heart disease and stroke statistics–2018 update: a report from the American Heart Association. *Circulation* 137, E67–E492. doi: 10.1161/CIR.0000000000000558

Bernhardt, J., Hayward, K. S., Kwakkel, G., Ward, N. S., Wolf, S. L., Borschmann, K., et al. (2017). Agreed definitions and a shared vision for new standards in stroke recovery research: the stroke recovery and rehabilitation roundtable taskforce. *Int. J. Stroke* 12, 444–450. doi: 10.1177/1747493017711816

Bertani, R., Melegari, C., De Cola, M. C., Bramanti, A., Bramanti, P., and Calabrò, R. S. (2017). Effects of robot-assisted upper limb rehabilitation in stroke patients: a systematic review with meta-analysis. *Neurol. Sci.* 38, 1561–1569. doi: 10.1007/s10072-017-2995-5

Bertrand, O., Perrin, F., and Pernier, J. (1985). A theoretical justification of the average reference in topographic evoked potential studies. *Electroencephalogr. Clin. Neurophysiol.* 62, 462–464.

Biabani, M., Farrell, M., Zoghi, M., Egan, G., and Jaberzadeh, S. (2018). The minimal number of TMS trials required for the reliable assessment of corticospinal excitability, short interval intracortical inhibition, and intracortical facilitation. *Neurosci. Lett.* 674, 94–100. doi: 10.1016/j.neulet.2018.03.026

Billingham, S. A. M., Whitehead, A. L., and Julious, S. A. (2013). An audit of sample sizes for pilot and feasibility trials being undertaken in the United Kingdom registered in the United Kingdom clinical research network database. *BMC Med. Res. Methodol.* 13:104. doi: 10.1186/1471-2288-13-104

Blankertz, B., Tomioka, R., Lemm, S., Kawanabe, M., and Müller, K.-R. (2008). Optimizing spatial filters for robust EEG single-trial analysis. *IEEE Signal Process. Mag.* 25, 41–56. doi: 10.1109/MSP.2007.909009

Borschmann, K. N., and Hayward, K. S. (2020). Recovery of upper limb function is greatest early after stroke but does continue to improve during the chronic phase: a two-year, observational study. *Physiotherapy* 107, 216–223. doi: 10.1016/j.physio.2019.10.001

Branco, J. P., Oliveira, S., Sargento-Freitas, J., Laíns, J., and Pinheiro, J. (2019). Assessing functional recovery in the first six months after acute ischemic stroke: a prospective, observational study. *Eur. J. Phys. Rehabil. Med.* 55, 1–7. doi: 10.23736/S1973-9087.18.05161-4

Brooke, J. (1996). "SUS–a 'quick and dirty' usability scale," in *Usability Evaluation in Industry*, eds P. W. Jordan, B. Thomas, B. A. Weerdmeester, and A. L. McClelland (London: Taylor and Francis).

Bruce, D. (2005). Rehabilitation after stroke. *N. Engl. J. Med.* 352, 1677–1684.

Bustamante, E., and Spain, R. (2012). Measurement invariance of the Nasa TLX. *Proc. Hum. Factors Ergon. Soc. Annu. Meet.* 52, 1522–1526. doi: 10.1177/154193120805201946

Cantillo-Negrete, J., Carino-Escobar, R., Carrillo-Mora, P., and Gutierrez-Martinez, J. (2017). "Increasing stroke patients motor imagery classification by selecting features with particle swarm optimization," in *Proceedings of the 7th Graz Brain-Computer Interface Conference 2017*, Graz.

Cantillo-Negrete, J., Carino-Escobar, R. I., Carrillo-Mora, P., Barraza-Madrigal, J. A., and Arias-Carrión, O. (2019). Robotic orthosis compared to virtual hand for brain–computer interface feedback. *Biocybern. Biomed. Eng.* 39, 263–272. doi: 10.1016/j.bbe.2018.12.002

Cantillo-Negrete, J., Carino-Escobar, R. I., Carrillo-Mora, P., Elias-Vinas, D., and Gutierrez-Martinez, J. (2018). Motor imagery-based brain-computer interface coupled to a robotic hand orthosis aimed for neurorehabilitation of stroke patients. *J. Healthc. Eng.* 2018:1624637. doi: 10.1155/2018/1624637

Carino-Escobar, R. I., Carrillo-Mora, P., Valdés-Cristerna, R., Rodriguez-Barragan, M. A., Hernandez-Arenas, C., Quinzaños-Fresnedo, J., et al. (2019). Longitudinal analysis of stroke patients' brain rhythms during an intervention with a brain-computer interface. *Neural Plast.* 2019:7084618. doi: 10.1155/2019/7084618

Carrillo-de-la-Peña, M. T., Galdo-Álvarez, S., and Lastra-Barreira, C. (2008). Equivalent is not equal: primary motor cortex (MI) activation during motor imagery and execution of sequential movements. *Brain Res.* 1226, 134–143. doi: 10.1016/j.brainres.2008.05.089

Cassidy, J. M., and Cramer, S. C. (2017). Spontaneous and therapeutic-induced mechanisms of functional recovery after stroke. *Transl. Stroke Res.* 8, 33–46. doi: 10.1007/s12975-016-0467-5

Cervera, M. A., Soekadar, S. R., Ushiba, J., Millán, J., del, R., Liu, M., et al. (2018). Brain-computer interfaces for post-stroke motor rehabilitation: a meta-analysis. *Ann. Clin. Transl. Neurol.* 5, 651–663. doi: 10.1002/acn3.544

Delavaran, H., Aked, J., Sjunnesson, H., Lindvall, O., Norrving, B., Kokaia, Z., et al. (2017). Spontaneous recovery of upper extremity motor impairment after ischemic stroke: implications for stem cell-based therapeutic approaches. *Transl. Stroke Res.* 8, 351–361. doi: 10.1007/s12975-017-0523-9

Delvaux, V., Alagona, G., Gérard, P., De Pasqua, V., Pennisi, G., and de Noordhout, A. M. (2003). Post-stroke reorganization of hand motor area: a 1-year prospective follow-up with focal transcranial magnetic stimulation. *Clin. Neurophysiol* 114, 1217–1225. doi: 10.1016/S1388-2457(03)00070-1

Demeurisse, G., Demol, O., and Robaye, E. (1980). Motor Evaluation in vascular hemiplegia. *Eur. Neurol.* 19, 382–389.

Edlinger, G., Allison, B. Z., and Guger, C. (2015). "How many people can use a BCI system?," in *Clinical Systems Neuroscience*, eds K. Kansaku, L. Cohen, and N. Birbaumer (Tokyo: Springer), 33–66.

FDA (2011). *Investigational Device Exemptions (IDEs) for Early Feasibility Medical Device Clinical Studies, Including Certain First in Human (FIH) Studies*. Silver Spring, MD: FDA.

Franck, J. A., Smeets, R. J. E. M., and Seelen, H. A. M. (2017). Changes in arm-hand function and arm-hand skill performance in patients after stroke during and after rehabilitation. *PLoS One* 12:e0179453. doi: 10.1371/journal.pone.0179453

Frolov, A. A., Mokienko, O., Lyukmanov, R., Biryukova, E., Kotov, S., Turbina, L., et al. (2017). Post-stroke rehabilitation training with a motor-imagery-based Brain-Computer Interface (BCI)-controlled hand exoskeleton: a randomized controlled multicenter trial. *Front. Neurosci.* 11:400. doi: 10.3389/fnins.2017.00400

Goodglass, H., Kaplan, E., and Barresi, B. (2005). *Evaluación de la afasia y de trastornos relacionados*, 3rd Edn. Argentina: Editorial Médica Panamericana.

Hart, S. G. (2012). Nasa-Task Load Index (NASA-TLX); 20 years later. *Proc. Hum. Factors Ergon. Soc. Annu. Meet.* 50, 904–908. doi: 10.1177/154193120605000909

Hart, S. G., and Staveland, L. E. (1988). "Development of NASA-TLX(Task Load Index): results of empirical and theoretical research," in *Human Mental Workload*, eds P. Hancock and M. Meshkati, (Amsterdam: North Holland Press), 139–183.

Hatem, S. M., Saussez, G., della Faille, M., Prist, V., Zhang, X., Dispa, D., et al. (2016). Rehabilitation of motor function after stroke: a multiple systematic review focused on techniques to stimulate upper extremity recovery. *Front. Hum. Neurosci.* 10:442. doi: 10.3389/fnhum.2016.00442

Irimia, D. C., Ortner, R., Poboroniuc, M. S., Ignat, B. E., and Guger, C. (2018). High classification accuracy of a motor imagery based brain-computer interface for stroke rehabilitation training. *Front. Robot. AI* 5:130. doi: 10.3389/frobt.2018.00130

Kraeutner, S., Gionfriddo, A., Bardouille, T., and Boe, S. (2014). Motor imagery-based brain activity parallels that of motor execution: evidence from magnetic source imaging of cortical oscillations. *Brain Res.* 1588, 81–91. doi: 10.1016/j.brainres.2014.09.001

Kroemer, K. H. E., and Marras, W. S. (1980). Towards an objective assessment of the "maximal voluntary contraction" component in routine muscle strength measurements. *Eur. J. Appl. Physiol. Occup. Physiol.* 45, 1–9. doi: 10.1007/BF00421195

Krug, E., and Cieza, A. (2017). Strengthening health systems to provide rehabilitation services. *Bull. World Health Organ.* 95:167. doi: 10.2471/BLT.17.191809

Lang, C. E., Wagner, J. M., Dromerick, A. W., and Edwards, D. F. (2006). Measurement of upper-extremity function early after stroke: properties of the action research arm test. *Arch. Phys. Med. Rehabil.* 87, 1605–1610. doi: 10.1016/j.apmr.2006.09.003

Lee, K. B., Lim, S. H., Kim, K. H., Kim, K. J., Kim, Y. R., Chang, W. N., et al. (2015). Six-month functional recovery of stroke patients. *Int. J. Rehabil. Res.* 38, 173–180. doi: 10.1097/MRR.0000000000000108

Li, M., Liu, Y., Wu, Y., Liu, S., Jia, J., and Zhang, L. (2014). Neurophysiological substrates of stroke patients with motor imagery-based brain-computer interface training. *Int. J. Neurosci.* 124, 403–415. doi: 10.3109/00207454.2013.850082

López-Larraz, E., Sarasola-Sanz, A., Irastorza-Landa, N., Birbaumer, N., and Ramos-Murguialday, A. (2018). Brain-machine interfaces for rehabilitation in stroke: a review. *NeuroRehabilitation* 43, 77–97. doi: 10.3233/NRE-172394

Martinez-Valdes, M., Vargaz-Criz, J., Gutierrez-Martinez, J., Cantillo-Negrete, J., Elias-Vinas, D., and Castaneda-Galvan, A. (2014). "A mechanical structure prototype and control unit for an active orthosis for a human hand," in *Proceedings of the Health Care Exchanges (PAHCE)* (Brasilia: Institute of Electrical and Electronics Engineers (IEEE)), 1–4.

Monge-Pereira, E., Ibañez-Pereda, J., Alguacil-Diego, I. M., Serrano, J. I., Spottorno-Rubio, M. P., and Molina-Rueda, F. (2017). Use of electroencephalography brain-computer interface systems as a rehabilitative approach for upper limb function after a stroke: a systematic review. *PM R* 9, 918–932. doi: 10.1016/j.pmrj.2017.04.016

Müller-putz, G. R., Scherer, R., Brunner, C., Leeb, R., and Pfurtscheller, G. (2008). Better than random? A closer look on BCI results. *Int. J. Bioelectromagn.* 10, 52–55.

Ono, T., Shindo, K., Kawashima, K., Ota, N., Ito, M., Ota, T., et al. (2014). Brain-computer interface with somatosensory feedback improves functional recovery from severe hemiplegia due to chronic stroke. *Front. Neuroeng.* 7:19. doi: 10.3389/fneng.2014.00019

Ostrosky, F., Gomez, E., Matute, E., Rosseli, M., Ardilla, A., and Pineda, D. (2019). *Neuropsi Atención y Memoria*, 3rd Edn. Mexico: Manual Moderno.

Page, S. J., Fulk, G. D., and Boyne, P. (2012). Clinically important differences for the upper-extremity Fugl-Meyer scale in people with minimal to moderate impairment due to chronic stroke. *Phys. Ther.* 92, 791–798. doi: 10.2522/ptj.20110009

Pekna, M., Pekny, M., and Nilsson, M. (2012). Modulation of neural plasticity as a basis for stroke rehabilitation. *Stroke* 43, 2819–2828. doi: 10.1161/STROKEAHA.112.654228

Pfurtscheller, G., and Lopes Da Silva, F. H. (1999). Event-related EEG/MEG synchronization and desynchronization: basic principles. *Clin. Neurophysiol.* 110, 1842–1857.

Pfurtscheller, G., and Neuper, C. (2001). Motor imagery and direct brain-computer communication. *Proc. IEEE* 89, 1123–1134. doi: 10.1109/5.939829

Prasad, G., Herman, P., Coyle, D., McDonough, S., and Crosbie, J. (2010). Applying a brain-computer interface to support motor imagery practice in people with stroke for upper limb recovery: a feasibility study. *J. Neuroeng. Rehabil.* 7:60. doi: 10.1186/1743-0003-7-60

Ramos-Murguialday, A., Broetz, D., Rea, M., Läer, L., Yilmaz, Ö, Brasil, F. L., et al. (2013). Brain-machine interface in chronic stroke rehabilitation: a controlled study. *Ann. Neurol.* 74, 100–108. doi: 10.1002/ana.23879

Remsik, A., Young, B., Vermilyea, R., Kiekhoefer, L., Abrams, J., Evander Elmore, S., et al. (2016). A review of the progression and future implications of brain-computer interface therapies for restoration of distal upper extremity motor function after stroke. *Expert Rev. Med. Devices* 13, 445–454. doi: 10.1080/17434440.2016.1174572

Rossini, P. M., Burke, D., Chen, R., Cohen, L. G., Daskalakis, Z., Di Iorio, R., et al. (2015). Non-invasive electrical and magnetic stimulation of the brain, spinal cord, roots and peripheral nerves: basic principles and procedures for routine clinical and research application. An updated report from an I.F.C.N. committee. *Clin. Neurophysiol.* 126, 1071–1107. doi: 10.1016/j.clinph.2015.02.001

Shi, Y., and Eberhart, R. (1998). "A modified particle swarm optimizer," in *Proceedings of the IEEE International Conference on Evolutionary Computation* (Anchorage, AK: IEEE), 69–73.

Stern, Y. (2009). Cognitive reserve. *Neuropsychologia* 47, 2015–2028. doi: 10.1016/j.neuropsychologia.2009.03.004

Stinear, C. M., Byblow, W. D., Ackerley, S. J., Smith, M. C., Borges, V. M., and Barber, P. A. (2017). PREP2: a biomarker-based algorithm for predicting upper limb function after stroke. *Ann. Clin. Transl. Neurol.* 4, 811–820. doi: 10.1002/acn3.488

Tallon-Baudry, C., Bertrand, O., Tallon-Baudry, C., Bertrand, O., Tallon-Baudry, C., and Bertrand, O. (1999). Oscillatory gamma activity in humans and its role in object representation. *Trends Cogn. Sci.* 3, 151–162. doi: 10.1016/S1364-6613(99)01299-1

Tecuapetla-Trejo, J. E., Cantillo-Negrete, J., Valdés-Cristerna, R., Carrillo-Mora, P., Arias-Carrion, O., Ortega-Robles, E., et al. (2020). "Automatic recognition and feature extraction of motor-evoked potentials elicited by transcranial magnetic stimulation BT," in *VIII Latin American Conference on Biomedical Engineering and XLII National Conference on Biomedical Engineering*, eds C. A. González Díaz, C. Chapa González, E. Laciar Leber, H. A. Vélez, N. P. Puente, D.-L. Flores, et al. (Cham: Springer International Publishing), 1037–1042.

Van Der Lee, J. H., Beckerman, H., Lankhorst, G. J., and Bouter, L. M. (2001). The responsiveness of the action research arm test and the Fugl-Meyer assessment scale in chronic stroke patients. *J. Rehabil. Med.* 33, 110–113. doi: 10.1080/165019701750165916

Ward, N. S., Brown, M. M., Thompson, A. J., and Frackowiak, R. S. J. (2003). Neural correlates of motor recovery after stroke: a longitudinal fMRI study. *Brain* 126, 2476–2496. doi: 10.1093/brain/awg245

Winstein, C. J., Stein, J., Arena, R., Bates, B., Cherney, L. R., Cramer, S. C., et al. (2016). Guidelines for adult stroke rehabilitation and recovery . *Stroke* 47, e98–e169. doi: 10.1161/STR.0000000000000098

Wolpaw, J. R., Birbaumer, N., McFarland, D. J., Pfurtscheller, G., and Vaughan, T. M. (2002). Brain–computer interfaces for communication and control. *Clin. Neurophysiol.* 113, 767–791. doi: 10.1016/S1388-2457(02)00057-3

Woodbury, M. L., Velozo, C. A., Richards, L. G., and Duncan, P. W. (2013). Rasch analysis staging methodology to classify upper extremity movement impairment after stroke. *Arch. Phys. Med. Rehabil.* 94, 1527–1533. doi: 10.1016/j.apmr.2013.03.007

Conflict of Interest: The authors declare that the research was conducted in the absence of any commercial or financial relationships that could be construed as a potential conflict of interest.

Copyright © 2021 Cantillo-Negrete, Carino-Escobar, Carrillo-Mora, Rodriguez-Barragan, Hernandez-Arenas, Quinzaños-Fresnedo, Hernandez-Sanchez, Galicia-Alvarado, Miguel-Puga and Arias-Carrion. This is an open-access article distributed under the terms of the Creative Commons Attribution License (CC BY). The use, distribution or reproduction in other forums is permitted, provided the original author(s) and the copyright owner(s) are credited and that the original publication in this journal is cited, in accordance with accepted academic practice. No use, distribution or reproduction is permitted which does not comply with these terms.

frontiers in Neural Circuits

ORIGINAL RESEARCH
published: 14 June 2021
doi: 10.3389/fncir.2021.693073

Cortical Electrical Stimulation Ameliorates Traumatic Brain Injury-Induced Sensorimotor and Cognitive Deficits in Rats

*Chi-Wei Kuo[1,2†], Ming-Yuan Chang[3,4†], Hui-Hua Liu[5], Xiao-Kuo He[6,7], Shu-Yen Chan[8,9], Ying-Zu Huang[10,11], Chih-Wei Peng[12], Pi-Kai Chang[13], Chien-Yuan Pan[1] and Tsung-Hsun Hsieh[2,11,14]**

[1]Department of Life Science, National Taiwan University, Taipei, Taiwan, [2]School of Physical Therapy and Graduate Institute of Rehabilitation Science, Chang Gung University, Taoyuan, Taiwan, [3]Division of Neurosurgery, Department of Surgery, Min-Sheng General Hospital, Taoyuan, Taiwan, [4]Department of Early Childhood and Family Educare, Chung Chou University of Science and Technology, Yuanlin, Taiwan, [5]Sun Yat-sen Memorial Hospital, Sun Yat-sen University, Guangzhou, China, [6]Fifth Hospital of Xiamen, Xiamen, China, [7]Fujian University of Traditional Chinese Medicine, Fuzhou, China, [8]Department of Internal Medicine, Far Eastern Memorial Hospital, New Taipei, Taiwan, [9]College of Medicine, Taipei Medical University, Taipei, Taiwan, [10]Department of Neurology, Chang Gung Memorial Hospital and Chang Gung University College of Medicine, Taoyuan, Taiwan, [11]Neuroscience Research Center, Chang Gung Memorial Hospital, Taoyuan, Taiwan, [12]School of Biomedical Engineering, College of Biomedical Engineering, Taipei Medical University, Taipei, Taiwan, [13]School of Medicine, College of Medicine, Chang Gung University, Taoyuan, Taiwan, [14]Healthy Aging Research Center, Chang Gung University, Taoyuan, Taiwan

OPEN ACCESS

Edited by:
Ti-Fei Yuan,
Shanghai Jiao Tong University, China

Reviewed by:
Zhang Yanming,
Capital Medical University, China
Hsiao-Yun Chang,
Asia University, Taiwan
Min-Fang Kuo,
Leibniz Research Centre for Working Environment and Human Factors (IfADo), Germany
Wei-Hsin Wang,
Taipei Veterans General Hospital, Taiwan

***Correspondence:**
Tsung-Hsun Hsieh
hsiehth@mail.cgu.edu.tw

†These authors have contributed equally to this work

Received: *09 April 2021*
Accepted: *14 May 2021*
Published: *14 June 2021*

Citation:
Kuo C-W, Chang M-Y, Liu H-H, He X-K, Chan S-Y, Huang Y-Z, Peng C-W, Chang P-K, Pan C-Y and Hsieh T-H (2021) Cortical Electrical Stimulation Ameliorates Traumatic Brain Injury-Induced Sensorimotor and Cognitive Deficits in Rats. Front. Neural Circuits 15:693073. doi: 10.3389/fncir.2021.693073

Objective: Individuals with different severities of traumatic brain injury (TBI) often suffer long-lasting motor, sensory, neurological, or cognitive disturbances. To date, no neuromodulation-based therapies have been used to manage the functional deficits associated with TBI. Cortical electrical stimulation (CES) has been increasingly developed for modulating brain plasticity and is considered to have therapeutic potential in TBI. However, the therapeutic value of such a technique for TBI is still unclear. Accordingly, an animal model of this disease would be helpful for mechanistic insight into using CES as a novel treatment approach in TBI. The current study aims to apply a novel CES scheme with a theta-burst stimulation (TBS) protocol to identify the therapeutic potential of CES in a weight drop-induced rat model of TBI.

Methods: TBI rats were divided into the sham CES treatment group and CES treatment group. Following early and long-term CES intervention (starting 24 h after TBI, 1 session/day, 5 days/week) in awake TBI animals for a total of 4 weeks, the effects of CES on the modified neurological severity score (mNSS), sensorimotor and cognitive behaviors and neuroinflammatory changes were identified.

Results: We found that the 4-week CES intervention significantly alleviated the TBI-induced neurological, sensorimotor, and cognitive deficits in locomotor activity, sensory and recognition memory. Immunohistochemically, we found that CES mitigated the glial fibrillary acidic protein (GFAP) activation in the hippocampus.

Conclusion: These findings suggest that CES has significant benefits in alleviating TBI-related symptoms and represents a promising treatment for TBI.

Keywords: traumatic brain injury (TBI), cortical electrical stimulation, neuromodulation, sensorimotor impairment, cognitive dysfunction

INTRODUCTION

Traumatic brain injury (TBI) is a common brain injury caused by an external mechanical force, such as rapid acceleration or deceleration impact, crushing, or projectile penetration (Faul et al., 2010). TBI has been estimated to affect approximately 1.7 million American residents, resulting in the cost of over $76.5 billion to the medical care systems each year in the United States (Faul et al., 2010). Following TBI, damage to the brain can be identified as primary injury and secondary injury. Primary injury is direct damage to the intracranial contents resulting from mechanical forces, such as an object, rapid acceleration/deceleration, as seen in motor vehicle accidents, penetrating injury, and blast waves. Acute injury of the parenchyma can manifest as contusions, hematomas, shearing of white matter tracts, and cerebral edema (Popernack et al., 2015). Secondary injury is the subsequent damage that occurs over hours to days and results in the alternation of cerebral blood flow and inflammatory processes. In addition, cerebral blood flow is often altered and causes vasospasm, focal microvascular occlusion, and vascular injury, resulting in brain edema. This secondary ischemia can lead to hypoxia and neuronal hyperactivity or excessive inhibition (Ping and Jin, 2016). Individuals with different severities of TBI suffer long-lasting motor, sensory, neurological, cognitive, or behavioral disturbances. To date, no neuromodulation-based therapies have been used to manage the development of pathological deficits associated with TBI.

A number of alternative nonpharmacological procedures have been suggested as new therapeutic strategies for neurological disorders, including TBI. Electrical or magnetic neuromodulation approaches are promising tools for inducing changes in neural activity and plasticity. Repetitive transcranial magnetical stimulation (rTMS) or cortical electrical stimulation (CES) are used as neuromodulatory means for neurological disorders. Recent research suggests that rTMS or CES can alter the neural activities *via* plasticity-like mechanisms, which have been applied for the treatment of neurological or psychiatric disorders and might have the therapeutic potential for TBI (Gaynes et al., 2014; Kamble et al., 2014; Sokal et al., 2019; Zaninotto et al., 2019; Pink et al., 2021). However, the results exploring the therapeutic effects of such neuromodulatory tools on TBI are still inconclusive. The major concern with rTMS is the risk of seizure-induction (Cavinato et al., 2012; Dhaliwal et al., 2015). Under this consideration, individuals with TBI are frequently excluded from rTMS studies making it difficult to assess the efficacy and safety of rTMS as a treatment for TBI (Rossi et al., 2009).

Recently, increasing attention has focused on cortical electrical stimulation (CES). This technique was initially used as an experimental treatment to control neuropathic and intractable central pain (Son et al., 2006; Fagundes-Pereyra et al., 2010; Alm and Dreimanis, 2013). It has been reported that the CES can improve motor and sensory functions in stroke patients (Brown and Pilitsis, 2005). Similar to the rTMS, a recent animal study suggests that CES can modulate motor cortical excitability *via* plasticity-like mechanisms (Hsieh et al., 2015a). Earlier preclinical studies also show that CES coupled with motor rehabilitative training promotes synaptic plasticity and improves motor function after ischemic stroke (Adkins-Muir and Jones, 2003; Adkins et al., 2006, 2008). However, the therapeutic value of such a stimulatory approach for TBI is still unclear.

For the purpose of translational research, an animal model of disease could be the best way to study the pathogenesis of TBI, as it may provide a stable condition to eliminate any discrepancies and clarify the existence of a treatment effect. A suitable TBI animal model could help explore an effective therapeutic strategy, allowing the rapid screening of a stimulation protocol and identifying the detailed mechanisms of the CES protocol in TBI animal studies through neurophysiological and molecular analysis. Although the CES methodology has been reported in a few animal studies, studies with the application of CES as a long-term treatment in TBI animals are relatively rare. To date, the long-term effects of CES on detailed TBI-related motor and nonmotor symptoms, as well as its neuroprotective effects, have not been studied in TBI animal models. The current study was, therefore, designed to identify the therapeutic effects of CES in rats with weight drop-induced TBI. The therapeutic effects of CES were measured by behavioral assessments, including detailed time-course analysis of motor and nonmotor symptoms, such as the modified neurological severity score (mNSS), adhesion removal test, beam walking, novel object recognition (NOR), and histological assessment. It is hypothesized that long-term CES treatment may result in the improvement of TBI-related motor and nonmotor symptoms in weight drop-induced TBI rats. The knowledge obtained in these procedures may have translational relevance for establishing new therapeutic applications as neuromodulation therapy in clinical use.

MATERIALS AND METHODS

Animal Preparation

Experiments were carried out on male Sprague-Dawley rats (350–400 g) obtained from the Animal Center of Chang Gung University. The rats were housed in standard cages in a temperature (25°C) and humidity (50%) controlled facility with a 12 h light/dark cycle. All animal assessment and surgical procedures were approved by the guidelines of the Institutional Animal Care and Use Committee at Chang Gung University

(IACUC Approval No. CGU107-104). All efforts were made to minimize the number of rats required in the present study.

TBI Rat Model

To provide a stable and controllable environment and obtain detailed mechanical insights from the TBI animal model, researchers have widely used one of the typical TBI rodent models, known as the weight-drop model, to mimic diffuse axonal injury and concussion caused by falls or motor vehicle accidents in individuals with TBI (Foda and Marmarou, 1994; Marmarou et al., 1994). The weight drop model is the use of weights that are freely dropped or through a guiding tube to generate an impact on the head. The widely recognized weight drop induced TBI model is Marmarou's impact acceleration model, which has been described as resulting in diffused brain injury in rats (Marmarou et al., 1994; Smith et al., 2015). In this model, weight-drop procedures can provide a secure and inexpensive method for producing different graded brain injuries in animals by adjusting the height during the weight drop (1–2 m; Foda and Marmarou, 1994; Marmarou et al., 1994; Hsieh et al., 2017). In the current study, for the induction of TBI in rats, the Marmarou's impact acceleration model was modified and applied. Animal preparations for the induction of the TBI rat model were described previously (Hsieh et al., 2017). Briefly, to minimize animal suffering and distress during TBI lesions, we anesthetized the animals using an intraperitoneal administration of tiletamine-zolazepam (50 mg/kg, i.p.; Zoletil, Vibac, France) with xylazine (10 mg/kg; Rompun, Bayer, Leverkusen, Germany) 30 min before impact. A 2-cm incision was made, and the area was carefully cleared to expose the line of bregma. The stainless steel disc (10 mm in diameter, 3 mm in thickness) was fixed with the self-adherent wrap (1582, 3M, St. Paul, MN, USA) to the central portion of the rat skull vault between the bregma and lambdoid sutures. The rats were placed prone on flexible foam and secured by using two belts. A Plexiglas tube was then positioned vertically, and the lower end of the tube was centered directly above the stainless steel disc. TBI was induced using a 450-g brass weight falling from 2 m through a vertical transparent Plexiglas tube (**Figure 1A**). Based on our earlier study, the averaged response of impact force and acceleration are 9.43 ± 0.27 kg and 370.28 ± 9.98 g (Hsieh et al., 2017). Under this weight drop TBI model, the different graded severity of brain injury can be reproducibly and reliably induced. Following the TBI lesion, the body temperature was monitored throughout surgery, and the temperature was maintained at 37.0 ± 0.5°C using an adjustable heating pad during recovery from anesthesia.

CES Electrode Implantation

After the TBI lesion, a CES electrode was implanted in the rat's skull. Four burr holes were made using a dental drill (NE213, NSK-Nakanishi Inc, Tochigi, Japan) with a 1.5-mm burr for screw electrodes (1.6-mm-diameter pole; Plastics One, Inc., Roanoke, VA). According to the stereotaxic brain atlas of Paxinos and Watson, cortical electrodes were placed epidurally (A = + 4.0 mm, L = ± 2 mm for the frontal cortex; A = −3.6 mm, L = ± 4 mm for the parietal cortex; Paxinos and Watson, 2005; **Figure 1B**). All electrodes were inserted into a six-channel pedestal (MS363, Plastics One, Inc., Roanoke, VA, USA). The surgical incision was closed with three stitches. The screw electrodes and pedestal were secured to the skull surface with dental acrylic (Lang Dental Mfg., Wheeling, IL, USA; **Figures 1C,D**). Following TBI lesion and CES electrode implantation, the analgesia (Carprofen, 5 mg/kg; Pfizer Animal Health Inc., PA, USA) was administered subcutaneously every 24 h for 48 h postoperatively.

CES Treatment and Experimental Design

Twenty-three rats were used for the present experiment. Following TBI lesion, a 30.4% (7/23) mortality rate was observed following weight-drop induced TBI. 16 TBI rats were utilized to observe the efficacy of CES treatment. Animals were randomly divided into the sham CES treatment group and CES treatment group (n = 8 in each group). For the stimulation protocol of CES, we applied a popular and specific rTMS paradigm, the continue theta-burst stimulation (TBS; cTBS) and intermittent theta-burst stimulation (iTBS) protocol, have been proposed for inducing more efficient long-term potentiation (LTP) or long-term depression (LTD)-like plasticity in the motor cortex beyond the short period of stimulation and lower intensity (Huang et al., 2005; Fitzgerald et al., 2006; Khedr et al., 2007). The basic pattern of cTBS or iTBS consisted of three pulses at 50 Hz and repeated every 200 ms (**Figure 2**). In the cTBS paradigm, the stimuli were given in a continuous train lasting 40 s (i.e., 600 bursts; Huang et al., 2005). The iTBS scheme was given in a 2-s train and repeated every 10 s for 20 cycles (190 s, total 600 pulses). The stimulus intensity was set at 80% resting motor threshold (RMT). The RMT was defined as the minimal intensity of CES required for eliciting minimal forelimb muscle twitches. Under the intensity at 80% RMT for CES treatment, no obvious muscle twitches were observed during CES treatment.

In the CES treatment group, the CES intervention protocols were divided into two stages: the acute stage and the chronic stage. In the acute stage (24 h-1 week post-TBI), the CES treatment protocol using continuous theta-burst stimulation (cTBS) was designed for the suppression of the hyperexcitability cascade, which may prevent or minimize some of the disabling consequences of TBI and have a potential therapeutic effect (Demirtas-Tatlidede et al., 2012; Villamar et al., 2012). In the chronic stages (>1 week), the CES parameter using intermittent theta-burst stimulation (iTBS) was set to modulate or increase brain plasticity, which could be useful to reduce functionally maladaptive changes to counter disability (Demirtas-Tatlidede et al., 2012). One day after the TBI lesion, the TBI animals in the CES group received the CES-cTBS protocol at an intensity of 80% RMT for 40 s daily for five consecutive days on the first 7 days. In the subacute and chronic stage, from 7 days to 28 days post-TBI, the CES-iTBS protocol (1 session/day, five consecutive days/week, pulse intensity = 80% of the RMT) was carried out to evoke neural facilitation (**Figure 2**). In the sham CES treatment group, the TBI rats also experienced the same CES protocol but did not receive any electrical stimulation at the same

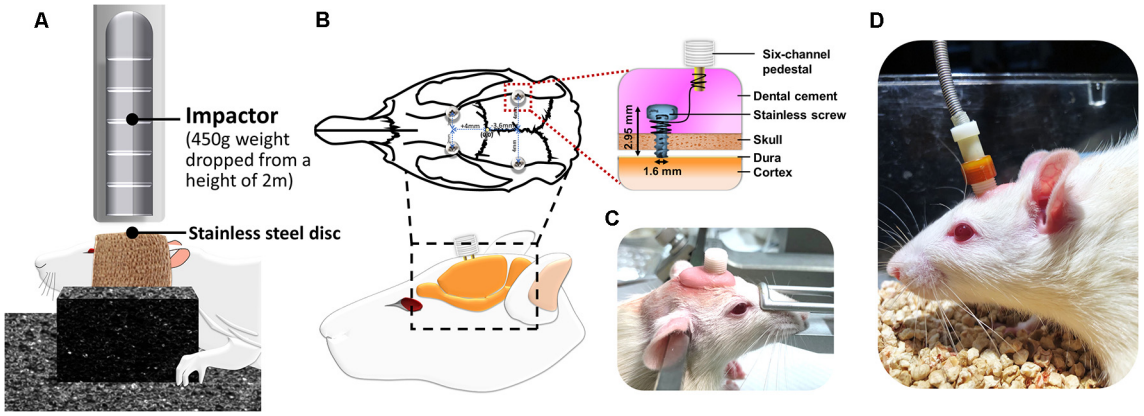

FIGURE 1 | Instrumentation setup of the traumatic brain injury (TBI) rat model and the placement and assembly of the cortical electrical stimulation (CES) electrode. **(A)** TBI rat model was induced using a 450-g brass weight falling from 2 m through a vertical transparent Plexiglas tube. **(B,C)** The CES electrodes were positioned at the frontal and parietal cortex and connected with wires in the six-channel pedestal and fixed with dental cement. **(D)** During CES treatment, the head electrode pedestal served as the plugin site of the electrode pin to conduct electrical current *via* the screw electrode on the cortex.

time points. All TBI rats were allowed to move freely during the CES or sham CES intervention. Behavioral tests, including open field locomotor activity tests, adhesion removal tests, beam walking, and mNSS, were performed at baseline (pre-TBI) and 1, 3, 7, 14, 21, and 28 days post-TBI lesion. For the cognitive measure in TBI rats, because the exploratory behavior could be influenced by the impairment of locomotor ability during the novel object recognition test, to avoid this potential confound, the novel object recognition test was assessed pre-lesion and at 28 days post-TBI lesion. Immunohistochemistry analysis was applied on day 28 post-TBI lesion to identify the changes in neural inflammation levels following CES treatment.

Behavioral Tests

A well-trained examiner was blinded to the type of intervention and performed all examinations before and after sham or CES treatment. All experimental animals were trained and pretested for these tasks at least 3 days before TBI lesion to record the baseline level (as pre-TBI data). After habituation and training, all behavioral test sessions were performed at our set time points under the same environmental conditions. Behavioral tests measured the time-course changes in sensorimotor and cognitive functions associated with TBI, i.e., mNSS, adhesion removal tests for sensory function, beam walking tests for balance function, and novel object recognition tests for short-term recognition memory. There was at least a 4-h break between behavioral tests to avoid possible interference.

Assessment of Motor Symptoms in TBI Rats

Beam-Walking Test

Balance and coordination were assessed by the beam-walking test (Dixon et al., 1987). Animals were pretrained to walk along the Plexiglas beam (120 cm long, 1.5 cm wide) toward their home cage at the opposite end. The latency of walking across within five testing trials after injury was calculated (Yu et al., 2016; Hsieh et al., 2017).

Adhesion-Removal Test

Sensory function was evaluated by the adhesion-removal test (Albertsmeier et al., 2007; Hsieh et al., 2017). Rats were familiarized with the environment. Two small dot stickers were attached to the bilateral forelimb. The removal duration was recorded.

Modified Neurological Severity Score (mNSS)

The mNSS is one of the most common neurological scales applied in animal studies of stroke. Severe TBI shares similar symptoms and pathology with stroke. The mNSS might also be a good test to evaluate the cortical functions of TBI rats. The mNSS includes a composite of balance, motor (muscle status and abnormal movement), sensory (visual, tactile, and proprioceptive), and reflex tests (Schaar et al., 2010; Hsieh et al., 2017).

short-term Recognition Memory

A novel object recognition (NOR) test was used to evaluate short-term recognition memory based on the tendency of rats to discriminate between familiar and new objects (Cheng et al., 2015). Before the acquisition phases, rats were habituated in the open field box for 10 min on day 3 and were then transferred to the home cage for 2 min. After that, the animals were placed back in the box for 10 min with the addition of two objects made of the same material placed in a symmetrical position. After 1 h, one of the objects was replaced with a novel object, and exploratory behavior was again analyzed for 10 min (day 3). The exploration duration was defined as sniffing, rearing on the object at a distance of less than 2 cm, or touching it with the nose (Zhang et al., 2019). The data was further analyzed as the discrimination index, which is defined as the exploration time at the novel object—the exploration time at the familiar object / the exploration time at the novel object + the exploration time at the familiar object (Aggleton et al., 2010; Antunes and Biala, 2012).

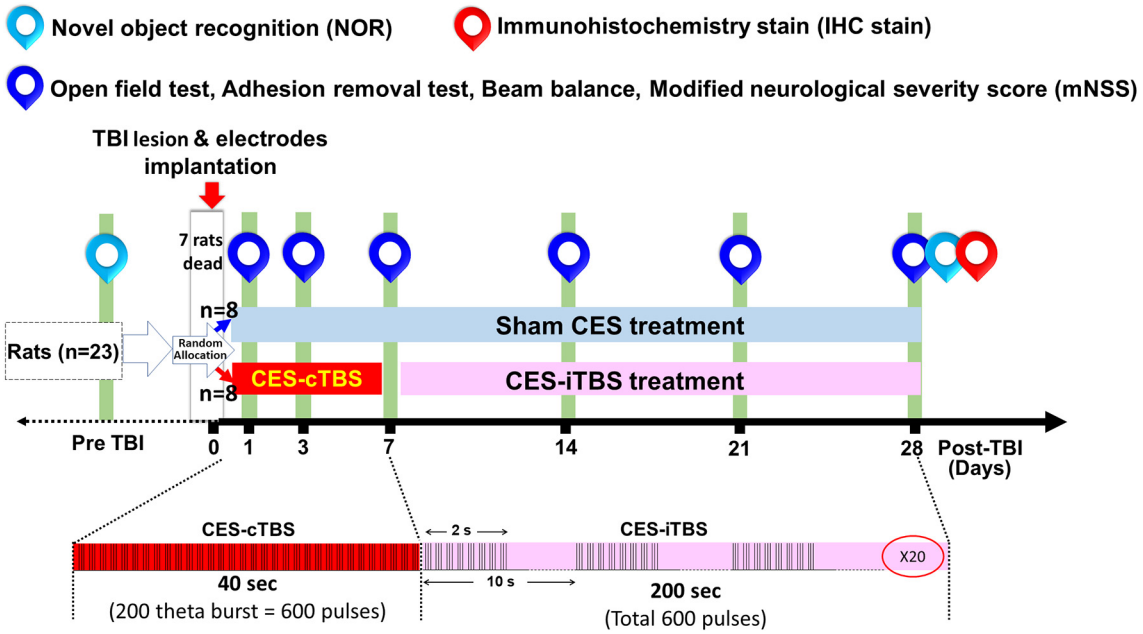

FIGURE 2 | Experimental design for the long-term treatment effects of CES. The TBI rats in the sham CES group remained in conditions identical to those of the CES group for the same period of time. In the treatment group, CES was performed in 20 sessions over 28 successive days, a session/day for 5 consecutive days per week. The inhibition and facilitation protocols were applied under the acute and subacute stages, respectively. The open field, adhesion removal, beam balance, and modified neurological severity score (mNSS) tests were performed every week to investigate long-term treatment effects. The novel object recognition (NOR) test was measured at baseline and 28 days post TBI lesion to identify the function of short-term recognition memory.

After each session, the objects were cleaned with 75% ethanol to prevent odor recognition from impacting the testing results.

Locomotor Activity

The open-field test was applied to measure general locomotor activity. In this test, each rat was monitored in an open field black plexiglass arena (60 × 60 × 100 cm in dimension) by a video camera. The total distance traveled and the movement time of each animal was recorded within a 10 min testing period (Feng et al., 2020). Each trial was recorded and analyzed using the tracking system (Smart 3.0, Panlab, Harvard Apparatus, Barcelona, Spain). The testing area was thoroughly cleaned with 75% ethanol between each testing period for each rat to avoid odor interference in the test response.

Immunohistochemistry Staining

After behavioral tests at 28 days post-lesion, TBI rats were sacrificed for glial fibrillary acidic protein (GFAP) staining. Briefly, brains were postfixed in a 4% paraformaldehyde fixative solution (PFA) and cytoprotected in 30% sucrose solution for 48 h at 4°C until the brain sank. The cerebral tissues between −3.00 and −3.36 mm to bregma were sectioned into coronal blocks at a thickness of 30 mm on a cryostat (Leica CM3050S Cryostat, FL, US), and the areas of the frontal cortex, corpus callosum, and hippocampus were selected. The sections were quenched with 0.3% H_2O_2/PBS for 10 min and 10% milk (Anchor Shape-up, New Zealand) for 1 h to block nonspecific antibodies and then incubated with rabbit primary anti-GFAP (1:1,000, AB7260, Millipore, USA) for 1 h at room temperature. After the sections were washed three times with PBS, they were incubated with the secondary anti-rabbit antibody (1:200, MP-7401, Vector Labs, USA) for 1 h at room temperature. The sections were developed by using a solution of 3.3-diaminobenzidine (DAB, SK-4105, Vector Labs, USA) for 5 min. Next, the sections were dehydrated in graded alcohols, cleared in xylene, and mounted with DPX. Mounted coronal sections were digitally imaged at 40x optical zoom (0.25 μM/pixel) using a digital pathology slide scanner (Aperio CS2, Leica Biosystems Inc. Buffalo Grove, IL, USA). For revealing the different expression levels of GFAP-positive cells between sham CES and CES rats, the higher magnification pictures were selected and captured from the Aperio ImageScope viewer software for further quantification and of GFAP-positive cells and observation of the morphology of GFAP-immunoreactive astrocytes. The consistent regions of interest for the frontal cortex, corpus callosum, and hippocampus were manually outlined according to the atlas of Paxinos and Watson (Paxinos and Watson, 2005). The obtained images with various degrees of GFAP expression were converted to binary (8-bit black-and-white) images. The binary threshold was determined to capture the GFAP-positive cells in the regions of interest while minimizing background staining and were kept constant for all images. The particle size used in particle analysis was set so that almost all astrocytes could be detected (Wakasa et al., 2009). The numbers of GFAP-positive cells in each region were counted by means of particle analysis under a computer-based image analysis system (Image-pro, Media Cybernetics, Bethesda,

MD, USA) and then manually validated by two investigators in order to ensure the correct identification of immunoreactivity patterns. The density of GFAP-positive cells was calculated by individually counting the number of GFAP-positive cells within the region and was expressed as the mean numbers of cells per mm^2 (cells/mm^2) for further statistical analysis.

Data Analysis

Data were analyzed using SPSS version 21.0 with the significance level set as $p < 0.05$ for each analysis. All data are presented as mean ± SEM. The effect of CES on the behavioral tests (i.e., beam-walking test, adhesion-removal test, mNSS, locomotor activity) was evaluated by a two-way repeated-measures analysis of variance (ANOVA) with the group (CES and sham CES treatment) as the between-subject factor and time (pre, every week after sham or CES treatment over 4 weeks) as a within-subject factor. For the short-term recognition memory, a two-way repeated measures ANOVA was used with two-way with the group (real CES and sham CES treatment) as the between-subject factor and time (pre and after sham or CES treatment over 4 weeks) as a within-subject factor. Unpaired *t*-tests were performed to compare groups at each time point when the main effect of the group was significant. Furthermore, the *post hoc* Fisher's LSD tests were also used to compare time points on behavioral and immunohistochemical data.

RESULTS

Effect of CES Treatment on Neurological Function in TBI Rats

The neurological function of rats was rated by the mNSS, which is a multifunctional evaluation scale that comprises balance, sensory, motor, and reflex tests. Repeated measures ANOVA identified significant main effects of time ($F_{6, 84} = 148.373$, $p < 0.001$) and group ($F_{1, 14} = 11.738$, $p = 0.004$) and a significant time × group interaction ($F_{6, 84} = 2.154$, $p = 0.04$). When compared with baseline value, subsequent *post hoc* Fisher's LSD tests demonstrate that the mNSS score was significantly increased at day 1 after TBI lesion ($p < 0.001$) and remained maintained in the high level for up to 28 days after TBI lesion (all $p < 0.001$ in both groups). For the comparison of the mNSS score between two groups, *post hoc t*-tests between the two groups showed that the scores reached significant differences at day 7 ($p = 0.02$), day 14 ($p = 0.031$), day 21 ($p = 0.015$), and day 28 ($p = 0.049$) after TBI lesion (**Figure 3**).

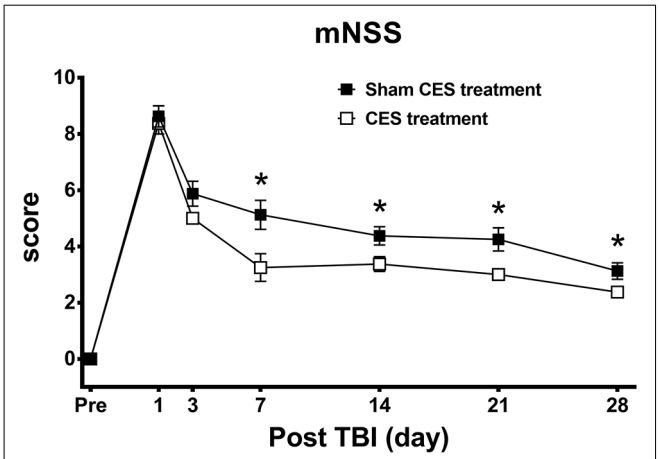

FIGURE 3 | Effect of CES treatment on neurological function evaluated by mNSS. Values are expressed as the mean ± SEM. *$p < 0.05$, significant difference between the two groups.

Effects of CES Treatment on Locomotor Dysfunction and Balance Function in TBI Rats

In the open field test, the overall distance traveled was calculated to investigate the general locomotor activity between the CES group and the sham CES group following the TBI lesion. Repeated measures ANOVA indicated a significant main effect of time ($F_{6, 84} = 21.010$, $p < 0.001$) and a time × group interaction ($F_{6, 84} = 2.575$, $p = 0.024$) but not an effect of group ($F_{1, 14} = 3.799$, $p = 0.072$). When compared with baseline value, subsequent *post hoc* Fisher's LSD tests show that locomotor activity was significantly decreased at day 1 after TBI lesion ($p < 0.001$) and remained maintained in the low level for up to 28 days after TBI lesion in the sham treatment group (all $p < 0.001$). However, in the CES treatment group, when compared with baseline value, *post hoc* tests show that the locomotor activity was significantly decreased on day 1 and day 3 after TBI lesion ($p < 0.01$). No significant differences were found between baseline and the time points of observation after 7 days post TBI lesion in the CES treatment group. For the comparison of locomotor activity between the two groups, *post hoc t*-tests between the two groups showed that the distance traveled in the open field test was significantly different at day 21 ($p = 0.031$) and day 28 ($p = 0.008$) after TBI (**Figure 4A**).

Furthermore, the beam walking test was applied to investigate the balance and motor coordination of the TBI rats with or without CES invention (**Figure 4B**). Repeated measures ANOVA identified significant main effects of time ($F_{6, 84} = 6.874$, $p < 0.001$) and group ($F_{1, 14} = 6.844$, $p = 0.02$) but not a time × group interaction ($F_{6, 84} = 1.722$, $p = 0.126$). When compared with baseline value, subsequent *post hoc* Fisher's LSD tests show that latency to traverse the beam was significantly increased at day 1 after TBI lesion ($p < 0.001$). No significant differences were found between baseline and the time points of observation after 3 days post TBI lesion in the sham treatment group. For the comparison of beam balance function between two groups, *post hoc t*-tests between the two groups showed that the latency in the beam walking test was significantly different at day 1 ($p = 0.049$) and at day 28 ($p = 0.039$) after TBI (**Figure 4B**).

Effect of CES Treatment on Sensory Function in TBI Rats

The adhesive removal test was adopted in this study to observe sensory function in TBI rats. Repeated measures ANOVA applied to the removal time indicated significant main effects of time ($F_{6, 84} = 7.012$, $p < 0.001$) but not group ($F_{1, 14} = 1.731$, $p = 0.209$) or the time × group interaction ($F_{6, 84} = 0.814$,

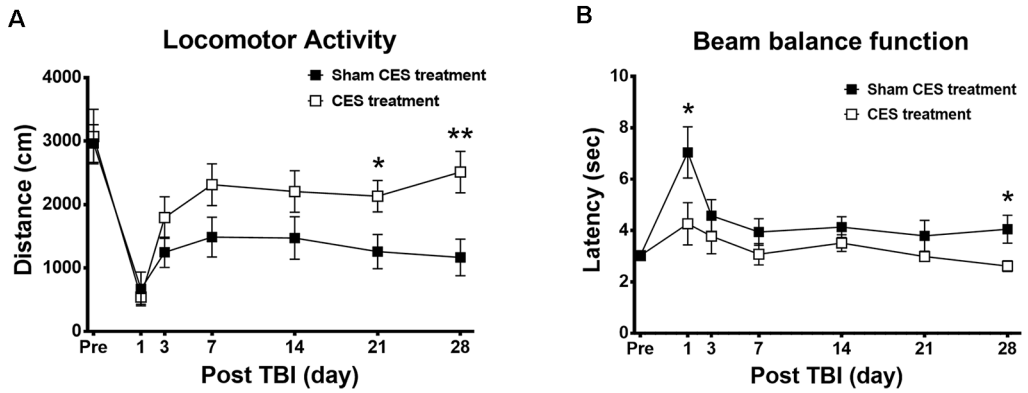

FIGURE 4 | Effects of CES treatment on **(A)** locomotor activity and **(B)** balance assessed by the open field test and beam walking test, respectively. Values are expressed as the mean ± SEM. $^{*}p < 0.05$, $^{**}p < 0.01$, significant difference between the two groups.

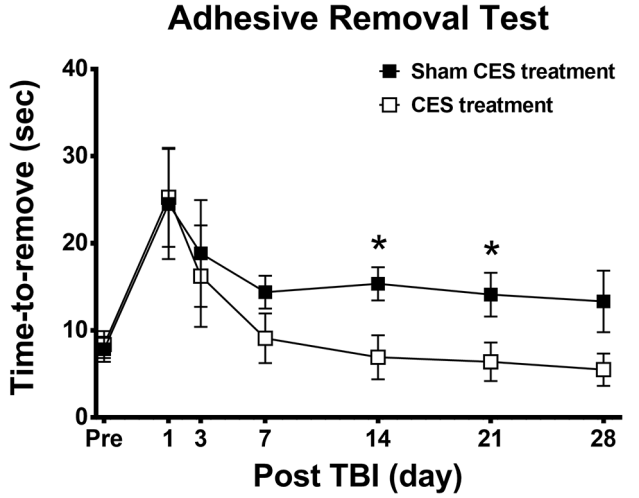

FIGURE 5 | Effect of CES treatment on sensory function assessed by adhesive removal test. Values are expressed as the mean ± SEM. $^{*}p < 0.05$, significant difference between the two groups.

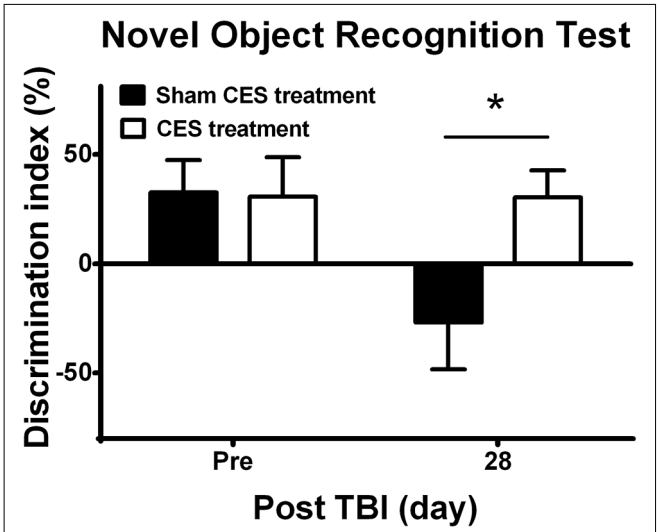

FIGURE 6 | Effect of CES treatment on recognition memory evaluated by the novel object recognition test. Values are expressed as the mean ± SEM. $^{*}p < 0.05$, significant difference between the two groups.

$p = 0.562$). When compared with baseline value, subsequent *post hoc* Fisher's LSD tests show that sensory function was significantly decreased at day 1 after TBI lesion in both groups ($p < 0.01$). No significant differences were found between baseline and the time points of observation after 3 days post-TBI lesion in both groups (all $p > 0.05$). For the comparison of locomotor activity between the two groups, *post hoc* *t*-tests between the two groups showed that removal time showed a significant difference at day 14 ($p = 0.019$) and day 21 ($p = 0.037$) after TBI lesion (**Figure 5**).

Effect of CES Treatment on Recognition Memory in TBI Rats

Novel object recognition was used to evaluate short-term recognition memory based on the tendency of rats to discriminate between familiar and new objects. Repeated measures ANOVA indicated a significant main effect of time ($F_{1, 14} = 5.28$, $p = 0.038$) and time × group interaction ($F_{1, 14} = 5.15$, $p = 0.04$) but not an effect of group ($F_{1, 14} = 2.92$, $p = 0.109$). Independent *t*-tests between the CES and sham CES groups showed that the discrimination index was significantly different at day 28 after TBI lesion (**Figure 6**; $t = 2.67$, $p = 0.018$).

Effect of CES Intervention Assessed by Immunohistochemistry in TBI Rats

With regard to the effects of the 4-week CES intervention on GFAP positive cells, the results of GFAP immunohistochemistry in the frontal cortex, corpus callosum, and hippocampus are shown in **Figure 7**. The densities of GFAP-immunoreactive astrocytes in the frontal cortex and corpus callosum were similar between the two groups (**Figures 7A,B,E,F**). When compared with sham CES-treated rat, lower density

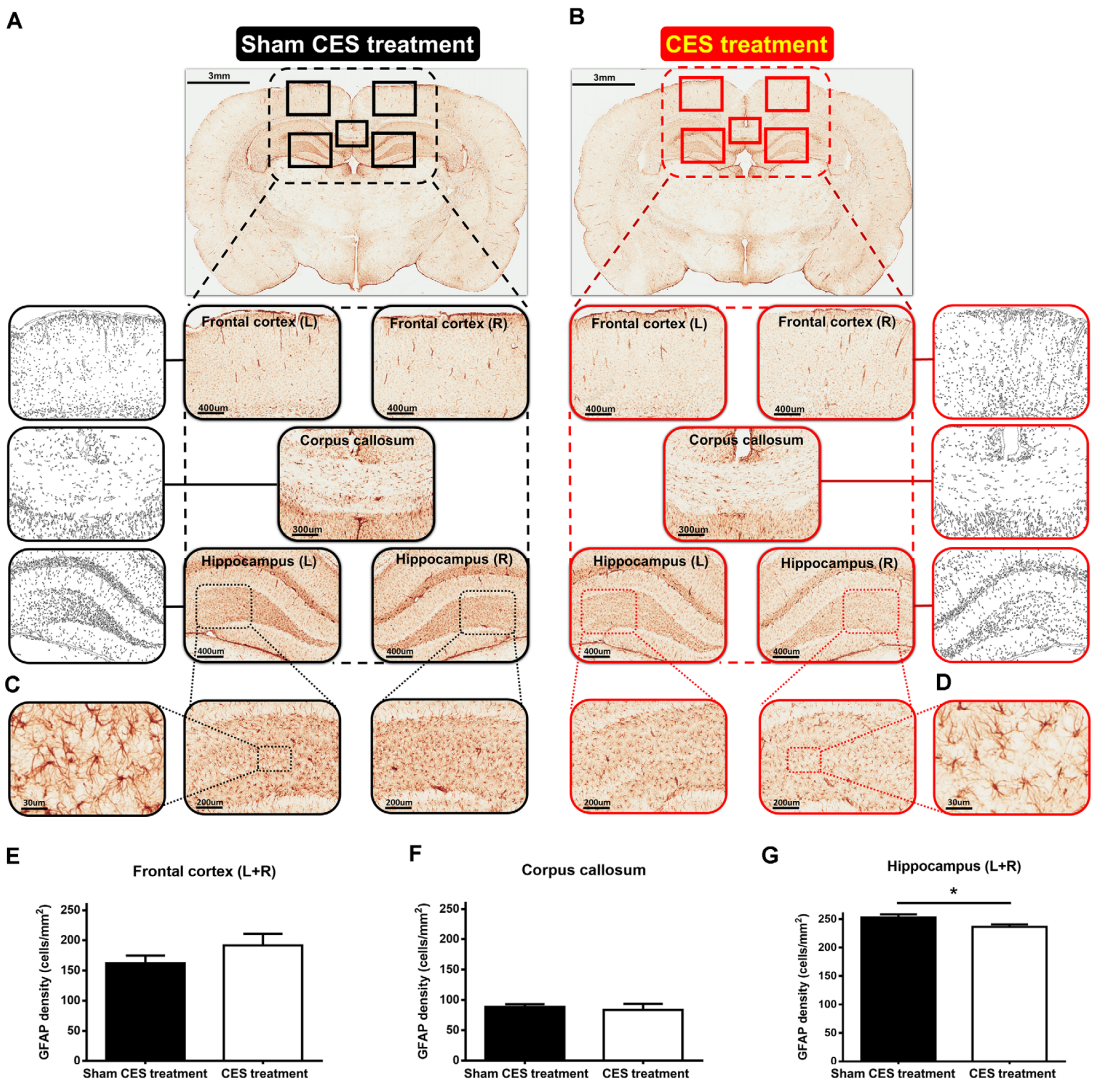

FIGURE 7 | (A,B) Representative of glial fibrillary acidic protein (GFAP) immunostaining and example of GFAP images to a binary image in the frontal cortex (L + R, Magnification, ×50; Scale bars = 400 μm), corpus callosum (Magnification, ×50; Scale bars = 300 μm), and hippocampus (L + R, Magnification, ×50; Scale bars = 400 μm) in TBI rat with sham CES treatment and TBI rat with 4 weeks of CES treatment. **(C,D)** Representative views of the morphology of GFAP-positive cells in the hippocampus (Magnification, ×300; Scale bars = 30 μm). **(E–G)** The averaged data (L + R) of the density of GFAP-positive cells in the frontal cortex, corpus callosum and hippocampus in the sham CES treatment and CES-treated groups. *$p < 0.05$, significant difference between the two groups.

of GFAP-positive cells in the hippocampus of CES-treated rat was found (**Figures 7C,D**). No morphological abnormalities or obvious hypertrophy in the GFAP-positive astrocytes were found between sham CES and CES rats. Independent *t*-tests between the CES and sham CES groups showed that the density of GFAP-positive cells was significantly lower in the CES treatment group compared with the sham CES group in the hippocampus ($p = 0.033$; **Figure 7G**).

DISCUSSION

In the current study, we applied a TBI rat model to investigate the effect of long-term CES treatment for 4 weeks on the TBI rats. We found that early and long-term CES intervention can ameliorate TBI-induced dysfunctions in sensorimotor and memory behavior. Moreover, the immunohistological results showed that long-term CES could ameliorate the TBI-induced elevations in GFAP in the hippocampus, suggesting that less central nervous system (CNS) damage was found in the CES treatment group. To date, the therapeutic efficacy and the underlying mechanisms of CES treatment for TBI remain unknown. An animal model would help provide more information on the benefits and underlying mechanism of CES treatment of TBI. Here, we performed several comprehensive and quantitative assessments of neurological severity score, sensory function, balance, and short-term memory, all of which are commonly affected in TBI patients, to identify the beneficial

effects during and after 4 weeks of CES. After treatment with CES for 4 weeks, a clear improvement in all parameters of the mNSS score was observed in the CES treatment group. Moreover, compared with the sham CES treatment, CES treatment for 4 weeks ameliorated and delayed disease progression in the TBI rats. To the best of our knowledge, this is the first study to confirm the therapeutic effect of CES on several comprehensive motor and nonmotor functions in a TBI rat model. These data strengthen the growing amount of basic research and clinical literature on the efficacy of CES in TBI treatment.

For the design of the potential CES stimulation protocol, in this study, two theta-burst stimulation (TBS) protocols, intermittent TBS (iTBS) and continuous TBS (cTBS), were applied to induce long-term potentiation-like or long-term depression-like plasticity at specific time points during disease development (Hsieh et al., 2015a,b). With regard to the natural development pattern of neuropathological changes following TBI, several key molecular and biochemical processes have been identified in earlier studies. For example, following TBI, excessive glutamate accumulation is induced and causes NMDA-mediated glutamatergic excitotoxicity (Faden et al., 1989). Additionally, increased NMDA receptor activation results in neuronal and glial depolarization. Intracellular calcium overload induces further inflammation, mitochondrial dysfunction, and apoptosis (Katsura et al., 1994; Forster et al., 1999; Bramlett and Dietrich, 2004). Furthermore, overactive calcium levels may trigger calcium-induced calpain proteolysis of cytoskeletal proteins and subsequent cellular collapse (Bramlett and Dietrich, 2004). Cellular destruction may also result from increased oxidative stress due to mitochondrial dysfunction and increased neuronal and inducible nitric oxide synthase, enhancing the production of free radicals and lipid peroxidation (Forster et al., 1999; Syntichaki and Tavernarakis, 2003; Bramlett and Dietrich, 2004). Therefore, in this acute stage, we tried to apply the inhibitory theta burst protocol using CES-cTBS to suppress the hyperexcitability cascade and prevent or minimize some of the disabling consequences. In the subacute stage, based on an animal imaging study, GABA levels were found to be increased at 1–2 days post-TBI, as shown by magnetic resonance spectroscopy (Pascual et al., 2007). Additionally, TBI induces long-lasting working memory deficits associated with increased GABA levels, and administration of GABA antagonists restores memory function, suggesting that lasting deficits following TBI are associated with overreactive GABA-mediated inhibition (Kobori and Dash, 2006). Thus, in this stage (>1 week), we applied the facilitation protocol using the CES-iTBS scheme to counter GABAergic tone and increase neuronal excitability to further reduce functional deficits. Finally, in the chronic stage, the recovery process operating through synaptic reorganization may not be complete and adequate. This process may cause concentration of and damage to critical neural networks. The maladaptive plasticity of the brain may limit functional recovery and promote lasting disability. Therefore, in the chronic stages (1–4 weeks), we continued the facilitation protocol using the CES-iTBS scheme to increase brain plasticity and reduce the functionally maladaptive changes to counter disability. Based on current results, we found that the use of different neuromodulatory CES approaches at different stages after TBI could have the potential to reduce the sensorimotor and memory and promote functional recovery. However, although the time-course assessments of several functional behaviors have been made at different time points after CES treatment, we cannot clearly differentiate whether the long-term beneficial effects of CES come solely from CES-cTBS protocol during the acute stage of TBI or from the combination of both CES-cTBS and CES-iTBS protocols. It is one of the limitations in this study; hence a well-designed experiment is still needed in the future to prove the efficacy of CES in different stages after TBI and define the optimal CES protocols that maximize the functional recovery. Moreover, when compared with the sham treatment group, we found that early and long-term CES treatment can ameliorate TBI-induced dysfunctions. However, in this study, to avoid the possible interference between two evaluation time points and behavioral tests, we did not compare the pre-treatment values between two groups before CES or sham treatment. Thus, it cannot rule out the possibility of the severity difference between groups before the intervention. It is another limitation of this study. To eliminate this possible confounding factor, in addition to performing the standard procedures of TBI lesion, following TBI lesion, the TBI rats were randomly assigned to the control or treatment group before sham/CES treatment. These efforts could reduce the differences between groups before intervention.

CES is a cortical stimulation technique that has been used in the control of neuropathic pain (Fagundes-Pereyra et al., 2010; Alm and Dreimanis, 2013). Previous preclinical studies have shown that cortical stimulation can enhance neuronal plasticity and improve the functional performance in stroke rat model (Adkins-Muir and Jones, 2003). Furthermore, recent research suggests that CES can modulate motor cortical excitability *via* plasticity-like mechanisms (Hsieh et al., 2015a), and might have therapeutic potential for TBI (Adkins, 2015). In the current study, we found that 4 weeks of CES treatment of TBI rats improved the recovery of locomotor function. These results parallel the findings from another TBI animal study, showing that CES is effective for the recovery of motor function, spatial memory (Yu et al., 2018). In addition, it has been found that the 100 Hz CES combined with daily motor training for 9 weeks significantly improved forelimb motor performance (Jefferson et al., 2016), encouraging further research into its therapeutic potential. To date, it is still unclear what the optimal stimulation parameters of CES are, although they are currently under exploration *in vivo* or in human studies for TBI. A suitable disease animal model could help identify an effective stimulation protocol, including adjustment and optimization of frequency, polarity, and current level, allowing rapid screening and neurophysiological analysis in TBI animal studies. Future research is still needed to clarify the mechanisms of action of CES to explore and optimize CES protocols in TBI.

Histological investigation of GFAP staining was performed in both groups and revealed that CES ameliorated TBI-induced the upregulation of GFAP in the hippocampus in the group that

received CES treatment compared with the group that received sham stimulation. GFAP is an astrocyte-specific intermediate filament component of the central nervous system (CNS) and is a common target used for observing the astroglial responses after TBI *in vivo* experiments (Myer et al., 2006; Chen et al., 2012). The astrocytes respond to TBI by pronounced changes in cell proliferation and cellular hypertrophy in the lesion site (Myer et al., 2006; Babaee et al., 2015; Cikriklar et al., 2016). In our earlier study using the same diffuse TBI rat model, the upregulation of GFAP has been found at day 1 and remained elevated for at least 1-week post TBI-lesion (Hsieh et al., 2017). In the current study, with the spontaneous recovery of functional behaviors, the GFAP-positive cells were found in the frontal cortex, corpus callosum, and hippocampus at day 28 after the TBI lesion, indicating sustained GFAP-positive astrocyte activation was still remarkably in the chronic stage after TBI. This finding was consistent with a previous TBI animal study using a controlled cortical impact rat model, showing GFAP-positive cells increased significantly in the cortex, corpus callosum, and hippocampus at 3 days, 14 days, and 28 days after TBI (Wang et al., 2018). Furthermore, when compared with the sham CES group, we found that long-term CES treatment significantly reduces the GFAP-positive astrocytes in the hippocampus at day 28 after the TBI lesion. The lower GFAP-positive astrocytes in the CES-treated group also support the beneficial effect on recognition memory and implies that the long-term CES treatment could be able to reduce the astroglial proliferation in the hippocampus, which may eventually alleviate the progressive deterioration of recognition memory in TBI rats. Although the CES electrodes were fixed on the skull and the electrical current was administered epidurally, the electric field could spread to 2–3 mm depth of rat's brain (Asan et al., 2019). It indicates that the hippocampus could be stimulated and further induced the plastic or functional changes after CES. However, the detailed and precise mechanisms are still unclear. Further investigations are still needed to clarify the underlying mechanisms of the beneficial effects of CES.

CONCLUSIONS

In conclusion, this study provides a clearer picture of the progressive symptom changes in induced TBI with or without CES treatment and documents the efficacy of CES in preventing several sensorimotor and memory dysfunctions. Future preclinical studies are still needed to further define the underlying mechanisms, leading to improved CES protocols for TBI.

DATA AVAILABILITY STATEMENT

The raw data supporting the conclusions of this article will be made available by the authors, without undue reservation.

ETHICS STATEMENT

The animal study was reviewed and approved by the Institutional Animal Care and Use Committee, Chang Gung University IACUC Approval No.: CGU107-104, Period of Protocol: valid from October 01, 2018 to September 30, 2021.

AUTHOR CONTRIBUTIONS

C-WK, Y-ZH, and T-HH conceived and designed the experiments. C-WK, S-YC, P-KC, and T-HH performed the experiments. M-YC, H-HL, X-KH, C-WP, and C-YP provided the equipment. C-WK, H-HL, X-KH, and T-HH analyzed the data. C-WK, M-YC, and T-HH contributed to writing and editing the manuscript. All authors contributed to the article and approved the submitted version.

FUNDING

This study was supported by grants from the Ministry of Science and Technology, Taiwan (MOST 109-2314-B-182-029-MY3, MOST 108-2314-B-182-015-MY3 to T-HH and MOST 109-2221-E-038-005-MY3 to C-WP), Chang Gung Medical Foundation, Taiwan (CMRPD1H0463 and CMRPD1K0671 to T-HH), Industry-Academy Cooperation Project of Chang Gung University (QCRPD657, SCRPD1H0061, SCRPD1K0351 and SCRPD1K0611 to T-HH), National Natural Science Foundation of China (Grant number 81902286 to H-HL) and Min-Sheng General Hospital (Grant number 1090003 and 2020003 to M-YC).

ACKNOWLEDGMENTS

We are grateful to the Neuroscience Research Center of Chang Gung Memorial Hospital, Linkou, Taiwan.

REFERENCES

Adkins, D. L. (2015). "Cortical stimulation-induced structural plasticity and functional recovery after brain damage," in *Brain Neurotrauma: Molecular, Neuropsychological, and Rehabilitation Aspects*, ed F. H. Kobeissy (Boca Raton, FL: CRC Press/Taylor & Francis). Chapter 43.

Adkins, D. L., Campos, P., Quach, D., Borromeo, M., Schallert, K., and Jones, T. A. (2006). Epidural cortical stimulation enhances motor function after sensorimotor cortical infarcts in rats. *Exp. Neurol.* 200, 356–370. doi: 10.1016/j.expneurol.2006.02.131

Adkins, D. L., Hsu, J. E., and Jones, T. A. (2008). Motor cortical stimulation promotes synaptic plasticity and behavioral improvements following sensorimotor cortex lesions. *Exp. Neurol.* 212, 14–28. doi: 10.1016/j.expneurol.2008.01.031

Adkins-Muir, D. L., and Jones, T. A. (2003). Cortical electrical stimulation combined with rehabilitative training: enhanced functional recovery and dendritic plasticity following focal cortical ischemia in rats. *Neurol. Res.* 25, 780–788. doi: 10.1179/016164103771953853

Aggleton, J. P., Albasser, M. M., Aggleton, D. J., Poirier, G. L., and Pearce, J. M. (2010). Lesions of the rat perirhinal cortex spare the acquisition of a complex configural visual discrimination yet impair object recognition. *Behav. Neurosci.* 124, 55–68. doi: 10.1037/a0018320

Albertsmeier, M., Teschendorf, P., Popp, E., Galmbacher, R., Vogel, P., and Bottiger, B. W. (2007). Evaluation of a tape removal test to assess neurological

deficit after cardiac arrest in rats. *Resuscitation* 74, 552–558. doi: 10.1016/j.resuscitation.2007.01.040

Alm, P. A., and Dreimanis, K. (2013). Neuropathic pain: transcranial electric motor cortex stimulation using high frequency random noise. Case report of a novel treatment. *J. Pain Res.* 6, 479–486. doi: 10.2147/JPR.S44648

Antunes, M., and Biala, G. (2012). The novel object recognition memory: neurobiology, test procedure, and its modifications. *Cogn. Process.* 13, 93–110. doi: 10.1007/s10339-011-0430-z

Asan, A. S., Gok, S., and Sahin, M. (2019). Electrical fields induced inside the rat brain with skin, skull, and dural placements of the current injection electrode. *PLoS One* 14:e0203727. doi: 10.1371/journal.pone.0203727

Babaee, A., Eftekhar-Vaghefi, S. H., Asadi-Shekaari, M., Shahrokhi, N., Soltani, S. D., Malekpour-Afshar, R., et al. (2015). Melatonin treatment reduces astrogliosis and apoptosis in rats with traumatic brain injury. *Iran. J. Basic Med. Sci.* 18, 867–872.

Bramlett, H. M., and Dietrich, W. D. (2004). Pathophysiology of cerebral ischemia and brain trauma: similarities and differences. *J. Cereb. Blood Flow Metab.* 24, 133–150. doi: 10.1097/01.WCB.0000111614.19196.04

Brown, J. A., and Pilitsis, J. G. (2005). Motor cortex stimulation for central and neuropathic facial pain: a prospective study of 10 patients and observations of enhanced sensory and motor function during stimulation. *Neurosurgery* 56, 290–297. doi: 10.1227/01.neu.0000148905.75845.98

Cavinato, M., Iaia, V., and Piccione, F. (2012). Repeated sessions of sub-threshold 20-Hz rTMS. Potential cumulative effects in a brain-injured patient. *Clin. Neurophysiol.* 123, 1893–1895. doi: 10.1016/j.clinph.2012.02.066

Chen, Z., Leung, L. Y., Mountney, A., Liao, Z., Yang, W., Lu, X. C., et al. (2012). A novel animal model of closed-head concussive-induced mild traumatic brain injury: development, implementation and characterization. *J. Neurotrauma* 29, 268–280. doi: 10.1089/neu.2011.2057

Cheng, T., Yang, B., Li, D., Ma, S., Tian, Y., Qu, R., et al. (2015). Wharton's jelly transplantation improves neurologic function in a rat model of traumatic brain injury. *Cell. Mol. Neurobiol.* 35, 641–649. doi: 10.1007/s10571-015-0159-9

Cikriklar, H. I., Uysal, O., Ekici, M. A., Ozbek, Z., Cosan, D. T., Yucel, M., et al. (2016). Effectiveness of GFAP in determining neuronal damage in rats with induced head trauma. *Turk. Neurosurg.* 26, 878–889. doi: 10.5137/1019-5149.JTN.13946-15.2

Demirtas-Tatlidede, A., Vahabzadeh-Hagh, A. M., Bernabeu, M., Tormos, J. M., and Pascual-Leone, A. (2012). Noninvasive brain stimulation in traumatic brain injury. *J. Head Trauma Rehabil.* 27, 274–292. doi: 10.1097/HTR.0b013e318217df55

Dhaliwal, S. K., Meek, B. P., and Modirrousta, M. M. (2015). Non-invasive brain stimulation for the treatment of symptoms following traumatic brain injury. *Front. Psychiatry* 6:119. doi: 10.3389/fpsyt.2015.00119

Dixon, C. E., Lyeth, B. G., Povlishock, J. T., Findling, R. L., Hamm, R. J., Marmarou, A., et al. (1987). A fluid percussion model of experimental brain injury in the rat. *J. Neurosurg.* 67, 110–119. doi: 10.3171/jns.1987.67.1.0110

Faden, A. I., Demediuk, P., Panter, S. S., and Vink, R. (1989). The role of excitatory amino acids and NMDA receptors in traumatic brain injury. *Science* 244, 798–800. doi: 10.1126/science.2567056

Fagundes-Pereyra, W. J., Teixeira, M. J., Reyns, N., Touzet, G., Dantas, S., Laureau, E., et al. (2010). Motor cortex electric stimulation for the treatment of neuropathic pain. *Arq. Neuropsiquiatr.* 68, 923–929. doi: 10.1590/s0004-282x2010000600018

Faul, M., Xu, L., Wald, M. M., and Coronado, V. G. (2010). *Traumatic Brain Injury in the United States: Emergency Department Visits, Hospitalizations and Deaths 2002–2006*. Atlanta, GA: Centers for Disease Control and Prevention NCfIPaC.

Feng, X.-J., Huang, Y.-T., Huang, Y.-Z., Kuo, C.-W., Peng, C.-W., Rotenberg, A., et al. (2020). Early transcranial direct current stimulation treatment exerts neuroprotective effects on 6-OHDA-induced Parkinsonism in rats. *Brain Stimul.* 13, 655–663. doi: 10.1016/j.brs.2020.02.002

Fitzgerald, P. B., Fountain, S., and Daskalakis, Z. J. (2006). A comprehensive review of the effects of rTMS on motor cortical excitability and inhibition. *Clin. Neurophysiol.* 117, 2584–2596. doi: 10.1016/j.clinph.2006.06.712

Foda, M. A., and Marmarou, A. (1994). A new model of diffuse brain injury in rats. Part II: morphological characterization. *J. Neurosurg.* 80, 301–313. doi: 10.3171/jns.1994.80.2.0301

Forster, C., Clark, H. B., Ross, M. E., and Iadecola, C. (1999). Inducible nitric oxide synthase expression in human cerebral infarcts. *Acta Neuropathol.* 97, 215–220. doi: 10.1007/s004010050977

Gaynes, B. N., Lloyd, S. W., Lux, L., Gartlehner, G., Hansen, R. A., Brode, S., et al. (2014). Repetitive transcranial magnetic stimulation for treatment-resistant depression: a systematic review and meta-analysis. *J. Clin. Psychiatry* 75, 477–489; quiz 489. doi: 10.4088/JCP.13r08815

Hsieh, T.-H., Huang, Y.-Z., Chen, J.-J. J., Rotenberg, A., Chiang, Y.-H., Chien, W.-S. C., et al. (2015a). Novel use of theta burst cortical electrical stimulation for modulating motor plasticity in rats. *J. Med. Biol. Eng.* 35, 62–68. doi: 10.1007/s40846-015-0006-y

Hsieh, T.-H., Huang, Y.-Z., Rotenberg, A., Pascual-Leone, A., Chiang, Y.-H., Wang, J. Y., et al. (2015b). Functional dopaminergic neurons in substantia nigra are required for transcranial magnetic stimulation-induced motor plasticity. *Cereb. Cortex* 25, 1806–1814. doi: 10.1093/cercor/bht421

Hsieh, T.-H., Kang, J.-W., Lai, J.-H., Huang, Y.-Z., Rotenberg, A., Chen, K.-Y., et al. (2017). Relationship of mechanical impact magnitude to neurologic dysfunction severity in a rat traumatic brain injury model. *PLoS One* 12:e0178186. doi: 10.1371/journal.pone.0178186

Huang, Y.-Z., Edwards, M. J., Rounis, E., Bhatia, K. P., and Rothwell, J. C. (2005). Theta burst stimulation of the human motor cortex. *Neuron* 45, 201–206. doi: 10.1016/j.neuron.2004.12.033

Jefferson, S. C., Clayton, E. R., Donlan, N. A., Kozlowski, D. A., Jones, T. A., and Adkins, D. L. (2016). Cortical stimulation concurrent with skilled motor training improves forelimb function and enhances motor cortical reorganization following controlled cortical impact. *Neurorehabil. Neural Repair.* 30, 155–158. doi: 10.1177/1545968315600274

Kamble, N., Netravathi, M., and Pal, P. K. (2014). Therapeutic applications of repetitive transcranial magnetic stimulation (rTMS) in movement disorders: a review. *Parkinsonism Relat. Disord.* 20, 695–707. doi: 10.1016/j.parkreldis.2014.03.018

Katsura, K., Kristián, T., and Siesjö, B. K. (1994). Energy metabolism, ion homeostasis and cell damage in the brain. *Biochem. Soc. Trans.* 22, 991–996. doi: 10.1042/bst0220991

Khedr, E. M., Rothwell, J. C., Ahmed, M. A., Shawky, O. A., and Farouk, M. (2007). Modulation of motor cortical excitability following rapid-rate transcranial magnetic stimulation. *Clin. Neurophysiol.* 118, 140–145. doi: 10.1016/j.clinph.2006.09.006

Kobori, N., and Dash, P. K. (2006). Reversal of brain injury-induced prefrontal glutamic acid decarboxylase expression and working memory deficits by D1 receptor antagonism. *J. Neurosci.* 26, 4236–4246. doi: 10.1523/JNEUROSCI.4687-05.2006

Marmarou, A., Foda, M. A., Van Den Brink, W., Campbell, J., Kita, H., and Demetriadou, K. (1994). A new model of diffuse brain injury in rats. Part I: pathophysiology and biomechanics. *J. Neurosurg.* 80, 291–300. doi: 10.3171/jns.1994.80.2.0291

Myer, D. J., Gurkoff, G. G., Lee, S. M., Hovda, D. A., and Sofroniew, M. V. (2006). Essential protective roles of reactive astrocytes in traumatic brain injury. *Brain* 129, 2761–2772. doi: 10.1093/brain/awl165

Pascual, J. M., Solivera, J., Prieto, R., Barrios, L., Lopez-Larrubia, P., Cerdan, S., et al. (2007). Time course of early metabolic changes following diffuse traumatic brain injury in rats as detected by (1)H NMR spectroscopy. *J. Neurotrauma* 24, 944–959. doi: 10.1089/neu.2006.0190

Paxinos, G., and Watson, C. (2005). *The Rat Brain in Stereotaxic Coordinates.* Amsterdam: Elsevier Academic Press.

Ping, X., and Jin, X. (2016). Transition from initial hypoactivity to hyperactivity in cortical layer V pyramidal neurons after traumatic brain injury *in vivo*. *J. Neurotrauma* 33, 354–361. doi: 10.1089/neu.2015.3913

Pink, A. E., Williams, C., Alderman, N., and Stoffels, M. (2021). The use of repetitive transcranial magnetic stimulation (rTMS) following traumatic brain injury (TBI): a scoping review. *Neuropsychol. Rehabil.* 31, 479–505. doi: 10.1080/09602011.2019.1706585

Popernack, M. L., Gray, N., and Reuter-Rice, K. (2015). Moderate-to-severe traumatic brain injury in children: complications and rehabilitation strategies. *J. Pediatr. Health Care* 29, e1–e7. doi: 10.1016/j.pedhc.2014.09.003

Rossi, S., Hallett, M., Rossini, P. M., Pascual-Leone, A., and Safety of TMS Consensus Group. (2009). Safety, ethical considerations and application

guidelines for the use of transcranial magnetic stimulation in clinical practice and research. *Clin. Neurophysiol.* 120, 2008–2039. doi: 10.1016/j.clinph.2009.08.016

Schaar, K. L., Brenneman, M. M., and Savitz, S. I. (2010). Functional assessments in the rodent stroke model. *Exp. Transl. Stroke Med.* 2:13. doi: 10.1186/2040-7378-2-13

Smith, D. H., Hicks, R. R., Johnson, V. E., Bergstrom, D. A., Cummings, D. M., Noble, L. J., et al. (2015). Pre-clinical traumatic brain injury common data elements: toward a common language across laboratories. *J. Neurotrauma* 32, 1725–1735. doi: 10.1089/neu.2014.3861

Sokal, P., Harat, M., Malukiewicz, A., Kiec, M., Switonska, M., and Jablonska, R. (2019). Effectiveness of tonic and burst motor cortex stimulation in chronic neuropathic pain. *J. Pain Res.* 12, 1863–1869. doi: 10.2147/JPR.S195867

Son, B. C., Lee, S. W., Choi, E. S., Sung, J. H., and Hong, J. T. (2006). Motor cortex stimulation for central pain following a traumatic brain injury. *Pain* 123, 210–216. doi: 10.1016/j.pain.2006.02.028

Syntichaki, P., and Tavernarakis, N. (2003). The biochemistry of neuronal necrosis: rogue biology? *Nat. Rev. Neurosci.* 4, 672–684. doi: 10.1038/nrn1174

Villamar, M. F., Santos Portilla, A., Fregni, F., and Zafonte, R. (2012). Noninvasive brain stimulation to modulate neuroplasticity in traumatic brain injury. *Neuromodulation* 15, 326–338. doi: 10.1111/j.1525-1403.2012.00474.x

Wakasa, S., Shiiya, N., Tachibana, T., Ooka, T., and Matsui, Y. (2009). A semiquantitative analysis of reactive astrogliosis demonstrates its correlation with the number of intact motor neurons after transient spinal cord ischemia. *J. Thorac. Cardiovasc. Surg.* 137, 983–990. doi: 10.1016/j.jtcvs.2008.10.002

Wang, M. L., Yu, M. M., Yang, D. X., Liu, Y. L., Wei, X. E., and Li, W. B. (2018). Longitudinal microstructural changes in traumatic brain injury in rats: a diffusional kurtosis imaging, histology, and behavior study. *Am. J. Neuroradiol.* 39, 1650–1656. doi: 10.3174/ajnr.A5737

Yu, Y.-W., Hsieh, T.-H., Chen, K.-Y., Wu, J. C.-C., Hoffer, B. J., Greig, N. H., et al. (2016). Glucose-dependent insulinotropic polypeptide ameliorates mild traumatic brain injury-induced cognitive and sensorimotor deficits and neuroinflammation in rats. *J. Neurotrauma* 33, 2044–2054. doi: 10.1089/neu.2015.4229

Yu, K. P., Yoon, Y.-S., Lee, J. G., Oh, J.-S., Lee, J. S., Seog, T., et al. (2018). Effects of electric cortical stimulation (ECS) and transcranial direct current stimulation (tDCS) on rats with a traumatic brain injury. *Ann. Rehabil. Med.* 42, 502–513. doi: 10.5535/arm.2018.42.4.502

Zaninotto, A. L., El-Hagrassy, M. M., Green, J. R., Babo, M., Paglioni, V. M., Benute, G. G., et al. (2019). Transcranial direct current stimulation (tDCS) effects on traumatic brain injury (TBI) recovery: a systematic review. *Dement. Neuropsychol.* 13, 172–179. doi: 10.1590/1980-57642018dn13-020005

Zhang, Y., Chopp, M., Rex, C. S., Simmon, V. F., Sarraf, S. T., Zhang, Z. G., et al. (2019). A small molecule spinogenic compound enhances functional outcome and dendritic spine plasticity in a rat model of traumatic brain injury. *J. Neurotrauma* 36, 589–600. doi: 10.1089/neu.2018.5790

Conflict of Interest: The authors declare that the research was conducted in the absence of any commercial or financial relationships that could be construed as a potential conflict of interest.

Copyright © 2021 Kuo, Chang, Liu, He, Chan, Huang, Peng, Chang, Pan and Hsieh. This is an open-access article distributed under the terms of the Creative Commons Attribution License (CC BY). The use, distribution or reproduction in other forums is permitted, provided the original author(s) and the copyright owner(s) are credited and that the original publication in this journal is cited, in accordance with accepted academic practice. No use, distribution or reproduction is permitted which does not comply with these terms.

frontiers in Neural Circuits

ORIGINAL RESEARCH
published: 27 October 2021
doi: 10.3389/fncir.2021.655502

Cerebellar Intermittent Theta-Burst Stimulation Reduces Upper Limb Spasticity After Subacute Stroke: A Randomized Controlled Trial

Yi Chen[1,2], *Qing-Chuan Wei*[1,2], *Ming-Zhi Zhang*[3], *Yun-Juan Xie*[1,2], *Ling-Yi Liao*[1,2,4], *Hui-Xin Tan*[1,2], *Qi-Fan Guo*[1,2] *and Qiang Gao*[1,2]*

[1] *Department of Rehabilitation Medicine, West China Hospital, Sichuan University, Chengdu, China,* [2] *Key Laboratory of Rehabilitation Medicine in Sichuan Province, Chengdu, China,* [3] *Department of Ultrasound Medicine, West China Hospital, Sichuan University, Chengdu, China,* [4] *Daping Hospital, Third Military Medical University, Chongqing, China*

Objective: This study aims to explore the efficacy of cerebellar intermittent theta-burst stimulation (iTBS) on upper limb spasticity in subacute stroke patients.

Methods: A total of 32 patients with upper limb spasticity were enrolled and randomly assigned to treatment with cerebellar iTBS or sham stimulation before conventional physical therapy daily for 2 weeks. The primary outcomes included the modified Ashworth scale (MAS), the modified Tardieu scale (MTS), and the shear wave velocity (SWV). The secondary outcomes were the *H*-maximum wave/*M*-maximum wave amplitude ratio (H_{max}/M_{max} ratio), motor-evoked potential (MEP) latency and amplitude, central motor conduction time (CMCT), and the Barthel Index (BI). All outcomes were evaluated at baseline and after 10 sessions of intervention.

Results: After the intervention, both groups showed significant improvements in the MAS, MTS, SWV, and BI. In addition, patients treated with cerebellar iTBS had a significant increase in MEP amplitude, and patients treated with sham stimulation had a significant decrease in H_{max}/M_{max} ratio. Compared with the sham stimulation group, the MAS, MTS, and SWV decreased more in the cerebellar iTBS group.

Conclusion: Cerebellar iTBS is a promising adjuvant tool to reinforce the therapeutic effect of conventional physical therapy in upper limb spasticity management after subacute stroke (Chinese Clinical Trial Registry: ChiCTR1900026516).

Keywords: stroke, spasticity, intermittent theta-burst stimulation, upper limb, randomized controlled trial

OPEN ACCESS

Edited by:
Ti-Fei Yuan,
Shanghai Jiao Tong University, China

Reviewed by:
Matteo Bologna,
Sapienza University of Rome, Italy
Antonio Suppa,
Sapienza University of Rome, Italy
Elias Paolo Casula,
Santa Lucia Foundation (IRCCS), Italy
Ruiping Hu,
Fudan University, China

***Correspondence:**
Qiang Gao
gaoqiang_hxkf@163.com

Received: *19 January 2021*
Accepted: *22 September 2021*
Published: *27 October 2021*

Citation:
Chen Y, Wei Q-C, Zhang M-Z, Xie Y-J, Liao L-Y, Tan H-X, Guo Q-F and Gao Q (2021) Cerebellar Intermittent Theta-Burst Stimulation Reduces Upper Limb Spasticity After Subacute Stroke: A Randomized Controlled Trial. Front. Neural Circuits 15:655502. doi: 10.3389/fncir.2021.655502

INTRODUCTION

Poststroke spasticity (PSS) is a motor disorder clinically manifested as a velocity-dependent increase in stretch reflexes due to the hyperexcitability of alpha motor neurons in the spinal cord (Ward, 2012). It is one of the most common complications after stroke, affecting 19–43% of survivors (Aloraini et al., 2015; Cai et al., 2017). Around 36% of the patients suffered moderate or severe upper limb spasticity (Nam et al., 2019). Weakness, pain, loss of dexterity, stiffness, fibrosis, and atrophy followed by upper limb PSS always contribute to disordered motor control, functional limitations, and poor quality of life that result in an increased burden on caregivers (Leo et al., 2017; Li et al., 2019).

The treatments for managing PSS include pharmacological and non-pharmacological options (Bethoux, 2015). Oral medications are well-known and generally safe, but usually with side effects, especially sedation and weakness (Dvorak et al., 2011). Botulinum toxin A injection, the most widely used local management of spasticity, has a definite efficacy on severe PSS but has a more limited impact on function (Kinnear et al., 2014; Bethoux, 2015). Conventional physical therapy, one of the non-pharmacological options, is strongly recommended for patients with clinically significant spasticity (Khan et al., 2019).

Repetitive transcranial magnetic stimulation (rTMS) is one of the physical therapies for spasticity management, and the efficacy of rTMS on upper limb spasticity after stroke has been identified over the past 10 years (Barros Galvao et al., 2014; McIntyre et al., 2018). Intermittent theta-burst stimulation (iTBS) is a novel form of rTMS, which was developed by John Rothwell in his laboratory in 2005 (Rounis and Huang, 2020). It can lead to consistent and long-lasting therapeutic effects in regulating the excitability of neural structures (Huang et al., 2005). Previous studies have confirmed that iTBS can decrease upper limb spasticity and improve motor function in individuals with stroke (Kim et al., 2015; Chen et al., 2019).

The cerebellum works in concert with the cerebral cortex and plays an important role in muscle tone adjustment (Glickstein et al., 2009). The corticopontocerebellar pathway and the cerebellothalamocortical system are the two main connections. In addition, the cerebellum as a promising stimulation target of neuromodulation has been investigated by accruing studies in recent years. Relevant research revealed that the cerebellum suppresses cortical excitability of the motor cortex via cerebellar brain inhibition (CBI) (Fernandez et al., 2018). Koch et al. found that cerebellar iTBS has efficacy in reconstructing cerebello-cortical plasticity and recovering motor function in individuals with stroke (Koch et al., 2018). However, no study has been conducted to investigate the effect of cerebellar iTBS on PSS since now. Therefore, the objective of this study was to preliminarily explore the short-term efficacy of cerebellar iTBS coupled with conventional physical therapy on upper limb spasticity in subacute stroke patients. We hypothesized that iTBS over ipsilesional cerebellum combined with conventional physical therapy could improve PSS significantly more than by applying conventional physical therapy alone.

MATERIALS AND METHODS

Participants

A total of 32 patients [25 males (78%); mean (SD) age, 54.14 (9.02) years] were enrolled from Sichuan University West China Hospital Rehabilitation Medicine (Chengdu, Sichuan Province, China) between September 2019 and September 2020. Inclusion criteria were as follows: (1) age between 18 and 80 years (Koch et al., 2018); (2) first-ever unilateral ischemic or hemorrhagic stroke confirmed by computed tomography or magnetic resonance imaging; (3) subacute stroke survivors (stroke onset ranged from 2 weeks to 6 months) (Chien et al., 2020; Soulard et al., 2020); (4) having affected elbow flexors and wrist flexors spasticity with the modified Ashworth scale (MAS) score between 1+ and 3 (Barros Galvao et al., 2014); and (5) absence of cognitive impairment that is determined by the mini-mental state examination score is over 27 (Sun et al., 2014). Exclusion criteria included the following: (1) coexisting other neurological diseases; (2) cerebellar or brain stem injury; (3) used anti-spasticity drugs or injected botulinum toxin type A within 3 months before enrollment; (4) severe general impairment or concomitant diseases; and (5) contraindications for rTMS (e.g., history of seizures, intracranial metallic implants, cardiac pacemakers, and pregnancy).

Trial Design

This randomized, double-blind, sham-controlled trial was designed to explore the safety and the short-term efficacy of cerebellar iTBS on upper limb spasticity after subacute stroke. Eligible participants were randomly allocated in a 1:1 ratio to either cerebellar iTBS group or sham stimulation group. The randomization sequences were generated based on the table of random digits and were concealed in opaque numbered envelopes, which were opened in numerical order by a neutral non-involved researcher. All outcome measures were evaluated at baseline (T0) and after 10 sessions of intervention (T1). Each evaluation was performed by a clinician or by a physical therapist who was blinded to the experimental condition of the patient. Patients themselves were also unaware of the group assignment.

The sample size was estimated using G*power of 3.1.9.2 (Faul et al., 2007), with the following parameters: effect size (d) = 1.35, $\alpha = 0.05$ (two tails), power ($1–\beta$) = 90%, and allocation ratio $n2/n1 = 1$. The effect size was determined based on the result of our pilot study. After calculation, the necessary sample size of $n = 26$ was obtained. Considering the compliance of subjects, a total of 32 patients were required to allow for a 20% dropout rate.

Ethics Committee

This study was approved by the local institutional biomedical Ethics Committee on September 30, 2019, and complied with the Declaration of Helsinki. All patients provided written informed consent before the experiment. The trial was then registered on October 13, 2019, in the Chinese Clinical Trial Registry (registration number: ChiCTR1900026516).

Interventions

Each patient received 1 session of cerebellar iTBS or sham stimulation daily, always before conventional physical therapy, for a total of 10 sessions. The overall intervention periods were 5 days/week for 2 consecutive weeks. All the patients did not use anti-spasticity drugs or injected botulinum toxin type A throughout the whole trial.

Intermittent Theta-Burst Stimulation

Before each daily conventional physical therapy, one session of cerebellar iTBS was applied over the ipsilesional lateral cerebellum, which was carried out using a 70-mm figure 8 coil attached to a magnetic stimulator (Yiruide Medical Company, Wuhan, China). The coil was positioned tangentially to the scalp, with the handle pointing superiorly. The center of the coil was positioned at 1 cm inferior and 3 cm lateral to the inion based on

previously reported studies (Hardwick et al., 2014; Olfati et al., 2020). The stimulation intensity was determined by the active motor threshold (aMT), defined as the lowest intensity which evoked at least 5 out of 10 motor-evoked potentials (MEP) with an amplitude >200 μV peak to peak in the abductor pollicis brevis muscle during 10% of maximum contraction (Popa et al., 2013; Koch et al., 2019). iTBS protocol was used with a total of 600 pulses over 200 s delivered at 80% aMT (Schwippel et al., 2019). For sham stimulation, the stimulation coil was rotated 90° so that the minimal current flow was induced in the brain, and it was still centered on the same scalp position with the same parameter as the cerebellar iTBS group (Wang et al., 2020).

Conventional Physical Therapy

Conventional physical therapy program was composed of exercises designed to improve spasticity and promote recovery of voluntary motor function of the upper limb, including limb positioning, postural training, stretching, task-oriented therapy, and sensory stimulation (Winstein et al., 2016; Kucukdeveci et al., 2018), lasting 50 min per session (**Supplementary Material**).

Outcome Measures

Primary Outcome Measures

The primary outcomes were the measurements to assess the elbow flexors and wrist flexors spasticity of the affected upper limb, including the modified Ashworth scale (MAS), the modified Tardieu scale (MTS), and the shear wave velocity (SWV).

Modified Ashworth Scale

The MAS is a reliable scale for evaluating the muscle tone in individuals with stroke, which has shown satisfactory inter- and intra-rater reliability and agreement (Meseguer-Henarejos et al., 2018; Chen et al., 2019). It was scored using a six-point (0, 1, 1+, 2, 3, 4) scale, ranging from 0 (normal muscle tone) to 4 (limb rigid in flexion or extension) (Li et al., 2020).

Modified Tardieu Scale

The MTS measures spasticity using three parameters: angle of fast-stretch R1, angle of relatively slow-stretch R2, and angle differences between R2 and R1 (Ben-Shabat et al., 2013). The differences between R2 and R1 indicate the level of the dynamic component of spasticity in the muscle (Singh et al., 2011). A standard goniometer was utilized to measure the range of motion of the elbow and wrist joints.

Shear Wave Ultrasound Elastography

The muscle hardness of the affected biceps brachii and flexor carpi radialis was measured at a relaxed position using the shear wave ultrasound elastography images obtained by an ultrasonic apparatus (Resona 7, Mindray, Shenzhen, China). The transducer (L9-3U type) was placed over the bellies of biceps brachii or flexor carpi radialis and was perpendicular to the muscle fibers in the transverse axis (Wu et al., 2017). In the image, a region of interest (ROI, 0.5 cm*0.5 cm) was set near the center part where the muscle was thickest. During SWV acquisition, a warm thin layer of acoustic gel was kept on the skin and the transducer was held stationary. After that, three measurements of SWV with the lowest coefficient of variation were acquired and averaged for further statistical analysis (Akagi and Takahashi, 2013).

Secondary Outcome Measures

The secondary outcomes included the H-maximum wave/M-maximum wave amplitude ratio (H_{max}/M_{max} ratio) to assess the intrinsic excitability of the alpha motor neurons, neurophysiological parameters to assess the cortical activity, and the Barthel Index (BI) to assess the ability of activities of daily living (ADL).

H_{max}/M_{max} Ratio

Compound muscle action potentials and Hoffmann (H) reflex were obtained using an electromyography (EMG) unit (Keypoint, Dantec, Denmark) with a bandpass filter at 20 Hz to 2 kHz, sweep speed at 10 ms/division, and sensitivity at 200–500 μV. Ag–AgCl surface electrodes were utilized to record the EMG activity. A bipolar stimulus probe was used to stimulate the median nerve at the antecubital fossa. After skin preparation, the active electrode was placed over the bellies of the affected flexor carpi radialis at one-third of the proximal distance between the medial epicondyle of the humerus and the radial styloid, the reference electrode was 4 cm distal and lateral to the active electrodes, and the ground electrode was between the stimulating and the active electrode (Pizzi et al., 2005; Naghdi et al., 2014). Stimulus intensity was gradually increased until an H-reflex emerged. And then, the H_{max}/M_{max} ratio was recorded to estimate the intrinsic excitability of the alpha motor neurons.

Neurophysiological Parameters

Neurophysiological parameters were recorded by the above-mentioned TMS instrument. The MEP latency and amplitude, and central motor conduction time (CMCT) were detected in the unaffected hemisphere recorded by the contralateral abductor pollicis brevis. Before the MEP measurement, the resting motor threshold (rMT) was determined as the lowest intensity to evoke at least 5 MEPs of peak-to-peak amplitude higher than 50 μV on 10 consecutive stimulations during a resting period. Later, latencies and amplitudes of 5 MEPs were obtained by stimulating at 120% of the rMT intensity (Pisa et al., 2020), and three intermediate values were acquired and averaged for further statistical analysis. In addition, the CMCT was calculated as the latency difference between MEPs elicited by stimulating the motor cortex and those evoked by spinal (motor root) stimulation (Cakar et al., 2016).

Barthel Index

The BI is a 10-item measure of ADL (i.e., feeding, bathing, personal hygiene, dressing, bowel control, bladder control, using the toilet, chair/bed transfer, ambulation, and stair climbing) used to quantify functional change after rehabilitation intervention (Silveira et al., 2018). It is a self-reported scale with excellent inter-rater reliability for standard administration after stroke (Duffy et al., 2013).

Statistical Analysis

Professional physical therapists monitored adverse effects throughout the trial. Data management and analyses were

performed using GraphPad Prism 7.00 (GraphPad Software, Inc., La Jolla, CA, USA). Before undergoing statistical analyses, the normal distribution of data was evaluated by the Shapiro–Wilk test. Continuous variables, ordinal variables, and categorical variables were, respectively, presented as mean (±standard deviation, SD), medians (interquartile range, IQR), and number (percentage, %). The level of significance was set at $\alpha = 0.05$. Descriptive analyses were conducted to show the demographic and clinical characteristics of subjects. Fisher's exact test and unpaired *t*-test were used to evaluate the differences between the groups in the distribution of the characteristics of the subject at baseline.

For the MAS, the scores 0, 1, 1+, 2, 3, and 4 were converted to 0, 1, 2, 3, 4, and 5. The intervention efficacy within the group and between groups was analyzed with the Wilcoxon matched-pairs signed-rank test and the Mann–Whitney *U* test, respectively. For other outcome measures, a paired *t*-test of raw data was performed to evaluate the treatment effects within groups. Additionally, an unpaired *t*-test of changes between T0 and T1 was conducted to analyze the difference between groups.

RESULTS

Participant Characteristics and Flow of the Trial

After the screening based on the inclusion and exclusion criteria, a total of 32 out of 404 patients recruited were identified as being eligible for the trial. The whole procedure was well-tolerated, and no adverse events were reported in either group. During the intervention period, three subjects withdrew because two subjects were discharged in advance and one subject was transferred to another hospital that is near home (**Figure 1**). At baseline, no significant between-group differences were found in age, sex,

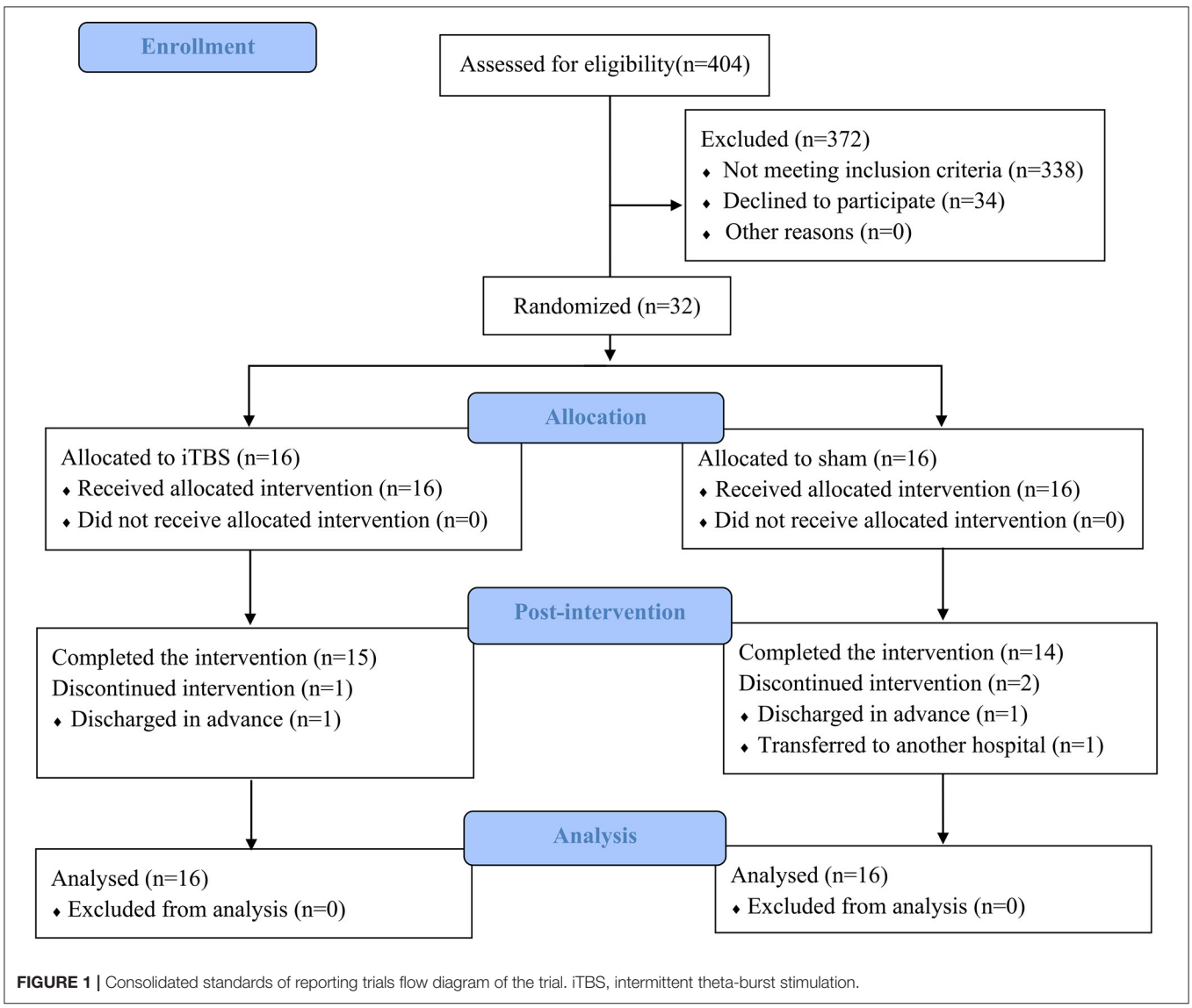

FIGURE 1 | Consolidated standards of reporting trials flow diagram of the trial. iTBS, intermittent theta-burst stimulation.

TABLE 1 | Characteristics of the participants.

Variable	Cerebellar iTBS ($n = 16$)	Sham stimulation ($n = 16$)	*P*-value
Age (y), mean ± SD	57.38 ± 8.04	51.44 ± 9.19	0.061[a]
Gender: male, *n* (%)	13 (81.25%)	12 (75.00%)	>0.999[b]
Time since the stroke (d), mean ± SD	80.13 ± 35.19	101.50 ± 54.15	0.196[a]
Type of stroke: ischemic, *n* (%)	10 (62.50%)	8 (50.00%)	0.722[b]
Paretic side: left, *n* (%)	12 (75.00%)	7 (43.75%)	0.149[b]
NIHSS score, *n* (%)			0.685[b]
0∼4	13 (81.25%)	11 (68.75%)	
5∼15	3 (18.75%)	5 (31.25%)	

iTBS, intermittent theta-burst stimulation; y, years; d, days; SD, standard deviation; NIHSS, National Institute of Health Stroke Scale.
[a]*Analyzed by unpaired t-test.*
[b]*Analyzed by Fisher's exact test.*

time since stroke, types of stroke, paretic side, and the severity of stroke assessed by NIHSS (**Table 1**).

Outcome Measures

Table 2 lists the descriptive data for all outcome measures in both groups at T0 and T1. **Figure 2** provides the statistical analysis results between groups.

The Results of Primary Outcomes

The Mann–Whitney *U* test showed that 2 weeks of cerebellar iTBS coupled with conventional physical therapy resulted in the decreases of the MAS scores for affected elbow flexors and wrist flexors compared with sham stimulation (elbow flexors: $P = 0.004$, wrist flexors: $P = 0.002$). After the intervention, Wilcoxon matched-pairs signed-rank test revealed that both groups showed a significant decrease in the MAS scores of elbow flexors (cerebellar iTBS group: $P < 0.001$, sham stimulation group: $P = 0.031$), and the cerebellar iTBS group also showed the improvement in the MAS scores of wrist flexors ($P < 0.001$).

Consistent with the result of MAS, significant differences in MTS scores (elbow flexors: $P < 0.001$, wrist flexors: $P < 0.0001$) and SWV values (biceps brachii: $P = 0.015$, flexor carpi radialis: $P < 0.001$) of upper limb were also found between cerebellar iTBS and sham stimulation groups. The analysis of effectiveness within groups indicated that MTS scores and SWV values of upper limb significantly improved after interventions both in the cerebellar iTBS group (MTS scores: elbow flexors, $P < 0.001$; wrist flexors, $P < 0.001$. SWV values: biceps brachii, $P < 0.001$; flexor carpi radialis, $P < 0.001$) and the sham stimulation group (MTS scores: elbow flexors, $P = 0.005$; wrist flexors, $P < 0.001$. SWV values: biceps brachii, $P = 0.002$; flexor carpi radialis, $P = 0.023$) (**Figure 2**).

The Results of Secondary Outcomes

After the intervention, the patients of both groups showed significant improvements in the BI (cerebellar iTBS group, $P < 0.001$; sham stimulation group, $P < 0.001$) scores compared with baseline. For the MEP amplitude, a significant increase was detected only in the cerebellar iTBS group at T1 compared with T0 ($P = 0.003$). For the H_{max}/M_{max} ratio, a significant decrease was detected only in the sham stimulation group at T1 compared with T0 ($P = 0.009$). However, there were no differences between the groups for all the secondary outcomes (**Figure 3**).

DISCUSSION

This randomized, double-blind, sham-controlled study was designed to explore the short-term efficacy of cerebellar iTBS coupled with conventional physical therapy on upper limb spasticity in subacute stroke patients. Our results show that cerebellar iTBS coupled with conventional physical therapy improves PSS of the upper limb and ADL in individuals with stroke, as demonstrated by the decreased MAS and MTS scores, the reduced SWV values, and the increased BI scores after intervention. Importantly, the effectiveness of cerebellar iTBS on spasticity is promising, as significant improvements in the MAS scores, MTS scores, and SWV values were detected in the cerebellar iTBS group when compared with the sham stimulation group.

The Effect of Cerebellar iTBS on Spasticity

Our study systematically assessed elbow flexors and wrist flexors spasticity by clinical, electrophysiological, and biomechanical measurements. Both clinical and biomechanical measurements showed significant improvements after cerebellar iTBS when compared with sham stimulation.

From a clinical point of view, we found that cerebellar iTBS coupled with conventional physical therapy decreased MAS scores of elbow flexors and wrist flexors from 3 to 2 points, passing from a marked increase level (2) to a slight increase level (1+) (Bohannon and Smith, 1987). In addition, the result of the difference between groups showed that the median changes of MAS scores of both elbow flexors and wrist flexors decreased one level in the cerebellar iTBS group when compared with the sham stimulation group, revealing that the efficacy of the cerebellar iTBS combined with conventional physical therapy was significantly better than that of the conventional physical therapy alone. Notably, the above changes reached the minimal clinically important difference that indicates a clinical significance was detected (Chen et al., 2019). Consistent with the result of MAS, MTS was also significantly improved by the 2 weeks of cerebellar iTBS coupled with conventional physical therapy, with the average angle differences between R2 and R1 of elbow flexors and wrist flexors reduced 43.00 degrees and 51.93 degrees, respectively. The range of motion at the upper limb is associated with cosmesis, hygiene, and active movement capabilities (Malhotra et al., 2011). Therefore, the increase in the range of motion at the upper limb can remove some participation restrictions and improve the quality of life in individuals with stroke.

From an electrophysiological point of view, spasticity is associated with the over hyperexcitability of spinal alpha motor neurons. The H-reflex is commonly used to quantify the level of spinal alpha motor neuron excitability (Pizzi et al., 2005). The

TABLE 2 | The descriptive data for all outcome measures in both groups at T0 and T1.

Outcome measures	T0		T1		Difference within groups (T1–T0)	
	Cerebellar iTBS	Sham stimulation	Cerebellar iTBS	Sham stimulation	Cerebellar iTBS	Sham stimulation
MAS						
Elbow flexors	3.00 (3.00,3.00)	3.00 (2.00,3.00)	2.00 (2.00,2.00)	2.00 (2.00, 3.00)	−1.00 (−1.00, −1.00)[a,***]	0.00 (−1.00, 0.00)[a,*]
Wrist flexors	3.00 (2.75,3.00)	3.00 (2.00,3.00)	2.00 (1.00,2.00)	2.00 (2.00, 3.00)	−1.00 (−2.00, −1.00)[a,***]	0.00 (−1.00, 0.00)[a]
MTS (R2–R1) (deg.)						
Elbow flexors	80.00 (75.00, 88.00)	79.50 (57.50, 81.25)	36.73 ± 22.26	55.71 ± 19.91	−40.27 ± 15.29[a,***]	−16.36 ± 16.84[a,**]
Wrist flexors	71.57 ± 19.76	62.14 ± 22.45	19.64 ± 15.87	45.14 ± 22.64	−51.93 ± 23.55[b,***]	−17.00 ± 11.58[b,***]
SWV (m/s)						
Biceps brachii	3.07 ± 0.50	2.73 ± 0.75	2.15 ± 0.35	2.25 ± 0.59	−0.92 ± 0.45[b,***]	−0.48 ± 0.44[b,**]
Flexor carpi radialis	3.17 ± 0.42	2.57 ± 0.39	2.30 ± 0.32	2.32 ± 0.37	−0.87 ± 0.43[b,***]	−0.25 ± 0.35[b,*]
H_{max}/M_{max} ratio	0.60 ± 0.49	0.79 ± 0.47	0.33 ± 0.26	0.46 ± 0.22	−0.05 (−0.53, 0.00)[b]	−0.33 ± 0.37[b,**]
MEP latency (ms)	22.14 ± 1.32	21.33 ± 2.21	21.72 ± 1.56	21.45 ± 2.10	−0.42 ± 1.24[b]	0.00 (−1.13, 0.73)[b]
MEP amplitude (μV)	140.47 ± 48.45	188.00 ± 97.41	170.00 (136.00, 238.67)	176.34 ± 69.01	30.67 (12.00, 62.00)[a,**]	2.67 (−43.97, 46.67)[b]
CMCT (ms)	8.17 ± 2.41	7.23 ± 2.36	6.37 ± 2.26	6.50 ± 2.34	−0.85 (−2.72, −0.17)[b]	−0.74 ± 2.91[b]
BI	60.00 ± 21.68	70.94 ± 13.32	69.06 ± 16.75	78.13 ± 12.76	9.06 ± 8.61[b,***]	7.19 ± 5.76[b,***]

T0, at baseline; T1, after 10 sessions of intervention; iTBS, intermittent theta burst stimulation; MAS, modified Ashworth scale; MTS, modified Tardieu scale; deg., degree; SWV, shear wave velocity; H_{max}/M_{max} ratio, H-maximum wave/M-maximum wave amplitude ratio; MEP, motor-evoked potential; CMCT, central motor conduction time; BI, the Barthel Index.
**Within group: P < 0.05, when compared with baseline.*
***Within group: P < 0.01, when compared with baseline.*
****Within group: P < 0.001, when compared with baseline.*
[a] *Wilcoxon matched-pairs signed-rank test.*
[b] *Paired t-test.*

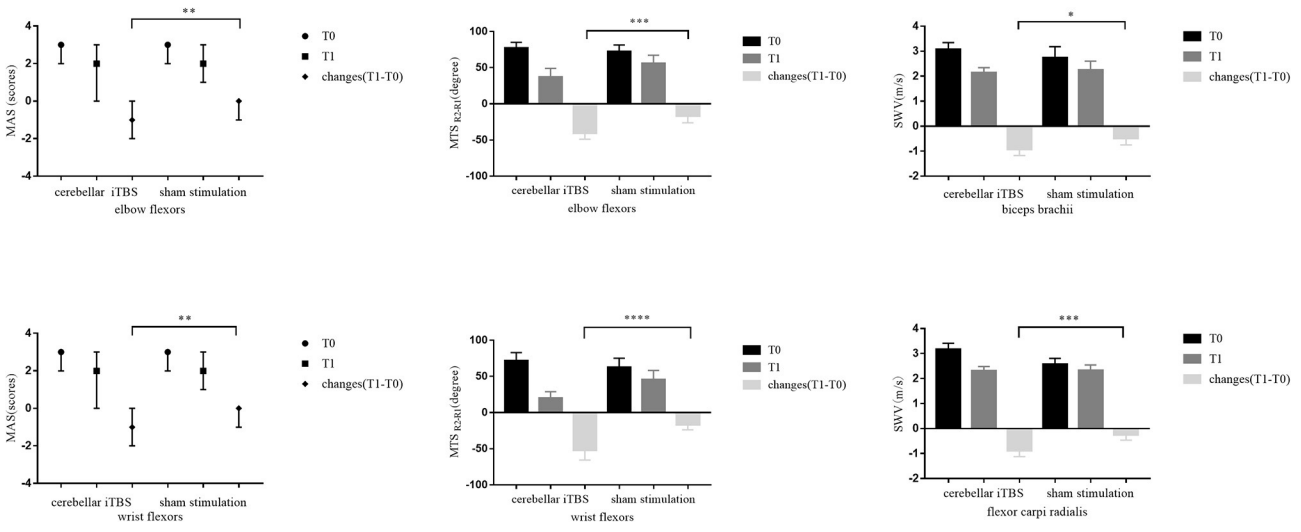

FIGURE 2 | The statistical analysis results between groups for the primary outcomes. The data are expressed as the Median with IQR or Mean with 95%CI. *$P < 0.05$, **$P < 0.01$, ***$P < 0.001$, ****$P < 0.0001$.

H_{max}/M_{max} ratio is proposed as a measure of the percentage of motoneurons activated by eliciting the monosynaptic H-reflex compared with those directly activated (Okuyama et al., 2018), which presents high reliability and good sensitivity in detecting changes in spasticity (Levin and Hui-Chan, 1993). In this study, no significant improvements in the H_{max}/M_{max} ratio were found between groups. It may be attributed to the high variability of H-reflex in measuring the median nerve (Kim et al., 2015). Another possible reason is that the stimulation intensity of iTBS (80% aMT) was lower than the intensity of conventional rTMS (100% rMT) to induce electrophysiological changes in PSS improvement. Kim et al. also reported similar findings that iTBS over the affected motor cortex did not affect the H-reflex evoked in flexor carpi radialis (Kim et al., 2015).

From a biomechanical point of view, shear wave ultrasound elastography is feasible in muscle hardness assessment that may

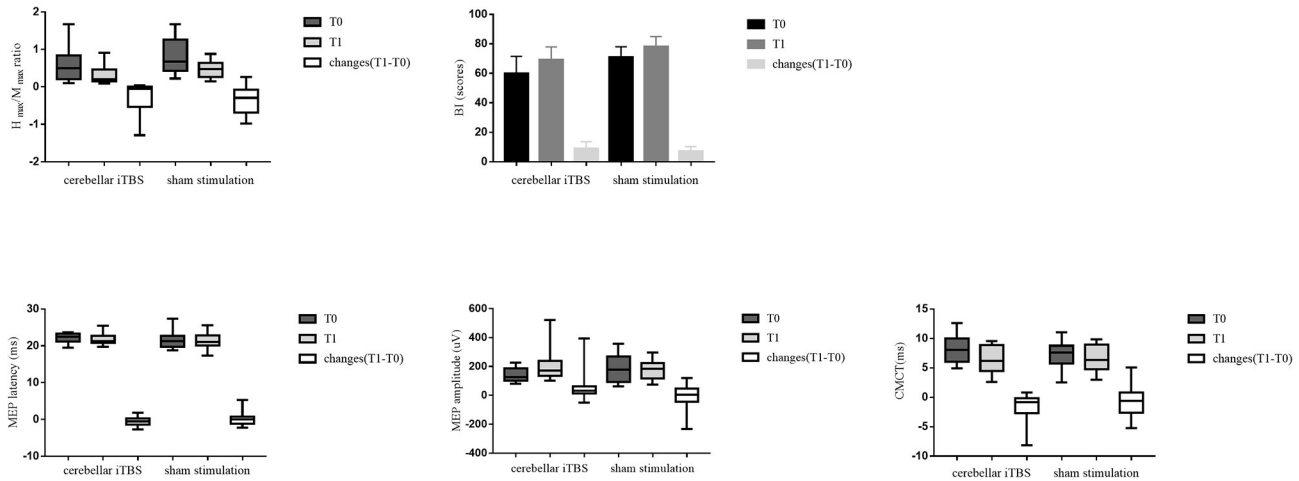

FIGURE 3 | The statistical analysis results between groups for the secondary outcomes. The data are expressed as the Median with IQR or Mean with 95%CI.

offer a better quantification of spasticity compared with clinical and electrophysiological measurements (Gao et al., 2018; Chen et al., 2019). In contrast to normal muscle cells, spastic muscle cells from stroke had shorter resting sarcomeres and increased elastic moduli, indicating that muscle stiffness can reflect the disease-related alterations in tissue properties (Wu et al., 2017). As shear waves travel faster in stiffer tissues, greater SWV and echo intensity were detected in spastic muscles (Lee et al., 2015). Our data demonstrated that the average SWV values of both biceps brachii and flexor carpi radialis were decreased in both groups after the intervention, and the cerebellar iTBS coupled with conventional physical therapy significantly decreased more SWV than sham stimulation. It implied that the therapeutic effect of cerebellar iTBS on changing muscle tissue properties was relatively obvious.

In agreement with relevant reported research published in 2014 (Barros Galvao et al., 2014), it was found that physiotherapy combined with additional low-frequency rTMS on unaffected primary motor cortex was more effective than physiotherapy alone in reducing upper limb spasticity in patients with chronic stroke (Barros Galvao et al., 2014). Furthermore, the benefits of iTBS on the affected motor cortex as an effective intervention to improve PSS had been identified by Kim et al. (2015). Their research found that a single session of iTBS contributed to a transient improvement in upper limb spasticity after stroke, which proved that iTBS seems to be an effective adjuvant to manage upper limb spasticity. Consistent with the above-reported studies, our study revealed significant improvements in upper limb spasticity after cerebellar iTBS in individuals with subacute stroke.

It is important to point out that the mean age of the subjects in the cerebellar iTBS group was 5.94 years older than that in the sham stimulation group, although it did not reach statistical significance. Age is a significant predictor of upper limb spasticity after stroke, with an odds ratio of 0.01 (Tedesco Triccas et al., 2019). The increase in aging individuals could have an impact on a higher incidence of upper limb spasticity. Besides, age is also a critical factor for predicting stroke outcome, with a negative correlation between age and the score of the motor component of the Functional Independence Measure and an active correlation between age and the length of hospital stay (Koyama et al., 2020). In our study, a significant decrease in upper limb spasticity was detected in the older cerebellar iTBS group patients.

Possible Mechanism

The mechanism of iTBS over the ipsilesional lateral cerebellum reducing upper limb spasticity is still unclear. iTBS consists of high-frequency stimulation bursts, and the stimulus pattern is based on the natural theta rhythm occurring in the hippocampus of the brain, which can strongly modulate the neural activity of the cerebellum (Klomjai et al., 2015; Koch et al., 2019). An animal study reported that there were two modes of synaptic plasticity in the cerebellum, long-term depression (LTD) and long-term potentiation (LTP) (Jörntell and Hansel, 2006). Cerebellar iTBS can induce plasticity changes in the cerebellum of stroke patients (Koch et al., 2018). Besides, the molecular evidence also suggested that high-frequency rTMS could induce neural plasticity in the cerebellum associated with LTD (Lee et al., 2014). iTBS over the ipsilesional lateral cerebellum can increase the activation of Purkinje cells; the inhibitory synaptic connections between Purkinje cells and deep cerebellar nuclei are enhanced so that the neural plasticity in the cerebellum has been regulated (Fernandez et al., 2018). Besides, cerebellum iTBS can influence the activities of spinal neurons involved in the muscle tone adjustments in two ways: the inhibitory synaptic connections between Purkinje cells and dentate nucleus reduce the tonic excitatory effect of the dentate nucleus over the contralateral cerebral cortex through the ventrolateral nucleus of the thalamus; alternatively, interposed nuclei (globose and emboliform) and fastigial nucleus directly affect both the medial and lateral descending motor systems to reduce muscle spasticity (Teixeira et al., 2015). The relevant descending pathways include the corticospinal, reticulospinal, vestibulospinal, rubrospinal, and tectospinal tracts (Matsugi and Okada, 2020). Considering the results of our study, no significant

difference in corticospinal excitability assessments (MEP latency and amplitude, and CMCT) was observed between groups. Therefore, the cerebellar iTBS improved upper limb spasticity may attribute to promoting the functional connection between the cerebellum and other brain areas rather than concerting with the cerebral cortex.

Physiological evidence shows that the cerebellum can interfere in the muscle tone adjustment by regulating neuronal discharge in different brain stem nuclei, primarily the reticular formation, red nucleus, and vestibular nucleus. Besides, the vestibular nucleus is involved in the alpha motor neuron activation, while the reticular formation and red nucleus are involved in the gamma motor neuron activation (D'Angelo, 2018). Chothia et al. found that anodal cerebellar direct current stimulation regulated the reticular spinal tract and rubrospinal tract to affect the motor neurons of the spinal cord (Chothia et al., 2016).

Other than motor areas, cerebellar iTBS also affects non-motor areas. Casula et al. found that the induction of cerebellar plasticity by iTBS was also associated with relevant changes in the neural activity of the posterior parietal cortex (Casula et al., 2016). The posterior parietal cortex participates in the perception and processing of action-related information and encodes the more abstract aspects of sensorimotor control processes, which is involved in the upper limb rehabilitation in patients with PSS (Veverka et al., 2019).

The Effects of Cerebellar iTBS on ADL

In our study, increases in BI scores were shown in both groups after interventions. These effects are likely due to the course of coupled 2 weeks of daily conventional physical therapy, independently from the cerebellar iTBS treatment. Conventional physical therapy has been confirmed as an effective way for the recovery of function after stroke (McDonnell and Stinear, 2017), whereas iTBS is an adjuvant tool to reinforce the therapeutic effect of conventional physical therapy.

Limitations

We acknowledge that some limitations still existed in this study. First, the lack of follow-up did not allow us to explore the long-term efficacy of cerebellar iTBS. Second, the potential mechanisms of cerebellar iTBS need to explore further to confirm our hypothesis. Therefore, high-quality randomized controlled trials with larger sample sizes to investigate the long-term efficacy and potential mechanisms of cerebellar iTBS are recommended for future studies.

CONCLUSION

Our study is the first study to provide novel evidence that combining cerebellar iTBS with conventional physical therapy is an effective strategy to promote upper limb PSS recovery in patients with subacute stroke. The result of the effectiveness of cerebellar iTBS in terms of the MAS, MTS, and SWV at the upper limb is significant. Therefore, cerebellar iTBS is a promising adjuvant tool to reinforce the therapeutic effect of conventional physical therapy in spasticity management for patients after subacute stroke.

DATA AVAILABILITY STATEMENT

The original contributions presented in the study are included in the article/**Supplementary Material**, further inquiries can be directed to the corresponding author/s.

ETHICS STATEMENT

The studies involving human participants were reviewed and approved by Biomedical Ethics Committee of West China Hospital, Sichuan University. The patients/participants provided their written informed consent to participate in this study.

AUTHOR CONTRIBUTIONS

YC and QG: concept, idea, research design, and writing. YC, Q-CW, and M-ZZ: research implementation. Y-JX and L-YL: data collection. H-XT and Q-FG: data analysis. QG: project management.

SUPPLEMENTARY MATERIAL

The Supplementary Material for this article can be found online at: https://www.frontiersin.org/articles/10.3389/fncir.2021.655502/full#supplementary-material

REFERENCES

Akagi, R., and Takahashi, H. (2013). Acute effect of static stretching on hardness of the gastrocnemius muscle. *Med. Sci. Sports Exerc.* 45, 1348–1354. doi: 10.1249/MSS.0b013e3182850e17

Aloraini, S. M., Gäverth, J., Yeung, E., and MacKay-Lyons, M. (2015). Assessment of spasticity after stroke using clinical measures: a systematic review. *Disabil. Rehabil.* 37, 2313–2323. doi: 10.3109/09638288.2015.1014933

Barros Galvao, S. C., Borba Costa dos Santos, R., Borba dos Santos, P., Cabral, M. E., and Monte-Silva, K. (2014). Efficacy of coupling repetitive transcranial magnetic stimulation and physical therapy to reduce upper-limb spasticity in patients with stroke: a randomized controlled trial. *Arch. Phys. Med. Rehabil.* 95, 222–229. doi: 10.1016/j.apmr.2013.10.023

Ben-Shabat, E., Palit, M., Fini, N. A., Brooks, C. T., Winter, A., and Holland, A. E. (2013). Intra- and interrater reliability of the Modified Tardieu Scale for the assessment of lower limb spasticity in adults with neurologic injuries. *Arch. Phys. Med. Rehabil.* 94, 2494–2501. doi: 10.1016/j.apmr.2013.06.026

Bethoux, F. (2015). Spasticity management after stroke. *Phys Med. Rehabil. Clin. North Am.* 26, 625–639. doi: 10.1016/j.pmr.2015.07.003

Bohannon, R. W., and Smith, M. B. (1987). Interrater reliability of a modified Ashworth scale of muscle spasticity. *Phys. Ther.* 67, 206–207. doi: 10.1093/ptj/67.2.206

Cai, Y., Zhang, C. S., Liu, S., Wen, Z., Zhang, A. L., Guo, X., et al. (2017). Electroacupuncture for poststroke spasticity: a systematic review and meta-analysis. *Arch. Phys. Med. Rehabil.* 98, 2578–2589.e4. doi: 10.1016/j.apmr.2017.03.023

Cakar, E., Akyuz, G., Durmus, O., Bayman, L., Yagci, I., Karadag-Saygi, E., et al. (2016). The relationships of motor-evoked potentials to hand dexterity, motor function, and spasticity in chronic stroke patients: a transcranial magnetic stimulation study. *Acta Neurol. Belgica* 116, 481–487. doi: 10.1007/s13760-016-0633-2

Casula, E. P., Pellicciari, M. C., Ponzo, V., Stampanoni Bassi, M., Veniero, D., Caltagirone, C., et al. (2016). Cerebellar theta burst stimulation modulates the neural activity of interconnected parietal and motor areas. *Sci. Rep.* 6:36191. doi: 10.1038/srep36191

Chen, C. L., Chen, C. Y., Chen, H. C., et al. (2019). Responsiveness and minimal clinically important difference of Modified Ashworth Scale in patients with stroke. *Eur. J. Phys. Rehabil. Med.* 55, 754–760. doi: 10.23736/S1973-9087.19.05545-X

Chien, W. T., Chong, Y. Y., Tse, M. K., Chien, C. W., and Cheng, H. Y. (2020). Robot-assisted therapy for upper-limb rehabilitation in subacute stroke patients: a systematic review and meta-analysis. *Brain Behav.* 10:e01742. doi: 10.1002/brb3.1742

Chothia, M., Doeltgen, S., and Bradnam, L. V. (2016). Anodal cerebellar direct current stimulation reduces facilitation of propriospinal neurons in healthy humans. *Brain Stimul.* 9, 364–371. doi: 10.1016/j.brs.2016.01.002

D'Angelo, E. (2018). Physiology of the cerebellum. *Handb. Clin. Neurol.* 154, 85–108. doi: 10.1016/B978-0-444-63956-1.00006-0

Duffy, L., Gajree, S., Langhorne, P., Stott, D. J., and Quinn, T. J. (2013). Reliability (inter-rater agreement) of the Barthel Index for assessment of stroke survivors: systematic review and meta-analysis. *Stroke* 44, 462–468. doi: 10.1161/STROKEAHA.112.678615

Dvorak, E. M., Ketchum, N. C., and McGuire, J. R. (2011). The underutilization of intrathecal baclofen in poststroke spasticity. *Topics Stroke Rehabil.* 18, 195–202. doi: 10.1310/tsr1803-195

Faul, F., Erdfelder, E., Lang, A. G., and Buchner, A. (2007). G*Power 3: a flexible statistical power analysis program for the social, behavioral, and biomedical sciences. *Behav. Res. Methods* 39, 175–191. doi: 10.3758/BF03193146

Fernandez, L., Major, B. P., Teo, W. P., Byrne, L. K., and Enticott, P. G. (2018). Assessing cerebellar brain inhibition (CBI) via transcranial magnetic stimulation (TMS): a systematic review. *Neurosci. Biobehav. Rev.* 86, 176–206. doi: 10.1016/j.neubiorev.2017.11.018

Gao, J., He, W., Du, L. J., Chen, J., Park, D., Wells, M., et al. (2018). Quantitative ultrasound imaging to assess the Biceps Brachii muscle in chronic post-stroke spasticity: preliminary observation. *Ultrasound Med. Biol.* 44, 1931–1940. doi: 10.1016/j.ultrasmedbio.2017.12.012

Glickstein, M., Strata, P., and Voogd, J. (2009). Cerebellum: history. *Neuroscience* 162, 549–559. doi: 10.1016/j.neuroscience.2009.02.054

Hardwick, R. M., Lesage, E., and Miall, R. C. (2014). Cerebellar transcranial magnetic stimulation: the role of coil geometry and tissue depth. *Brain Stimul.* 7, 643–649. doi: 10.1016/j.brs.2014.04.009

Huang, Y. Z., Edwards, M. J., Rounis, E., Bhatia, K. P., and Rothwell, J. C. (2005). Theta burst stimulation of the human motor cortex. *Neuron* 45:201–206. doi: 10.1016/j.neuron.2004.12.033

Jörntell, H., and Hansel, C. (2006). Synaptic memories upside down: bidirectional plasticity at cerebellar parallel fiber-Purkinje cell synapses. *Neuron* 52, 227–238. doi: 10.1016/j.neuron.2006.09.032

Khan, F., Amatya, B., Bensmail, D., and Yelnik, A. (2019). Non-pharmacological interventions for spasticity in adults: an overview of systematic reviews. *Ann. Phys. Rehabil. Med.* 62, 265–273. doi: 10.1016/j.rehab.2017.10.001

Kim, D. H., Shin, J. C., Jung, S., Jung, T.-M., and Kim, D. Y. J. N. (2015). Effects of intermittent theta burst stimulation on spasticity after stroke. *Neuroreport* 26, 561–566. doi: 10.1097/WNR.0000000000000388

Kinnear, B. Z., Lannin, N. A., Cusick, A., Harvey, L. A., and Rawicki, B. (2014). Rehabilitation therapies after botulinum toxin-A injection to manage limb spasticity: a systematic review. *Phys. Ther.* 94, 1569–1581. doi: 10.2522/ptj.20130408

Klomjai, W., Katz, R., and Lackmy-Vallee, A. (2015). Basic principles of transcranial magnetic stimulation (TMS) and repetitive TMS (rTMS). *Ann. Phys. Rehabil. Med.* 58, 208–213. doi: 10.1016/j.rehab.2015.05.005

Koch, G., Bonni, S., Casula, E. P., Iosa, M., Paolucci, S., Pellicciari, M. C., et al. (2018). Effect of cerebellar stimulation on gait and balance recovery in patients with hemiparetic stroke: a randomized clinical trial. *JAMA Neurol.* 76, 170–178. doi: 10.1001/jamaneurol.2018.3639

Koch, G., Esposito, R., Motta, C., Casula, E. P., Di Lorenzo, F., Bonni, S., et al. (2019). Improving visuo-motor learning with cerebellar theta burst stimulation: behavioral and neurophysiological evidence. *Neuroimage* 208:116424. doi: 10.1016/j.neuroimage.2019.116424

Koyama, T., Uchiyama, Y., and Domen, K. (2020). Outcome in stroke patients is associated with age and fractional anisotropy in the cerebral peduncles: a multivariate regression study. *Prog. Rehabil. Med.* 5:20200006. doi: 10.2490/prm.20200006

Kucukdeveci, A. A., Stibrant Sunnerhagen, K., Golyk, V., Delarque, A., Ivanova, G., Zampolini, M., et al. (2018). Evidence-based position paper on Physical and Rehabilitation Medicine professional practice for persons with stroke. European PRM position (UEMS PRM Section). *Eur. J. Phys. Rehabil. Med.* 54, 957–970. doi: 10.23736/S1973-9087.18.05501-6

Lee, S. A., Oh, B. M., Kim, S. J., and Paik, N. J. (2014). The molecular evidence of neural plasticity induced by cerebellar repetitive transcranial magnetic stimulation in the rat brain: a preliminary report. *Neurosci. Lett.* 575, 47–52. doi: 10.1016/j.neulet.2014.05.029

Lee, S. S., Spear, S., and Rymer, W. Z. (2015). Quantifying changes in material properties of stroke-impaired muscle. *Clin. Biomech.* 30, 269–275. doi: 10.1016/j.clinbiomech.2015.01.004

Leo, A., Naro, A., Molonia, F., Tomasello, P., Sacc,à I., Bramanti, A., et al. (2017). Spasticity management: the current state of transcranial neuromodulation. *PM R* 9, 1020–1029. doi: 10.1016/j.pmrj.2017.03.014

Levin, M. F., and Hui-Chan, C. (1993). Are H and stretch reflexes in hemiparesis reproducible and correlated with spasticity? *J. Neurol.* 240, 63–71. doi: 10.1007/BF00858718

Li, G., Yuan, W., Liu, G., Qiao, L., Zhang, Y., Wang, Y., et al. (2020). Effects of radial extracorporeal shockwave therapy on spasticity of upper-limb agonist/antagonist muscles in patients affected by stroke: a randomized, single-blind clinical trial. *Age Ageing* 49, 246–252. doi: 10.1093/ageing/afz159

Li, S., Chen, Y. T., Francisco, G. E., Zhou, P., and Rymer, W. Z. (2019). A unifying pathophysiological account for post-stroke spasticity and disordered motor control. *Front. Neurol.* 10:468. doi: 10.3389/fneur.2019.00468

Malhotra, S., Pandyan, A. D., Rosewilliam, S., Roffe, C., and Hermens, H. (2011). Spasticity and contractures at the wrist after stroke: time course of development and their association with functional recovery of the upper limb. *Clin. Rehabil.* 25, 184–191. doi: 10.1177/0269215510381620

Matsugi, A., and Okada, Y. (2020). Cerebellar transcranial direct current stimulation modulates the effect of cerebellar transcranial magnetic stimulation on the excitability of spinal reflex. *Neurosci. Res.* 150, 37–43. doi: 10.1016/j.neures.2019.01.012

McDonnell, M. N., and Stinear, C. M. (2017). TMS measures of motor cortex function after stroke: a meta-analysis. *Brain Stimul.* 10, 721–734. doi: 10.1016/j.brs.2017.03.008

McIntyre, A., Mirkowski, M., Thompson, S., Burhan, A. M., Miller, T., and Teasell, R. (2018). A systematic review and meta-analysis on the use of repetitive transcranial magnetic stimulation for spasticity poststroke. *PM R* 10, 293–302. doi: 10.1016/j.pmrj.2017.10.001

Meseguer-Henarejos, A. B., Sanchez-Meca, J., Lopez-Pina, J. A., and Carles-Hernandez, R. (2018). Inter- and intra-rater reliability of the Modified Ashworth Scale: a systematic review and meta-analysis. *Eur J. Phys. Rehabil. Med.* 54, 576–590. doi: 10.23736/S1973-9087.17.04796-7

Naghdi, S., Ansari, N. N., Abolhasani, H., Mansouri, K., Ghotbi, N., and Hasson, S. (2014). Electrophysiological evaluation of the Modified Tardieu Scale (MTS) in assessing poststroke wrist flexor spasticity. *Neuro Rehabil.* 34, 177–184. doi: 10.3233/NRE-131016

Nam, K. E., Lim, S. H., Kim, J. S., Hong, B. Y., Jung, H. Y., Lee, J. K., et al. (2019). When does spasticity in the upper limb develop after a first stroke? A nationwide observational study on 861 stroke patients. *J. Clin. Neurosci.* 66, 144–148. doi: 10.1016/j.jocn.2019.04.034

Okuyama, K., Kawakami, M., Hiramoto, M., Muraoka, K., Fujiwara, T., and Liu, M. (2018). Relationship between spasticity and spinal neural circuits in patients with chronic hemiparetic stroke. *Exp. Brain Res.* 236, 207–213. doi: 10.1007/s00221-017-5119-9

Olfati, N., Shoeibi, A., Abdollahian, E., Ahmadi, H., Hoseini, A., Akhlaghi, S., et al. (2020). Cerebellar repetitive transcranial magnetic stimulation (rTMS) for essential tremor: a double-blind, sham-controlled, crossover, add-on clinical trial. *Brain Stimul.* 13, 190–196. doi: 10.1016/j.brs.2019.10.003

Pisa, M., Chieffo, R., Giordano, A., Gelibter, S., Comola, M., Comi, G., et al. (2020). Upper limb motor evoked potentials as outcome measure in progressive multiple sclerosis. *Clin. Neurophysiol.* 131, 401–405. doi: 10.1016/j.clinph.2019.11.024

Pizzi, A., Carlucci, G., Falsini, C., Verdesca, S., and Grippo, A. (2005). Evaluation of upper-limb spasticity after stroke: a clinical and neurophysiologic study. *Arch. Phys. Med. Rehabil.* 86, 410–415. doi: 10.1016/j.apmr.2004.10.022

Popa, T., Russo, M., Vidailhet, M., Roze, E., Lehericy, S., Bonnet, C., et al. (2013). Cerebellar rTMS stimulation may induce prolonged clinical benefits in essential tremor, and subjacent changes in functional connectivity: an open label trial. *Brain Stimul.* 6, 175–179. doi: 10.1016/j.brs.2012.04.009

Rounis, E., and Huang, Y. Z. (2020). Theta burst stimulation in humans: a need for better understanding effects of brain stimulation in health and disease. *Exp. Brain Res.* 238, 1707–1714. doi: 10.1007/s00221-020-05880-1

Schwippel, T., Schroeder, P. A., Fallgatter, A. J., and Plewnia, C. (2019). Clinical review: the therapeutic use of theta-burst stimulation in mental disorders and tinnitus. *Progr. Neuro Psychopharmacol. Biol. Psychiatry* 92, 285–300. doi: 10.1016/j.pnpbp.2019.01.014

Silveira, L., Silva, J. M. D., Soler, J. M. P., Sun, C. Y. L., Tanaka, C., and Fu, C. (2018). Assessing functional status after intensive care unit stay: the Barthel Index and the Katz Index. *Int. J. Qual. Health Care* 30, 265–270. doi: 10.1093/intqhc/mzx203

Singh, P., Joshua, A. M., Ganeshan, S., and Suresh, S. (2011). Intra-rater reliability of the modified Tardieu scale to quantify spasticity in elbow flexors and ankle plantar flexors in adult stroke subjects. *Ann. Indian Acad. Neurol.* 14, 23–26. doi: 10.4103/0972-2327.78045

Soulard, J., Huber, C., Baillieul, S., Thuriot, A., Renard, F., Aubert Broche, B., et al. (2020). Motor tract integrity predicts walking recovery: a diffusion MRI study in subacute stroke. *Neurology* 94, e583–e593. doi: 10.1212/WNL.0000000000008755

Sun, J. H., Tan, L., and Yu, J. T. (2014). Post-stroke cognitive impairment: epidemiology, mechanisms and management. *Ann. Transl. Med.* 2:80. doi: 10.3978/j.issn.2305-5839.2014.08.05

Tedesco Triccas, L., Kennedy, N., Smith, T., and Pomeroy, V. (2019). Predictors of upper limb spasticity after stroke? A systematic review and meta-analysis. *Physiotherapy* 105, 163–173. doi: 10.1016/j.physio.2019.01.004

Teixeira, M. J., Schroeder, H. K., and Lepski, G. (2015). Evaluating cerebellar dentatotomy for the treatment of spasticity with or without dystonia. *Br. J. Neurosurg.* 29, 772–777. doi: 10.3109/02688697.2015.1025697

Veverka, T., Hok, P., Otruba, P., Zapletalova, J., Kukolova, B., Tudos, Z., et al. (2019). Botulinum toxin modulates posterior parietal cortex activation in post-stroke spasticity of the upper limb. *Front. Neurol.* 10:495. doi: 10.3389/fneur.2019.00495

Wang, Q., Zhang, D., Zhao, Y. Y., Hai, H., and Ma, Y. W. (2020). Effects of high-frequency repetitive transcranial magnetic stimulation over the contralesional motor cortex on motor recovery in severe hemiplegic stroke: a randomized clinical trial. *Brain Stimul.* 13, 979–986. doi: 10.1016/j.brs.2020.03.020

Ward, A. B. (2012). A literature review of the pathophysiology and onset of post-stroke spasticity. *Eur. J. Neurol.* 19, 21–27. doi: 10.1111/j.1468-1331.2011.03448.x

Winstein, C. J., Stein, J., Arena, R., Bates, B., Cherney, L. R., Cramer, S. C., et al. (2016). Guidelines for adult stroke rehabilitation and recovery: a guideline for healthcare professionals from the American Heart Association/American Stroke Association. *Stroke* 47, e98–e169. doi: 10.1161/STR.0000000000000098

Wu, C. H., Ho, Y. C., Hsiao, M. Y., Chen, W. S., and Wang, T. G. (2017). Evaluation of post-stroke spastic muscle stiffness using shear wave ultrasound elastography. *Ultrasound Med. Biol.* 43, 1105–1111. doi: 10.1016/j.ultrasmedbio.2016.12.008

Conflict of Interest: The authors declare that the research was conducted in the absence of any commercial or financial relationships that could be construed as a potential conflict of interest.

Publisher's Note: All claims expressed in this article are solely those of the authors and do not necessarily represent those of their affiliated organizations, or those of the publisher, the editors and the reviewers. Any product that may be evaluated in this article, or claim that may be made by its manufacturer, is not guaranteed or endorsed by the publisher.

Copyright © 2021 Chen, Wei, Zhang, Xie, Liao, Tan, Guo and Gao. This is an open-access article distributed under the terms of the Creative Commons Attribution License (CC BY). The use, distribution or reproduction in other forums is permitted, provided the original author(s) and the copyright owner(s) are credited and that the original publication in this journal is cited, in accordance with accepted academic practice. No use, distribution or reproduction is permitted which does not comply with these terms.

Advantages of publishing in Frontiers

OPEN ACCESS
Articles are free to read for greatest visibility and readership

FAST PUBLICATION
Around 90 days from submission to decision

HIGH QUALITY PEER-REVIEW
Rigorous, collaborative, and constructive peer-review

TRANSPARENT PEER-REVIEW
Editors and reviewers acknowledged by name on published articles

Frontiers
Avenue du Tribunal-Fédéral 34
1005 Lausanne | Switzerland

Visit us: www.frontiersin.org
Contact us: frontiersin.org/about/contact

REPRODUCIBILITY OF RESEARCH
Support open data and methods to enhance research reproducibility

DIGITAL PUBLISHING
Articles designed for optimal readership across devices

FOLLOW US
@frontiersin

IMPACT METRICS
Advanced article metrics track visibility across digital media

EXTENSIVE PROMOTION
Marketing and promotion of impactful research

LOOP RESEARCH NETWORK
Our network increases your article's readership